



# **Migration and Cyclisation Reactions of Selected Organic Anions**

A Thesis Submitted Towards the Degree of

Doctor of Philosophy

by

**John Michael Hevko B.Sc. (Hons)**



**THE UNIVERSITY OF ADELAIDE**

Department of Chemistry  
The University of Adelaide  
December 1998



1.4	Mass Analysed Ion Kinetic Energy Mass Spectrum	14
1.5	Linked $B^2/E$ Scanning	15
1.6	Structural Identification of Ions	16
1.6.1	Collisional Activation (CA)	17
1.6.2	Charge Reversal (CR) MIKE Scanning	17
1.6.3	Kinetic Energy Release (Peak Profiles)	19
1.7	Theoretical <i>Ab Initio</i> Molecular Orbital Calculations	22
1.8	Negative Ion Fragmentations	29
1.8.1	Simple Homolytic Cleavage	29
1.8.2	Formation of an Ion-Neutral Complex	30
1.8.3	Proton Transfer or Rearrangement Preceding Fragmentation	30
1.8.4	Remote Fragmentations	32
1.9	Migration of Anions	33

## **Chapter 2 - Cross-Ring Phenyl Anion Initiated Reactions as Fragmentations of (M-H)<sup>-</sup> Species.**

2.1	Introduction	35
2.2	Results and Discussion	37
2.2.1	N-(Methoxyphenyl) benzamide Series	37
2.2.2	N-(Ethoxyphenyl) benzamide Series	48
2.2.3	Methyl-benzoylaminobenzoate Series	51
2.3	Summary, Conclusions and Future Work	55

### Chapter 3 - Ion Mobility in Keto Substituted Alkoxide Anions

3.1	Introduction	57
3.2	Results and Discussion	61
3.2.1	Migration of the Hydride Ion	62
3.2.1.1	Reactions of Deprotonated 6-Hydroxy-hexan-2-one	62
3.2.1.2	Reactions of Deprotonated 5-Hydroxy-pentan-2-one	74
3.2.1.3	Reactions of Deprotonated 7-Hydroxy-heptan-2-one	79
3.2.2	Possible Migration of the Methyl Ion	83
3.2.2.1	Reactions of Deprotonated 2-Dimethyl Substituted Keto-Alcohols	83
3.3	Summary and Conclusions	89

### Chapter 4 - Competitive Cyclisations of Epoxy-Alkoxide Ions

4.1	Introduction	90
4.2	Results and Discussion	95
4.2.1	Competitive Cyclisations of the 3,4-Epoxybutoxide Anion	95
4.2.1.1	<i>Ab Initio</i> Calculations for Competing Cyclisations of the 3,4-Epoxybutoxide Anion	96
4.2.1.2	Gas Phase Reactions of <b>1</b> , <b>2</b> and <b>3</b>	98



4.2.1.3	Condensed Phase Reactions of <b>1</b> , <b>2</b> and <b>3</b>	111
4.2.1.4	Summary	112
4.2.2	Competitive Cyclisations of 4,5-Epoxy pentoxide Anion	113
4.2.2.1	<i>Ab Initio</i> Calculations for Competing Cyclisations of the 4,5-Epoxy pentoxide Anion	114
4.2.2.2	Gas Phase Reactions of <b>7</b> , <b>8</b> and <b>9</b>	115
4.2.2.3	Condensed Phase Reactions of <b>7</b> , <b>8</b> and <b>9</b>	130
4.2.2.4	Summary	131
4.2.3	Competitive Cyclisations of 5,6-Epoxy hexoxide Anion	131
4.2.3.1	<i>Ab Initio</i> Calculations for Competing Cyclisations of 5,6-Epoxy hexoxide Anion	132
4.2.3.2	Gas Phase Reactions of <b>10</b> , <b>11</b> and <b>12</b>	133
4.2.3.3	Condensed Phase Reactions of <b>10</b> , <b>11</b> and <b>12</b>	144
4.2.3.4	Summary	145
4.3	Competing $S_Ni$ Reactions - The Arrhenius Factor	146
4.4	Conclusions	161

## Chapter 5 - Experimental

5.1	General Experimental	163
5.2	Compounds Described in Chapter 2	166
5.3	Compounds Described in Chapter 3	170

5.4	Compounds Described in Chapter 4	180
5.4.1	Compounds Described in Section 4.2.1	180
5.4.2	Compounds Described in Section 4.2.2	185
5.4.3	Compounds Described in Section 4.2.3	191
<b>Appendices</b>		200
<b>References</b>		228
<b>Publications</b>		246

# List of Figures

- Figure 1.1 Potential energy curves for MX and  $\text{MX}^-$  where the electron affinity of MX is less than zero (a) and greater than zero (b). page 5
- Figure 1.2 Potential curves for MX and  $\text{MX}^-$  showing attractive (a) and repulsive (b) states for  $\text{MX}^-$ . page 7
- Figure 1.3 Potential energy curve for MX and  $\text{MX}^*$  for an ion-pair process. page 8
- Figure 1.4 The VG ZAB 2HF Mass Spectrometer. page 13
- Figure 1.5 CR MIKE spectrum of the  $(\text{M-H})^-$  ion of methyl vinyl ketone. page 19
- Figure 1.6 Different orientations of (field free) ion decompositions leading to kinetic energy release. page 20
- Figure 1.7 Metastable peaks observed due to different extremes of kinetic energy release. page 21
- Figure 1.8 Saddle-shaped Energy Surface in the region of a Transition State. page 24

Figure 2.1	Methoxy (a), ethoxy (b) and methylcarboxylate (c) substituted phenyl benzamides to be investigated for possible phenyl anion 'cross-ring' reactions.	page 37
Figure 2.2	CA MIKE spectrum for deprotonated N-(4-methoxyphenyl) benzamide.	page 38
Figure 2.3	Linked scans at constant $B^2/E$ showing the parent ions of $m/z$ 134 for deprotonated (a) <i>ortho</i> - , (b) <i>meta</i> - , and (c) <i>para</i> - N-(methoxyphenyl) benzamide.	page 42
Figure 2.4	Stable radical anions formed from deprotonated N-(methoxy phenyl) benzamide isomers.	page 43
Figure 2.5	CA MS/MS data for $o\text{-CH}_3\text{O-C}_6\text{H}_4\text{-}^-\text{NCOC}_6\text{D}_5$ .	page 47
Figure 2.6	The CA MIKES spectrum of deprotonated N-(4-ethoxyphenyl) benzamide.	page 48
Figure 2.7	Phenyl anion initiated reactions observed for (a) deprotonated N-(4-methoxyphenyl) benzamide and (b) deprotonated N-(4-ethoxyphenyl) benzamide.	page 51
Figure 2.8	CA MIKES spectrum for deprotonated methyl 4-benzoylaminobenzoate.	page 53

- Figure 2.9 Stable radical anions resulting from loss of (a)  $\text{H}^\cdot$ , (b)  $\text{CH}_3^\cdot$ , (c)  $\text{CH}_3\text{O}^\cdot$ , and (d)  $\text{CH}_3\text{CO}_2^\cdot$  from Methyl-Benzoylaminobenzoate isomers. page 54
- Figure 3.1 Collision-induced  $\text{HO}^-$  negative chemical ionisation mass spectrum (MS/MS) of the  $(\text{M-D})^-$  ion of  $\text{MeCO}(\text{CH}_2)_4\text{OD}$ . page 63
- Figure 3.2 CA MIKE spectrum for dedeuterated 5-hydroxy-pentan-2-one (**1**). page 74
- Figure 3.3 The CA MIKE spectrum for the  $(\text{M-D})^-$  ion of 7-hydroxy-heptan-2-one (**12**). page 80
- Figure 3.4 The CA MIKE spectrum of  $(\text{M-D})^-$  ion of 5-methyl-hydroxy-OD-hexan-2-one (**4**). page 85
- Figure 4.1 *ab initio* calculations for the competitive  $\text{S}_{\text{N}}\text{i}$  calculations of the epoxybutoxide anion. page 97
- Figure 4.2 Collisional activated  $\text{HO}^-$  negative ion chemical ionisation MIKE spectrum of the 3,4-epoxybutoxide anion. page 99
- Figure 4.3 Peak profile of the broad peaks in the spectra of the  $(\text{M-H})^-$  ion of (A) 1,1- $d_2$ -2-(2-oxiranyl)-1-ethanol (**4**), and (B) 2-(2-oxiranyl)ethan-1- $^{18}\text{O}$ ol (**5**). page 101

Figure 4.4	Collisional activated HO <sup>-</sup> negative ion chemical ionisation MIKE spectrum of the 2-oxetanylmethanol alkoxide ion (2).	page 104
Figure 4.5	Collisional activated HO <sup>-</sup> negative ion chemical ionisation MIKE spectrum of the tetrahydro-3-furanol alkoxide ion (3).	page 105
Figure 4.6	<i>Ab initio</i> calculations for the competitive S <sub>N</sub> i cyclisations of the 4,5-epoxypentoxide anion.	page 115
Figure 4.7	Collisional activated mass spectrum (MS/MS) of 7. Produced by the S <sub>N</sub> 2 reaction between the methyl ether and <sup>-</sup> OH.	page 117
Figure 4.8	Collisional activated mass spectrum (MS/MS) of 8. Produced by the S <sub>N</sub> 2 reaction between the methyl ether and <sup>-</sup> OH	page 117
Figure 4.9	Collisional activated mass spectrum (MS/MS) of 9. Produced by the S <sub>N</sub> 2 reaction between the methyl ether and <sup>-</sup> OH	page 118
Figure 4.10.	CA MIKE Spectra for the <sup>18</sup> O-labelled analogues of 7 and 8.	page 128
Figure 4.11	<i>Ab initio</i> calculations for the competitive S <sub>N</sub> i cyclisations of the 5,6-epoxyhexoxide anion.	page 133

Figure 4.12 Collisionally activated MS/MS data for **10**. page 134

Figure 4.13 Collisionally activated MS/MS data for **11**. page 135

Figure 4.14 Collisionally activated MS/MS data for **12**. page 135

Figure 4.15 Density of states for the transition states leading to cyclisation products of 5,6-epoxyhexoxide anion. page 156

# List of Tables

Table 2.1.	CA MIKE data for deprotonated N-(methoxyphenyl) benzamide series.	page 38
Table 2.2.	Collisional activation MS/MS data for production of $m/z$ 134.	page 41
Table 2.3	CA MIKE data for deprotonated N-(ethoxyphenyl) benzamide isomers.	page 49
Table 2.4.	Collisional activated MIKE data for methyl-benzoylamino benzoate series.	page 53
Table 3.1	Compounds examined in this study.	page 61
Table 3.2	Collisional activated mass spectra (MS/MS) of (M-D) <sup>-</sup> or (M-H) <sup>-</sup> ions.	page 63
Table 3.3	Comparison of collisional activated or charge reversal (positive ion) mass spectra of product anions from the (M-D) <sup>-</sup> ion from <b>7</b> , with the spectra of authentic anions (formed by deprotonation of the appropriate neutral).	page 65
Table 3.4	Collisional activated negative ion spectra for (M-H) <sup>-</sup> or (M-D) <sup>-</sup> ions of <b>1</b> , <b>2</b> , and <b>3</b> .	page 75



Table 3.5	Comparison of Collisional Activated or Charge Reversal (positive ion) Mass Spectra of Product Anions from the (M-D) <sup>-</sup> ion of <b>1</b> , with the Spectra of Authentic Anions (formed by deprotonation of the appropriate neutral).	page 76
Table 3.6.	Comparison of Collisional Activated and/or Charge Reversal (positive ion) mass spectra of product anions from the (M-D) <sup>-</sup> ion of <b>12</b> , with the spectra of authentic anions (formed by deprotonation of the appropriate neutrals).	page 81
Table 3.7	CA negative ion spectra for (M-D) <sup>-</sup> or (M-H) <sup>-</sup> ions of <b>4</b> , <b>5</b> , <b>10</b> and <b>11</b> .	page 84
Table 3.8	Comparison of Collisional Activated or Charge Reversal (positive ion) mass spectra of product anions from the (M-D) <sup>-</sup> ion of <b>4</b> , with the spectra of authentic anions (formed by deprotonation of the appropriate neutrals).	page 86
Table 4.1	Mass spectra of labelled 3,4-epoxybutoxide anions.	page 100
Table 4.2	Spectra of product anions from <b>1</b> and known anions.	page 102
Table 4.3	Peak width measurements of <i>m/z</i> 69 and/or <i>m/z</i> 59 from anions <b>1</b> , <b>2</b> and <b>3</b> .	page 106

Table 4.4	Spectra of product anions from <b>2</b> and <b>3</b> .	page 106
Table 4.5.	Base catalysed solution reactions of the neutrals of <b>1</b> , <b>2</b> and <b>3</b> .	page 112
Table 4.6	Peak width measurements of $m/z$ 71 and 83 from <b>7</b> , <b>8</b> and <b>9</b> .	page 118
Table 4.7	Product Ion Studies using Charge Reversal spectra.	page 120
Table 4.8	CA MS/MS of Labelled Derivatives.	page 127
Table 4.9	Base Catalysed Solution Reactions of 3-(2-oxiranyl)propyl acetate, tetrahydrofurfuryl alcohol and tetrahydro-2H-3-pyranol.	page 130
Table 4.10	Peak width measurements of $m/z$ 97, and/or 85 and 67 from <b>10</b> , <b>11</b> and <b>12</b> .	page 136
Table 4.11	Product ion studies using CA and CR spectra.	page 137
Table 4.12	CA MS/MS data for $^{18}\text{O}$ -labelled derivatives of <b>10</b> and <b>11</b> .	page 144
Table 4.13	Condensed Phase Reactions of 4-(2-oxiranyl)-1-butanol, tetrahydropyran-2-methanol, and 3-oxepanol.	page 145

Table 4.14	Parameters Influencing the Kinetics of the $S_Ni$ Processes. Major Products.	page 148
Table 4.15	Harmonic Vibrational Partition Functions of $S_Ni$ Transition States at 298K.	page 154
Table 4.16	Mulliken Charge Ratios for the Oxirane Carbons for the Reactant Anions.	page 157

# Abstract

In this thesis the investigation of anionic migration reactions in the gas phase, and rearrangement reactions of selected organic anions in the gas and condensed phases were examined.

"Long-range" phenyl anion "cross-ring" reactions occur when  $(M-H)^-$  ions of methoxy-, ethoxy-, and carbomethoxy- $C_6H_4^-NCOPh$  are subjected to collisional activation. These reactions are generally minor processes: a particular example is the "cross-ring" elimination  $p-C_2H_5O-C_6H_4^-NCOPh \rightarrow [Ph^- (p-C_2H_5O-C_6H_4-NCO)] \rightarrow p-(^-O)-C_6H_4-NCO + C_2H_4 + Ph$ . Major processes of these  $(M-H)^-$  ions involve losses of radicals to form stabilised radical anions, e.g. (a) loss of a ring  $H^\cdot$  or (b)  $CH_3^\cdot$ , (or  $C_2H_5^\cdot$ , or  $^\cdot CO_2CH_3$ ) from the alkoxy group.

Keto alcohols of the formula  $MeCO(CH_2)_nOH$  ( $n = 3 - 5$ ) are deprotonated by  $HO^-$  at both  $-OH$  or  $\alpha$  to the carbonyl group. The various deprotonated species interconvert under the conditions of collisional activation. The fragmentations of  $(M-H)^-$  ions are varied and complex, with most fragmentations being directed from the alkoxide centre. These fragmentations have been investigated by product ion and deuterium labelling studies. An interesting hydride transfer reaction occurs when  $n = 3$  and 4, i.e.  $H^-$  transfer occurs from the  $CH_2$  group next to the alkoxide centre to the carbon of the carbonyl group to form  $^-CH_2CHO$  as the product anion. This reaction does not occur when  $n = 5$ . The corresponding  $Me^-$  transfer from deprotonated  $MeCO(CH_2)_nC(Me)_2OH$  ( $n = 2$  and 3) is not observed.

*Ab initio* calculations [at the MP2(fc)/6-31+G(d) level] indicate that the 3,4-epoxybutoxide anion, the 4,5-epoxypentoxide anion, and the 5,6-

epoxyhexoxide anion should undergo competitive  $S_Ni$  cyclisations (through four- and five-, five- and six-, and six- and seven-membered transition states respectively) to yield the corresponding  $(M-H)^-$  ions of the respective cyclic products. These systems have been studied experimentally in both the condensed and gas phases. A comparison is made of the reported competitive  $S_Ni$  reactions for the 2,3-epoxypropoxide anion, with those processes observed for 3,4-epoxybutoxide, 4,5-epoxypentoxide and 5,6-epoxyhexoxide anions. For all but the 3,4-epoxybutoxide system, the exclusive or major product is that which contains the smaller of the two ring systems for both gas phase and condensed phase reactions. In the case of the 3,4-epoxybutoxide system:- (i) in the gas phase, both four- and five-membered ring  $S_Ni$  products are formed in comparable yield, and (ii) in the condensed phase, the major product is that with the larger ring.

# Statement of Originality

This work contains no material which has been accepted for the award of any other degree or diploma in any other university or other tertiary institution and, to the best of my knowledge and belief, this thesis contains no material previously published or written by any other person, except where due reference has been made in the text.

I give consent to this copy of my thesis, when deposited in the University library, being available for loan or photocopying.

23/12/98

.....  
Date

# Acknowledgments

I would like to express my sincere thanks and gratitude to my supervisor Professor John H. Bowie. His enthusiasm and support over the past four years is second to none. He is a fascinating man and his research interests are equally as fascinating, and I am indebted to him for giving me the opportunity to study a very interesting and intellectually challenging aspect of ion chemistry.

I would also like to thank Tom Blumenthal for the initial training on the ZAB 2HF and for the general maintenance of this invaluable instrument. I also wish to thank Dr. Suresh Dua for his help and guidance throughout my post graduate period, and in particular for proof reading this thesis during the festive season. Suresh is a wonderful person and more importantly a very good friend, I wish him and his family all the best for the future. Special thanks to Mark Taylor and Dr. Mark Buntine who have patiently helped me grasp an understanding of theoretical and physical aspects of organic chemistry. Mark and Mark are both academically brilliant people and have in many cases inspired me to view chemistry from an entirely different point of view from which I would otherwise. One of these Marks also provided me with free accommodation close to a computer during the final stages of this Ph.D., for which I am grateful.

I would also like to thank my research group for being great friends and a wonderful group of people to work with, in particular Stephen Blanksby for always lending an ear when I felt that I needed advise, and Brian Chia, an amazing human being with extreme focus and dedication of which I feel has influenced myself throughout the closing stages of my Ph.D. (and also for providing me with a multitude of cheap second hand CD's).

I would like to thank Dr. Wayne Pearce, Spencer Clarke, and David Cluse (and their respective partners: Colleen, Joanne and Kathy) for being good house mates and providing me with fun times and entertainment over the past two years.

In no particular order I would like to thank Dr. David Ward for the help he has offered, Dr. George Gream for general advice, Jane Wannan for helping me with literature searches when at times things looked bleak, Tom Rozek for spray painting my car, amongst other things, Paul Wabnitz, Kate Wegener, Simon Steinborner, Andrew McAnoy, Daniela Caiazza, Tom Avery, Karl Cornelius, Marc Kimber and Christie Moule, I wish them both a happy future together, Peter Turner for a memorable trip to Ayers Rock, amongst other things, Jason Geue, Ian Milne for all the Macintosh guidance I have required over the last three years, Wendy Holstein and Ella Robinson for all of the sweets that kept me going during the stages of writing up, Gino Farese, Peter Apoeffis, John Cameron the ever patient 'store control freak', Prof. Michael Bruce, Dr. Lou Rendina, Dr. Dennis Taylor and the rest of the Chemistry Department, it has been a great pleasure to work with and amongst so many different people.

I would like to thank my family and friends for their encouragement throughout my University life. In particular I would like to thank my Parents for encouraging me to not become a motor mechanic or a chef, and in doing so leading me down the path I have now taken. I would like to thank my Uncle Bob and Auntie Marcia for providing me with entertainment and food whenever I made unexpected visits. I would also like to thank my grandparents, Helen and Michael Hevko, who I haven't seen as much of as I would have liked to due to the hectic lifestyle of a Ph.D. student. I would also like to thank Mike and Adrian Middleton for fun, relaxing, and sometimes stressful times outside of University. The Lowndes



family also deserve thanks for all those dinners and glasses of red wine over the last year, and more importantly for welcoming me into their family with open arms and allowing me to watch National Geographic on cable. I would also like to acknowledge my brother Steven and my sister to be Tammie. I wish them both well for their future together.

On a more personal note, I would also like to thank: Coopers Brewery (SA's own) for supplying me with the best beer known to man (Fig. A). Coopers was always there for me when I needed a break from the hard work. Triple J for providing a great range of music, in particular up and coming Australian bands, and NO-IS-Y, one of those up and coming Australian bands also deserves recognition.



Figure A. Coopers Brewery, Pale Ale label; Proudly South Australian.

Finally, I would like to thank my fiancée Melanie Lowndes for standing by me when my patience was at a minimum. I look forward to spending a wonderful life of fun and adventure with this lady.



# Chapter 1

## Introduction

### 1.1 General Introduction

For many years negative ion mass spectrometry had not received the deserved recognition as far as organic chemical applications were concerned. It was mainly of interest to physicists, and very few classes of compounds except quinones and nitroaromatics<sup>1</sup> gave useful negative ion mass spectra when investigated with an electron impact (EI) ion source mass spectrometer. This was due to the difficulty of obtaining a sufficiently intense beam of thermal electrons with an energy of 0-5 eV with the standard EI ion source. Negative ion (NI) mass spectrometry became recognised as a useful addition to mass spectrometry when chemical ionisation (CI) ion sources and quadrupole instruments, which allow for an easy change from positive to negative ionisation, were introduced to the market.<sup>2</sup>

The fragmentation behaviour of radical anions  $M^{\cdot-}$  derived by electron capture of organic molecules was studied extensively in the 1970's and early 1980's. Since then the study of negative ion chemistry in the gas phase has emerged as a powerful method for investigating the behaviour of anions and radical anions in the absence of solvent and counter ions.

The past two decades has brought about improvement in instrumentation,<sup>3</sup> leading to a surge of interest in the field of negative ions, which due to several factors<sup>1</sup> such as claimed difficulties in generating negative ions,<sup>4</sup> lack

of fragmentations observed from negative ions, and the low sensitivity of negative ion detection, had been lagging behind that of positive ions.

Important advances in "soft ionisation"<sup>5,6</sup> techniques including chemical ionisation, fast atom bombardment (FAB),<sup>7</sup> plasma desorption<sup>8</sup> and electrospray<sup>9</sup> has allowed for the easy formation of deprotonated organic molecules (M-H)<sup>-</sup>. The use of collisional activation has resulted in a better understanding of the structures and fragmentations of ions,<sup>10</sup> and has led to the classification of the general fragmentations of even-electron organic anions into particular reaction types.<sup>11</sup> As a consequence, negative ion mass spectrometry has become an increasingly useful analytical tool, proving in some cases to be more informative than traditional positive ion techniques.<sup>4</sup> Presently, it is playing an important role in the understanding of the reactivity of organic anions in the absence of solvent and counter ion effects.<sup>12</sup>

## 1.2 Formation of Negative Ions

### 1.2.1 Primary Ions

Direct electron impact results in the formation of positive and negative ions<sup>13</sup> in the source of the mass spectrometer. The formation of primary negative ions by electron impact is dependent on both the energy of the ionising electrons, the pressure and the temperature in the ion source<sup>14</sup>, and on the nature of the neutral precursor molecule.<sup>15</sup>

Electron capture by a molecule may result in the formation of a short lived negative ion state. The term "resonance" is applied to these states and they only form over a narrow range of energies. Negative ions are produced as a

result of electron/molecule interactions by three general processes depicted for the molecule MA.

1. Resonance capture (electron attachment)
2. Dissociative resonance capture (dissociative electron attachment), and
3. Ion-pair formation.

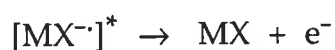
A better understanding of these processes may be obtained by examining potential energy diagrams for diatomic molecules and the negative ion.

#### 1.2.1.1. Resonance Capture (electron attachment)<sup>5</sup>

Resonance capture produces a parent negative ion and occurs at near 0 eV (equation 1.1).



For resonance capture two cases arise depending on whether the electron affinity of MX is less than or greater than zero (Fig. 1.1). When the electron affinity is less than zero, transitions from the ground state molecule occur according to the Franck-Condon principle, where electron motions are considered to be much more rapid than nuclear motions, leading to an unstable molecular anion  $[\text{MX}^-]^*$  which may undergo autodetachment.



Alternatively, if the anion radical is excited above the dissociation asymptote, it may dissociate to  $M\cdot$  and  $X^-$ . The anion  $[MX^{\cdot-}]^*$  may be stabilised by collision with a neutral molecule (although this is unlikely at low pressures) or by radiation emission. However, autodetachment is a very rapid process, and since this occurs within a vibrational period, there is often little possibility for collisional stabilisation to occur. When the electron affinity of  $MX$  is greater than zero there are two possibilities, viz (a) the potential energy curve for  $MX^{\cdot-}$  crosses the Franck-Condon region and reaction and/or dissociation processes similar to those shown in Figure 1.1(a) may occur, and (b) the  $MX^{\cdot-}$  curve does not intersect the vertical transition region. Given this scenario, long interaction times may result due to the low energy (thermal) of the electron, and therefore, the Born-Oppenheimer approximation may break down resulting in a change of position of the nuclei on the negative ion curve. If the excess energy of  $[MX^{\cdot-}]^*$  can be distributed into the vibrational modes of the anion, significant lifetimes (with respect to autodetachment) for the molecular anion may be observed and collisional stabilisation can occur more readily.

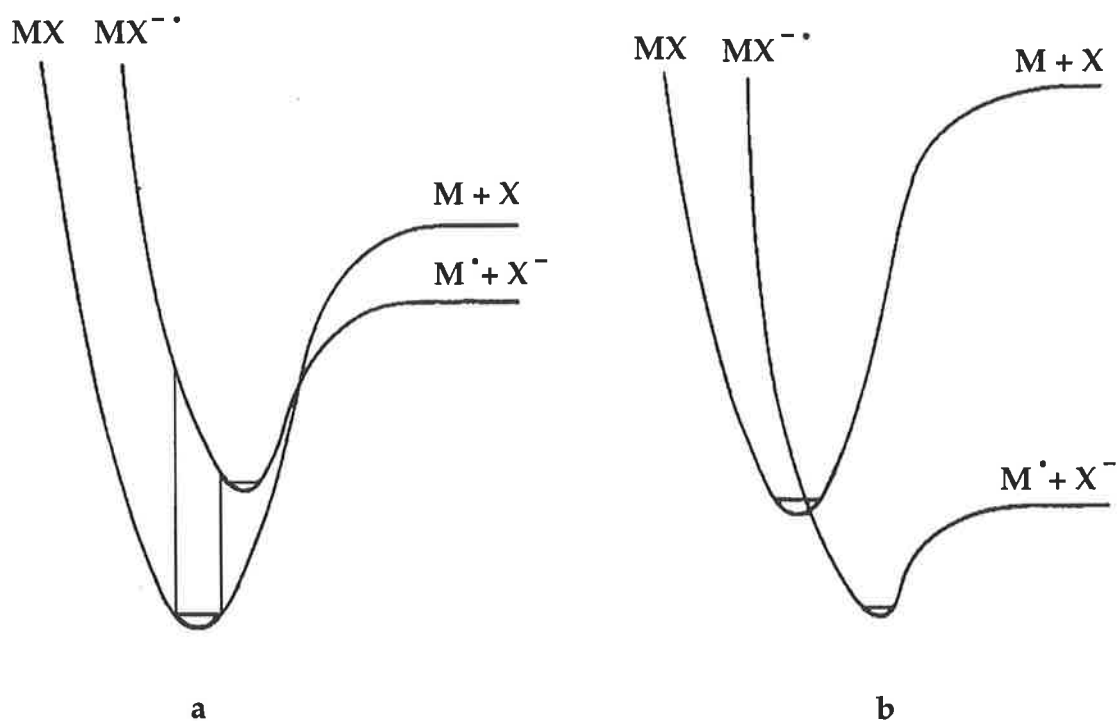


Figure 1.1 Potential energy curves for  $MX$  and  $MX^{\cdot-}$  where the electron affinity of  $MX$  is less than zero (a) and greater than zero (b).<sup>16</sup>

Ions having lifetimes  $> 10^{-6}$  seconds can be studied using conventional mass spectrometers. At low pressures ( $< 10^{-4}$  Torr), the lifetimes of the ions may vary from  $10^{-7}$  to  $10^{-12}$  seconds,<sup>17</sup> and at high pressures ( $> 1$  Torr), the formation of certain long lived molecular ions becomes favourable. The high pressures required can be generated by the use of an inert buffer gas.

#### 1.2.1.2 Dissociative Resonance Capture (dissociative electron attachment)<sup>5</sup>

The capture of an electron may result in the formation of a molecular anion ( $MX^{\cdot-}$ ) lying on the repulsive region of its potential energy surface; the resulting unstable anion fragments rapidly to yield an anion and a neutral radical (equation 1.2).



This process generally occurs over an electron energy range of 0 to 15 eV, and may be explained by the use of the Morse curves shown in Figure 1.2. The potential energy curve for  $\text{MX}^-$  is shown as an attractive state in Figure 1.2a and as a repulsive state in Figure 1.2b. Franck-Condon transitions to the attractive state will produce  $\text{M}^\cdot$  and  $\text{X}^-$  provided (a) that levels above the dissociation limit of  $\text{MX}^-$  are populated, and (b)  $\text{EA}(\text{X}) > \text{EA}(\text{M})$ . In such cases the molecular ion  $[\text{MX}^-]^*$  may also be formed.

A repulsive state of  $\text{MX}^-$  is shown in Figure 1.2b: this dissociates to produce  $\text{M}^\cdot$  and  $\text{X}^-$ . Due to a vertical transition of  $\text{MX}$ ,  $\text{MX}^-$  is produced in an unstable repulsive state which dissociates to form  $\text{M}^\cdot$  and  $\text{X}^-$ . The two products may have excess translational and excitational energy partitioned between  $\text{M}^\cdot$  and  $\text{X}^-$ .



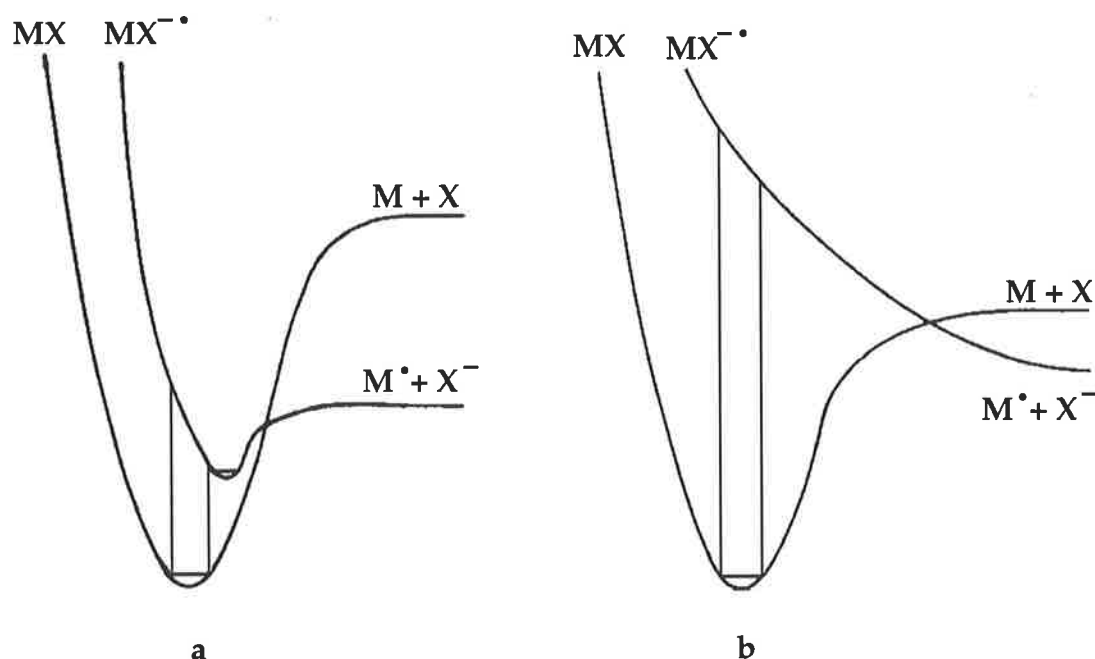


Figure 1.2. Potential curves for MX and MX<sup>-•</sup> showing attractive (a) and repulsive (b) states for MX<sup>-•</sup>.<sup>16</sup>

### 1.2.1.3 Ion-Pair Formation<sup>5</sup>

In ion-pair formation (Fig. 1.3), the electron provides the energy necessary to excite the molecule to an electronic level which can dissociate or pre-dissociate to give a positive ion and a negative ion. If the vertical transition to MX occurs to levels above the dissociation limit, then M<sup>+</sup> and X<sup>-</sup> may be formed with excess energy in a manner similar to that noted for dissociative resonance capture. The thresholds for such processes usually occur over a wide range of electron energies between 10 and 15 eV. In the chemical ionisation source "high energy" electrons can be "thermalised" as shown in equation 1.3.<sup>5</sup>

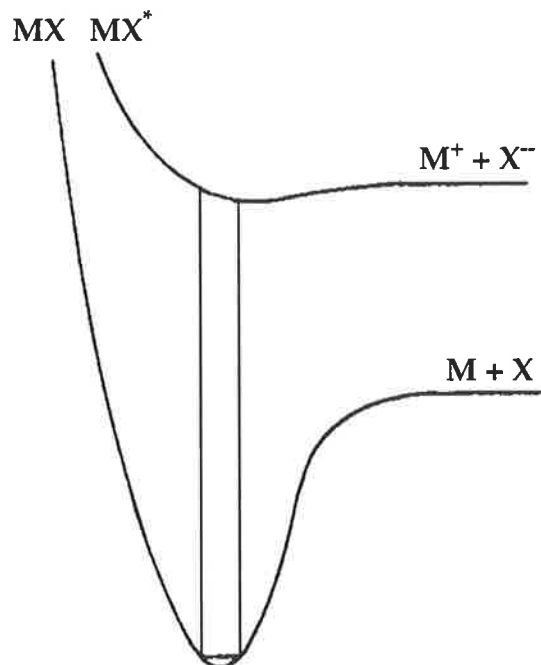
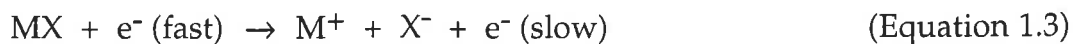


Figure 1.3. Potential energy curve for MX and MX\* for an ion-pair process.<sup>16</sup>

### 1.2.2 Secondary Ions Formed *via* Ion-Molecule Reactions

The majority of ions formed in a negative ion chemical ionisation (NICI) source are formed as a consequence of ion-molecule reactions between primary ions and a neutral molecule.<sup>18</sup> The chemical ionisation (CI) source operates at a pressure of 0.2-2 Torr: this should be compared to the pressures in the flight tube, generally  $\leq 10^{-7}$  Torr. Electrons and primary ions under these conditions undergo multiple collisions, and the ions may transfer their excess internal energies to the buffer gas. The primary ions may then react with a neutral molecule to generate secondary ions. To ensure electron capture by the sample does not occur, the proportion of sample to reagent gas

is kept very low.<sup>19</sup> There are four major classes of ion-molecule reactions that result in the formation of negative ions.

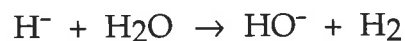
#### 1.2.2.1 Proton Transfer

Proton transfer processes are an important class of reactions since many organic compounds contain acidic hydrogens. Deprotonation is arguably the most important process for the generation of even electron anions in the CI source. This process is described in equation 1.4.



The proton transfer process will be exothermic if (a) the gas-phase acidity of BH is greater than the gas-phase acidity of AH, or (b) the proton affinity of  $A^-$  is greater than the proton affinity of  $B^-$ . Such proton transfer reactions are of importance in chemical ionisation mass spectrometry not only because of their high efficiency but also because they lead to formation of  $[M-H]^-$  ions which provide molecular weight information<sup>2</sup> and may be collisionally activated to yield characteristic fragmentations which may aid in structure determination.<sup>20</sup>

The usual primary ions employed are the Brønsted bases<sup>21</sup>  $^-NH_2$ ,  $MeO^-$  and  $HO^-$ . The primary ion  $HO^-$  is formed by electron impact on  $H_2O$  in the source as summarised in equation 1.5.



The  $\text{HO}^-$  ion is a strong base [ $\Delta G_{\text{acid}}^\circ \text{H}_2\text{O} = 1607 \text{ kJ mol}^{-1}$ ]<sup>22</sup> and as such is capable of abstracting a proton from a wide range of organic molecules. In addition, the electron affinity is high enough [ $\text{EA}, \text{HO}^\cdot = 173.6 \text{ kJ mol}^{-1}$ ]<sup>23</sup> so that charge exchange reactions are minimised.

#### 1.2.2.2 Charge Exchange

The electron affinity of a molecule is a quantitative measure of the ability to capture an electron. The charge exchange reaction shown in equation 1.6 will occur, provided the electron affinity of B is greater than that of A.<sup>24,25</sup>



#### 1.2.2.3 Nucleophilic Addition<sup>26</sup>

Stable addition complexes may be formed when weak Brønsted bases that do not readily deprotonate molecules, are allowed to react with neutral molecules (equation 1.7).



The  $\text{AB}^-$  addition complexes may be either "adducts" if covalently bound<sup>27</sup> or "solvated ions".<sup>28</sup>

#### 1.2.2.4 Nucleophilic Displacement

Nucleophilic displacement reactions may occur provided (a) the reaction is exothermic or thermoneutral and (b) does not compete with a facile deprotonation reaction.<sup>29</sup> For example, DePuy<sup>30</sup> has used an  $\text{S}_{\text{N}}2$  (Si) reaction to generate highly reactive anions (e.g. equation 1.8).



### **1.3 The VG ZAB 2HF Mass Spectrometer**

Conventional 'Nier-Johnson' mass spectrometers consist of an electric sector followed by a magnetic sector. The electric sector is an energy (or velocity) focussing device while the magnetic sector is angular (or directional) focussing.

If  $V$  is the potential through which the ions are initially accelerated and  $E$  is the field in the electric sector then equation 1.9 is obtained.<sup>31</sup>

$$r = \frac{2V}{E} \quad (\text{Equation 1.9})$$

where  $r$  is the radius of the ion path.

Ions accelerated through a potential ( $V$ ) and passing through a uniform field ( $E$ ) have the same radius of curvature ( $r$ ). Therefore keeping the field  $E$  constant allows the electric sector to focus ions according to their translational energies irrespective of their mass to charge ratios. The energy focussed ion beam then passes through a magnetic field where mass separation is effected according to equation 1.10.<sup>31</sup>

$$m/z = \frac{B^2 r^2}{2V} \quad (\text{Equation 1.10})$$

where  $B$  is the magnetic field.

The radius of curvature for ions of different  $m/z$  will be different at constant magnetic field ( $B$ ) and accelerating potential ( $V$ ), thereby allowing separation of ions depending on their  $m/z$  values.

This combined use of electric and magnetic sectors affords a double-focussing mass spectrometer because the ion beam is focussed first for translational energy and then for mass to charge ratio.

The ZAB is a double-focussing reverse sector mass spectrometer (Fig. 1.4) which means that unlike conventional 'Nier-Johnson' two sector instruments, the magnetic sector precedes the electric sector with the overall geometry being similar to that derived by Hintenberger and Konig.<sup>32</sup> Ions may be produced in either the combined electron impact (EI) and chemical ionisation (CI) source or with the fast atom bombardment (FAB) source. The reverse sector instrument is capable of performing in the same way as conventional instruments, but has additional advantages. The major advantage is that the magnetic field may be set to focus ions of predetermined  $m/z$  into the second field free region (FFR) while sweeping the voltage of the electric sector to identify all product ions. This technique is known as mass

analysed ion kinetic energy spectroscopy (MIKES). The ZAB is equipped with a variable potential gas cell in the 2nd FFR to allow collisional induced decompositions (CID) or collisional activation (CA) to extend the MIKES capability.

A disadvantage of the ZAB is that artefact peaks<sup>33,34</sup> may arise in a CA-MIKE spectrum due to metastable decompositions of ions in the 1st FFR which may lead to ions of differing mass but coincident momentum to the mass analysed species. Mass selection with the magnet alone is therefore insufficient to create a pure ion beam and the subsequent spectra may contain peaks due to this contamination. This problem may be overcome by adding a third sector to the instrument, thus the beam could be focussed using both the first magnetic and first electric sectors ensuring that the ion beam is free from all but the mass ion of interest.

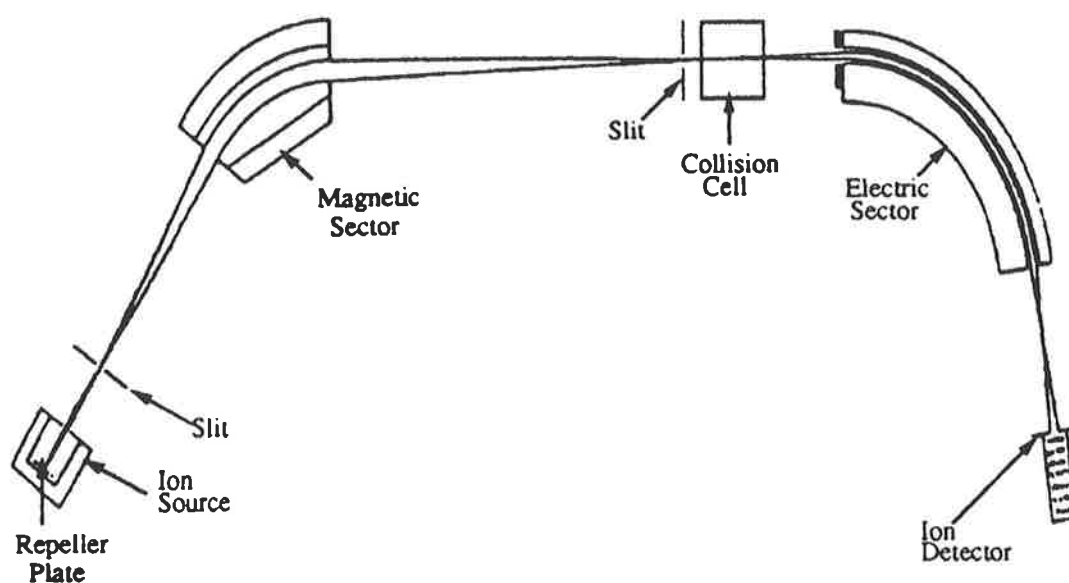


Figure 1.4 The VG ZAB 2HF Mass Spectrometer

The modern reverse sector mass spectrometer has been referred to as a complete chemical laboratory<sup>35</sup> with the ion source being analogous to synthesis, purification occurs at the magnet, the reaction takes place in the collision cell and sample analysis is obtained with the electric sector.

#### 1.4 Mass Analysed Ion Kinetic Energy Mass Spectrum

The MIKES technique is a powerful tool which can be used to directly analyse a mixture of samples, and as such has been suggested as an alternative to combined chromatography/mass spectrometry.<sup>31</sup>

If a mixture of three compounds of molecular weights  $M_1$ ,  $M_2$  and  $M_3$  are ionised in the source, the magnetic sector can be set to allow only  $M_1^-$  through the magnetic sector and down the flight tube towards the electric sector, upon which  $M_1^-$  may fragment into  $m_2^-$  and  $m_3$  on collisional activation (equation 1.11).



The initial translational (kinetic) energy of  $M_1^-$  is partitioned in the ratio of the masses of  $m_2^-$  and  $m_3$ . The electric sector separates the daughters of  $M_1^-$  according to their kinetic energies. The electric sector can be scanned from the maximum kinetic energy ( $V$ ) of the surviving  $M_1^-$  ion down to 0 volts. Fragmentation products will be detected at the electric sector voltage  $V_2$  (equation 1.12).



$$V_2 = V \times \frac{m_2}{M_1} \quad (\text{Equation 1.12})$$

Generally the electric sector is scanned automatically to detect all fragment ions produced from the collisionally activated parent ion to produce a collisionally activated mass analysed ion kinetic energy spectrum (CA MIKE).

MIKE spectra show peaks which are broadened due to energy release arising from the dynamics of fragmentation. Peak shapes can be analysed for distributions of translational energy release and for energy change in collision processes that are not accompanied by fragmentation.<sup>36</sup> The amount of kinetic energy released during any fragmentation can be accurately measured from the peak width.<sup>37</sup>

The ZAB 2HF mass spectra reported in this thesis are CA MIKE spectra unless otherwise stated.

## 1.5 Linked $B^2/E$ Scanning

There are numerous linked scanning techniques<sup>38</sup> in which two or more of the fields in the mass spectrometer are varied simultaneously in a controlled manner depending on the type of information required. Arguably the most commonly utilised link scan of this type is that in which the ratio  $B/E$  of the magnetic field strength to the electric sector voltage is maintained constant while both are varied.<sup>39</sup> If the mass spectrometer is adjusted to transmit an ion  $M_1^-$ , by scanning down  $B$  and  $E$  while keeping the value of  $B/E$  fixed, a spectrum of all the daughter ions  $m_2^-$  formed from  $M_1^-$  in the first field free region will be obtained, often with better resolution than that obtained by a MIKE scan.

The  $B^2/E$  linked scan complements a  $B/E$  scan in that it yields a mass spectrum of all the parent ions of a selected daughter ion. The instrument is set such that  $m_2^-$  ions are collected under normal operating conditions,  $B$  and  $E$  are then scanned such that the ratio  $B^2/E$  remains constant. This scan identifies all precursor ions forming  $m_2^-$  ions: in this case,  $M_1^-$ .

## 1.6 Structural Identification of Ions

In order to identify mechanisms for the fragmentations (or unimolecular rearrangements) of organic anions it is crucial to determine the structures of the daughter ions formed. It can be quite difficult and challenging to uniquely identify the structures of the product ion species formed, since often product ions can, in principle, have several possible structures. Where a number of isomeric product anions have to be considered, thermochemical data including gas phase acidity, electron affinity and hydride affinity can be applied to determine the probability of such processes. Many fragmentation reaction processes of anions in the gas phase can be rationalised using the same “arrow-pushing” nomenclature adopted for solution chemistry. Methods that we have used for product anion identification using the ZAB 2HF include:-

1. Collisional activation mass spectra,
2. Charge reversal mass spectra, and
3. Peak widths of product anions formed in MIKE spectra.

Since mass spectra are often characteristic for an organic ion, the structures of daughter ions may be identified by comparison of their spectra with those of ions obtained from independently synthesised neutral precursors.

### 1.6.1 Collisional Activation (CA)

Parent anions produced from soft ionisation techniques such as CI are generally formed with low internal energies. As a consequence, the parent anion undergoes minimal fragmentation, thus limiting the amount of structural information obtained from the spectrum.

Accelerated ion species possess large amounts of translational energy (~7000 eV in the ZAB 2HF). When these accelerated ions collide with a neutral species, as much as 10 eV of energy may be transferred to the ion mainly as vibrational and rotational energy, but sometimes as electronic energy.<sup>40</sup> The excited ion then fragments to give a mass spectrum, often called collisional activated (CA) or collision induced dissociation (CID) spectrum.<sup>41</sup>

In the ZAB this is achieved by focussing the ion beam into a small collision cell containing an inert gas, typically helium or argon, generally at a pressure of  $\sim 10^{-6}$  torr (measured outside the collision cell). Such a pressure has been shown to produce (on average) a single collision between a given ion and the inert gas.<sup>42</sup>

This CA spectrum often provides information concerning the structure of the product ion.

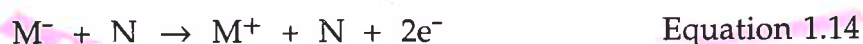
### 1.6.2 Charge Reversal (CR) MIKE Scanning

A useful method for the generation of decomposing positive ions from non-decomposing negative ions is the collisionally induced charge reversal technique first reported for organic anions in 1975 by Bowie and Blumenthal.<sup>43</sup>

In 1973 Beynon and Cooks <sup>37</sup>*et al.*<sup>44</sup> reported that positive ions ( $M^+$ ) may be converted to the corresponding anion ( $M^-$ ) if subjected to collisional activation with a suitable target gas (N) at high pressure (equation 1.13).



Bowie and Blumenthal demonstrated that source formed anions accelerated into a collision cell would undergo collisions with a suitable target gas atom which literally strips the anion of two electrons to form the decomposing cation (Equation 1.14).



The parent ions  $M^+$  that are formed within  $10^{-12}$  seconds of the collision process are generally unstable and are either not observed or detected in low abundance. The decomposing forms of  $M^+$  fragment in less than  $10^{-8}$  of a second and the intense daughter ions are resolved by MIKE scanning.

The CR MIKE process affords additional information concerning the structure of the anion  $M^-$ . In addition, this CR spectrum may be compared with those of anions of known structures in order to identify the initial anion species. The CR technique has also been used to generate cations in cases where such ions cannot be formed by conventional methods.<sup>44</sup> A typical CR spectrum is shown in Figure 1.5.

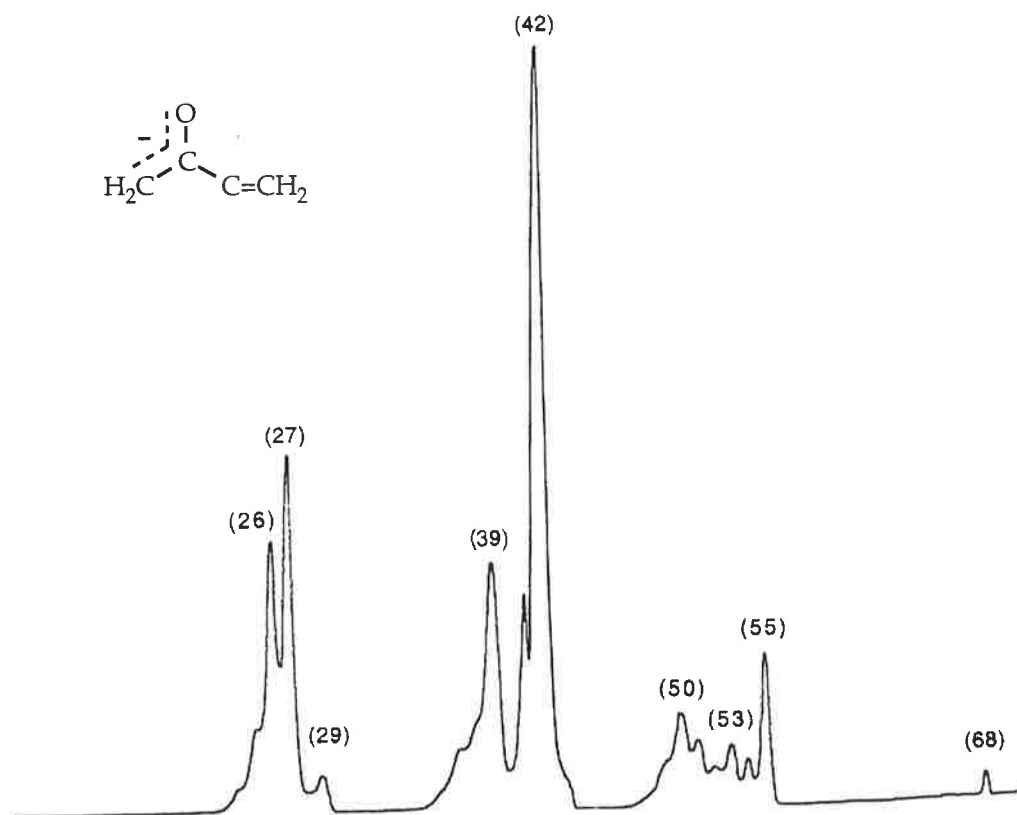


Figure 1.5. CR MIKE spectrum of the  $(M-H)^-$  ion of methyl vinyl ketone, using a collision pressure of  $10^{-5.5}$  torr using  $O_2$  collision gas. Peaks are shown with the  $m/z$  value in brackets. Note that there is no observed parent ion recovery signal at  $m/z$  69 (VG ZAB 2HF mass spectrometer).

### 1.6.3 Kinetic Energy Release (Peak Profiles)

There are distinct advantages in studying the mechanisms of ion reactions in the gas phase. Not only are the solvent and counter ion effects observed in solution avoided, but also the kinetic energy release associated with a reaction can be easily and accurately obtained. In solution experiments collisions lead to rapid interconversions of the internal energy of the system among the various rotational, vibrational and translational modes that are available. A Maxwell-Boltzman energy distribution is set up, and any energy released

during the course of the reaction is quickly absorbed into this common energy pool. Therefore the kinetic energy release associated with a reaction cannot be distinguished from that component which goes into the internal energy of the products.<sup>45</sup>

In the gas phase, any kinetic energy release accompanying dissociation is evidenced by a broadening of the peak profile, providing a distinct peak shape for the process concerned.

Ions  $M_1^-$  admitted into the 2nd field free region of the ZAB 2HF instrument will contain a range of energies below that required for fragmentation (ions containing excess energy will have decomposed earlier). As these  $M_1^-$  ions are activated in the collision cell they gain internal energy,<sup>46</sup> consequently decomposing to  $m_2^-$  (denoted by black circles) and  $m_3$  (denoted by the white circles) (Fig. 1.6).

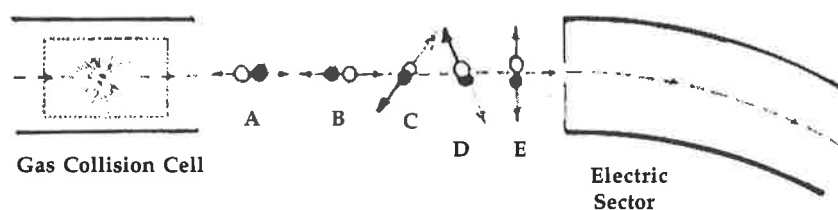


Figure 1.6. Different orientations of (field free) ion decompositions leading to kinetic energy release.

In the absence of repulsion between the neutral and the fragment ion, a relatively slow separation occurs and the molecules drift apart resulting in a narrow gaussian shaped peak (Fig. 1.7a), common for endothermic processes. If, however,  $m_2^-$  and  $m_3$  repel one another, there will be a discrete kinetic

energy release accompanying the dissociation giving the ion and neutral equal and opposite momenta. Decompositions arising from process A (Fig. 1.6) give rise to fragment ions with slightly more momentum than that observed in the absence of kinetic energy release, as ions A are pushed along the beam. Consequently, the ions are deflected slightly less readily in the electric sector and appear at an  $m/z$  value slightly higher than that expected (Fig. 1.7b). Conversely, decompositions arising from orientation B give rise to fragment ions with slightly less momentum because these ions are pushed back along the beam. As a result, they are deflected somewhat more readily by the electric sector and are displaced at an  $m/z$  value marginally lower than that expected (Fig. 1.7b).

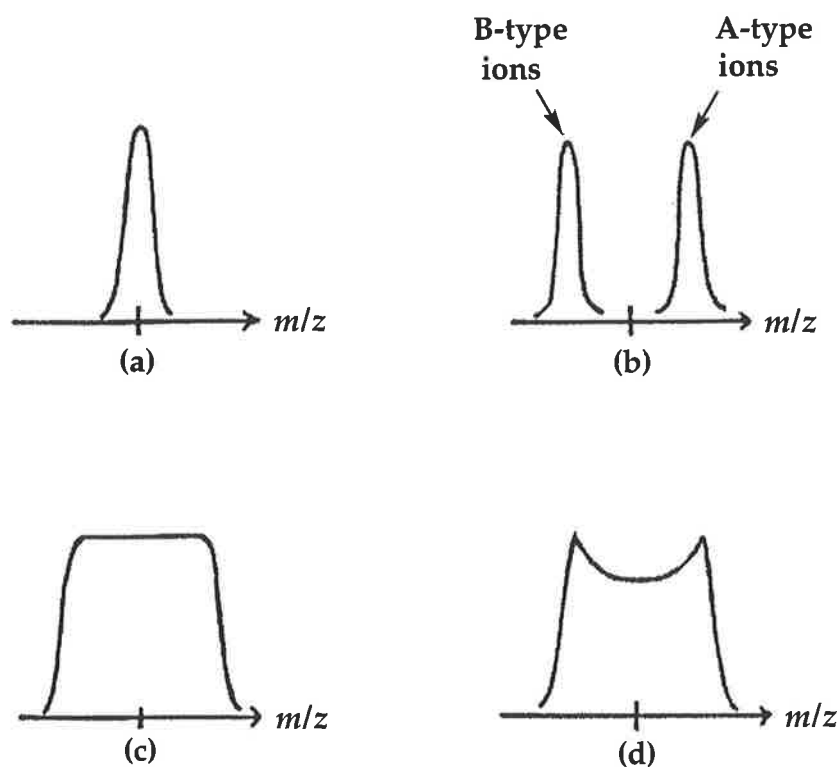


Figure 1.7. Metastable peaks observed due to different extremes of kinetic energy release.

Dissociations from C, D and E (Fig. 1.6) also occur giving rise to what is known as an exploding sphere of ions. The size of the sphere is determined by the amount of energy released.<sup>45</sup> As the magnitude of the kinetic energy release is increased the peak shape changes from a narrow gaussian shaped peak to a broad gaussian peak, then to a flat topped peak (Fig. 1.7c) at intermediate energies and then to a dish shaped peak (Fig. 1.7d) when the kinetic energy release is large.

Occasionally the peak shape is not simply gaussian, flat topped or dish shaped. A composite peak (for example a gaussian peak superimposed on a dish shaped peak) may indicate that two competing processes are occurring. The most plausible explanation for this observation is that either two fragment ions are generated, and/or the daughter ion is formed by two different mechanisms, each of which is characterised by a different kinetic energy release.<sup>47</sup>

In this thesis, recorded kinetic energy release values correspond to the width of the peak at half height. It has been shown<sup>48</sup> for a peak of exactly gaussian shape that the kinetic energy release at half height stands in a fixed relationship to the average kinetic energy released.<sup>49</sup>

## 1.7 Theoretical *Ab Initio* Molecular Orbital Calculations

Computational chemistry simulates chemical structures and reactions, based on the fundamental laws of physics. It allows chemists to study chemical phenomena by running calculations on computers as well as examining the reactions experimentally. There are different computational procedures, some methods can be used to model not only stable molecules, but also short lived intermediates and transition states. In this way calculations can provide information which is often difficult to obtain by experimental observations



alone. Computational chemistry is therefore a vital adjunct to the experimental studies in this thesis.

There are two broad areas within computational chemistry devoted to the structure of molecules and their reactivity: molecular mechanics and electronic structure theory, both of which perform the same basic types of calculations. Molecular mechanics calculations do not explicitly treat the electrons in a molecular system. Instead, they perform computations based upon the interactions among the nuclei. For this reason, molecular mechanics calculations are computationally less intensive and therefore employed in large systems containing large numbers of atoms. There are, limitations however; neglect of electrons means that such methods cannot treat chemical problems where electronic effects predominate, i.e.; they should not be used to describe processes which involve bond breakage or formation.

Electronic structure methods are based on the laws of quantum mechanics, which relates molecular properties to the motion and interactions of electrons and nuclei. It involves solving the Schrödinger differential equation (equation 1.15)<sup>50</sup> which allows for the direct quantitative prediction of the energy and many other properties of a stationary state of a chemical species.

$$H\Psi = E\Psi$$

Equation 1.15

*Ab initio* methods compute solutions to the Schrödinger equation using a series of rigorous mathematical approximations, providing high quality quantitative predictions for a broad range of systems.

By utilising these calculations, the experimental chemist can obtain a more detailed insight into reaction mechanisms, which in turn provides the initial knowledge of whether certain species are stable enough to be experimentally investigated.

The *ab initio* calculations reported in this thesis were obtained using the Gaussian 94 software package<sup>51</sup> which consists of algorithms that allow for the optimisation of the molecular potential energy by varying the molecular geometry of the species of interest. These geometry optimisation calculations can predict equilibrium geometries of molecules to within experimental error when calculated at high levels of theory. Geometry optimisations converge to a structure on the potential energy surface where the forces on the system are essentially zero. The final structure may correspond to a minimum on the potential energy surface, or it may represent a saddle point, which is a minimum with respect to some directions on the surface and a maximum in one or more others (Fig. 1.8).

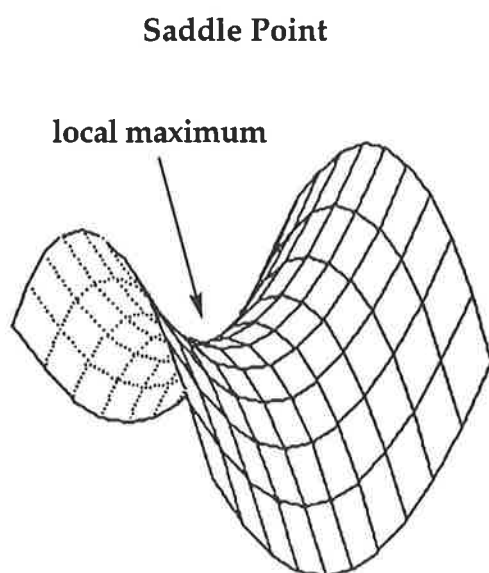


Figure 1.8. Saddle-shaped Energy Surface in the region of a Transition State.

At both minima and saddle points, the first derivative of the energy is zero. At such a point the forces are also zero since the gradient is the negative of the forces, and such a point on the potential energy surface is called a stationary point. All successful optimisations locate a stationary point of some description.

*Ab initio* molecular orbital theory calculates vibrational frequencies and normal modes of vibration belonging to any stable molecule, reactive intermediate or transition state. This type of frequency calculation can serve a number of different purposes such as: predict the IR and RAMAN spectra of molecules, compute force constants for a geometry optimisation, compute zero-point vibrational energy corrections to total energies and (most importantly for this work) the characterisation of a nuclear geometry as either a local minimum or a transition state. Local minima possess all real vibrational frequencies, whereas a transition state is characterised by having only one imaginary frequency.

A final theoretical tool used in this thesis is the Intrinsic Reaction Coordinate (IRC) calculation<sup>52</sup> which serve to identify the correct transition state. It examines the reaction path leading down from a transition structure on a potential energy surface, starting at the saddle point it traces the path in both directions from the transition state. This optimises the geometry of the molecular system at each point along the path. In this way, an IRC calculation definitively connects two minima on the potential energy surface by a path which passes through the transition state between them. An IRC characterises the local minima (reactants and products) that a particular transition state links. It also predicts the minimum energy reaction coordinate that a molecular system follows as it undergoes a reaction.

Thus, through the potential energies of equilibrium structures and transition states, *ab initio* molecular orbital theory allows for the accurate calculation of

reaction barriers, and through frequency calculation data. reaction probabilities \*

*Ab initio* techniques solve the electronic wavefunction only approximately. There exists a diverse range of theoretical implementations of varying sophistication and computational expense to address this problem. The Gaussian program contains a hierarchy of procedures corresponding to different approximation methods (levels of theory). The lowest (simplest) level used is Hartree-Fock (HF) theory. HF theory is very useful for providing initial, first level predictions for many systems. It is also reasonably good at computing the structures and vibrational frequencies of stable molecules and some transition states. As such, it is a good base level theory. This technique, however, suffers from its lack of accounting for a phenomenon known as electron correlation. Stated simply, HF theory treats the motion of an electron as if it moves in an average field of stationary electrons. In reality, the motion between electrons is correlated, that is, they move to keep out of each others way. These limitations result in HF energies which are higher than the exact values, The difference being the correlation energy (equation 1.16).

$$E(\text{exact}) = E(\text{HF}) + E(\text{correlation}) \quad \text{Equation 1.16}$$

Another approach to electron correlation is Moller-Plesset (MP) perturbation theory. Qualitatively, MP perturbation theory adds higher excitation to HF theory as a non-iterative correction, drawing upon techniques from the area of mathematical physics known as *many body perturbation* theory. The order that the perturbations are truncated at, is defined in the MP name: MP2 includes one perturbation correction to the HF energy. The MP2 method is

\* See appendix (after appendix G, p 227)

one of the least computationally expensive ways to improve on HF theory. It can successfully model a wide variety of systems, and MP2 geometries are usually quite accurate, and as such, the calculations in this thesis, for relatively large systems, are carried out firstly using HF theory and then corrected at the MP2 level of theory.

The next approximation involves expressing the molecular orbitals as linear combinations of a pre-defined set of one-electron functions known as basis functions. These basis functions are usually centred on the atomic nuclei and so bear some resemblance to atomic orbitals.

A basis set is a mathematical description of the molecular orbitals within a molecule.<sup>53</sup> It can be interpreted as restricting each electron to a particular region of space. Larger basis sets more accurately approximate exact molecular orbitals by imposing fewer restrictions on the locations of the electrons in space, thus making them more flexible. Larger basis sets, however, require correspondingly more computational resources and thus can become expensive in that they use significant amounts of super-computer time.

Standard basis sets for electronic structure calculations use linear combinations of gaussian functions to form orbitals.<sup>53</sup> Gaussian offers a wide range of pre-defined basis sets, which may be classified by the number and types of basis functions that they contain. Basis sets assign a group of basis functions to each atom within a molecule to approximate the orbital of the atom. The smallest basis set would be the minimal basis set which contain the minimum number of basis functions needed to accommodate each atom, for example:

H: 1s

C: 1s, 2s, 2p<sub>x</sub>, 2p<sub>y</sub>, 2p<sub>z</sub>

Increasing the number of basis functions per atom is the first way of increasing a basis set. Split valence basis sets such as 3-21G and 6-31G, have more than one size of basis function for each valence orbital. i.e.

H: 1s, 1s'

C: 1s, 2s, 2s', 2p<sub>x</sub>, 2p<sub>y</sub>, 2p<sub>z</sub>, 2p<sub>x</sub>', 2p<sub>y</sub>', 2p<sub>z</sub>'

where primed and unprimed orbitals differ in size. Split valence basis sets allow orbitals to change size but not to change shape. Polarised basis sets, however, remove this limitation by adding orbitals with angular momentum beyond what is required for the ground state to the description of each atom, for example, the 6-31G(d) basis set adds d functions to the carbon atoms.

Basis sets with diffuse functions are important for systems where electrons are relatively far from the nucleus such as the case for anions, lone pairs and other systems with significant electron density. Diffuse functions are large size versions of s- and p-type functions. They allow orbitals to occupy a larger region of space. The 6-31+G(d) basis set is the 6-31G(d) basis set with diffuse functions added to heavy atoms.

Choosing a model chemistry involves a trade off between accuracy and computational time and cost. The more accurate methods and the longer basis sets, not surprisingly, make jobs run longer and cost more in computational time. The basis set 6-31+G(d) has been chosen for the calculations reported in this thesis.

The level of theory used is indicated by the correlation technique and the basis set. For example, HF/6-31+G(d) denotes the use of Hartree-Fock theory in combination with the 6-31+G(d) basis set. Each such unique pairing of method with basis set represents a different approximation to the Schrödinger equation. *Ab initio* results from different chemical systems should only be

compared when they have been determined *via* the same unique combination i.e. at the same level of theory).

## 1.8 Negative Ion Fragmentations

The fragmentations of even electron (closed shell) negative ions of organic compounds have been reviewed.<sup>1,12</sup> It has been proposed that fragmentations can be rationalised in terms of a number of 'rules' classified as follows:-

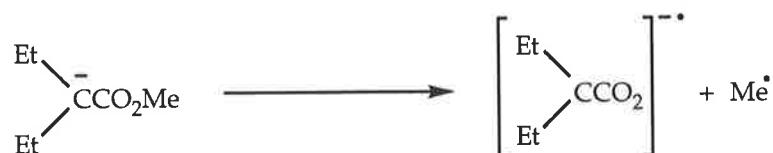
### 1.8.1 Simple Homolytic Cleavage

Most (M-H)<sup>-</sup> species lose a hydrogen radical (H<sup>•</sup>) to some extent. However, in systems where formation of a stabilised radical anion (in many cases a distonic radical anion) can occur, the loss is more pronounced (scheme 1.1).<sup>54</sup> This stability can also be the driving force to the loss of higher alkyl radicals such as Me<sup>•</sup> (scheme 1.2).

Scheme 1.1



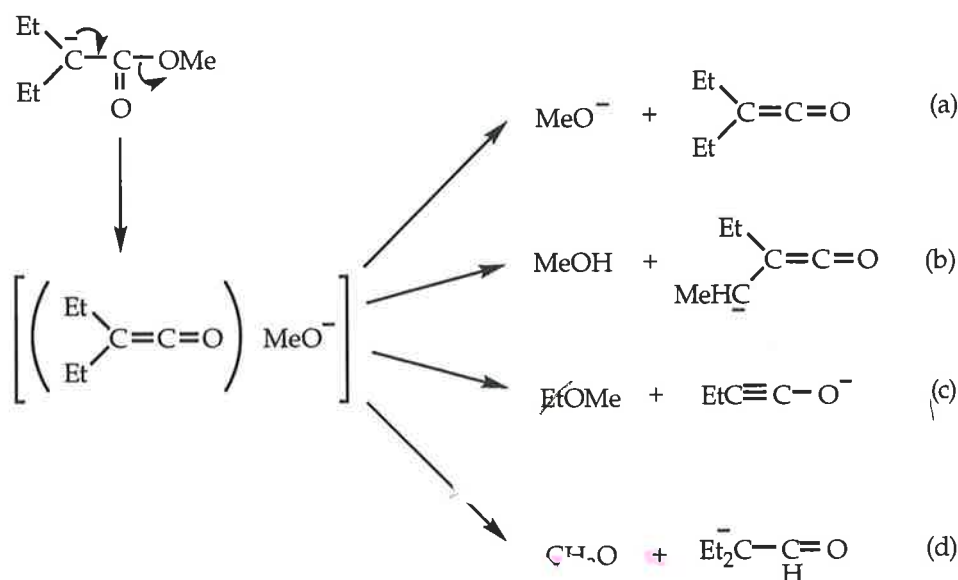
Scheme 1.2



### 1.8.2 Formation of an Ion-Neutral Complex

Ion-neutral complexes are formed when a heterolytic cleavage of a parent anion occurs to produce two species which are bound by ion-induced dipole interactions and hydrogen bonding. These complexes may decompose by displacing the anion (scheme 1.3a), or the anion may deprotonate the neutral portion of the complex prior to dissociation (scheme 1.3b). There are also examples of the bound anion effecting an S<sub>N</sub>2 displacement (scheme 1.3c) as well as cases of hydride transfer from the ion to the neutral (scheme 1.3d).<sup>55</sup>

Scheme 1.3



### 1.8.3 Proton Transfer or Rearrangement Preceding Fragmentation

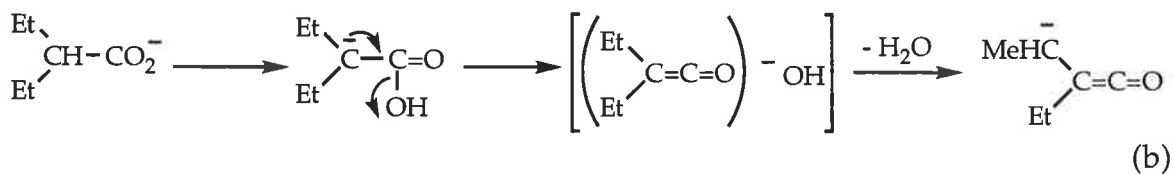
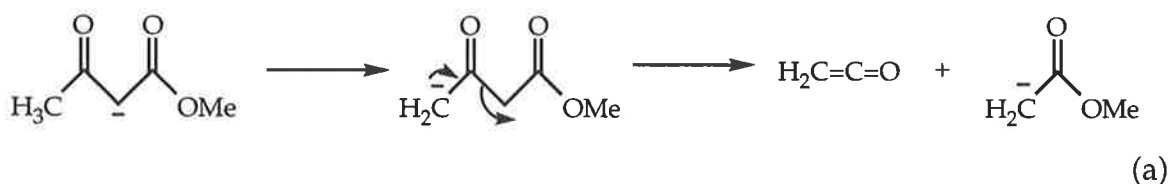
In some cases fragmentation of the initial deprotonated anion is unfavourable. In these cases; (a) proton transfer may produce a different anion, which may then fragment or (b) a skeletal rearrangement may precede fragmentation.



### (a) Proton Transfer Preceding Fragmentation

Proton transfer may occur when an additional site is present in the anion with similar acidity to that where initial deprotonation was effected<sup>56</sup> (scheme 1.4a). Alternatively, if simple fragmentation does not occur readily from a particular (M-H)<sup>-</sup> species proton transfer may be effected (by collisional activation) to produce a different anion which may then fragment (scheme 1.4b).<sup>54</sup>

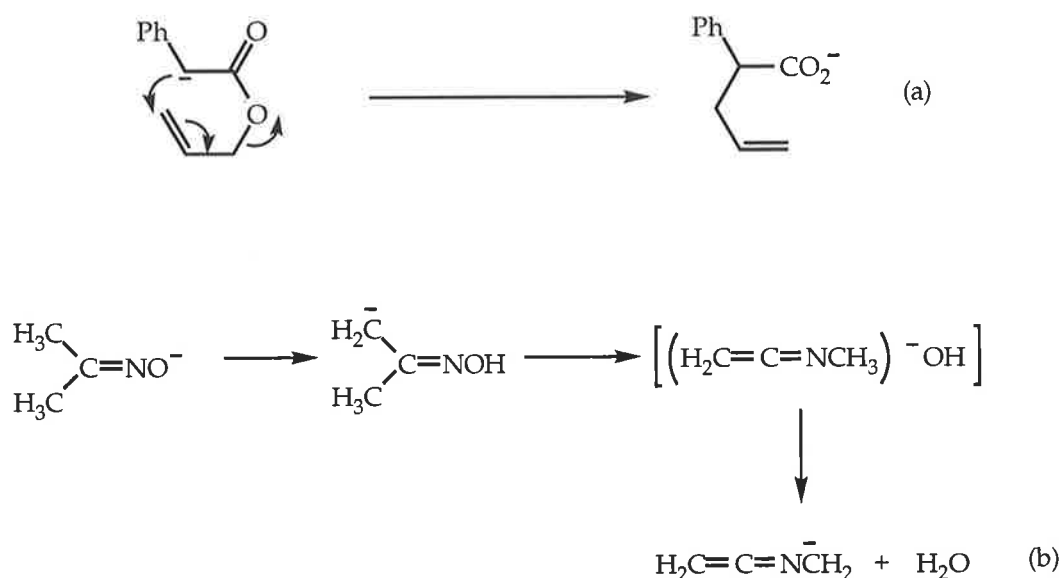
Scheme 1.4



### (b) Rearrangement Preceding Fragmentation

If simple cleavage is unfavourable, rearrangement of the anion may produce a different anion which may then fragment. For example, (i) the Claisen ester enolate rearrangement<sup>57</sup> (scheme 1.5a) and (ii) the negative ion Beckmann rearrangement<sup>58</sup> (scheme 1.5b).

Scheme 1.5



#### 1.8.4 Remote Fragmentations

All decompositions of  $(M-H)^-$  ions previously described have been charge mediated. That is they have been brought about by either direct interactions of the charged site or by the formation of a stable radical-anion species. There is, however, evidence to suggest that charge-remote fragmentations take place where bond cleavage reactions occur at a site physically removed from the locality of the charge.<sup>59,60</sup> One of the best examples of such behaviour is the loss of  $C_4H_{10}$  from the decanoate anion (scheme 1.6).<sup>60</sup> This process also occurs in the case of the nonenoate anion.<sup>61</sup>

Scheme 1.6



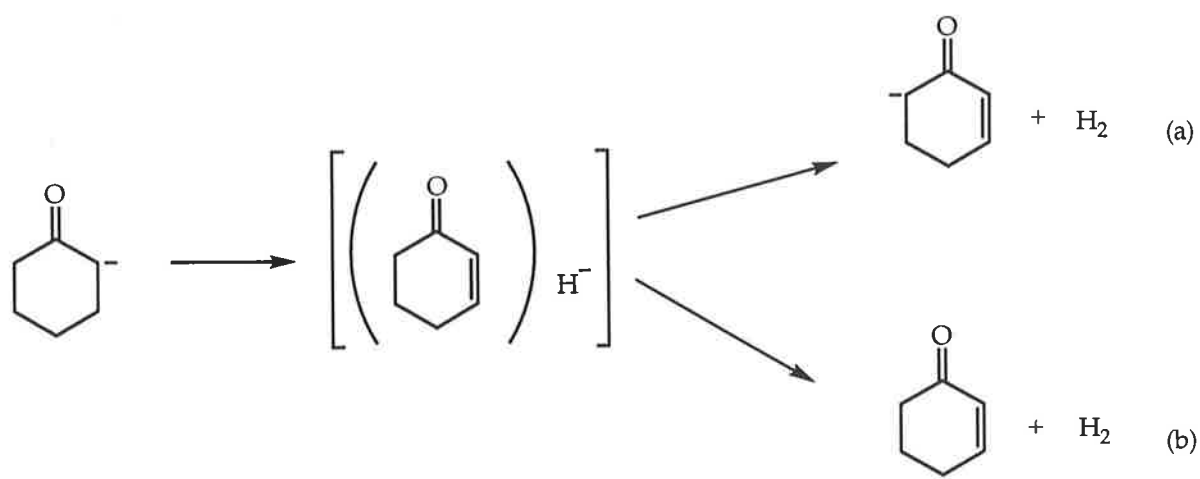
In some cases, the fragmenting and charged centres cannot approach closely because of the rigidity of the system.<sup>59,60</sup> In some cases it is not known whether these decompositions occur by high-energy processes uninfluenced by the charge centre, or by proton transfer to, or hydride ion transfer from the charged centre.<sup>62</sup> In other cases it has been demonstrated that charge remote fragmentations of anions may involve either radical or neutral loss.<sup>63</sup>

## 1.9 Migration of Anions

One of the interesting questions concerning anion reactions within ion-complexes, is how far the anion is free to move within that complex. There are examples where the anions are free to move within the complex and effect reactions at more than one centre: the classical example involves the loss of H<sub>2</sub> from the (M-H)<sup>-</sup> ion of cyclohexanone to yield the two products shown in schemes 1.7a and 1.7b.<sup>64</sup> This example seems to suggest the ability of the hydride anion to migrate within the anion-neutral complex, to deprotonate at both the  $\beta$  and 6 positions.

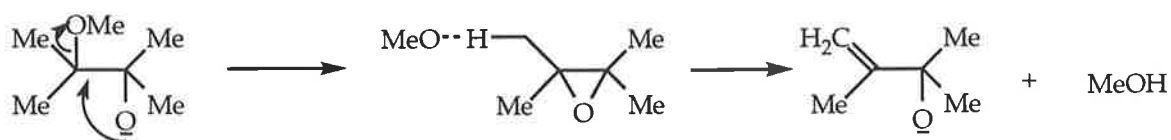
4

Scheme 1.7



In contrast, there are also examples where the incipient anion appears not to be mobile since it reacts solely at an adjacent position. For example, the loss of methanol from deprotonated  $\beta$ -methoxyhydrins occurs exclusively by deprotonation at the carbon directly adjacent to the site of methoxide loss<sup>65</sup> (scheme 1.8).

Scheme 1.8



These findings lead to one of the interesting questions concerning anion reactions within ion-neutral complexes: how far is the anion free to move within that complex? This question has been addressed for particular series of organic compounds in Chapters 2 and 3 of this thesis.

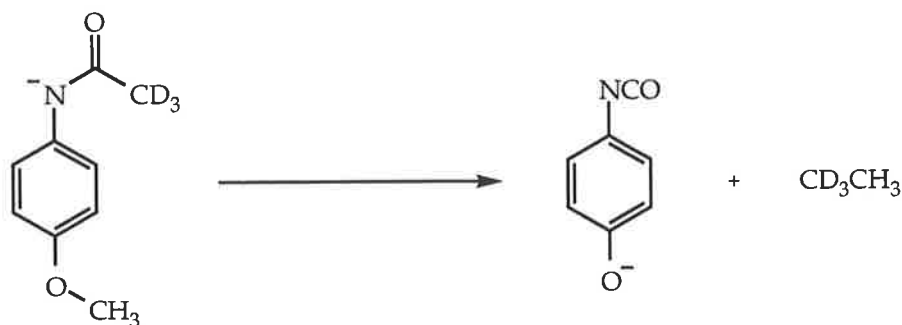
# Chapter 2

## Cross-Ring Phenyl Anion Initiated Reactions as Fragmentations of (M-H)<sup>-</sup> Species

### 2.1 Introduction

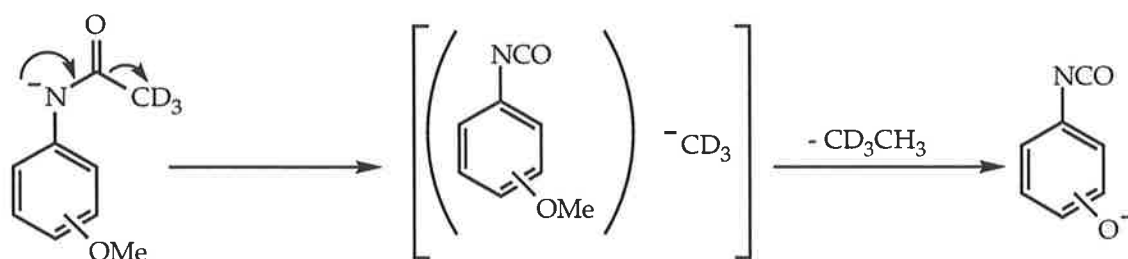
Blanksby *et al.* have reported an anionic migration where an incipient anion may move either around, or across an aromatic ring to induce an internal S<sub>N</sub>2 reaction.<sup>66</sup> The collision induced tandem mass spectra of the *ortho*-, *meta*-, and *para*- isomers of methoxyacetanilide anions each showed the loss of ethane, and furthermore, the *d*<sub>3</sub>-labelled isomer shown in scheme 2.1 incurred the loss of the elements of 'CD<sub>3</sub>CH<sub>3</sub>' from the parent anion.

Scheme 2.1



It was suggested that the reaction proceeds through an ion complex where the methyl anion is free to move across, or around the  $\pi$ -system of the neutral and perform an  $S_N2$  substitution on the methoxide moiety at any of the substitution positions on the aromatic ring (scheme 2.2).

Scheme 2.2



The mobility or otherwise of the anion within an anion/neutral complex is a topic of much interest.<sup>64,65,67,68</sup> We are interested in the structure of intermediate complexes formed during the decomposition of even-electron anions, and in the extent of the mobility of an anion within an anion/neutral complex. This unusual, and to date rare 'cross-ring' example provides a vehicle for the investigation of migratory aptitudes and reactive abilities of anions within anion/neutral complexes of this type. Such a system should allow the study of migratory abilities for a diverse series of organic anions, i.e. to determine the distance a migratory anion may travel across or around a  $\pi$ -system in order to effect such a reaction. It would also be of interest to investigate the types of 'cross-ring' reactions which can be induced by a mobile anion in suitable anion/neutral complexes. For the above reasons it was decided to pursue this matter further, and for the scope of this thesis, the migratory ability of the phenyl anion would be considered. In addition, we would focus on a series of possible reactions of the phenyl

anion in an anion/neutral complex analogous to that described in scheme 2.2, utilising methoxy, ethoxy and methylcarboxylate moieties as the reaction sites (Fig. 2.1).

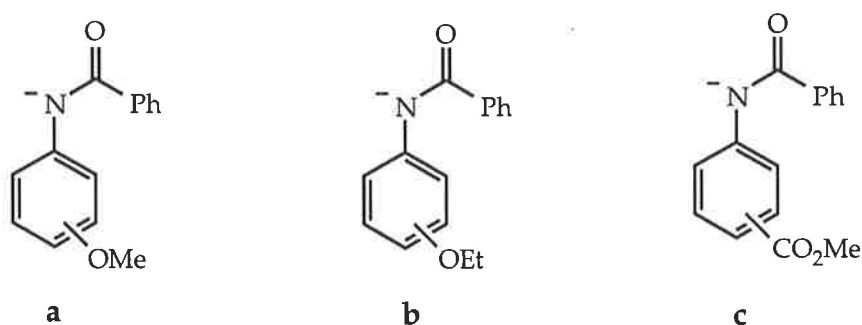


Figure 2.1. Methoxy (a), ethoxy (b) and methylcarboxylate (c) substituted phenyl benzamides to be investigated for possible phenyl anion 'cross-ring' reactions.

## 2.2 Results and Discussion

### 2.2.1 N-(Methoxyphenyl) benzamide Series

The collisionally activated MIKE spectrum of deprotonated N-(4-methoxyphenyl) benzamide is shown in Figure 2.2 and is typical for the three isomers studied (Table 2.1). In all three isomers the predominant fragmentation is the loss of a hydrogen radical (H<sup>•</sup>), however, all isomers also show a minor peak at  $m/z$  134. The formation of this daughter is consistent with that observed for the methoxy acetanilide system studied by Blanksby.<sup>66</sup>

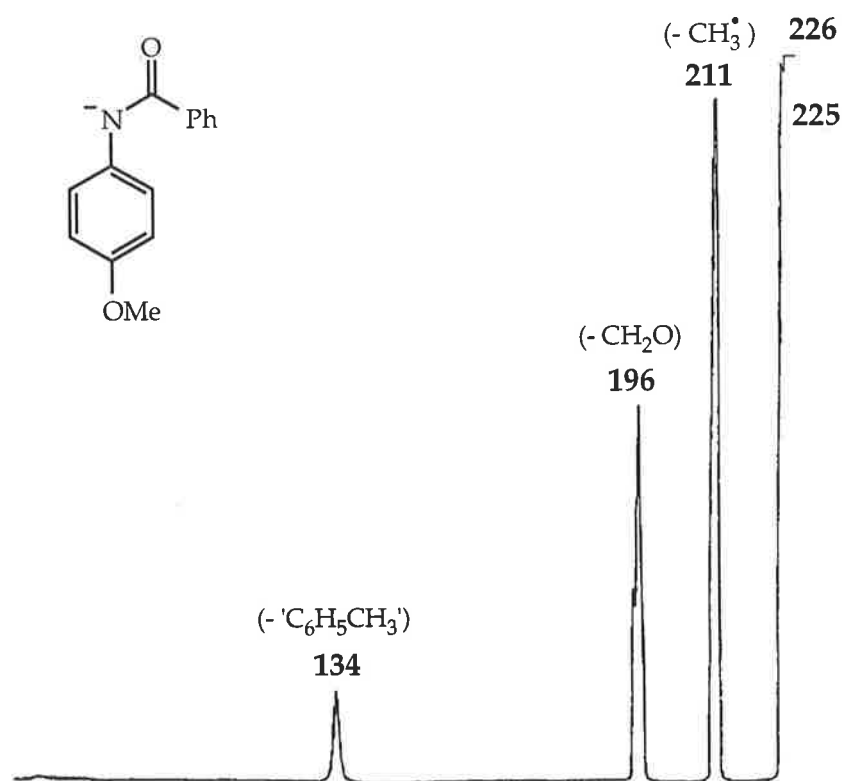


Figure 2.2. CA MIKE spectrum for deprotonated N-(4-methoxyphenyl) benzamide.

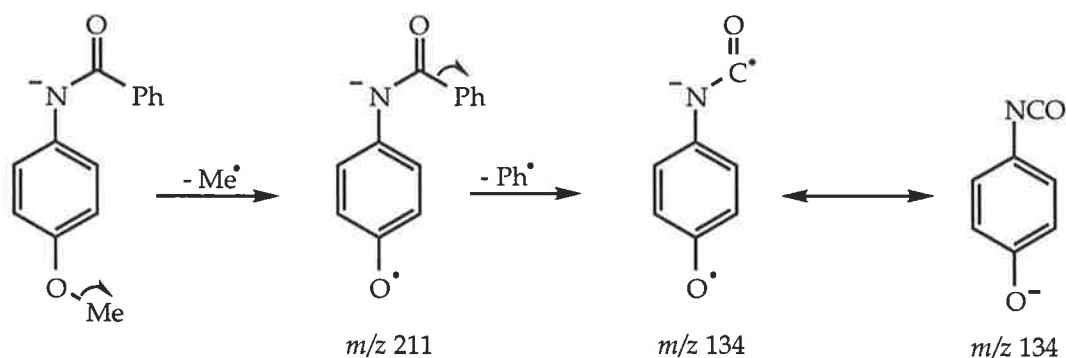
Table 2.1. CA MIKE data for deprotonated N-(methoxyphenyl) benzamide series.

Isomer	Loss					
	H <sup>•</sup>	H <sub>2</sub>	•CH <sub>3</sub>	CH <sub>2</sub> O	CH <sub>3</sub> OH	'C <sub>6</sub> H <sub>5</sub> CH <sub>3</sub> '
<i>ortho</i> -	100	2	8	0.3	3	1
<i>meta</i> -	100	2	6	3	-	8
<i>para</i> -	100	-	20	7	-	3

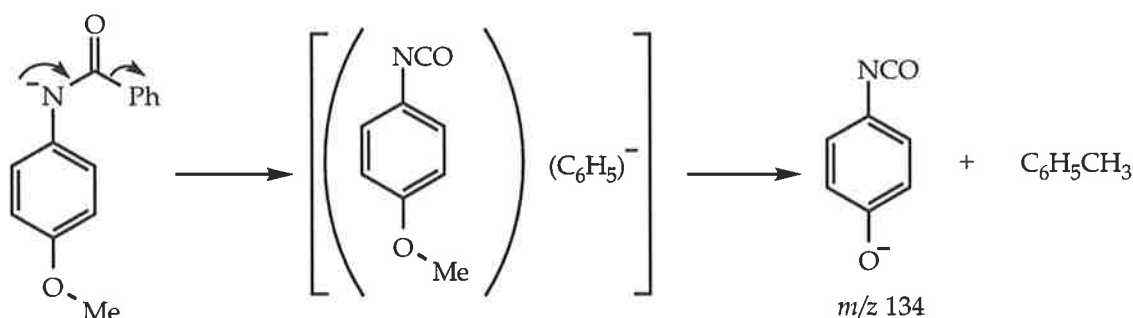


Other typical fragmentations observed for the isomers include some or all of the following: losses of  $\text{H}_2$ , methyl radical ( $\cdot\text{CH}_3$ ), formaldehyde ( $\text{CH}_2\text{O}$ ), and methanol ( $\text{CH}_3\text{OH}$ ) (Table 2.1). The peaks resulting from loss of  $\cdot\text{CH}_3$  are more pronounced than those arising from the loss of " $\text{C}_6\text{H}_5\text{CH}_3$ " in the spectra for both the *ortho*- and *para*- isomers, and the relative losses are almost 1:1 in the spectrum of the *meta*- isomer. The loss of " $\text{C}_6\text{H}_5\text{CH}_3$ " could occur by (i) sequential loss of  $\cdot\text{CH}_3$  followed by the loss of phenyl radical ( $\text{Ph}\cdot$ ) (scheme 2.3), or (ii) a one step process directly analogous to the mechanistic rationale proposed for the methoxy acetanilide (scheme 2.4, and *cf.* scheme 2.2).<sup>66</sup>

Scheme 2.3



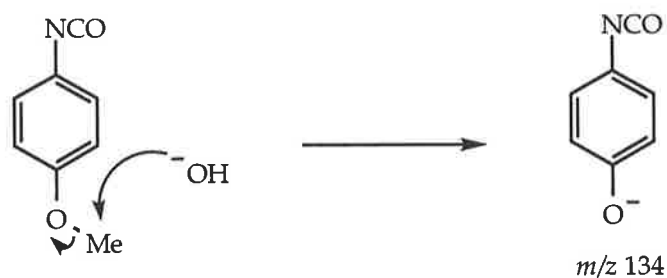
Scheme 2.4



### 'Long-range' $S_N2$ reactions of N-(methoxy phenyl) benzamide isomers

To attempt to show that a 'cross-ring' phenyl anion process is in operation it is first necessary to identify and confirm the structure of the observed  $m/z$  134 daughter ion, even though the same product ions should be formed irrespective of whether the process proceeds indirectly *via*  $m/z$  211 (scheme 2.3), or directly from the parent anion (scheme 2.4). The product ion  $m/z$  134 for each isomer was prepared in the ion-source of the VG ZAB 2HF mass spectrometer by the  $S_N2$  reaction between hydroxide ion and the appropriate isomer of methoxy phenylisocyanate (scheme 2.5).

Scheme 2.5



The characteristic CA MIKE spectrum for the  $m/z$  134 ion derived from *p*-methoxy phenylisocyanate was identical (within experimental error) to that of the source-formed  $m/z$  134 ion from N-(4-methoxy phenyl) benzamide (Table 2.2). The spectra of the analogous ions from the *ortho*- and *meta*-isomers of methoxy phenylisocyanate were also identical with the  $m/z$  134 ions from the corresponding parent ion and are similar to that of the *para*-isomer, with the only differences being in the abundances of the fragment peaks.

Table 2.2. Collisional activation MS/MS data for production of  $m/z$  134

Precursor ion	Spectrum [ $m/z$ (loss) relative abundance]
$m/z$ 134 from deprotonated $p$ -CH <sub>3</sub> O-C <sub>6</sub> H <sub>4</sub> -NHCOPh	133(H <sup>•</sup> )45, 106(CO)100, 78(2 × CO)38, 77(CO + <sup>•</sup> CHO)21
$m/z$ 134 from $p$ -CH <sub>3</sub> O-C <sub>6</sub> H <sub>4</sub> -NCO	133(H <sup>•</sup> )45, 106(CO)100, 78(2 × CO)40, 77(CO + <sup>•</sup> CHO)20

Confirmation of the product ion  $m/z$  134 indicates that the isocyanate species is formed in the source of the mass spectrometer. Pronounced peaks corresponding to  $m/z$  134, 211, and 226 are present in the beam of ions leaving the ion source for each isomer studied. If we are witnessing a 'cross-ring' migration of the phenyl anion displacing the methyl group *via* an S<sub>N</sub>2 type process, then  $m/z$  226 would be required as the immediate precursor ion, whereas a two step radical radical loss mechanism would require that the precursor ion be that of  $m/z$  211 since the first process would be loss of CH<sub>3</sub><sup>•</sup> followed by loss of Ph<sup>•</sup>. The stepwise process consisting of loss of the Ph<sup>•</sup> prior to loss of CH<sub>3</sub><sup>•</sup> is not considered a plausible process as evidenced by the lack of a peak at  $m/z$  149 produced by Ph<sup>•</sup> loss directly from the parent (M-H)<sup>-</sup> ion. To identify the operation of one or perhaps both of the processes outlined in schemes 2.3 and 2.4, linked scans at constant  $B^2/E$  were performed on  $m/z$  134 in order to identify the immediate precursor(s).

The results obtained from the  $B^2/E$  linked scans (Fig. 2.3) show peaks at both  $m/z$  211 and 225 indicating that  $m/z$  134 is the product of both stepwise radical losses (scheme 2.3), and the single step 'cross-ring' process (scheme 2.4). Furthermore, the competitive nature of these two processes may be observed by analysing the ratio of abundances of  $m/z$  225 and 211 from the linked  $B^2/E$  experiments and comparing the results for each studied isomer. The  $m/z$  134 ion is produced predominantly from the parent (M-H)<sup>-</sup> ion for

all isomers, however, formation of  $m/z$  134 from 211 is more pronounced for the *meta*- isomer, and the ratio of  $m/z$  225<sup>6</sup>:211 is further reduced in the  $B^2/E$  spectrum for the *para*- isomer. This is the expected trend since the  $S_N2$  process is more predominant when the two substituents are adjacent to each other as the phenyl anion has a shorter distance to traverse.

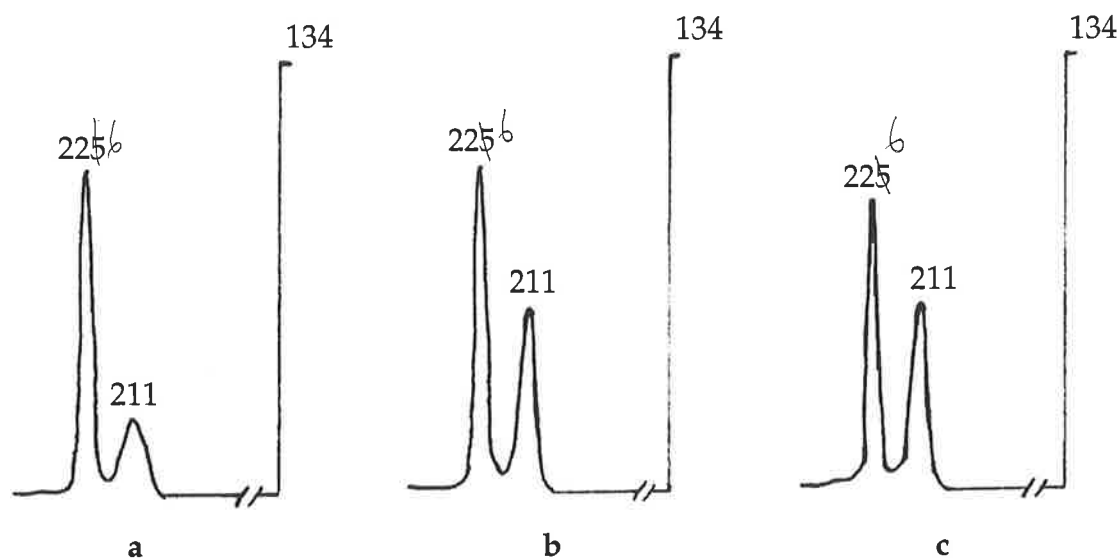


Figure 2.3. Linked scans at constant  $B^2/E$  showing the parent ions of  $m/z$  134 for deprotonated (a) *ortho*- , (b) *meta*- , and (c) *para*- N-(methoxyphenyl) benzamide.

The data appear to suggest that the  $m/z$  134 ion is formed, at least to some extent, directly from the parent species for each of the three studied isomers. This implies that: (i) an incipient phenyl anion may effect internal  $S_N2$  reactions in all three of these systems, and (ii) in the formation of the phenyl anion/neutral complex (scheme 2.4), at least for the scenario of the *meta*- and *para*- isomers, the anion must migrate either across and/or around the aromatic ring in order to interact with the methoxide function.

It has been shown that the unusual 'cross-ring' migration may occur for the phenyl anion, however, this is a minor process when compared with the other fragmentations (listed in Table 2.1) which are examined below.

#### Radical losses and unusual neutral losses for N-(Methoxy phenyl) benzamide isomers

The major processes observed in the spectra of this series of compounds involve radical losses resulting in the formation of stable radical anions (Table 2.1). The major fragmentation of these  $(M-H)^-$  ions involves loss of  $H^\cdot$  from the aromatic ring to produce the species shown in Figure 2.4a. A major fragmentation observed in the negative ion spectra of all of the N-(methoxy phenyl) benzamide isomers involves loss of  $CH_3^\cdot$  from the methoxy group to afford the radical anions shown in Figure 2.4b.

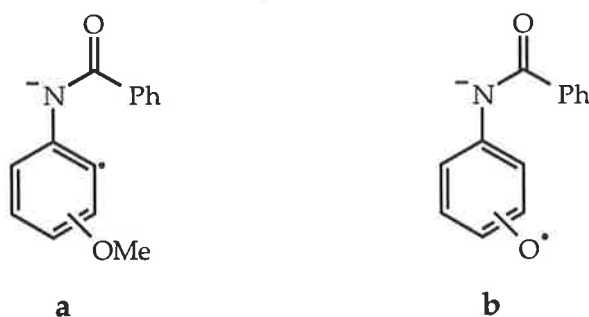


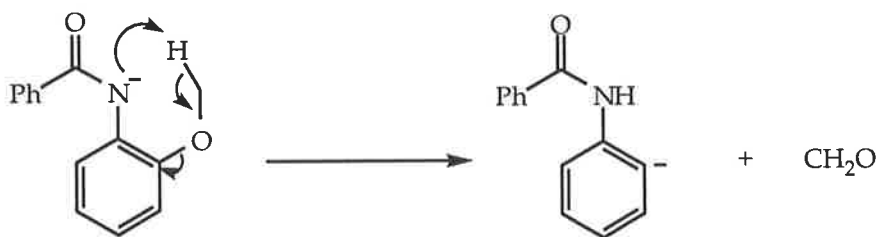
Figure 2.4 Stable radical anions formed from deprotonated N-(methoxy phenyl) benzamide isomers.

Loss of formaldehyde is also a characteristic process of the three isomeric anions. The loss of formaldehyde has been reported from anisole anions previously.<sup>69,70</sup> Deprotonated anisole undergoes partial ring *ortho*

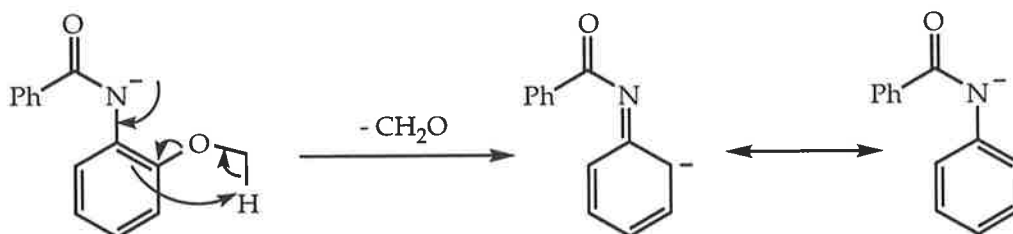
H/methyl H interchange, indicating that proton transfer from CH<sub>3</sub> to the anionic centre on the aromatic ring precedes or accompanies loss of CH<sub>2</sub>O. In the system we have studied, the charge is localised on the nitrogen atom, and this charge, at least initially, is remote from the fragmenting site. We suggest that the losses of CH<sub>2</sub>O from all isomers are initiated from anionic centres. Consider first the loss of formaldehyde from that of the *ortho*-isomer. This loss is minor compared to other fragmentations of the *ortho*-compound: for example, it is less pronounced than that forming *m/z* 134 (the 'cross-ring' product).

Two possible mechanisms are proposed for formaldehyde loss from the *ortho*- isomer, i.e. the transfer/elimination process shown in scheme 2.6, or the internal *ipso* proton transfer/elimination as described in scheme 2.7. We are unable to differentiate between these two processes on available evidence.

Scheme 2.6

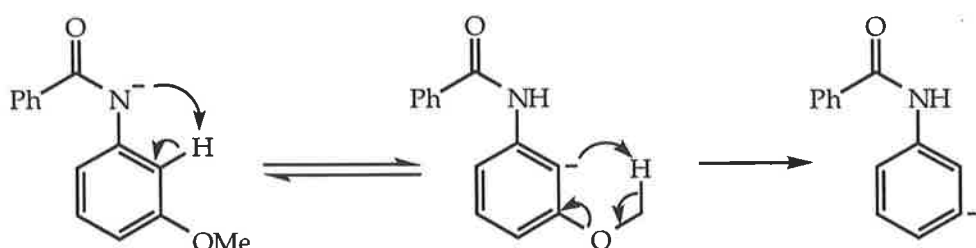


Scheme 2.7

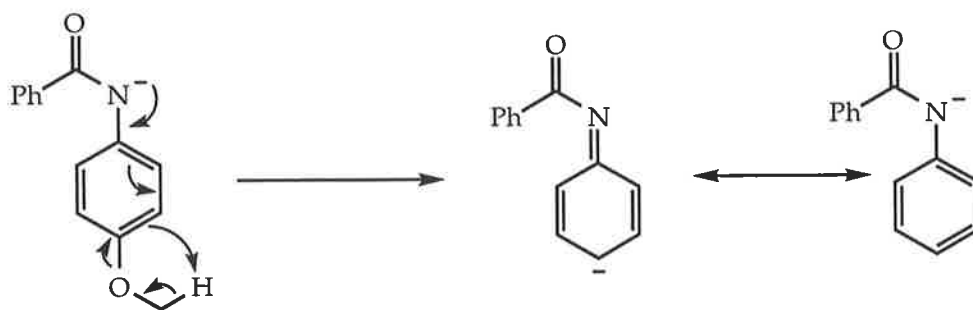


Loss of formaldehyde from the *meta*- isomer can be explained in terms of an initial *ortho* proton transfer from the ring to the nitrogen, followed by a proton transfer/elimination process as outlined in scheme 2.8. The formaldehyde loss from the *para*- isomer can also be explained in terms of an *ipso* process similar to that proposed for the *ortho*- compound (scheme 2.9).

Scheme 2.8



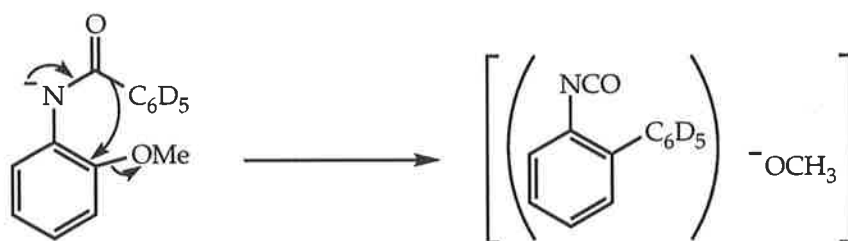
Scheme 2.9



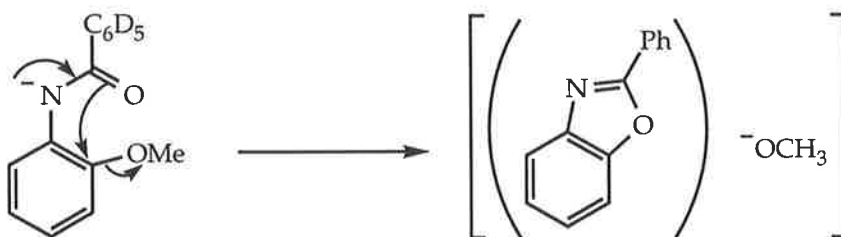
The loss of methanol occurs only for the *ortho*- isomer. This fragmentation is quite unusual. The CA MIKE spectrum for the  $d_5$ -labelled *ortho*- isomer is reproduced in Figure 2.5 and shows the losses of both  $\text{CH}_3\text{OH}$  and  $\text{CH}_3\text{OD}$  ( $m/z$  199 and 198 respectively). This spectrum shows that the extra

hydrogen originates from either aromatic ring. The ratio of methanol *vs* methanol-*d* loss may be due to a hydrogen/deuterium isotope effect. Two mechanistic proposals for methanol loss are shown in schemes 2.10 and 2.11. The first mechanism (scheme 2.10) is initiated by a phenyl anion, and results in the formation of a methoxide anion/neutral complex following an *ipso* nucleophilic substitution. In contrast the mechanism shown in scheme 2.11 involves liberation of a methoxide complex following *ipso* cyclisation *via* the carbonyl oxygen.

Scheme 2.10



Scheme 2.11





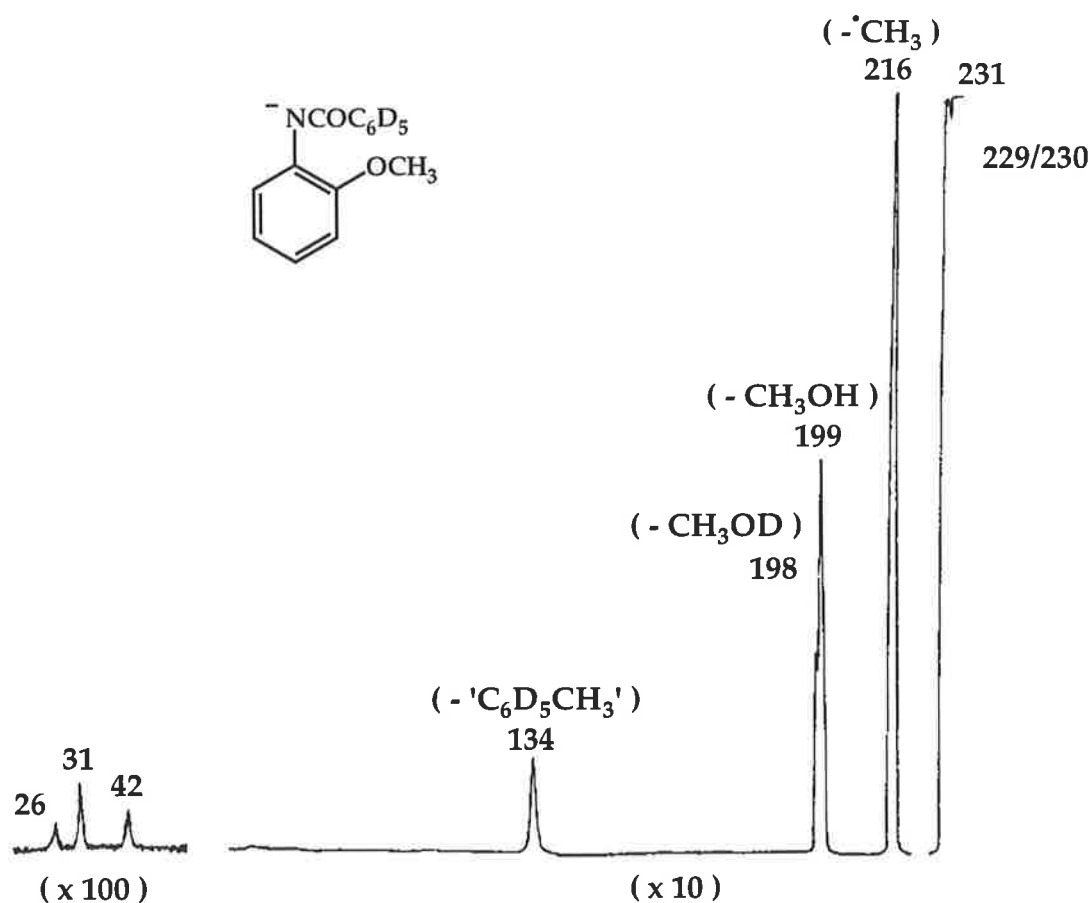


Figure 2.5. CA MS/MS data for  $o\text{-CH}_3\text{O-C}_6\text{H}_4\text{-NCOC}_6\text{D}_5$ .

Both proposed mechanisms allow for the methoxide anion in the ion/neutral complexes to both deprotonate or dedeuterate the formed neutral, resulting in product ions which for each process would be significantly different. Unfortunately the product ion  $m/z$  194 from the unlabelled  $(\text{M-H})^-$  ion was formed in low abundance in the ion-source of the ZAB 2HF, and as a consequence, the mass spectrum (both CA and CR) of  $m/z$  194 was too weak for a meaningful comparison of these spectra with those of deprotonated 2-phenylbenzisocyanate and 2-phenylbenzoxazole.

It has been reported<sup>66</sup> that loss of methanol also occurs for the (M-H)<sup>-</sup> ion of *o*-methoxybenzacetamide. Deuterium labelling experiments and product ion studies show this process to be analogous to that shown in scheme 2.11. Thus we favour the mechanism of scheme 2.11: i.e. loss of methanol from deprotonated N-(2-methoxyphenyl) benzamide affords deprotonated 2-phenylbenzoxazole as the product anion.

### 2.2.2 N-(Ethoxyphenyl) benzamide Series

The collisionally activated MIKE spectrum of deprotonated N-(4-ethoxyphenyl)-benzamide is shown in Figure 2.6. This spectrum is similar to those of the *ortho*- and *meta*- isomers (see Table 2.3).

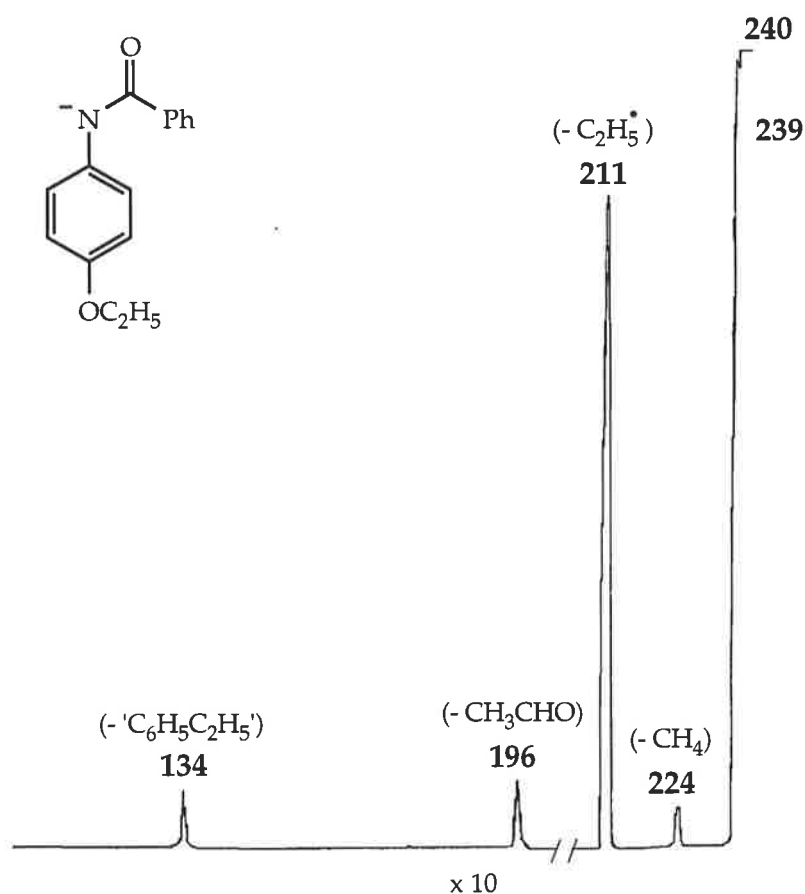


Figure 2.6. The CA MIKES spectrum of deprotonated N-(4-ethoxyphenyl) benzamide.

Table 2.3 CA MIKE data for deprotonated N-(ethoxyphenyl) benzamide isomers.

Isomer	Loss					
	H <sup>•</sup>	CH <sub>4</sub>	<sup>•</sup> C <sub>2</sub> H <sub>5</sub>	CH <sub>3</sub> CHO	C <sub>2</sub> H <sub>5</sub> OH	'C <sub>6</sub> H <sub>5</sub> C <sub>2</sub> H <sub>5</sub> '
<i>ortho</i> -	100	-	8	0.5	3	1
<i>meta</i> -	100	2	10	0.8	-	1
<i>para</i> -	100	7	40	4	-	2

The predominant fragmentations observed for all three isomers are the losses of H<sup>•</sup>, and Et<sup>•</sup> (which is directly analogous to the loss of Me<sup>•</sup> observed from anions of the N-(methoxyphenyl) benzamide series (Fig. 2.4)).

#### 'Long-range' reactions of N-(ethoxyphenyl) benzamide isomers

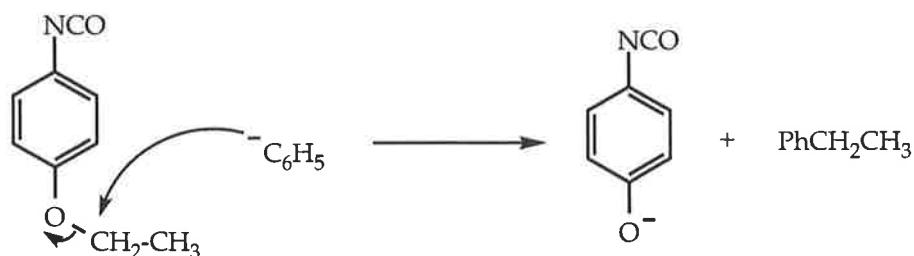
Apart from the major processes just described, all three spectra show peaks at  $m/z$  134. These three daughter ions were identified by product ion studies and shown to be *o*-, *m*-, or *p*- OCN-C<sub>6</sub>H<sub>4</sub>-O<sup>-</sup> from the corresponding parent (M-H)<sup>-</sup> ions (as previously described).

$B^2/E$  linked scans of source-formed  $m/z$  134 confirm that these ions are formed both directly from the parent (M-H)<sup>-</sup> ion and also by the stepwise sequence [(M-H)<sup>-</sup>-Et<sup>•</sup>-Ph<sup>•</sup>], exactly analogous processes as those observed for the corresponding N-(methoxyphenyl) benzamide isomers.

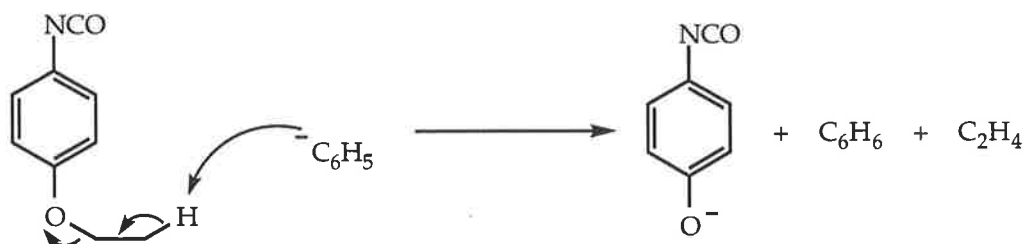
The product ion studies and the  $B^2/E$  linked scans indicate that the phenyl anion participates, at least in the case of the *meta*- and *para*- isomers, in some kind of 'long-range cross-ring' migration initiating some reaction at

the ethoxy substituent. There are two possible mechanisms for this interaction, i.e. the phenyl anion attacks the methylene carbon in an  $S_N2$  type process (scheme 2.12), or an elimination reaction occurs (scheme 2.13).

Scheme 2.12



Scheme 2.13



It has been shown, by a deuterium kinetic isotope study, that the analogous loss of the elements of  $\text{C}_3\text{H}_4$  from deprotonated  $p\text{-EtO-C}_6\text{H}_4\text{-NH-CO-CH}_3$  occur by stepwise loss of  $\text{CH}_4$  and  $\text{C}_2\text{H}_4$ .<sup>71</sup> By analogy, we propose the operation of the elimination process (scheme 2.13) in the system under study.

### 2.2.3 Methyl-Benzoylaminobenzoate Series

In summary, we have presented evidence to suggest that amide anions  $\text{Ar-N}^-\text{CO-Ph}$ , on collisional activation yield incipient  $\text{Ph}^-$  ions reacting within ion complexes  $[(\text{ArNCO})\text{Ph}]^-$ . The produced phenyl anion is able to effect 'long-range' reactions around or across the aromatic ring, for example,  $\text{S}_{\text{N}}2$  processes are observed from (a) and elimination reactions are observed from (b) (Fig. 2.7). These reactions are, however, minor in comparison to more facile radical losses to form stable radical anions, e.g. losses of  $\text{CH}_3^\cdot$  from (a) and  $\text{Et}^\cdot$  from (b) (Fig. 2.7).

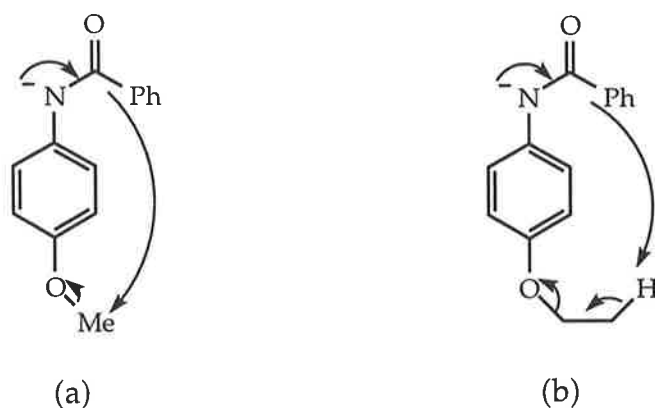
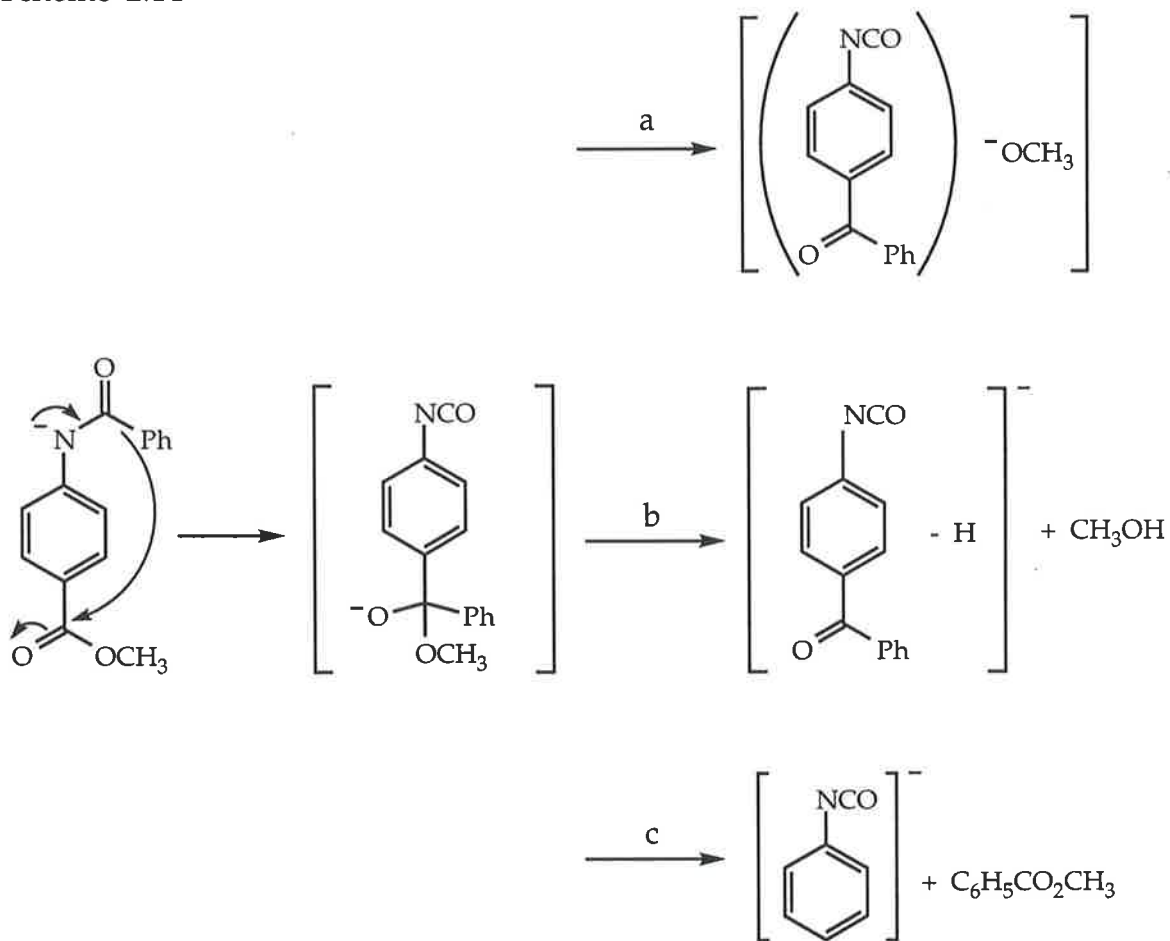


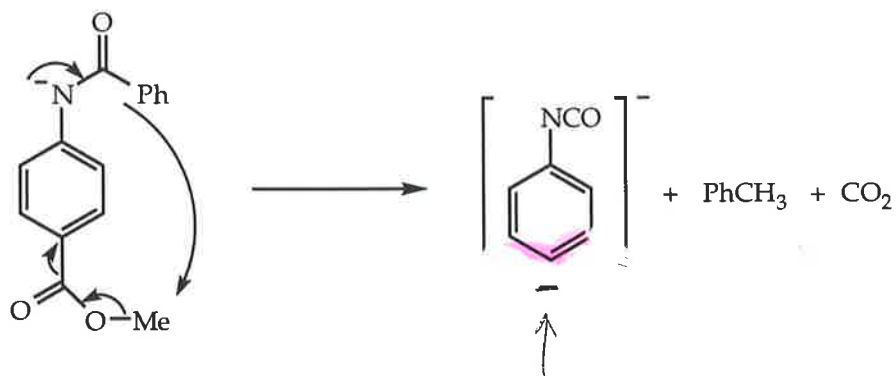
Figure 2.7. Phenyl anion initiated reactions observed for (a) deprotonated N-(4-methoxyphenyl) benzamide and (b) deprotonated N-(4-ethoxyphenyl) benzamide.

What 'cross-ring' reactions might take place if the ether functionality is replaced with a simple methyl ester? Perhaps phenyl anion attack at the carbonyl site would result in either direct formation of  $\text{CH}_3\text{O}^-$  (scheme 2.14a), loss of methanol resulting from deprotonation effected by the methoxy anion (2.14b), or the elimination of  $\text{C}_6\text{H}_5\text{CO}_2\text{CH}_3$  (2.14c). Alternatively, the phenyl anion might react *via* an  $\text{S}_{\text{N}}2$  process to effect loss of toluene and carbon dioxide (scheme 2.15).

Scheme 2.14



Scheme 2.15



The collisionally activated MIKE spectrum of deprotonated *para*-methylbenzoylaminobenzoate is shown in Figure 2.8: similar fragmentations are observed in the spectra of the *meta*- and *ortho*- analogues (see Table 2.4).

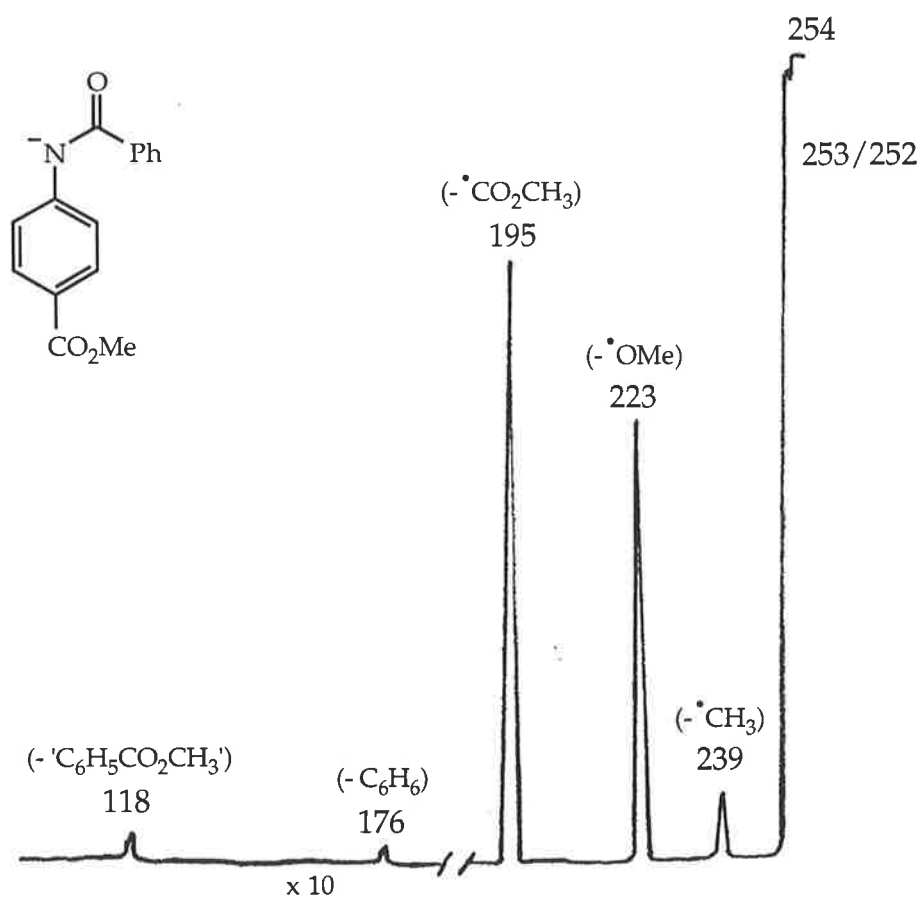


Figure 2.8. CA MIKES spectrum for deprotonated methyl 4-benzoylamino benzoate.

Table 2.4. Collisional activated MIKE data for methyl-benzoylamino benzoate series. *or formation*

Isomer	Spectrum [ $m/z$ (loss) relative abundance]
<i>ortho</i> -	253( $H^-$ )100, 252( $H_2$ )16, 239( $CH_3^-$ )33, 223( $CH_3O^-$ )2, 222( $CH_3OH$ )5, 195( $CO_2CH_3^-$ )5, 194( $HCO_2CH_3$ )2
<i>meta</i> -	253( $H^-$ )100, 252( $H_2$ )2, 239( $CH_3^-$ )1, 223( $CH_3O^-$ )2, 195( $CO_2CH_3^-$ )5
<i>para</i> -	253( $H^-$ )100, 252( $H_2$ )2, 239( $CH_3^-$ )2, 223( $CH_3O^-$ )5, 195( $CO_2CH_3^-$ )35, 176( $C_6H_6$ )1, 118( $C_6H_5CO_2CH_3^-$ )3

The major fragmentations observed for all isomers are the losses of radicals to afford stable radical anions. Losses of  $\text{H}^\bullet$ ,  $\text{CH}_3^\bullet$ ,  $\text{CH}_3\text{O}^\bullet$ , and  $\text{CH}_3\text{CO}_2^\bullet$  afford the radical anions represented in Figure 2.9.

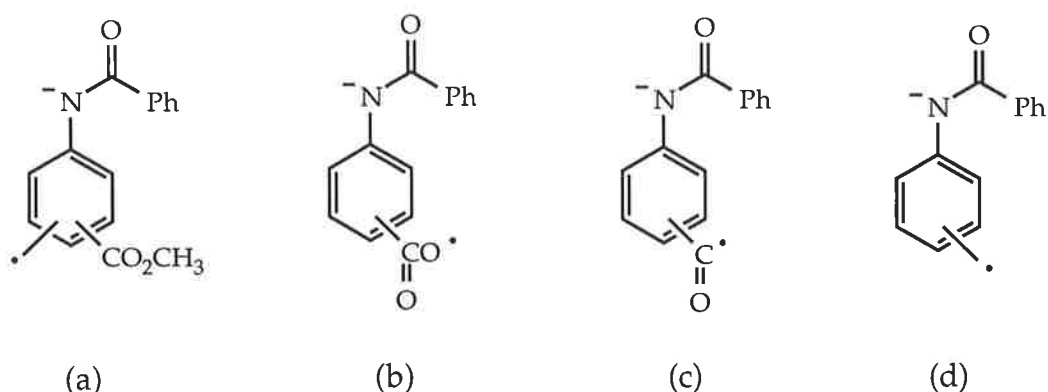
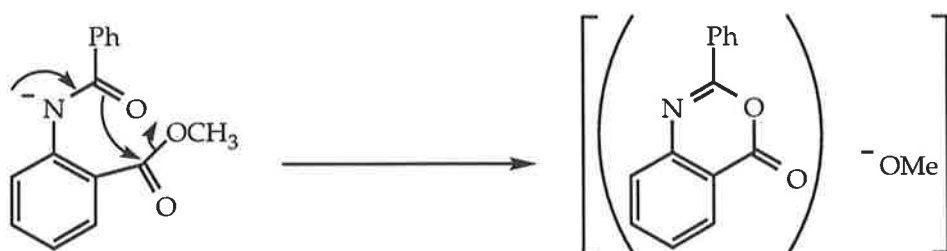


Figure 2.9. Radical anions resulting from loss of (a)  $\text{H}^\bullet$ , (b)  $\text{CH}_3^\bullet$ , (c)  $\text{CH}_3\text{O}^\bullet$ , and (d)  $\text{CH}_3\text{CO}_2^\bullet$  from methyl-benzoylaminobenzoate isomers.

The *meta*- isomer showed fragmentations occurring exclusively by the radical processes outlined above. The *ortho*- isomer, however, also loses methanol. This loss of methanol is analogous to a similar process already described, e.g. *ortho*-N-(methoxyphenyl)benzamide (scheme 2.11). Thus we suggest the formation of the ion complex shown in scheme 2.16.

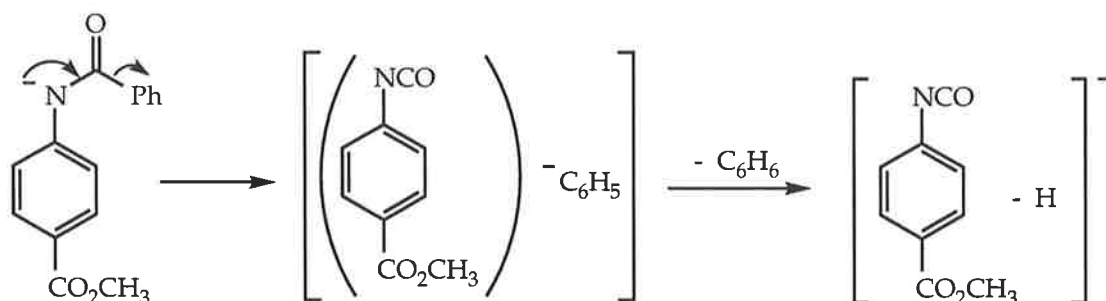
Scheme 2.16





The formation of daughter ions  $m/z$  176 and 118 in the spectrum of the *para*- isomer (Fig. 2.9) correspond to the losses of benzene and  $\text{C}_6\text{H}_5\text{CO}_2\text{CH}_3$  respectively. The loss of benzene indicates the formation of the phenyl anion/neutral complex shown in scheme 2.17, where the incipient phenyl anion deprotonates the aromatic ring.

Scheme 2.17



The ion  $m/z$  118 can only be formed by a 'cross-ring' migration reaction. It is not known whether  $m/z$  118 is formed by direct loss of  $\text{C}_6\text{H}_5\text{CO}_2\text{CH}_3$  (scheme 2.14c), or whether the mechanism involves the loss of toluene and carbon dioxide (scheme 2.15).

## 2.3 Summary, Conclusions and Future Work

It has been shown that the major collision-induced fragmentation processes of deprotonated phenyl-benzamides involve the loss of radicals to form stable radical anions.

The loss of  $\text{H}^\cdot$  from an aryl ring is the major process for all compounds concerned in this study, with the remaining radical losses being generated from the alkoxy or ester groups present on the aromatic ring. Competing

with these radical processes are specific *ortho* effects (loss of methanol and ethanol), and a number of reactions where the parent ions liberate a phenyl anion, which, through an ion/neutral complex is able to effect 'long-range cross-ring' reactions including deprotonation, S<sub>N</sub>2 displacement at -OCH<sub>3</sub> and elimination reactions at -OC<sub>2</sub>H<sub>5</sub> substituents. In each case, the phenyl anion migrates either around or across the aromatic ring to initiate the particular process at the appropriate functional group. This type of migration also occurs for the methyl anion.<sup>66,71,72</sup> \*

The question remains, however, as to whether this migrational behaviour is a function of aromaticity where the phenyl (or methyl) anion is free to move around the  $\pi$ -system or whether it is a through-space phenomenon. It would be interesting to extend this investigation to rigid aliphatic systems such as disubstituted adamantanes to establish whether such migrational behaviour would still be observed. The distance that the incipient anion is free to travel before such reactions cease to occur is also interesting and the investigations of extended aromatic systems such as disubstituted biphenyl compounds might prove to be interesting and provide insight towards this migrational distance.

\* See appendix p 277C

# Chapter 3

## Ion Mobility in Keto Substituted Alkoxide Anions

### 3.1 Introduction

Chapter 2 describes systems in which an incipient anion is free to migrate across, or around an aromatic ring in order to effect a reaction at a particular substituent. Both the methyl anion and phenyl anion react in this way.<sup>66,71,72</sup> However, to date, no such reactions have been observed with a hydride ion.

However, there are reactions where a hydride ion is mobile within the ion/neutral complex. For example, Raftery and Bowie<sup>64</sup> have observed by the aid of deuterium labelling studies, that deprotonated cyclohexanone undergoes two losses of H<sub>2</sub> as shown in scheme 1.7 (page 33).

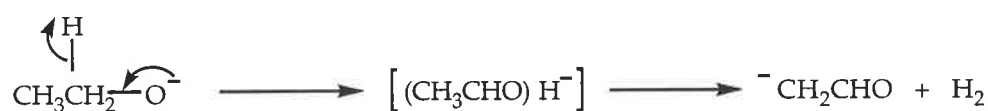
We extended the work on hydride mobility, to a system which will enable us to investigate the mobility of H<sup>-</sup> and the reactions, if any, that this anion might initiate.

The intramolecular reactions of gas phase alkoxide anions have generated interest for over more than 20 years. Collision-induced spectra for simple alkoxide anions are characteristic and informative. The analytical applicability of this technique for alkoxide anions can be illustrated for the example of PhCH(Me)O<sup>-</sup>, which undergoes competitive losses of H<sub>2</sub>, methane, acetaldehyde or benzene.<sup>73</sup> These processes are rationalised in

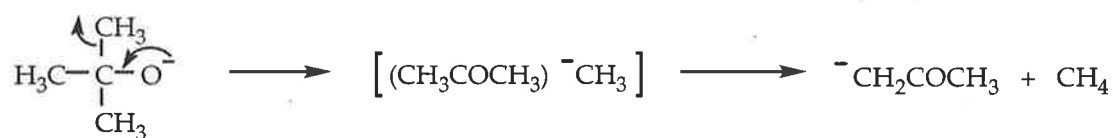
terms of the formation of ion/neutral complexes which fragment in a variety of ways.

The basic fragmentation of primary alkoxides involves the loss of H<sub>2</sub> and the mechanism for this process has been studied extensively both experimentally and theoretically. For example, Boand *et al.*<sup>74</sup> have recorded the collision induced mass spectra for a series of alkoxide ions and observed the characteristic elimination of H<sub>2</sub> from these activated anions. They deduced, with the aid of isotopic labelling, that specific 1,2 eliminations were responsible for this fragmentation. This conclusion is supported by the studies of Hayes *et al.*,<sup>75,76</sup> who also concluded, from *ab initio* calculations and a study of isotopic effects that this elimination process is stepwise, and for the case of the ethoxide ion, the key intermediate is a hydride ion solvated by acetaldehyde (scheme 3.1), whereas for *tert*-butoxide the intermediate is a methyl anion solvated by acetone (scheme 3.2). The conclusions that the elimination reactions are specifically 1,2 eliminations and that they occur in a stepwise fashion are in agreement with the conclusions reached by Tumas *et al.*<sup>77-80</sup> from a study of the infra-red multiphoton dissociation of an assortment of alkoxide ions. Noest and Nibbering<sup>81</sup> have investigated negative ion molecule reactions of aliphatic nitrites in an ion cyclotron resonance mass spectrometer. They report the facile formation of alkoxide ions from nitrites, and also observe loss of H<sub>2</sub> which they describe as occurring exclusively by a 1,2 elimination promoted by a collisionally induced decomposition of the alkoxide ions.

Scheme 3.1

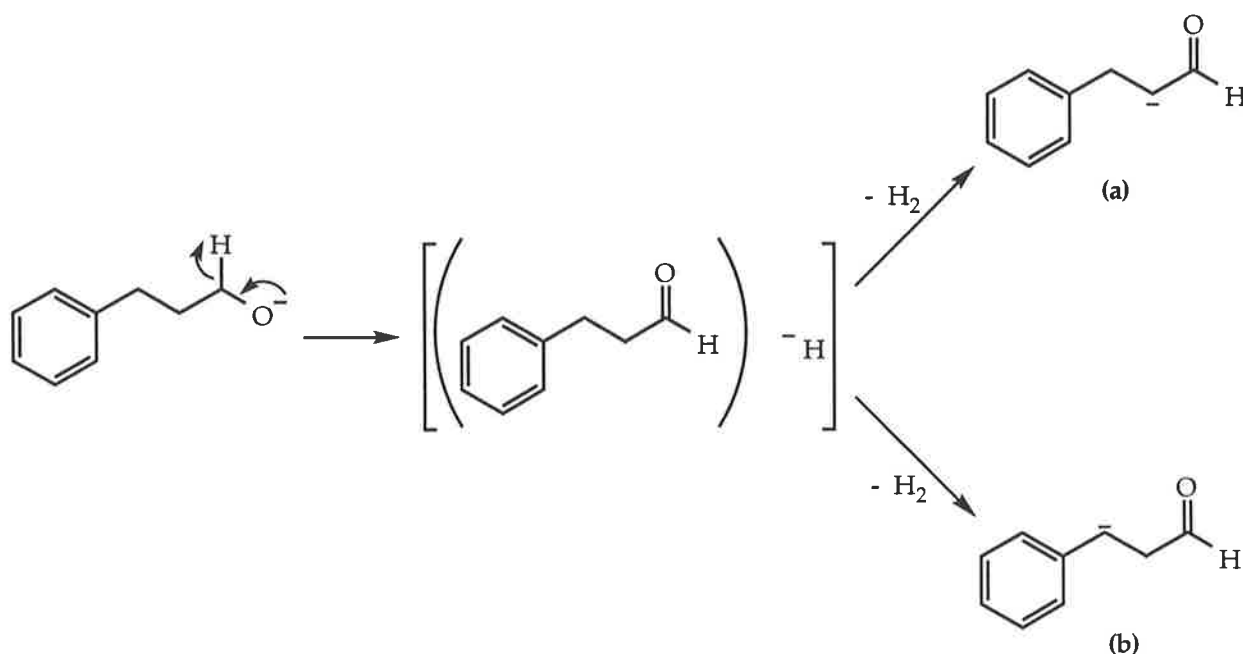


Scheme 3.2



Raftery *et al.*<sup>73</sup> have investigated the collision induced dissociations of aryl-substituted alkoxide ions and have reported that the spectra for deprotonated phenyl propanol is dominated by the loss of  $\text{H}_2$  which, from labelling data, is shown to occur by two processes through the same ion/neutral intermediate (scheme 3.3). The major process involves the typical 1,2 elimination to afford the stable enolate anion (scheme 3.3a), the second process, however, involves a stepwise 1,3 loss of  $\text{H}_2$  to afford a stable benzylic anion (scheme 3.3b). Thus the hydride ion is mobile, effecting deprotonation at both the 2- and 3- positions.

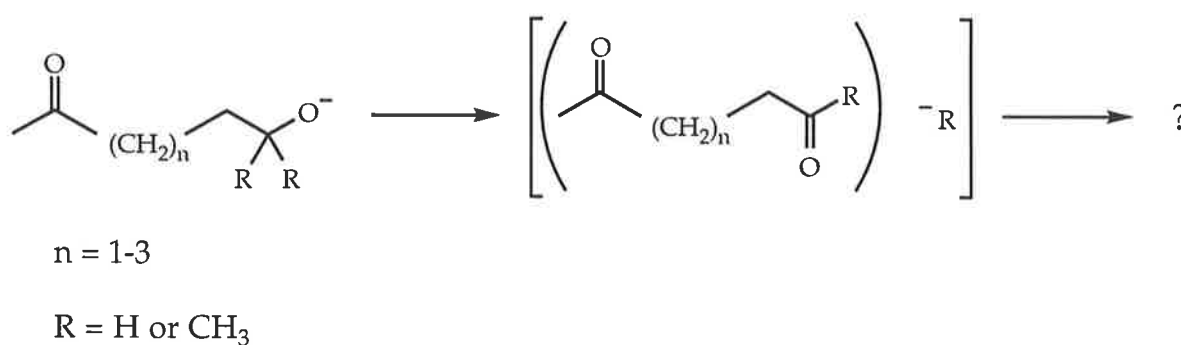
Scheme 3.3



One of the interesting questions concerning anion reactions within ion/neutral complexes is how far the anion is free to move within that complex.

In this chapter we explore the mobility of the hydride ion and methyl anion in the modified alkoxide system shown in scheme 3.4. Including a carbonyl as well as oxide functionality supports some interesting mechanistic possibilities. For example, we wish to explore this system in order to determine whether  $\text{H}^-$  and/or  $\text{CH}_3^-$  will competitively: (i) deprotonate  $\alpha$  to the carbonyl group at the other end of the carbonyl chain, and/or (ii) undergo nucleophilic addition to that carbonyl group, and (iii) if the answer to either of these questions is yes, what is the influence of the chain length on these reactions?

Scheme 3.4



## 3.2 Results and Discussion

The compounds listed in Table 3.1 were studied for the investigation of the hydride and methyl anion mobility in conformationally flexible keto-alkoxide systems. Raftery *et al.*<sup>73</sup> have observed that in addition to the characteristic 1,2 elimination of H<sub>2</sub> from primary alkoxide ions, competing 1,3 eliminations of H<sub>2</sub> may also occur. The systems we wish to study may enable us to observe a number of competing reactions. The alkoxide anion from compound **1**, for example, might eliminate H<sub>2</sub> by both the classical 1,2 elimination and a possible 1,3 elimination to afford stable enolate anions. A possible 1,4 elimination might occur for the alkoxide from compound **6**. In compounds **4** and **10** the two hydrogens at position 2 are replaced with methyl groups: the corresponding anions from these precursors may undergo methyl migration.

Table 3.1 Compounds examined in this study.

Compound	Number
MeCOCH <sub>2</sub> CH <sub>2</sub> CH <sub>2</sub> OD	<b>1</b>
MeCOCH <sub>2</sub> CH <sub>2</sub> CD <sub>2</sub> OH	<b>2</b>
CD <sub>3</sub> COCD <sub>2</sub> CH <sub>2</sub> CH <sub>2</sub> OH	<b>3</b>
MeCOCH <sub>2</sub> CH <sub>2</sub> C(Me) <sub>2</sub> OD	<b>4</b>
CD <sub>3</sub> COCD <sub>2</sub> CH <sub>2</sub> C(Me) <sub>2</sub> OH	<b>5</b>
MeCOCH <sub>2</sub> (CH <sub>2</sub> ) <sub>2</sub> CH <sub>2</sub> OH	<b>6</b>
MeCOCH <sub>2</sub> (CH <sub>2</sub> ) <sub>2</sub> CH <sub>2</sub> OD	<b>7</b>
MeCOCH <sub>2</sub> (CH <sub>2</sub> ) <sub>2</sub> CD <sub>2</sub> OH	<b>8</b>
CD <sub>3</sub> COCD <sub>2</sub> (CH <sub>2</sub> ) <sub>2</sub> CH <sub>2</sub> OH	<b>9</b>
MeCOCH <sub>2</sub> (CH <sub>2</sub> ) <sub>2</sub> C(Me) <sub>2</sub> OD	<b>10</b>
CD <sub>3</sub> COCD <sub>2</sub> (CH <sub>2</sub> ) <sub>2</sub> C(Me) <sub>2</sub> OH	<b>11</b>
MeCOCH <sub>2</sub> (CH <sub>2</sub> ) <sub>3</sub> CH <sub>2</sub> OD	<b>12</b>

The collisionally induced negative ion spectra for these compounds are amongst the most complex we have observed in the negative ion mode. The fragmentations of these systems are considered below.

### 3.2.1 Migration of the Hydride Ion

#### 3.2.1.1 Reactions of Deprotonated 6-Hydroxy-hexan-2-one

In order to examine and describe the fragmentation processes occurring for this series of compounds we first focus our attention on compound **6** and the labelled derivatives **7-9**. An understanding of the collision induced reactions of the alkoxide derived from **6** should allow a comparison with the fragmentation behaviour of other keto-alkoxides.

The spectrum of the (M-D)<sup>-</sup> ion of **7** is shown in Figure 3.1 and this also is summarised in Table 3.2 together with the spectra of the deuterium labelled (M-H)<sup>-</sup> ions derived from compounds **8** and **9**. We first need to identify the origin of deprotonation since, in principle, deprotonation of **6** with HO<sup>-</sup> could occur at the hydroxyl position or  $\alpha$  to the carbonyl group (eg.  $\Delta G_{acid}^{\circ}$  EtOH and CH<sub>3</sub>COCH<sub>3</sub> = 1552 and 1514 kJ mol<sup>-1</sup> respectively).<sup>82</sup>



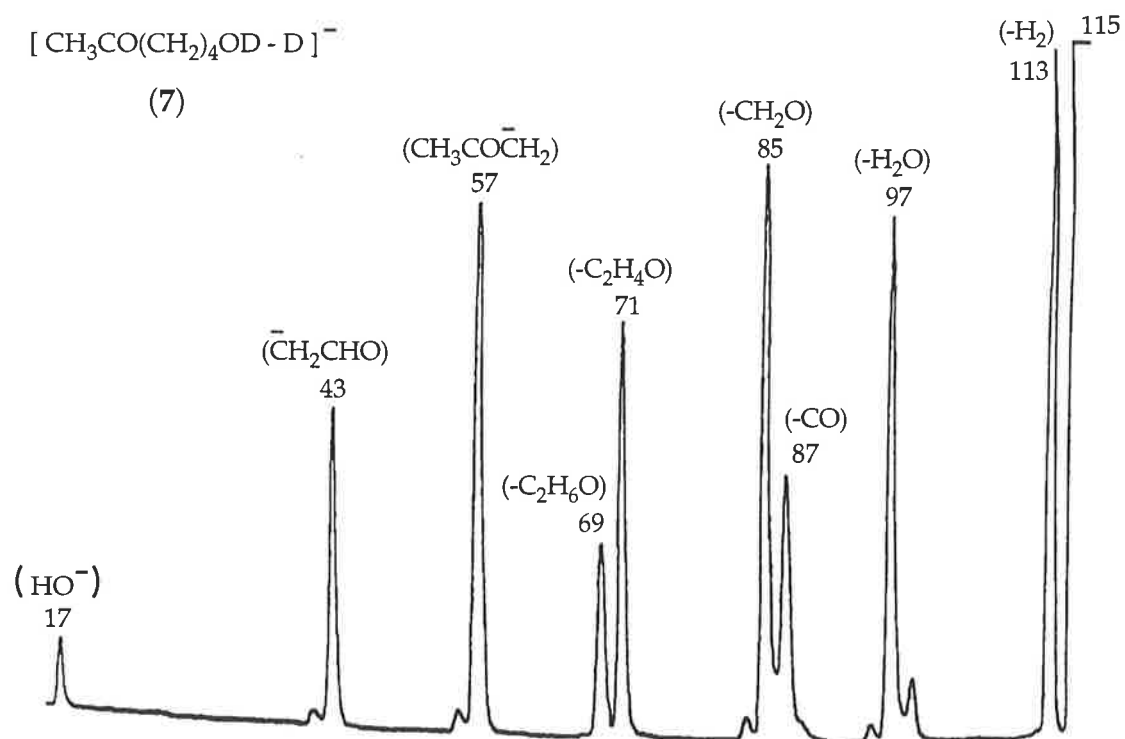


Figure 3.1 Collision-induced HO<sup>-</sup> negative chemical ionisation mass spectrum (MS/MS) of the (M-D)<sup>-</sup> ion of MeCO(CH<sub>2</sub>)<sub>4</sub>OD.

Table 3.2 Collisional activated mass spectra (MS/MS) of (M-D)<sup>-</sup> or (M-H)<sup>-</sup> ions.

Precursor	Spectrum [ <i>m/z</i> (loss of formation) relative abundance]
(M-D) <sup>-</sup> ion of MeCO(CH <sub>2</sub> ) <sub>4</sub> OD      7	113(H <sub>2</sub> )100, 99(CH <sub>4</sub> )8, 97(H <sub>2</sub> O)78, 87(CO)41, 85(CH <sub>2</sub> O)87, 71(C <sub>2</sub> H <sub>4</sub> O)63, 69(C <sub>2</sub> H <sub>6</sub> O)28, 57(C <sub>3</sub> H <sub>6</sub> O)76, 43(C <sub>4</sub> H <sub>8</sub> O)37, 41(HC <sub>2</sub> O <sup>-</sup> )3, 17(HO <sup>-</sup> )9
(M-H) <sup>-</sup> ion of MeCO(CH <sub>2</sub> ) <sub>3</sub> CD <sub>2</sub> OH      8	114(HD)65, 99(H <sub>2</sub> O)100, 89(CO)28, 86(CHDO)27, 85(CD <sub>2</sub> O)55, 73(C <sub>2</sub> H <sub>2</sub> D <sub>2</sub> O)16, 69(C <sub>2</sub> H <sub>4</sub> D <sub>2</sub> O)25, 57(C <sub>3</sub> H <sub>4</sub> D <sub>2</sub> O)40, 44(C <sub>4</sub> H <sub>7</sub> DO)23, 42(DC <sub>2</sub> O <sup>-</sup> )8, 41(HC <sub>2</sub> O <sup>-</sup> )18
(M-H) <sup>-</sup> ion of CD <sub>3</sub> COCD <sub>2</sub> (CH <sub>2</sub> ) <sub>3</sub> OH      9	118(H <sub>2</sub> )45, 102(H <sub>2</sub> O)100, 101(HOD)55, 92(CO)85, 90(CH <sub>2</sub> O)45, 89(CHDO)90, 76(C <sub>2</sub> H <sub>4</sub> O)8, 75(C <sub>2</sub> H <sub>3</sub> DO)5, 73(C <sub>2</sub> H <sub>5</sub> DO)28, 72(C <sub>2</sub> H <sub>4</sub> D <sub>2</sub> O)22, 62(C <sub>3</sub> H <sub>6</sub> O)32, 61(C <sub>3</sub> H <sub>5</sub> DO)18, 60(C <sub>3</sub> H <sub>4</sub> D <sub>2</sub> O)4, 45(C <sub>4</sub> H <sub>5</sub> D <sub>3</sub> O)15, 42(DC <sub>2</sub> O <sup>-</sup> )8, (DO <sup>-</sup> )4

In order to determine the origin of deprotonation, and to therefore identify the observed anion, the labelled compound **7** needs to be considered. The OD labelled derivative **7** yields (M-H)<sup>-</sup> and (M-D)<sup>-</sup> ions in the ratio 2:1 with both ions showing similar fragmentations when taking into account the D label in the former. Also, the spectra recorded for the (M-D)<sup>-</sup> ion of **7** is identical to that seen for the (M-H)<sup>-</sup> ion of **6** (Fig. 3.1). We conclude that deprotonation of **6** occurs both α to the carbonyl group and at the hydroxy position, with facile proton scrambling occurring between enolate anions and the alkoxide anion upon collisional activation. Such proton transfer is common between two acidic sites (see 1.8.3a, page 30).

The structures of the product ions formed from the (M-D)<sup>-</sup> ion of **7** have all been identified by comparing the collisional activation and charge reversal spectra of the source formed daughter ions with those of authentic anions prepared independently by deprotonation of the appropriate neutrals. The data obtained from product ion studies are listed in Table 3.3 and the structures for the daughter ions (together with their *m/z* values) are shown in scheme 3.5.

Table 3.3 Comparison of collisional activated or charge reversal (positive ion) mass spectra of product anions from the (M-D)<sup>-</sup> ion from 7, with the spectra of authentic anions (formed by deprotonation of the appropriate neutral).<sup>a,b,c</sup>

Ion ( <i>m/z</i> )	Spectrum type	Spectrum CA [ <i>m/z</i> (loss of formation) rel. abundance] CR [ <i>m/z</i> (rel. abundance)]
[-H <sub>2</sub> ] (113)	CA	112(H <sup>-</sup> )100, 111(H <sub>2</sub> )28, 95(H <sub>2</sub> O)8, 85(CO)4, 83(CH <sub>2</sub> O)22, 69(C <sub>2</sub> H <sub>4</sub> O)78, 57((C <sub>3</sub> H <sub>4</sub> O)100, 43(C <sub>4</sub> H <sub>6</sub> O)33.
[MeCO(CH <sub>2</sub> ) <sub>3</sub> CHO - H] <sup>-</sup> (113)	CA	112(H <sup>-</sup> )100, 111(H <sub>2</sub> )35, 95(H <sub>2</sub> O), 5, 85(CO)3, 83(CH <sub>2</sub> O)18, 69(C <sub>2</sub> H <sub>4</sub> O)85, 57(C <sub>3</sub> H <sub>4</sub> O)100, 43(C <sub>4</sub> H <sub>6</sub> O)38.
[-H <sub>2</sub> O] (97)	CA	96(H <sup>-</sup> )100, 95(H <sub>2</sub> )33, 81(CH <sub>4</sub> )35, 79(H <sub>2</sub> O)16, 69(C <sub>2</sub> H <sub>4</sub> )19, 55(42)22, 53(44)4, 41(HC <sub>2</sub> O <sup>-</sup> )17.
[MeCO(CH <sub>2</sub> ) <sub>2</sub> CH=CH <sub>2</sub> - H] <sup>-</sup> (97)	CA	96(H <sup>-</sup> )100, 95(H <sub>2</sub> )35, 81(CH <sub>4</sub> )36, 79(H <sub>2</sub> O)12, 69(C <sub>2</sub> H <sub>4</sub> )24, 55(42)28, 53(44)4, 41(HC <sub>2</sub> O <sup>-</sup> )28.
[-CO] (87)	CA	85(H <sub>2</sub> )100, 71(CH <sub>4</sub> )35, 43(C <sub>3</sub> H <sub>8</sub> )5.
MeCH(O <sup>-</sup> )CH <sub>2</sub> CH <sub>2</sub> Me (87)	CA	85(H <sub>2</sub> )100, 71(CH <sub>4</sub> )32, 43(C <sub>3</sub> H <sub>8</sub> )3.
[-CH <sub>2</sub> O] (85)	CA	84(H <sup>-</sup> )48, 83(H <sub>2</sub> )43, 69(CH <sub>4</sub> )100, 67(H <sub>2</sub> O)3, 57(C <sub>2</sub> H <sub>4</sub> )45, 41(HC <sub>2</sub> O <sup>-</sup> )3.
[MeCO(CH <sub>2</sub> ) <sub>2</sub> Me - H] <sup>-</sup> (85)	CA	84(H <sup>-</sup> )52, 83(H <sub>2</sub> )50, 69(CH <sub>4</sub> )100, 67(H <sub>2</sub> O)3, 57(C <sub>2</sub> H <sub>4</sub> )30, 41(HC <sub>2</sub> O <sup>-</sup> )3.
[-C <sub>2</sub> H <sub>4</sub> O] (71)	CR	57(3), 56(10), 55(16), 53(9), 44(52), 43(26), 42(36), 41(24), 39(22), 29(29), 28(31), 27(100), 26(78), 15(5), 14(5).
[MeCOCH <sub>2</sub> Me - H] <sup>-</sup> (71)	CR	57(3), 56(8), 55(17), 53(8), 44(55), 43(27), 42(38), 41(22), 39(14), 29(23), 28(33), 27(100), 26(74), 15(4), 14(4).
[Me(CH <sub>2</sub> ) <sub>2</sub> CHO - H] <sup>-</sup> (71)	CR	70(3), 69(15), 55(51), 54(11), 53(12), 41(69), 39(100), 29(75), 28(26), 27(72), 26(34), 15(3), 14(3).
CH <sub>2</sub> =CHCO <sub>2</sub> <sup>-</sup> (71)	CR	54(5), 53(11), 51(6), 44(100), 41(8), 29(10), 28(29), 27(100), 26(78), 25(27), 14(2), 13(2).
[-C <sub>2</sub> H <sub>6</sub> O] (69)	CR	68(10), 55(40), 53(18), 42(74), 39(68), 37(25), 27(100), 25(70), 14(6), 13(2).
<sup>-</sup> CH <sub>2</sub> COCH=CH <sub>2</sub> (69)	CR	68(8), 55(45), 53(22), 42(78), 39(66), 37(22), 27(100), 25(68), 14(5), 13(2).

Table 3.3 Cont.

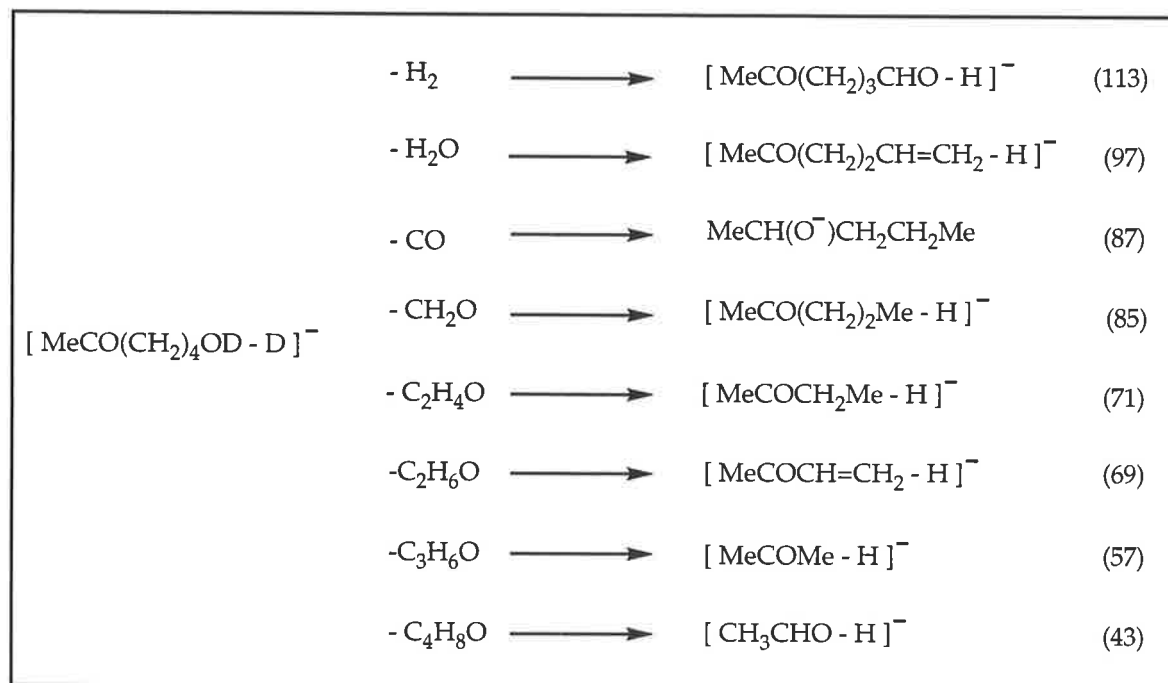
$[-C_3H_6O]$ (57)	CR	56(1), 55(8), 54(1), 53(4), 43(69), 42(100), 41(24), 39(54), 29(40), 28(10), 27(42), 26(18), 15(8), 14(6), 13(2).
$^-CH_2COMe$ (57)	CR	see reference <sup>83</sup>
$[-C_4H_8O]$ (43)	CR	42(100), 41(37), 40(6), 29(49), 28(16), 27(11), 25(3), 15(19), 14(8), 13(1).
$^-CH_2CHO$ (43)	CR	see reference <sup>84</sup>

<sup>a</sup>Both CA (negative) and charge reversal (CR, positive) mass spectra have been determined for the species listed in this table. For brevity, we have listed (in this table) whichever of the two spectra is more diagnostic.

<sup>b</sup>The relative abundances recorded for these spectra are very dependent upon source and focussing conditions and upon the pressure of collision gas. Differences of  $\pm 5$ -10% are not unusual for major peaks.

<sup>c</sup>Some of the precursors on deprotonation may form several enolate  $(M-H)^-$  anions. These enolate anions interconvert, on collisional activation, following proton transfer.<sup>85</sup> The CA and CR spectra of the  $(M-H)^-$  ions of such species are composite spectra of the equilibrated enolate anions.

Scheme 3.5



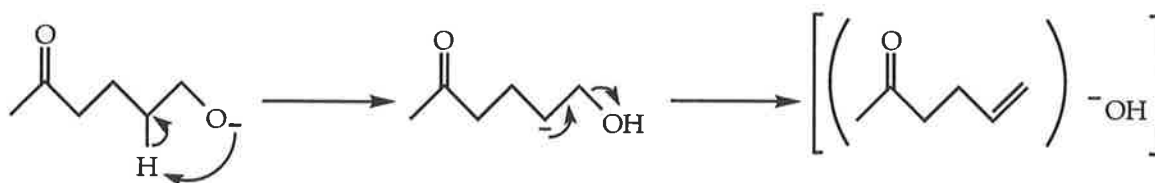
Having determined probable structures for the product anions, a mechanistic rationale for their formation must be now be postulated.

The information obtained from the labelled derivatives 8 and 9 (Table 3.2) plays a vital role in this study and needs to be considered in order to obtain an understanding of the mechanisms of these reactions.<sup>a</sup>

### Reactions not involving anion migration

Having determined the structures of the product anions, consider first those processes in which H<sup>-</sup> transfer is not implicated. The loss of water results in the formation of deprotonated allyl acetone (scheme 3.5 and Table 3.3). Loss of water is a standard reaction of simple alkoxide anions<sup>73</sup> and in this case, should occur as shown in scheme 3.6.

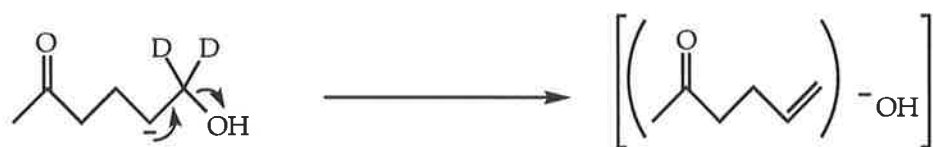
Scheme 3.6



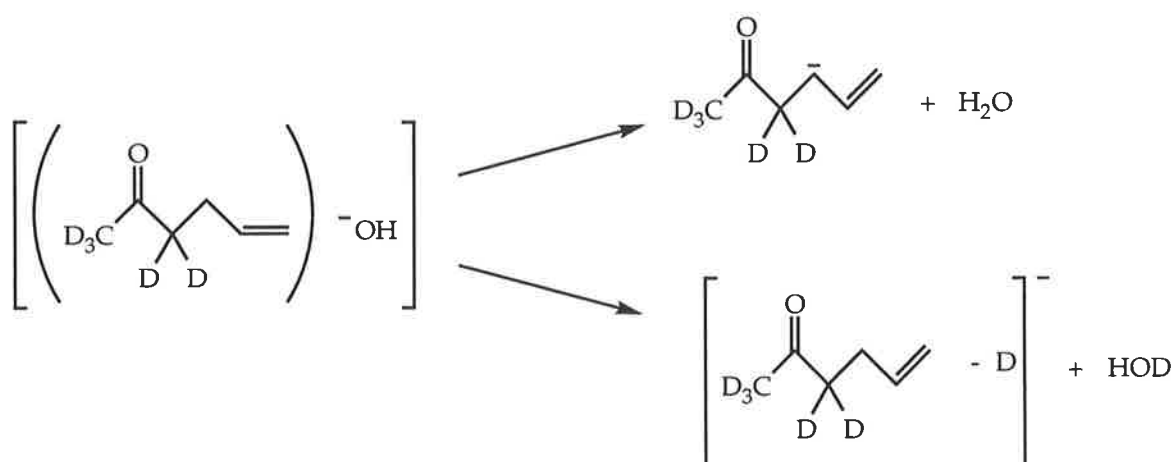
<sup>a</sup>It must be pointed out that in a recent study of the fragmentations of the 8-nonenoate anion, Dua *et. al.*<sup>61</sup> reported that the collisionally activated 8-nonenoate anion undergoes extensive hydrogen scrambling (without carbon scrambling) along the carbon chain, and that this H scrambling competes with high energy cleavage processes. Although we have not carried out such extensive labelling for our keto-alkoxide anions, the evidence available from the labelled derivatives suggests that the same scenario holds for certain reactions studied in this system.

The mechanism shown in scheme 3.6 is supported by the data obtained from the labelled (M-H)<sup>-</sup> ions of **8** and **9** (Table 3.2). The *d*<sub>2</sub>-labelled derivative **8** shows exclusive loss of H<sub>2</sub>O to afford product ion *m/z* 99: thus deprotonation by HO<sup>-</sup> occurs either at the enolate position or the allylic position (scheme 3.7). The *d*<sub>5</sub>-labelled derivative **9** undergoes losses of both H<sub>2</sub>O and HOD in the ratio 3:2. This result can be explained in terms of either: (i) HO<sup>-</sup> competitively removing H<sup>+</sup> from the allylic centre and D<sup>+</sup> from the enolate position (scheme 3.8), or (ii) specific removal of H<sup>+</sup> (D<sup>+</sup>) following H/D exchange between allylic and enolate positions. We cannot differentiate between these two possibilities.

Scheme 3.7

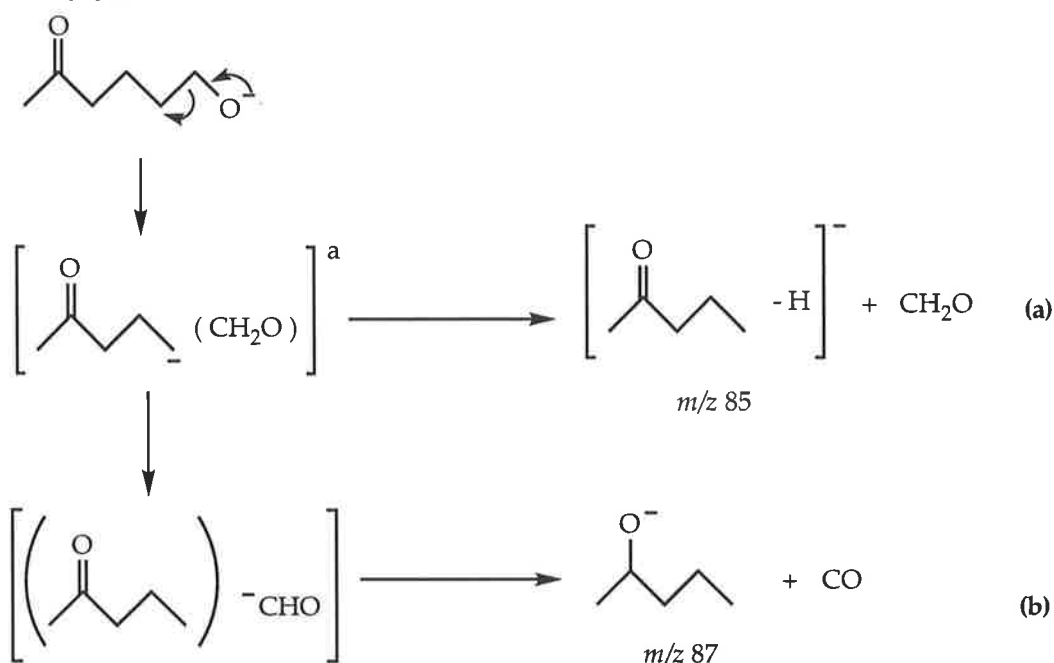


Scheme 3.8



The loss of formaldehyde to form  $m/z$  85 is a typical process observed for primary alkoxides<sup>73,86</sup>. This loss is discussed together with the loss of CO, since both processes are closely related. The loss of formaldehyde to afford deprotonated pentan-2-one (scheme 3.5 and Table 3.3) occurs by process 3.9a. This loss of formaldehyde competes with some minor H scrambling between the 1 ( $\text{CH}_2\text{O}^-$ ) and 4,6 (enolate) positions as evidenced by the losses of  $\text{CD}_2\text{O}$  and  $\text{CHDO}$  (2:1) for **8** and (1:2) for **9** (Table 3.2). The loss of CO to yield deprotonated 2-pentanol ( $m/z$  87), and the loss of formaldehyde are interconnected, since CO loss originates following  $\text{H}^-$  transfer from a formyl anion. This loss of CO is not a typical process of alkoxide ions and perhaps the stable alkoxide product ion is the driving force of the reaction. We propose that the mechanism for this CO loss proceeds through the same ion/neutral intermediate as illustrated for loss of formaldehyde (scheme 3.9b). Hydrogen exchange between the anion and neutral in the initial complex gives a formyl anion/complex: the formyl anion then transfers a hydride ion to the neutral, resulting in loss of CO and formation of anion  $m/z$  87.

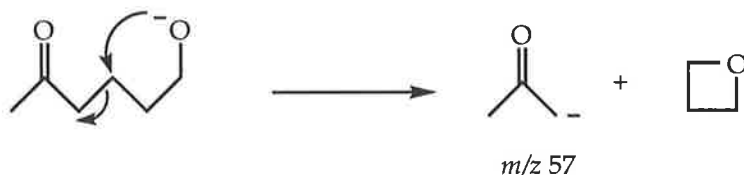
Scheme 3.9



<sup>a</sup>Proton transfer within this complex may yield a more stable anion.

Independent studies of aryl substituted alkoxide ions<sup>73,87</sup> have identified processes which involve  $S_Ni$  reactions which afford a stable anion together with a neutral cyclic ether. We propose a similar mechanism for the formation of  $m/z \ 57$  identified, in this system, by product ion studies, as the acetone enolate anion (Table 3.3). Loss of oxetane is rationalised *via* the  $S_Ni$  process shown in scheme 3.10.

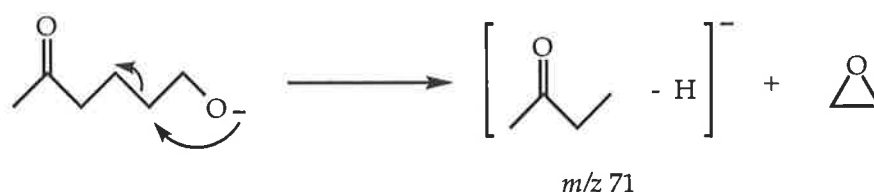
Scheme 3.10





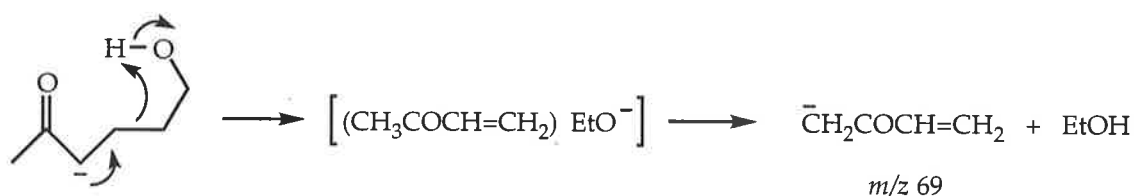
Product ion studies identify product ion  $m/z$  71 to be deprotonated butanone (Table 3.3). We propose that this process occurs *via* an  $S_Ni$  displacement reaction similar to that forming  $m/z$  57, except that attack occurs at the C2 position to eliminate oxirane (scheme 3.12). Both of these  $S_Ni$  processes occur with partial hydrogen scrambling as indicated from the spectra of the labelled derivatives (see Table 3.2).

Scheme 3.11

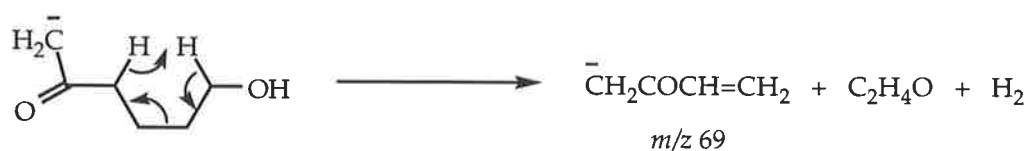


The formation of  $m/z$  69 identified as deprotonated methyl vinyl ketone (Table 3.3) is of particular interest since it is not formed directly from the alkoxide anion. Labelling data (Table 3.2) shows this process to be accompanied by partial hydrogen scrambling. The proposed mechanism for this reaction may be: (i) an anion-induced reaction (scheme 3.12), or (ii) a classical 'charge remote' reaction<sup>88,89</sup> (scheme 3.13). Either of these processes are energetically unfavourable: we cannot distinguish between them on available evidence.

Scheme 3.12



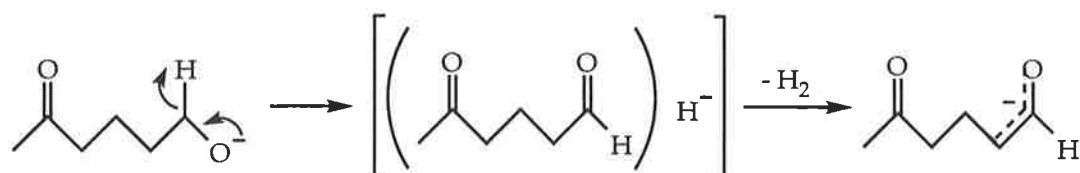
Scheme 3.13



### Reactions involving an $\text{H}^-$ migration

The focus of this investigation concerns what reactions are initiated by the  $\text{H}^-$  component of the anion/neutral complex  $[(\text{MeCO}(\text{CH}_2)_3\text{CHO}) \text{H}^-]$ . The classical fragmentation of alkoxide anions involves 1,2 elimination of  $\text{H}_2$  to form the allylic alkoxide anion (scheme 3.14). There are, however, other possible  $\text{H}^-$  ion reactions in this system. For example: (i) the  $\text{H}^-$  may migrate along the carbon chain and effect deprotonation  $\alpha$  to the ketone carbonyl as well, and (ii)  $\text{H}^-$  might attack the carbonyl next to the methyl initiating a reaction of some sort.

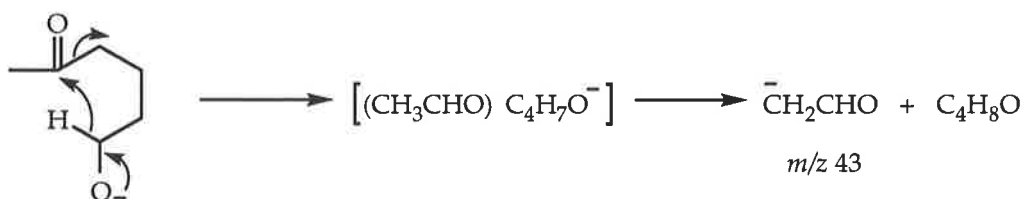
Scheme 3.14



Consider first, the loss of  $\text{H}_2$ . Loss of  $\text{H}_2$  produces the base peak in the spectrum in Figure 3.1. This process is so facile that the  $\text{H}_2$  loss proceeds without H/D scrambling as evidenced by the spectra of the labelled anions from 8 and 9 (Table 3.2). The labelling data shows exclusive loss of HD from  $\text{MeCO}(\text{CH}_2)_3\text{CD}_2\text{O}^-$  and loss of  $\text{H}_2$  from  $\text{CD}_3\text{COCD}_2(\text{CH}_2)_3\text{O}^-$ . Product ion studies indicate that  $m/z$  113 is deprotonated 3-acetyl-1-butanol and the reaction mechanism thus involves the classical 1,2 elimination summarised in scheme 3.14.

The formation of  $m/z$  43 turns out to be quite unusual. Product ion studies identify  $m/z$  43 as the acetaldehyde enolate anion. Deuterium labelling studies indicate that  $m/z$  43 (i) incorporates one hydrogen from the  $\text{CH}_2$  next to the alkoxide site, and (ii) this process is site specific occurring without any hydrogen scrambling. We propose that the acetaldehyde enolate anion is formed following  $\text{H}^-$  migration through a six centred state (scheme 3.15). The identity of the  $\text{C}_4\text{H}_8\text{O}$  neutral product formed in scheme 3.15 is not known: the most likely possibilities are butanal or cyclobutanol.

Scheme 3.15



### 3.2.1.2 Reactions of Deprotonated 5-Hydroxy-pentan-2-one

The CA MIKE spectrum of dedeuterated 5-hydroxy-pentan-2-one **1** is shown in Figure 3.2 and the spectral data for **1** and the (M-H)<sup>-</sup> ions of labelled derivatives **2** and **3** are reported in Table 3.4.

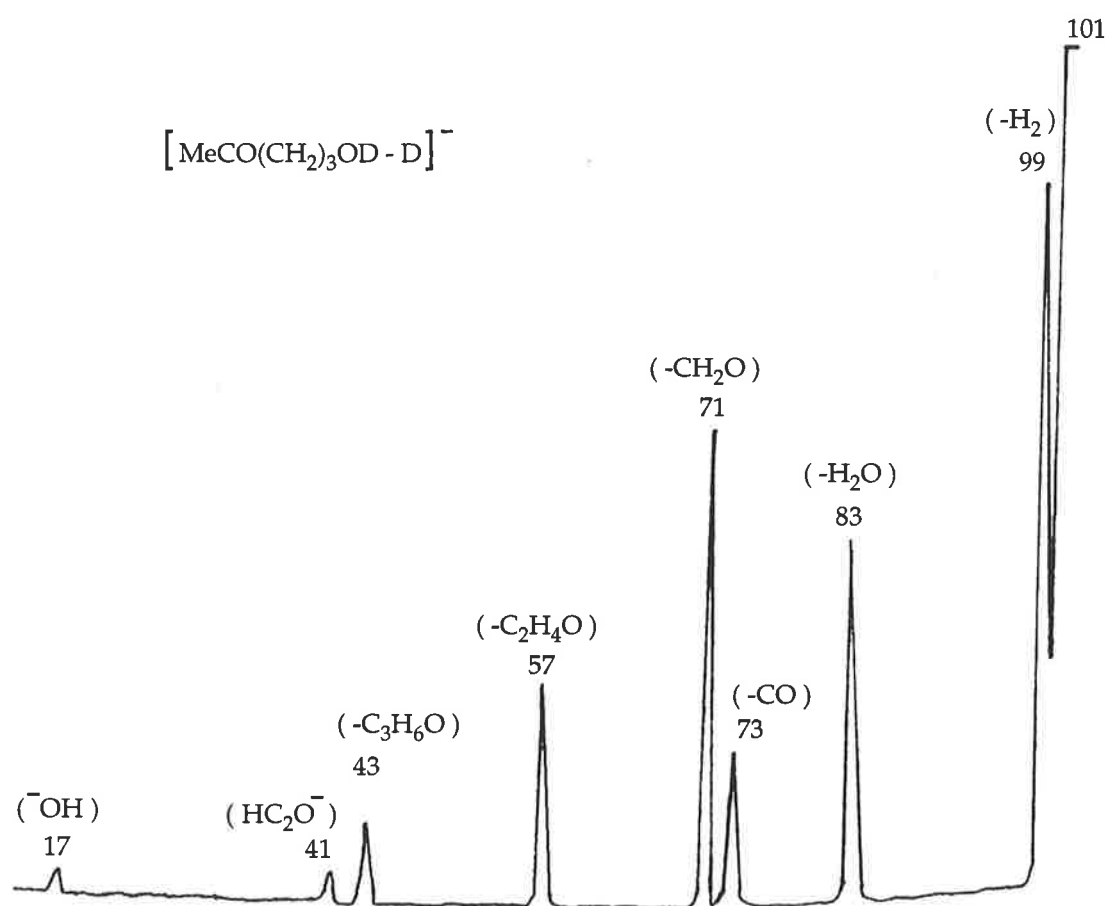


Figure 3.2 CA MIKE spectrum for dedeuterated 5-hydroxy-pentan-2-one (**1**).

Table 3.4 Collisional activated negative ion spectra for (M-H)<sup>-</sup> or (M-D)<sup>-</sup> ions of **1**, **2**, and **3**.

Precursor	Spectrum [ <i>m/z</i> (loss of formation) relative abundance]
(M-D) <sup>-</sup> ion of MeCO(CH <sub>2</sub> ) <sub>3</sub> OD <b>1</b>	99(H <sub>2</sub> )100, 85(CH <sub>4</sub> )17, 83(H <sub>2</sub> O)56, 73(CO)24, 71(CH <sub>2</sub> O)74, 57(C <sub>2</sub> H <sub>4</sub> O)34, 43(C <sub>3</sub> H <sub>6</sub> O)12, 41(HC <sub>2</sub> O <sup>-</sup> )6, 17(HO <sup>-</sup> )3.
(M-H) <sup>-</sup> ion of MeCO(CH <sub>2</sub> ) <sub>2</sub> CD <sub>2</sub> OH <b>2</b>	100(HD)98, 85(H <sub>2</sub> O)100, 75(CO)58, 73 <sup>a</sup> (CHDO)<10, 72(CD <sub>2</sub> O)32, 58(C <sub>2</sub> H <sub>3</sub> DO)38, 44(C <sub>3</sub> H <sub>5</sub> DO)9, 41(HC <sub>2</sub> O <sup>-</sup> )8.
(M-H) <sup>-</sup> ion of CD <sub>3</sub> COCD <sub>2</sub> (CH <sub>2</sub> ) <sub>2</sub> OH <b>3</b>	104(H <sub>2</sub> )100, 103(HD)80, 87(HOD)80, 78(CO)45, 76(CH <sub>2</sub> O)45, 75(CHDO)90, 59(C <sub>3</sub> H <sub>3</sub> D <sub>2</sub> O)45, 45(C <sub>3</sub> H <sub>3</sub> D <sub>3</sub> O)6.

<sup>a</sup>unresolved.

Most of the fragmentations observed for the (M-D)<sup>-</sup> ion of compound **1** can be directly compared to the losses previously described for MeCO(CH<sub>2</sub>)<sub>4</sub>O<sup>-</sup>. Product ion studies for the major processes observed in Figure 3.2 are tabulated in Table 3.5, and the major losses are summarised in scheme 3.16. For example, the losses of water, CO and formaldehyde are typical of primary keto-alkoxide ions and occur in exactly the same fashion as described for MeCO(CH<sub>2</sub>)<sub>4</sub>O<sup>-</sup>.

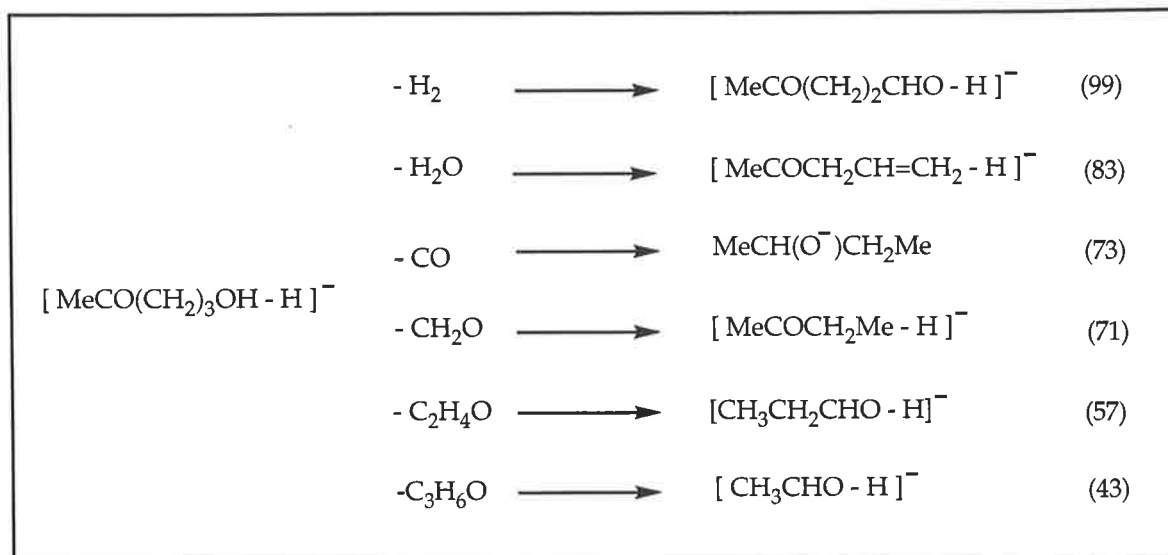
Table 3.5 Comparison of Collisional Activated or Charge Reversal (positive ion) Mass Spectra of Product Anions from the (M-D)<sup>-</sup> ion of **1**, with the Spectra of Authentic Anions (formed by deprotonation of the appropriate neutral).<sup>a, b</sup>

ion ( <i>m/z</i> )	Spectrum type	Spectrum CA [ <i>m/z</i> (loss of formation) rel. abundance] CR [ <i>m/z</i> (rel. abundance)]
[- H <sub>2</sub> ] (99)	CA	98(H <sub>2</sub> )75, 83(CH <sub>4</sub> )38, 81(H <sub>2</sub> O)28, 71(CO)3, 69(CH <sub>2</sub> O)77, 57(C <sub>2</sub> H <sub>2</sub> O)100, 43(C <sub>3</sub> H <sub>4</sub> O)9.
[MeCO(CH <sub>2</sub> ) <sub>2</sub> CHO - H] <sup>-</sup> (99)	CA	98(H <sub>2</sub> )79, 83(CH <sub>4</sub> )35, 81(H <sub>2</sub> O)20, 71(CO)2, 69(CH <sub>2</sub> O)71, 57(C <sub>2</sub> H <sub>2</sub> O)100, 43(C <sub>3</sub> H <sub>4</sub> O)6.
[- H <sub>2</sub> O] (83)	CR	83(50), 82(37), 81(24), 68(100), 55(31), 54(16), 53(29), 51(13), 50(13), 43(40), 42(37), 41(13), 39(55), 29(8), 27(11), 26(9).
[MeCOCH <sub>2</sub> CH=CH <sub>2</sub> - H] <sup>-</sup> (83)	CR	83(49), 82(35), 81(24), 68(100), 55(31), 54(14), 53(24), 51(13), 50(13), 43(39), 42(31), 41(16), 39(51), 29(7), 27(13), 26(10).
[- CO] (73)	CR	58(21), 57(38), 56(6), 55(7), 45(7), 44(28), 43(100), 42(27), 41(17), 39(12), 29(37), 28(15), 27(28), 26(15).
MeCH(O <sup>-</sup> )CH <sub>2</sub> Me (73)	CR	58(22), 57(38), 56(6), 55(7), 45(8), 44(29), 43(100), 42(28), 41(17), 39(13), 29(38), 28(14), 27(28), 26(14).
[- CH <sub>2</sub> O] (71)	CR	57(5), 56(10), 55(17), 53(7), 44(55), 43(22), 42(40), 41(20), 39(14), 29(21), 28(31), 27(100), 26(73), 15(4), 14(4).
[MeCOCH <sub>2</sub> Me - H] <sup>-</sup> (71)	CR	see Table 3.3.
[- C <sub>2</sub> H <sub>4</sub> O] (57)	CR	56(24), 55(43), 54(5), 53(5), 42(4), 41(13), 40(5), 39(20), 38(10), 37(8), 31(1.5), 29(100), 28(46), 27(52), 26(36), 25(8), 15(2.5), 14(6.5), 13(2.5).
[MeCH <sub>2</sub> CHO - H] <sup>-</sup> (57)	CR	56(23), 55(43), 54(5), 53(6), 42(4), 41(12), 40(5), 39(20), 38(10), 37(9), 31(1), 29(100), 28(45), 27(53), 26(36), 25(7), 15(3), 14(7), 13(3).
[- C <sub>3</sub> H <sub>6</sub> O] (43)	CR	42(100), 41(39), 40(8), 29(53), 28(18), 27(14), 25(5), 15(21), 14(8), 13(1).
[CH <sub>3</sub> CHO - H] <sup>-</sup> (43)	CR	see Table 3.3.

<sup>a</sup>Both CA (negative) and charge reversal (CR, positive) mass spectra have been determined for the species listed in this table. For brevity, we have listed (in this table) whichever of the two spectra is more diagnostic.

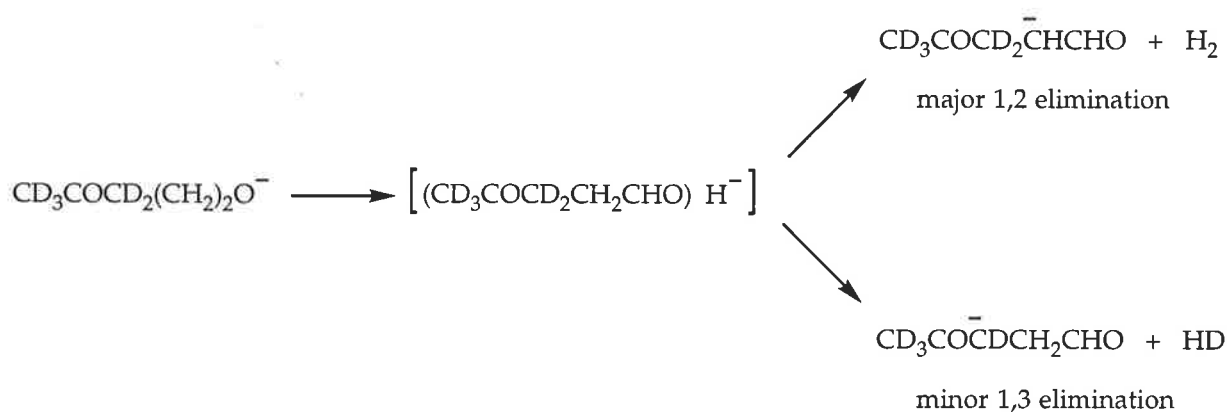
<sup>b</sup>The relative abundances recorded for these spectra are very dependent upon source and focussing conditions and upon the pressure of collision gas. Differences of ± 5-10% are not unusual for major peaks.

Scheme 3.16



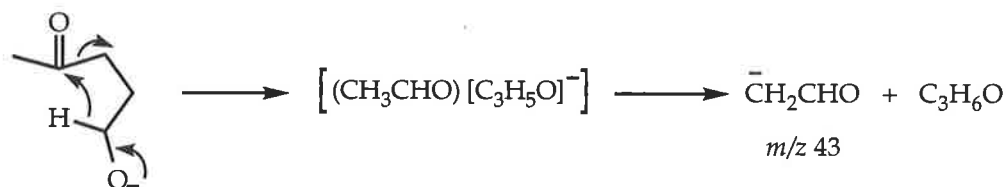
The losses of H<sub>2</sub> and C<sub>3</sub>H<sub>6</sub>O to afford *m/z* 99 and 43 respectively deserve particular attention since these processes could involve H<sup>-</sup> migration. In the case of MeCO(CH<sub>2</sub>)<sub>4</sub>O<sup>-</sup> loss of H<sub>2</sub> occurs exclusively *via* 1,2-elimination (scheme 3.7). The ion MeCO(CH<sub>2</sub>)<sub>3</sub>O<sup>-</sup>, however, consists of a carbon chain reduced by one methylene group and as a consequence, there is the possibility of competing losses of H<sub>2</sub> *via* 1,2 and 1,3 elimination processes. In order to characterise this H<sub>2</sub> loss we need to consider the appropriate fragmentations from the (M-H)<sup>-</sup> ions of the labelled derivatives **2** and **3** (Table 3.4). The *d*<sub>2</sub>-labelled ion shows exclusive loss of HD which is the expected loss for either a 1,2 or a 1,3 elimination. However, the spectrum of the *d*<sub>5</sub>-labelled derivative **3** shows losses of HD and H<sub>2</sub> in the ratio 5:4. The 1,2 elimination (loss of H<sub>2</sub>) yields the base peak. Loss of HD must occur *via* a 1,3 elimination (scheme 3.17). There is no evidence of H/D scrambling proceeding or accompanying either process.

Scheme 3.17



The formation of  $m/z$  43 is initiated by  $\text{H}^-$  migration, as evidenced by the deuterium labelling data (Table 3.4). The acetaldehyde enolate anion is formed *via* a five centred intermediate as shown in scheme 3.18: this process is directly comparable to that summarised in scheme 3.15.

Scheme 3.18

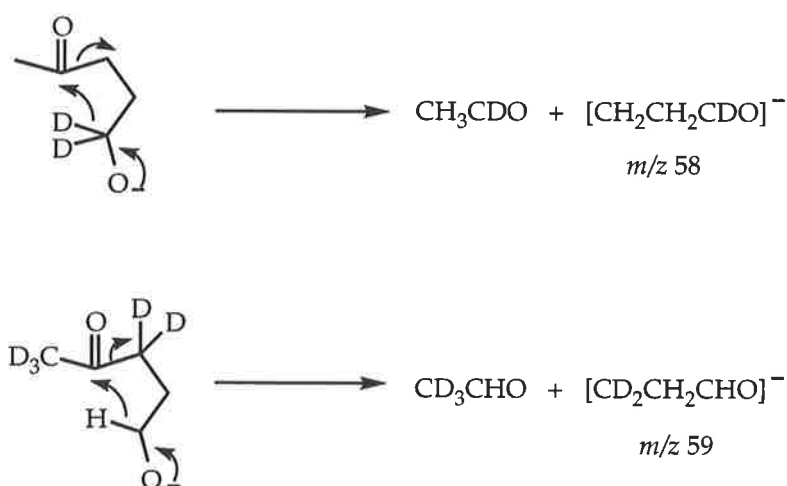


When comparing fragmentations of  $\text{MeCO}(\text{CH}_2)_n\text{O}^-$  ( $n=3$  and  $4$ ), perhaps the most interesting process involves the formation of  $m/z$  57. When  $n=4$ , loss of oxetane occurs by an  $\text{S}_{\text{Ni}}$  process to afford the acetone enolate anion (scheme 3.10). When  $n=3$ , the corresponding process would involve loss of oxirane to form the acetone enolate anion ( $m/z$  57). Both product ion studies (Table 3.5) and the labelling data (Table 3.4) disprove this prediction. From the product ion studies, the peak at  $m/z$  57 has been identified as



deprotonated propionaldehyde which gives a CR spectrum quite different from that of deprotonated acetone (Table 3.5). The (M-H)<sup>-</sup> ion of the *d*<sub>2</sub>-labelled derivative **2** fragments to give a daughter ion *m/z* 58 and the (M-H)<sup>-</sup> ion of the *d*<sub>5</sub>-labelled derivative **3** affords exclusively daughter ion *m/z* 59 (Table 3.4). These results may be accounted for by the process shown in scheme 3.18. The anion/neutral complex may simply fall apart to afford acetaldehyde and deprotonated propionaldehyde. This facile process occurs without any H/D scrambling (scheme 3.19) and the mechanism is consistent with the spectra of the (M-H)<sup>-</sup> ions of the labelled derivatives **2** and **3**.

Scheme 3.19



### 3.2.1.3 Reactions of Deprotonated 7-Hydroxy-heptan-2-one

The CA MIKE spectrum for  $\text{MeCO}(\text{CH}_2)_5\text{O}^-$  (**12**) is shown in Figure 3.3. The structures of the major product ions formed from the (M-D)<sup>-</sup> ion of **12** have been identified by comparing the collisional activation and charge reversal spectra of the source formed daughter ions with those of authentic anions prepared independently by deprotonation of the appropriate neutrals. The

data obtained from product ion studies are listed in Table 3.6 and the structures for the daughter ions (together with their  $m/z$  values) are shown in scheme 3.20.

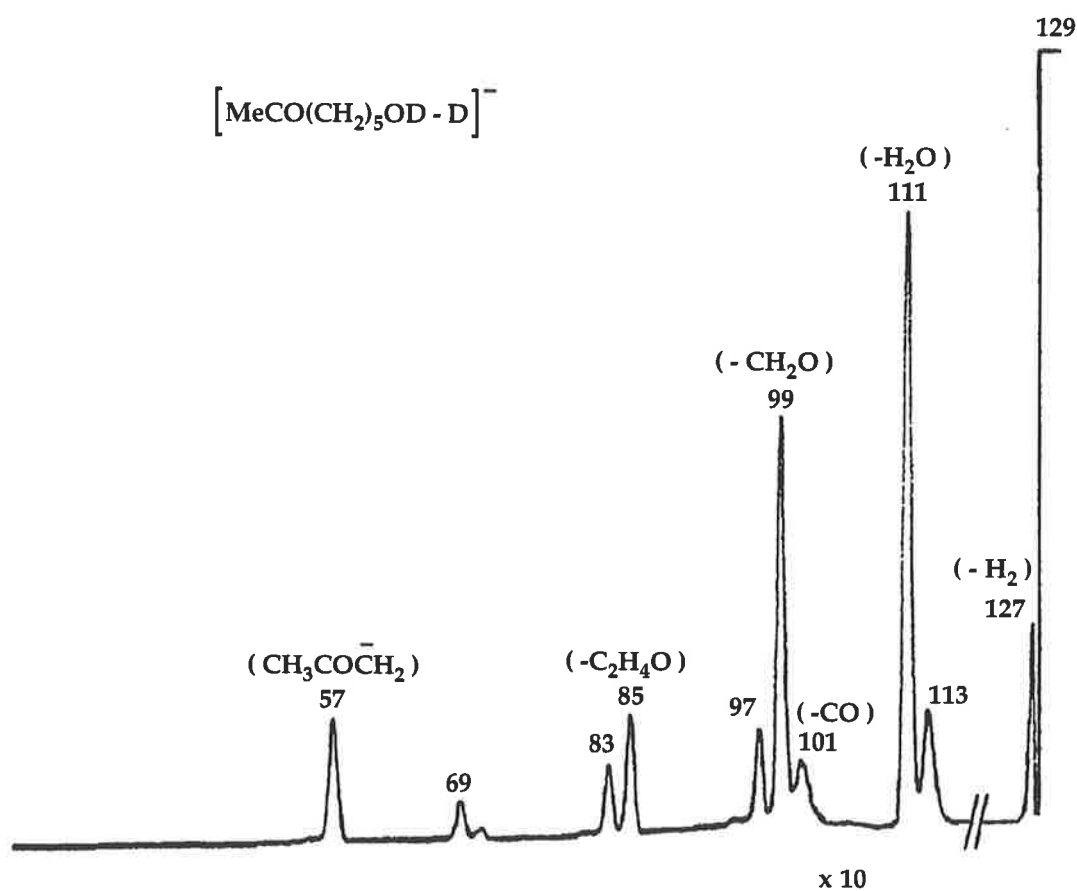


Figure 3.3 The CA MIKE spectrum for the  $(\text{M-D})^-$  ion of 7-hydroxy-heptan-2-one (12).

Table 3.6. Comparison of Collisional Activated and/or Charge Reversal (positive ion) mass spectra of product anions from the (M-D)<sup>-</sup> ion of **12**, with the spectra of authentic anions (formed by deprotonation of the appropriate neutrals).<sup>a, b</sup>

Ion ( <i>m/z</i> )	Spectra type	Spectra CA [ <i>m/z</i> (loss of formation) rel. abundance ] CR [ <i>m/z</i> (rel. abundance) ]
[-H <sub>2</sub> ] (127)	CA	126(H <sup>+</sup> )100, 125(H <sub>2</sub> )35, 109(H <sub>2</sub> O)34, 99(CO)8, 97(CH <sub>2</sub> O)7.
[MeCO(CH <sub>2</sub> ) <sub>4</sub> CHO - H] <sup>-</sup> (127)	CA	126(H <sup>+</sup> )100, 125(H <sub>2</sub> )40, 109(H <sub>2</sub> O)38, 99(CO)10, 97(CH <sub>2</sub> O)9.
[-H <sub>2</sub> O] (111)	CR	111(1), 110(1), 109(3), 107(1), 95(5), 93(5), 91(8), 83(4), 81(27), 79(20), 77(18), 69(8), 68(23), 67(34), 65(13), 63(7), 55(100), 53(27), 51(21), 41(49), 39(98), 29(7), 28 <sup>c</sup> , 27(27).
[MeCO(CH <sub>2</sub> ) <sub>3</sub> CH=CH <sub>2</sub> - H] <sup>-</sup> (111)	CR	111(1), 110(2), 109(4), 107(2), 95(5), 93(5), 91(8), 83(5), 81(28), 79(22), 77(19), 69(8), 68(26), 67(38), 65(13), 63(8), 55(100), 53(30), 51(24), 41(55), 39(87), 29(8), 28(14), 27(30).
[-CO] (101)	CA	99(H <sub>2</sub> )100, 85(CH <sub>4</sub> )100, 83(H <sub>2</sub> O)14, 57(C <sub>2</sub> H <sub>4</sub> O)6, 43(C <sub>4</sub> H <sub>10</sub> O)12.
MeCH(O <sup>-</sup> )(CH <sub>2</sub> ) <sub>3</sub> Me (101)	CA	99(H <sub>2</sub> )95, 85(CH <sub>4</sub> )100, 83(H <sub>2</sub> O)12, 57(C <sub>2</sub> H <sub>4</sub> O)4, 43(C <sub>4</sub> H <sub>10</sub> O)13.
[-CH <sub>2</sub> O] (99)	CR	99(1), 98(18), 97(4), 95(1), 85(5), 84(4), 83(20), 82(6), 81(20), 79(6), 71(3), 70(6), 69(12), 57(11), 56(15), 55(67), 53(15), 50(9), 49(9), 43(100), 42(61), 41(49), 39(41), 29(25), 28(17), 27(39).
[MeCO(CH <sub>2</sub> ) <sub>3</sub> Me - H] <sup>-</sup> (99)	CR	99(1), 98(26), 97(4), 95(2), 85(6), 84(9), 83(24), 82(7), 81(17), 79(7), 71(4), 70(5), 69(15), 57(9), 56(13), 55(63), 53(14), 50(7), 49(7), 43(100), 42(60), 41(47), 39(39), 29(26), 28(16), 27(39).
[-C <sub>2</sub> H <sub>4</sub> O] (85)	CR	84(2), 83(2), 71(7), 70(22), 69(25), 68(7), 67(8), 55(63), 53(8), 50(4), 43(100), 42(90), 41(40), 39(35), 29(12), 28(8), 27(25), 26(11).
[MeCO(CH <sub>2</sub> ) <sub>2</sub> Me - H] <sup>-</sup> (85)	CR	84(2), 83(2), 71(8), 70(23), 69(27), 68(8), 67(9), 55(69), 53(10), 50(6), 43(100), 42(94), 41(48), 39(37), 29(13), 28(9), 27(29), 26(13).

Table 3.6 Cont.

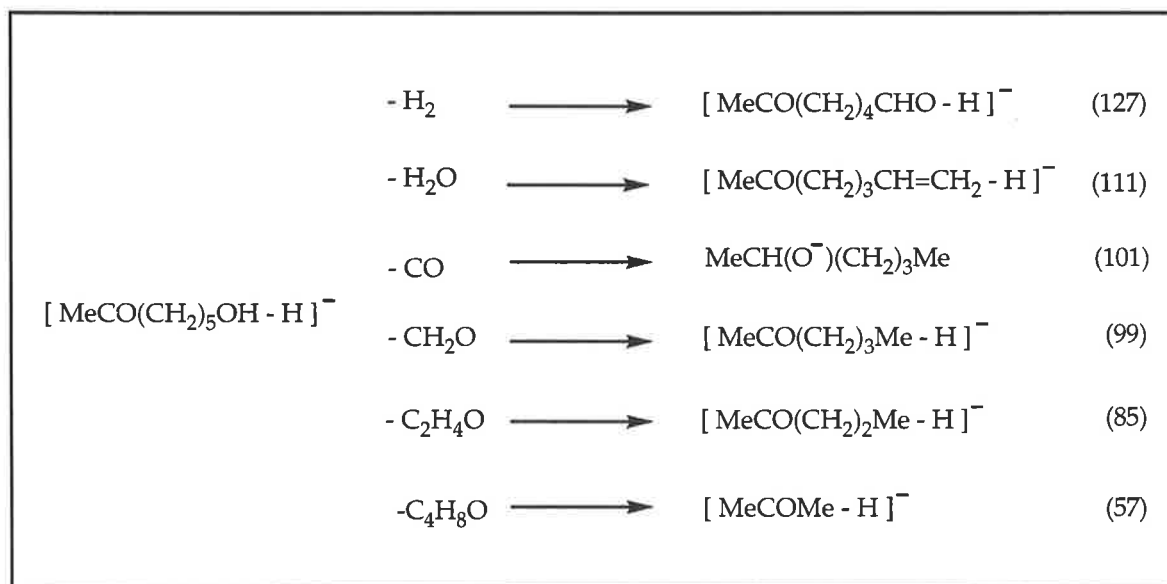
[Me(CH <sub>2</sub> ) <sub>3</sub> CHO - H] <sup>-</sup> (85)	CR	84(35), 83(23), 82(6), 81(2), 70(7), 69(13), 68(6), 67(6), 57(11), 55(100), 53(15), 50(7), 43(6), 41(22), 39(31), 29(35), 28(13), 27(29), 26(11).
[-C <sub>4</sub> H <sub>8</sub> O] (57)	CR	56(1), 55(9), 54(2), 53(4), 43(69), 42(100), 41(25), 39(54), 29(41), 28(11), 27(42), 26(20), 14(6), 13(1).
[MeCOMe - H] <sup>-</sup> (57)	CR	see Table 3.3

<sup>a</sup>Both CA (negative) and charge reversal (CR, positive) mass spectra have been determined for the species listed in this table. For brevity, we have listed (in this table) whichever of the two spectra is more diagnostic.

<sup>b</sup>The relative abundances recorded for these spectra are very dependent upon source and focussing conditions and upon the pressure of collision gas. Differences of  $\pm 5$ -10% are not unusual for major peaks.

<sup>c</sup>Unresolved.

Scheme 3.20

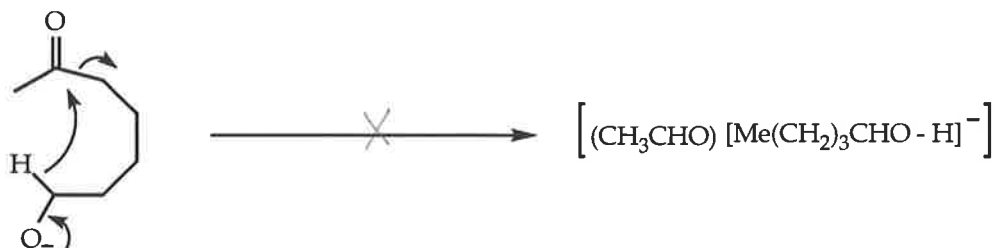


The major fragmentations summarised in scheme 3.20 reveal characteristic losses of H<sub>2</sub>, water, carbon monoxide, and formaldehyde: the product ion

studies indicate that these processes are analogous to similar processes listed in scheme 3.5. The formation of the acetone enolate anion  $m/z$  57 occurs *via* an  $S_Ni$  process to eliminate tetrahydrofuran similar to the oxetane loss shown in scheme 3.10.

This spectrum lacks the peak at  $m/z$  43 which would correspond to  $(CH_2CHO)^-$  occurring by the  $S_Ni$   $H^-$  'migration' through a seven centred state (scheme 3.21, *cf.* schemes 3.15 and 3.19). This process would afford an anion/neutral complex which may dissociate to yield deprotonated pentanal ( $m/z$  85). Data listed in Table 3.6 indicates that product ion  $m/z$  85 is not deprotonated pentanal. The product is deprotonated pentanone, formed following loss of oxirane (*cf.* the  $S_Ni$  process shown in scheme 3.11). The  $S_Ni$  process (scheme 3.21) involving loss of pentanal does not occur for this system.

Scheme 3.21



### 3.2.2 Possible Migration of the Methyl Ion

#### 3.2.2.1 Reactions of Deprotonated 2-Dimethyl Substituted Keto-Alcohols

Does methyl anion migration occur in similar keto-alkoxide systems to those investigated for  $H^-$  migration? If the potential migrating hydrogen atoms are replaced with methyl groups, are methyl anion/neutral

complexes involved in fragmentation? Table 3.7 lists the compounds studied in this series along with their respective CA MIKE data. The CA MIKE spectrum of the (M-D)<sup>-</sup> ion from 5-methyl-hydroxy-(OD)-hexan-2-one **4** is also shown in Figure 3.4.

Table 3.7 CA negative ion spectra for (M-D)<sup>-</sup> or (M-H)<sup>-</sup> ions of **4**, **5**, **10** and **11**.

Precursor	Spectrum [ <i>m/z</i> (loss of $\text{X}^{\cdot-}$ formation) relative abundance]
(M-D) <sup>-</sup> ion of MeCO(CH <sub>2</sub> ) <sub>2</sub> C(Me) <sub>2</sub> OD <b>4</b>	113(CH <sub>4</sub> )100, 111(H <sub>2</sub> O)11, 95(CH <sub>4</sub> + H <sub>2</sub> O)4, 71(Me <sub>2</sub> CO)48, 57(C <sub>4</sub> H <sub>8</sub> O)42.
(M-H) <sup>-</sup> ion of CD <sub>3</sub> COCD <sub>2</sub> CH <sub>2</sub> C(Me) <sub>2</sub> OH <b>5</b>	118(CH <sub>4</sub> )100, 116(H <sub>2</sub> O)45, 115 <sup>a</sup> (HOD)30, 76(Me <sub>2</sub> CO)28, 57(C <sub>4</sub> H <sub>3</sub> D <sub>5</sub> O).
(M-D) <sup>-</sup> ion of MeCO(CH <sub>2</sub> ) <sub>2</sub> C(Me) <sub>2</sub> OD <b>10</b>	127(CH <sub>4</sub> )62, 125(H <sub>2</sub> O)100, 85(Me <sub>2</sub> CO)22, 57(C <sub>5</sub> H <sub>10</sub> O)42
(M-H) <sup>-</sup> ion of CD <sub>3</sub> COCD <sub>2</sub> (CH <sub>2</sub> ) <sub>2</sub> C(Me) <sub>2</sub> OH <b>11</b>	134(CH <sub>4</sub> )50, 125(H <sub>2</sub> O)100, 90(Me <sub>2</sub> CO)18, 57(C <sub>5</sub> H <sub>5</sub> D <sub>5</sub> O)25.

<sup>a</sup>unresolved.

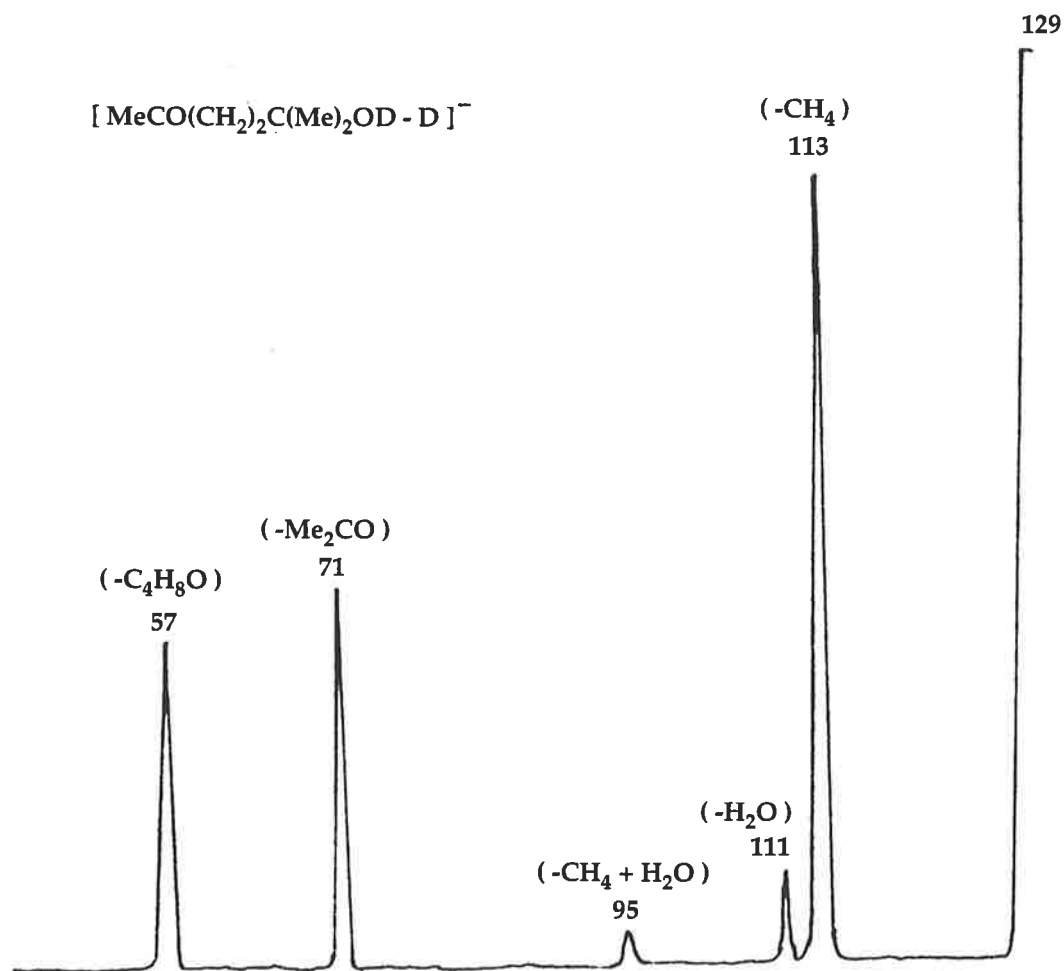


Figure 3.4 The CA MIKE spectrum of (M-D)<sup>-</sup> ion of 5-methyl-hydroxy-OD-hexan-2-one (4).

The spectra of the methyl derivatives are simpler than those of H substituted analogous considered previously. Major product ions are identified in Table 3.8 and the respective processes are summarised in scheme 3.22.

Table 3.8 Comparison of Collisional Activated or Charge Reversal (positive ion) mass spectra of product anions from the (M-D)<sup>-</sup> ion of **4**, with the spectra of authentic anions (formed by deprotonation of the appropriate neutrals).<sup>a, b</sup>

Ion ( <i>m/z</i> )	Spectrum type	Spectrum CA [ <i>m/z</i> (loss of formation)rel. abundance] CR[ <i>m/z</i> (rel. abundance)]
[-CH <sub>4</sub> ] (113)	CA	112(H <sup>•</sup> )100, 111(H <sub>2</sub> )92, 97(CH <sub>4</sub> )23, 95(H <sub>2</sub> O)98, 85(CO)2, 83(CH <sub>2</sub> O)1, 69(C <sub>2</sub> H <sub>4</sub> O)5, 43(C <sub>4</sub> H <sub>6</sub> O)2.
[MeCO(CH <sub>2</sub> ) <sub>2</sub> COMe - H] <sup>-</sup> (113)	CA	112(H <sup>•</sup> )100, 111(H <sub>2</sub> )98, 97(CH <sub>4</sub> )17, 95(H <sub>2</sub> O)100, 85(CO)2, 83(CH <sub>2</sub> O)1, 69(C <sub>2</sub> H <sub>4</sub> O)3, 43(C <sub>4</sub> H <sub>6</sub> O)2.
[-H <sub>2</sub> O] (111)	CR	111(26), 110(9), 109(7), 95(8), 93(3), 91 <sup>c</sup> , 82(6), 81(20), 79(14), 77(7), 69(18), 68(37), 67(61), 65(35), 63(15), 55(71), 53(39), 51(55), 41(70), 39(100), 29(9), 27(26).
[MeCOCH <sub>2</sub> CH=C(Me) <sub>2</sub> - H] <sup>-</sup> (111)	CR	111(27), 110(9), 109(9), 95(9), 93(5), 91(7), 82(8), 81(15), 79(11), 77(9), 69(12), 68(42), 67(57), 65(30), 63(16), 55(62), 53(36), 51(54), 41(74), 39(100), 29(9), 27(27).
[-CH <sub>3</sub> COCH <sub>3</sub> ] (71)	CR	57(5), 56(9), 55(18), 53(5), 44(55), 43(22), 42(40), 41(20), 39(14), 29(22), 28(31), 27(100), 26(73), 15(5), 14(4).
[MeCOCH <sub>2</sub> Me - H] <sup>-</sup> (71)	CR	see Table 3.3
[-C <sub>4</sub> H <sub>8</sub> O] (57)	CR	56(1), 55(10), 54(3), 53(4), 43(69), 42(100), 41(25), 39(54), 29(41), 28(12), 27(42), 26(19), 14(6), 13(1).
[MeCOMe - H] <sup>-</sup> (57)	CR	see Table 3.3

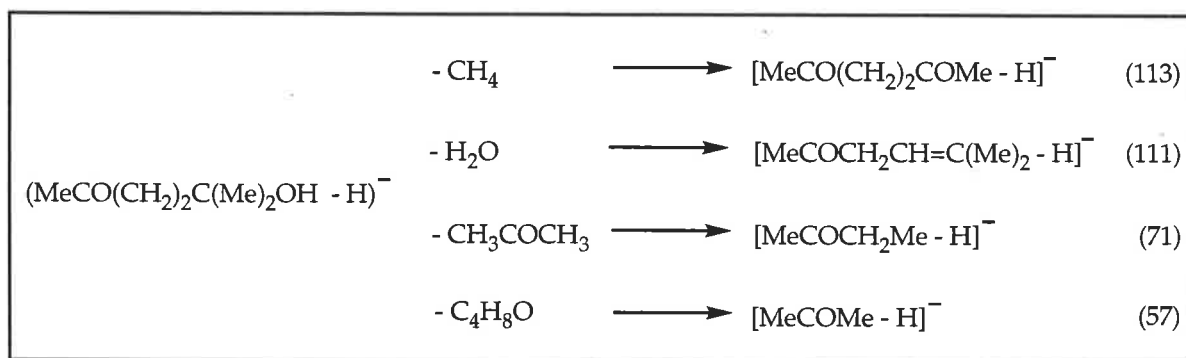
<sup>a</sup>Both CA (negative) and charge reversal (CR, positive) mass spectra have been determined for the species listed in this table. For brevity, we have listed (in this table) whichever of the two spectra is more diagnostic.

<sup>b</sup>The relative abundances recorded for these spectra are very dependent upon source and focussing conditions and upon the pressure of collision gas. Differences of ± 5-10% are not unusual for major peaks.

<sup>c</sup>Unresolved.



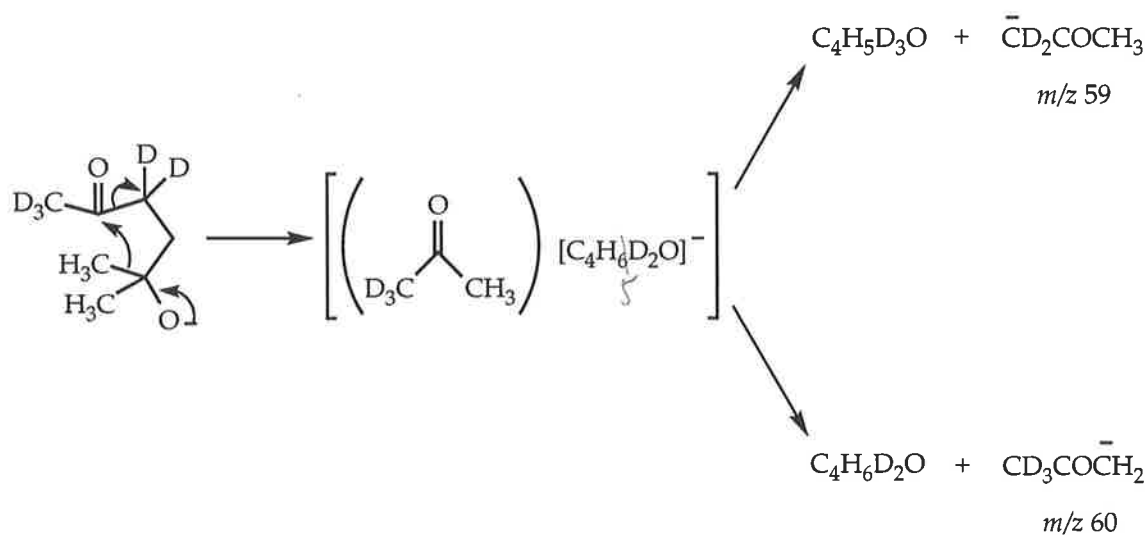
Scheme 3.22



The loss of water is straightforward and similar to processes described earlier. The loss of methane, analogous to the loss of H<sub>2</sub> described earlier, could involve an incipient Me<sup>-</sup> ion deprotonating either at the 2 position or 3 methylene position. The data obtained for the (M-H)<sup>-</sup> ion of labelled derivative **5** (Table 3.7) indicates exclusive loss of CH<sub>4</sub>. Thus the methyl anion deprotonates at only the 2 position, and the mobility of the methyl anion in this system is therefore not as facile as that of the hydride ion in the systems considered previously.

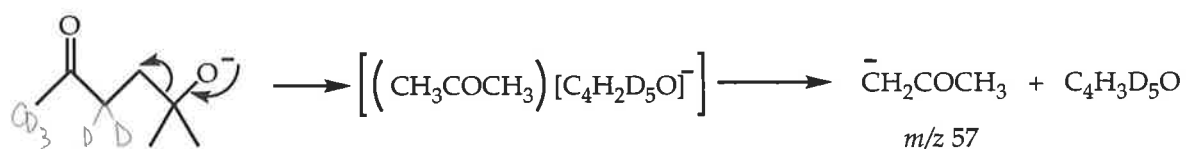
The acetone enolate anion should be produced if the methyl anion migrates along the chain to effect a nucleophilic attack on the carbonyl (*cf.* scheme 3.15, page 73). This process is illustrated in scheme 3.23 for the (M-H)<sup>-</sup> ion of the *d*<sub>5</sub>-labelled derivative **5** which should give both *m/z* 59 and 60 following Me<sup>-</sup> migration.

Scheme 3.23



The data obtained for the labelled derivative **5** (Table 3.7) reveals a product ion at only  $m/z$  57. No product ions  $m/z$  60 or 59 (scheme 3.23) are observed. Thus the acetone enolate anion is formed by the fragmentation shown in scheme 3.24, a process directly analogous to the formaldehyde loss shown in scheme 3.9.

Scheme 3.24



Alkoxide anions from the next homologue **10** (Table 3.7) and its labelled derivative **11** show the same fragmentations as those already described in

schemes 3.12 and 3.24. There is no evidence to suggest that the methyl anion can migrate to either: (i) deprotonate along the carbon chain or (ii) effect the reaction at the carbonyl centre earlier discussed for the hydride ion.

### 3.3 Summary and Conclusions

The negative ion mass spectra of the  $(M-H)^-$  ions  $\text{MeCO}(\text{CH}_2)_n\text{OH}$  ( $n=3-5$ ) are amongst the most complex yet reported for negative ions. The major processes for these keto-alkoxide ions have been identified and described in detail and the alkoxide anion is the initiating species for the majority of reactions. When  $n = 3$  we observe the mobility of a  $\text{H}^-$  ion (from position 1) which may migrate along the chain and effect a 1,3 elimination of  $\text{H}_2$ : This competes with the normal 1,2 elimination. When the alkyl chain is extended by 1 or more methylene groups,  $\text{H}^-$  migrations to effect competing  $\text{H}_2$  eliminations are not evident. Formation of  $(\text{CH}_2\text{CHO})^-$  from  $\text{MeCO}(\text{CH}_2)_4\text{O}^-$  involves the transfer of  $\text{H}^-$  from the methylene group next to the OH to the carbonyl group at the other end of the carbon chain. This  $\text{H}^-$  transfer may occur through five and six centred states (for  $n = 3$  and 4 respectively) but the analogous process when  $n = 5$  (which would require a seven centred intermediate) does not occur.

When the 'migrating' hydrogens are replaced with methyl groups, the corresponding spectra are simple. The only process involving  $\text{Me}^-$  is that where  $\text{Me}^-$  effects deprotonation at the adjacent position.

# Chapter 4

## Competitive cyclisations of Epoxy-Alkoxide ions

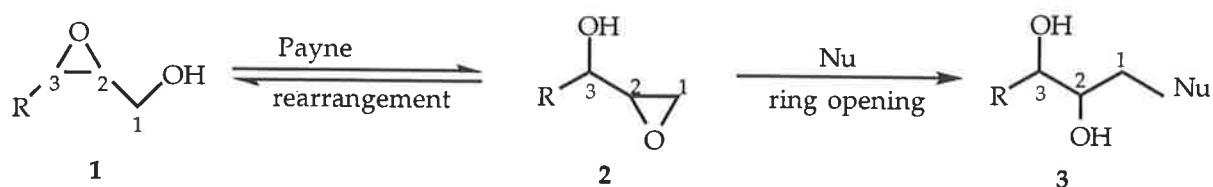
### 4.1 Introduction

*Epoxide compounds are extremely important as far as synthetic organic chemistry is concerned.*

This statement is verified by the considerable amount of interest epoxide chemistry has attracted in the past and indeed in the present.<sup>90-101</sup> The literature indicates that syntheses of natural products *via* epoxide-containing intermediates are of great interest. Epoxides are easily synthesised from a variety of compounds, and are easily opened under a wide range of conditions. One very favourable aspect of epoxide-opening reactions is that they are usually stereospecific, proceeding with inversion of configuration at the site of ring opening *via* an S<sub>N</sub>2 mechanism.

In 1962, Payne published a study of isomerisations of 2,3-epoxy alcohols under basic conditions,<sup>102</sup> a phenomenon already well known to sugar chemists.<sup>103</sup> Payne, however was the first to publish detailed observations of the epoxide migration reaction in simple acyclic compounds and as a result, this migration reaction is referred to as the 'Payne-rearrangement'. The Payne-rearrangement involves intramolecular nucleophilic attack by an alkoxide ion on an adjacent epoxide to form an isomeric alkoxide (scheme 4.1).

Scheme 4.1



The Payne-rearrangement is normally carried out at reflux in aqueous sodium hydroxide solution, usually in the presence of a co-solvent (no reaction is observed using NaH in tetrahydrofuran),<sup>102</sup> and the isomerisation produces an equilibrium mixture of the two epoxides (1) and (2). The Payne-rearrangement is not generally a useful preparative method because it often produces an equilibrium mixture of epoxy-alcohols. For example, Wood<sup>104</sup> achieved a high-yielding, enantioselective synthesis of medicinally active methyl 3,4-anhydroshikimate, which unfortunately suffered a Payne-rearrangement under mildly basic conditions to afford an inseparable equilibrium mixture of two isomeric epoxides. Carlson<sup>105</sup> reported a method for determining the extent of an unwanted Payne-rearrangement during the synthesis of atenolol, a  $\beta$ -receptor blocking agent used for the treatment of hypertension, angina and arrhythmia's. He investigated this reaction by studying the EI mass spectrum of deuteriated atenolol so as to follow attempts to eliminate the unwanted Payne side reaction. Tius,<sup>106</sup> however, had success with the Payne-rearrangement in his synthesis of disubstituted naphthalene 1,2-oxides. He was able to achieve a key Payne-rearrangement in a reported yield of 90%.

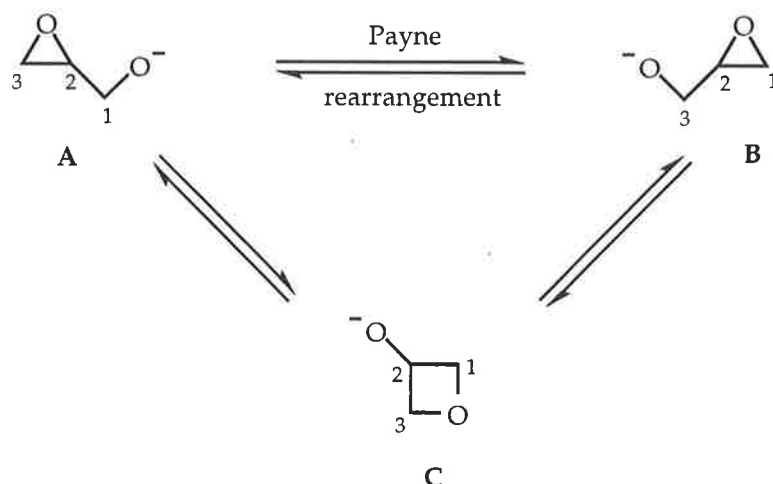
Ganem<sup>107</sup> and Sharpless<sup>108</sup> independently exploited the Payne-rearrangement to its full synthetic potential by utilising the often different reactivities of the two isomeric epoxides in a further reaction to displace the equilibrium and so give eventually one product. A major advance in the synthetic utility of the Payne-rearrangement came with the realisation that a

nucleophile which is introduced into an equilibrating mixture of epoxy alcohols may react selectively with one of the epoxy alcohols (scheme 4.1). Under basic conditions the terminal epoxide position of **2** is very much more reactive than the C<sub>2</sub> and C<sub>3</sub> positions of **1** and the C<sub>2</sub> position of **2** due to steric hinderance. Thus, with a suitable nucleophile, attack takes place selectively at C<sub>1</sub> of **2**, displacing the equilibrium to afford **3** as the sole product of the reaction. This process has been used to produce enantiomerically pure vicinal diol products.<sup>108-110</sup>

The condensed phase Payne-rearrangement has some notable features, namely:

- (i) in an unsymmetrical system the predominant product is normally that which has the more alkyl substitution on the epoxide ring; whether this is a feature of the thermodynamics or the kinetics has not been studied in solution;
- (ii) the requirement of a protic solvent with high dielectric constant suggests charge separation in the transition state if the reaction is proceeding under conditions of kinetic control; and
- (iii) there is no indication that the alternative cyclisation through a four-centred transition state to form an oxetane system **C** competes with the Payne-rearrangement.

Scheme 4.2



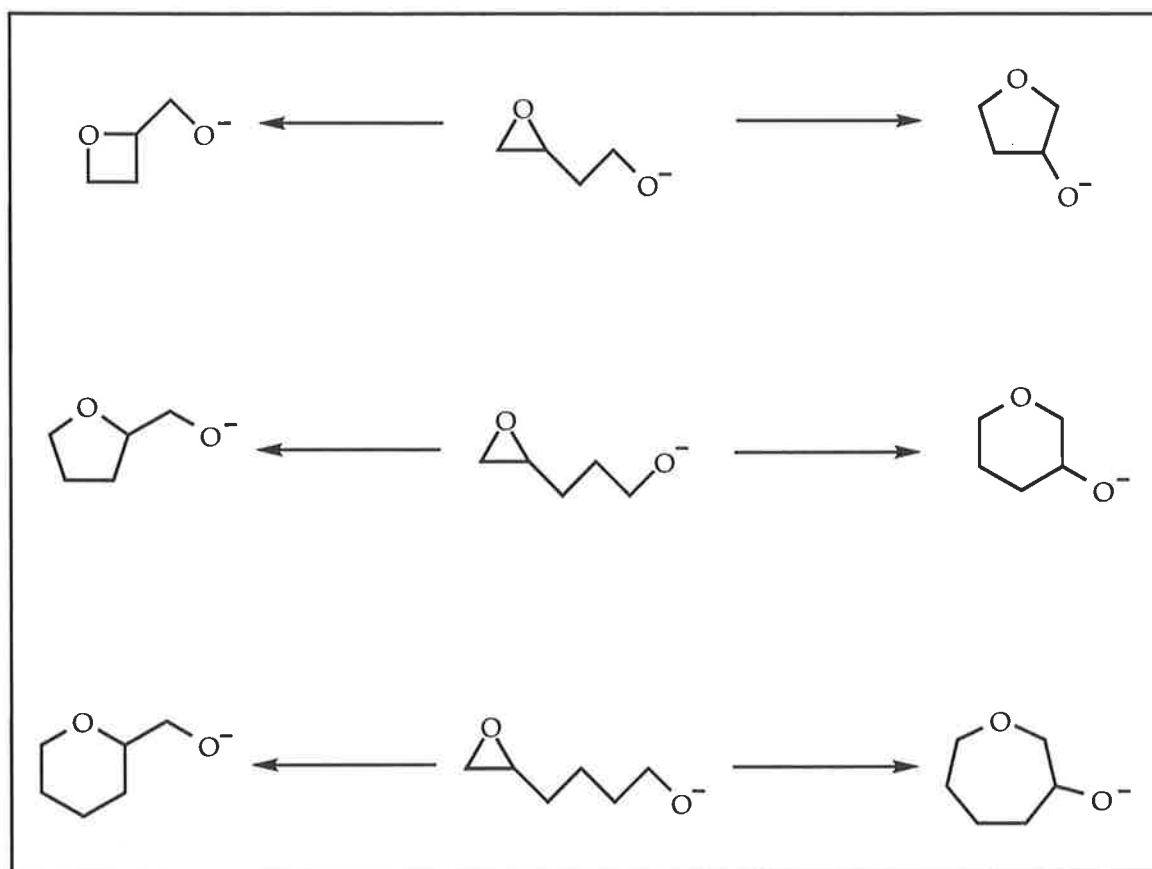
The Payne-rearrangement is clearly influenced by solvent effects,<sup>102</sup> as such, the fundamental reactivity of this reaction is best determined in the gas phase, in the absence of solvent and counter ions.<sup>111</sup>

The scenario outlined in scheme 4.2 has been extensively investigated in the gas phase both experimentally and theoretically.<sup>112</sup> Dua *et al.* demonstrated *via* computational *ab initio* calculations and extensive deuterium and <sup>18</sup>O labelling of the epoxide **A** (scheme 4.2) that the degenerate Payne-rearrangement occurs in the gas phase through a three-centred mechanism. By observing the facile loss of formaldehyde, characteristic for primary alkoxides, it was shown that in the gas phase the energised 2,3-epoxypropoxide anion also undergoes the competing cyclisation *via* a four-membered transition state to form the oxetane alkoxide species **C** (scheme 4.2), a phenomenon not observed in the solution phase studies originally carried out by Payne for similar systems.<sup>102</sup>

We have extended the study of Dua in order to explore the systems summarised in scheme 4.3. We wish to investigate the S<sub>N</sub>i reactions of epoxy-alkoxide anions with the alkyl chain extended by 1, 2 and 3 methylene

groups. By studying these three systems theoretically, and experimentally in both the gas and condensed phases, we should be able to achieve an insight into the cyclisation processes of base induced epoxy-alcohols and be able to understand the mechanisms of the formations of the resulting product ions.

Scheme 4.3



Ring forming reactions are important and common processes in organic chemistry, and as such, it is not surprising that there is a general set of rules for predicting the formation of cyclic compounds *via* internal cyclisation processes. Baldwin has enunciated a set of simple rules for predicting the relative facility of different ring closures.<sup>113</sup> "Baldwin's rules" for ring



closure are of a stereochemical nature and predict that opening three-membered rings to form cyclic structures generally favour formation of the smaller ring product. The physical basis of these rules lies in the stereochemical requirements of the transition states for various ring closure processes. Although "Baldwin's rules" generally apply to condensed phase reactions, it would be interesting to investigate, in both the gas and condensed phases, whether the systems described in scheme 4.3 undergo cyclisation processes according to "Baldwin's rules".

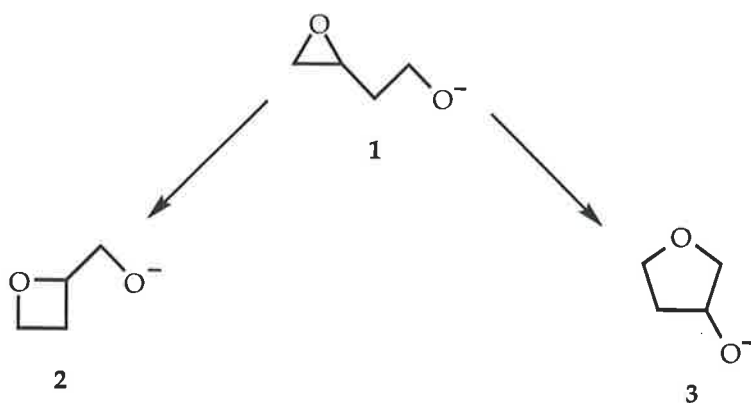
## 4.2 Results and Discussion

### 4.2.1 Competitive Cyclisations of the 3,4-Epoxybutoxide Anion

Scheme 4.4 summarises the scenario we now desire to study. We wish to explore the possible  $S_Ni$  reactions of the 3,4-epoxybutoxide anion (1) both theoretically and experimentally in the gas and solution phases in order to answer the following questions. Firstly, do the reactions where the alkoxide ion attacks the least substituted epoxide carbon to afford the tetrahydro-3-furanyl alkoxide ion (3) take place, or does attack of the nucleophilic alkoxide ion occur at the most substituted epoxide carbon to yield the 2-oxetanylmethanol alkoxide anion (2) (scheme 4.4). Secondly, if both cyclisations do occur, what information can we obtain from the transition state structures calculated by *ab initio* studies, since Dua<sup>112</sup> has shown that the angle of approach of  $O^-$  to the receptor carbon in the Payne process is a major feature influencing the relative barriers to the transition states. Dua has postulated that the closer the OCO angle is to  $180^\circ$  (i.e. the closer the geometry represents an ideal  $S_N2$  type transition state), the lower the barrier of the  $S_Ni$  process. This is true for the Payne system, since the strain

energies of the epoxide and the oxetane rings have only minor influence on the competition between the three- and four-centred cyclisations, since the strain energies of ethylene oxide and oxetane are comparable (112.5 and 107 kJ mol<sup>-1</sup> respectively).<sup>114</sup> Another interesting question is whether or not equilibria between **1**, **2** and **3** occur during the reaction conditions, or are processes **1** to **2** and **1** to **3** irreversible?

Scheme 4.4



#### 4.2.1.1 *Ab Initio* Calculations for Competing Cyclisations of the 3,4-Epoxybutoxide Anion

The results of an *ab initio* computational study at G2 level using Gaussian 94<sup>51</sup> are summarised in Figure 4.1. The data presented in Figure 4.1 show that the barriers to the two transition states **C** and **D** are comparable (70 and 69 kJ mol<sup>-1</sup> respectively). Gas phase ionic reactions are generally kinetically controlled and the rates of reaction are dependent principally on two factors, *viz.* the barrier to the transition state, and the probability of reaction (frequency factor, the pre-exponential Arrhenius factor).<sup>115</sup> Reaction

coordinate plots of the type shown in Figure 4.1 provide primary data concerning the barrier to the transition state, but do not describe the frequency factor.

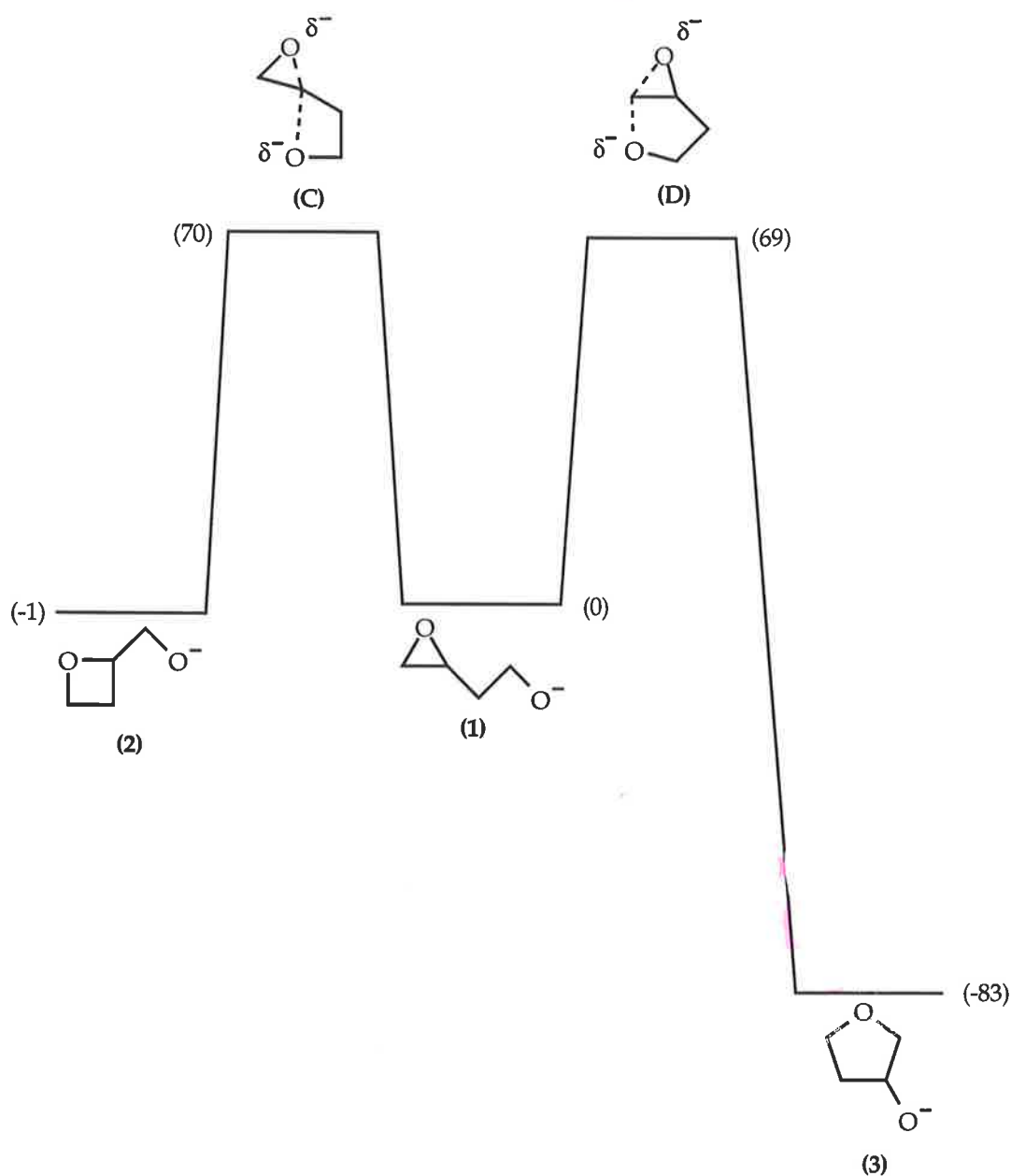


Figure 4.1 *ab initio* calculations [GAUSSIAN94, geometries RHF/6-31+G(d), energies MP2-Fc/6-31+G(d)] for the competitive  $S_Ni$  cyclisations of the 3,4-epoxybutoxide anion. Energies are shown as kJ mol<sup>-1</sup>. For discussion of the transition structures see section 4.3. Full details of geometries and energies are recorded in Appendix A.

The *ab initio* calculations (Fig. 4.1) predict that a suitably energised 3,4-epoxybutoxide anion may undergo  $S_Ni$  cyclisation. The energy barrier of the two competing processes are similar and the relative proportions of products **2** and **3** (from **1**) should be comparable if the rates of the two reactions are controlled by the relative barriers to the transition states. The calculations also predict that reaction of **1** to **2** should be reversible, and if this is true under appropriate experimental conditions, thermodynamic product **3** may be formed in the higher yield.

#### 4.2.1.2 Gas Phase Reactions of **1**, **2** and **3**

The CA tandem mass spectrum of 3,4-epoxybutoxide anion (**1**) obtained by deprotonation of 2-(2-oxiranyl)-1-ethanol by  $^-\text{OH}$  in the source of the ZAB is shown in Figure 4.2. The spectrum appears to be quite simple with product ion  $m/z$  59 exhibiting an unusual broad dish-shaped peak. Peak  $m/z$  59 is interesting in that it could be due to the loss of ethene or CO. The loss of CO is a process observed for keto-alkoxides (Chapter 3), but this loss usually produces a gaussian-shaped peak. In order to identify the neutral loss for this process we need to consider the data obtained from the CA MIKE spectra of the deuterium and  $^{18}\text{O}$  labelled analogues of **1** recorded in Table 4.1.

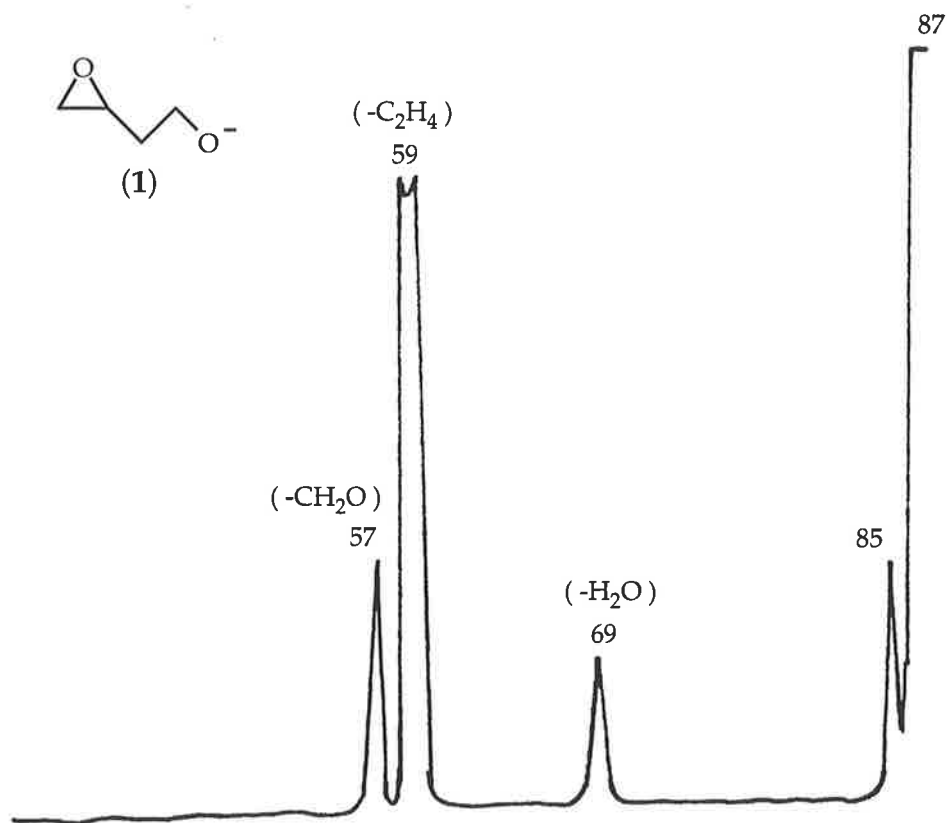
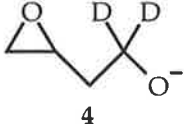
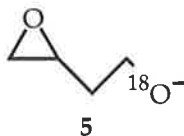
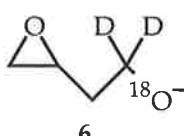


Figure 4.2 Collisional activated HO<sup>-</sup> negative ion chemical ionisation MIKE spectrum of the 3,4-epoxybutoxide anion.

Table 4.1 Mass spectra of labelled 3,4-epoxybutoxide anions.

Anion	$m/z$ (loss) abundance
 4	$88(\text{H}^+)55$ , $87(\text{H}_2, \text{D}^+)100$ , $71(\text{H}_2\text{O})20$ , $59(\text{C}_2\text{H}_2\text{D}_2, \text{CH}_2\text{O})85$ , $57(\text{CD}_2\text{O})17$ . <i>(m/z 89)</i>
 5	$88(\text{H}^+)45$ , $87(\text{H}_2)92$ , $71(\text{H}_2\text{O})7$ , $69(\text{H}_2^{18}\text{O})17$ , $61(\text{C}_2\text{H}_4)100$ , $59(\text{CH}_2\text{O})8$ , $57(\text{CH}_2^{18}\text{O})16$ . <i>(m/z 89)</i>
 6	$90(\text{H}^+)100$ , $89(\text{H}_2, \text{D}^+)82$ , $88(\text{HD})18$ , $71(\text{H}_2\text{O})3$ , $69(\text{H}_2^{18}\text{O})14$ , $61(\text{CH}_2\text{O}, \text{C}_2\text{H}_2\text{D}_2)85$ , $57(\text{CD}_2^{18}\text{O})15$ . <i>(m/z 91)</i>

The loss of CO from the labelled species **4**, **5** and **6** would result in the peaks  $m/z$  61, 61 and 63 respectively. The data in Table 4.1 clearly indicate that the observed dish-shaped peak at  $m/z$  59 (Fig. 4.2) does not arise by loss of CO since the spectra of **4** and **6** do not exhibit peaks corresponding to  $m/z$  61 and 63 respectively. The spectra from the labelled derivatives indicate that this unusual shaped peak is a result of the loss of neutral ethene, which has, in the case of **4** and **6**, incorporated 2 deuterium atoms. Peaks  $m/z$  59 and 61 from **4** and **6** may be attributed to the loss of formaldehyde (loss of 30 mass units), a process which forms a gaussian-shaped peak. The peaks at  $m/z$  59 and 61 for **4** and **5** are illustrated in Figure 4.3. The composite peak  $m/z$  59 (from **4**) shows two processes, i.e. the losses of  $\text{CH}_2\text{O}$  and  $\text{C}_2\text{H}_2\text{D}_2$ . The loss of  $d_2$ -ethene results in the dish-shaped peak, while the loss of  $\text{CH}_2\text{O}$  can be seen as the centre gaussian peak. Peak  $m/z$  61 from **5** is due exclusively to the loss of ethene and is therefore observed as a dish-shaped peak (Fig. 4.3b).

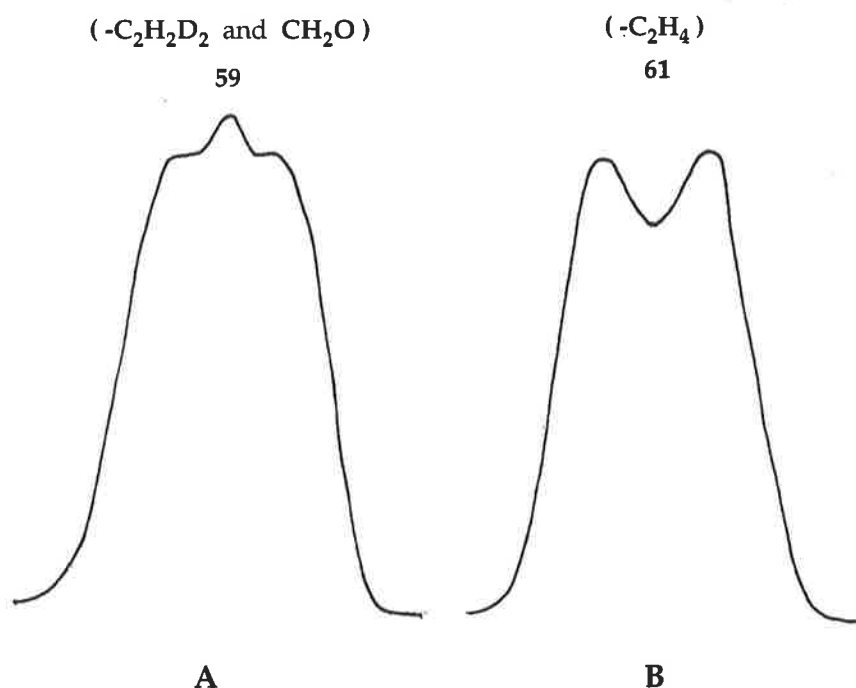
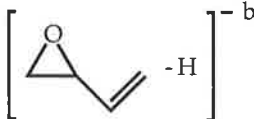


Figure 4.3 Peak profiles of the broad peaks in the spectra of the  $(M-H)^-$  ion of (A) 1,1- $d_2$ -2-(2-oxiranyl)-1-ethanol (**4**), and (B) 2-(2-oxiranyl)ethan-1- $[^{18}O]$ ol (**5**).

It is important to identify the structures of the product ions shown in Figure 4.2 and to assign mechanisms for their formation. Product ion studies of the daughter ions in the spectrum of **1** have been investigated and their spectra are recorded in Table 4.2. These spectra are compared with those of known anions prepared by unequivocal routes.

Table 4.2 Spectra of product anions from 1 and known anions.

Precursor ion ( <i>m/z</i> )	Product ion [ <i>m/z</i> (loss)]	Mode	Spectrum [CA, <i>m/z</i> (loss) abundance] [CR, <i>m/z</i> (abundance)] <sup>a</sup>
(1)	69 (-H <sub>2</sub> O)	CR	69(1), 68(73), 66(4), 55(11), 54(5), 53(8), 52(6), 51(8), 50(15), 42(43), 41(27), 40(8), 39(100), 38(20), 37(13), 29(15), 27(25), 26(41), 25(28).
	69	CR	69(1), 68(100), 66(6), 54(16), 53(12), 52(8), 51(12), 50(18), 42(6), 41(27), 40(10), 39(71), 38(21), 37(9), 29(18), 27(8), 26(10), 25(12).
		CA	68(H)65, 67(H <sub>2</sub> )100, 51(H <sub>2</sub> O)17, 41(CO)34, 39(CH <sub>2</sub> O)2.
[CH <sub>3</sub> COCH=CH <sub>2</sub> - H] <sup>- c</sup>	69	CR	68(2), 66(1), 55(33), 54(8), 53(12), 52(7), 51(9), 50(19), 42(100), 41(33), 39(38), 37(10), 29(5), 27(46), 26(28), 25(10), 14(1).
		CA	68(H)100, 67(H <sub>2</sub> )12, 41(C <sub>2</sub> H <sub>4</sub> )90
(1)	59 (-C <sub>2</sub> H <sub>4</sub> )	CA	58(H')100, 57(H <sub>2</sub> )65, 44(-CH <sub>3</sub> )8, 31(CO)32, 29(CH <sub>2</sub> O)11.
		CR	59(12), 58(29), 56(31), 45(11), 44(22), 43(15), 42(22), 41(20), 31(18), 30(22), 29(100), 28(29), 15(2).
<sup>-</sup> OCH <sub>2</sub> CHO <sup>d</sup>	59	CA	58(H')100, 57(H <sub>2</sub> )60, 31(CO)30, 29(CH <sub>2</sub> O)13.
		CR	59(8), 58(33), 56(19), 42(24), 41(27), 31(31), 30(44), 29(100), 28(39).
CH <sub>3</sub> CO <sub>2</sub> <sup>- e</sup>	59	CR	56(4), 45(28), 44(100), 43(36), 42(38), 41(18), 29(12), 28(13), 15(10), 14(5), 13(2), 12(1).
(1)	57 (CH <sub>2</sub> O)	CA	56(H')68, 55(H <sub>2</sub> )100, 41(CH <sub>4</sub> )28, 29(C <sub>2</sub> H <sub>4</sub> )36, 27(CH <sub>2</sub> O)58.
		CR	56(12), 55(58), 53(14), 42(18), 41(20), 39(62), 38(18), 37(16), 29(100), 28(19), 27(68), 26(48), 25(15).
CH <sub>2</sub> =CHCH <sub>2</sub> O <sup>- f</sup>	57	CA	56(H')65, 55(H <sub>2</sub> )100, 41(CH <sub>4</sub> )25, 29(C <sub>2</sub> H <sub>4</sub> )32, 27(CH <sub>2</sub> O)55.
		CR	56(10), 55(64), 53(12), 42(12), 41(16), 39(54), 38(14), 37(12), 29(100), 28(26), 27(75), 26(50), 25(12).

<sup>a</sup>the relative abundances of CR spectra are critically dependent upon the collision gas pressure. Discrepancies between the abundances of peaks in the charge reversal spectra of source formed product anions and in the spectra of authentic anions is to be expected. This is particularly apparent for the CR spectra of the [(M-H)<sup>-</sup>-C<sub>2</sub>H<sub>4</sub>]<sup>-</sup> ions and of CH<sub>3</sub>CO<sub>2</sub><sup>-</sup> and <sup>-</sup>OCH<sub>2</sub>CHO. Even so, the spectra are quite characteristic, and there can be no doubt as to the structures of the two [(M-H)<sup>-</sup>-C<sub>2</sub>H<sub>4</sub>]<sup>-</sup> species. <sup>b</sup>Formed by deprotonation of butadiene monoxide. <sup>c</sup>Formed by deprotonation of methyl vinyl ketone. <sup>d</sup>Formed by reaction of HO<sup>-</sup> with glycoaldehyde dimer. <sup>e</sup>Formed by deprotonation of acetic acid. <sup>f</sup>Formed by deprotonation of allyl alcohol.

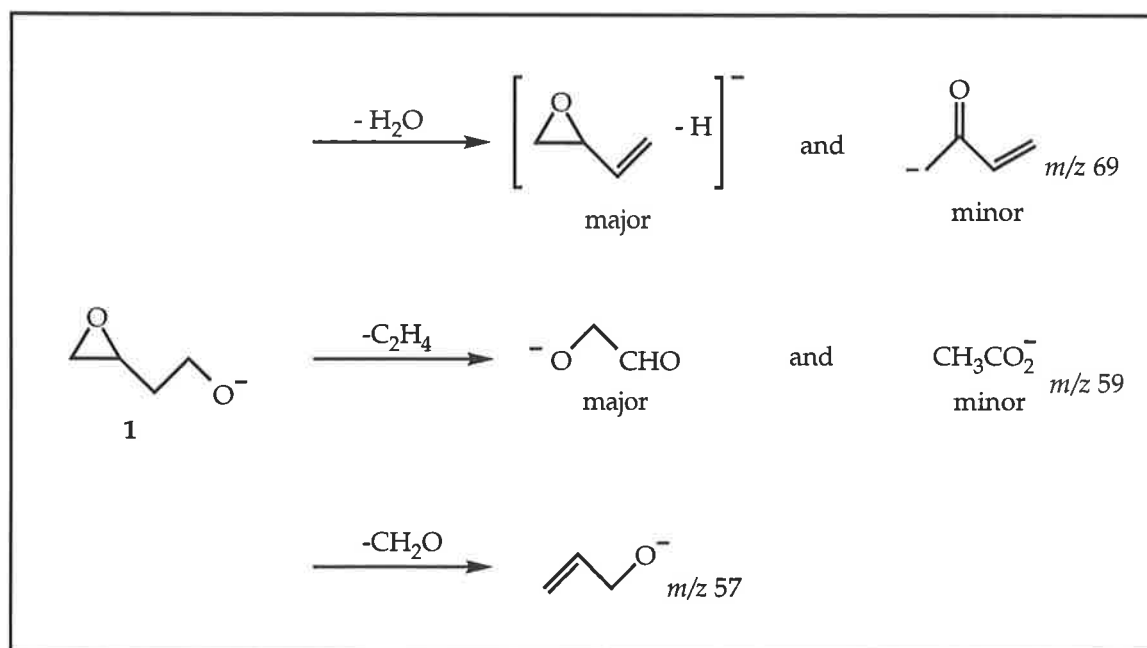


Scheme 4.5 summarises the processes occurring for anion **1**. Loss of water is quite complicated since peak  $m/z$  69 is seen to be a mixture of deprotonated methyl vinyl ketone and deprotonated butadiene monoxide. The latter would be the expected product for the characteristic loss of  $\text{H}_2\text{O}$  from a primary alkoxide anion but the formation of deprotonated methyl vinyl ketone is interesting and needs further investigation.

The loss of ethene is even more interesting since (i) the resulting dish-shaped product ion  $m/z$  59 is identified also as a mixture of isomers and (ii) loss of ethene cannot occur directly from **1**.

It appears that the characteristic loss of formaldehyde from primary alkoxides, in this case to afford deprotonated allyl alcohol may be the only process not requiring rearrangement of **1**.

Scheme 4.5



Before we propose mechanisms for processes shown in scheme 4.5, it is appropriate to consider the fragmentation processes of the oxetane anion (2) and the isomeric tetrahydrofuran anion (3).

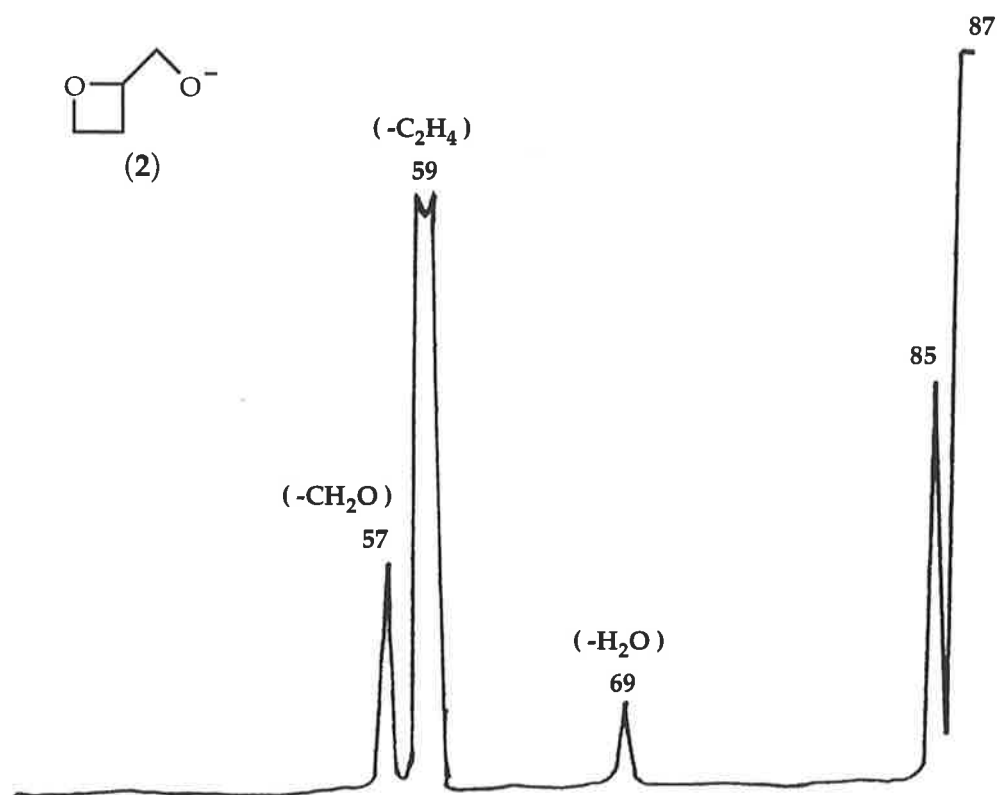


Figure 4.4 Collisional activated  $\text{HO}^-$  negative ion chemical ionisation MIKE spectrum of the 2-oxetanylmethanol alkoxide ion (2).

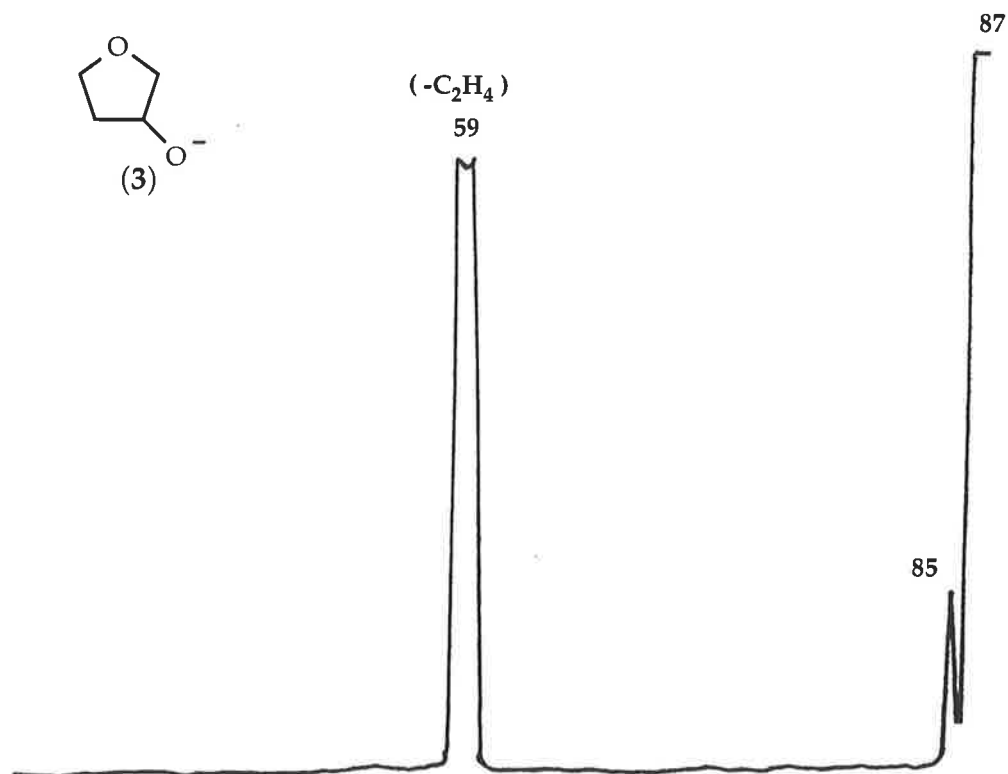


Figure 4.5 Collisional activated  $HO^-$  negative ion chemical ionisation MIKE spectrum of the tetrahydro-3-furanol alkoxide ion (3).

The collision induced MIKE spectra of **2** and **3** are shown in Figures 4.4 and 4.5 respectively. Both spectra show dish-shaped peaks at  $m/z$  59 both due to the loss of ethene. The spectrum of **2** (Fig. 4.4) is very similar to that of **1** (Fig. 4.2). However, the peak width measurements at half height of the major peaks (Table 4.3) are not identical. This suggests that either the product ions formed are different, or, if they are the same, then the mechanisms of formation of the two species must be different.

Table 4.3 Peak width measurements of  $m/z$  69 and/or  $m/z$  59 from anions 1, 2 and 3.

Isomer	Peak width [ $m/z$ (width at half height)]
1	59 ( $95.8 \pm 1.0$ v), 69 ( $75.2 \pm 1.0$ v)
2	59 ( $93.1 \pm 1.0$ v), 69 ( $72.0 \pm 1.0$ v)
3	59 ( $100 \pm 1.0$ v)

The collisionally activated or charge reversal spectra for the product ions from anions 2 and 3 are listed in Table 4.4. These spectra may be compared with the spectra of authentic anions previously investigated for the fragmentation processes of anion 1 (see Table 4.2).

Table 4.4 Spectra of product anions from 2 and 3.<sup>a</sup>

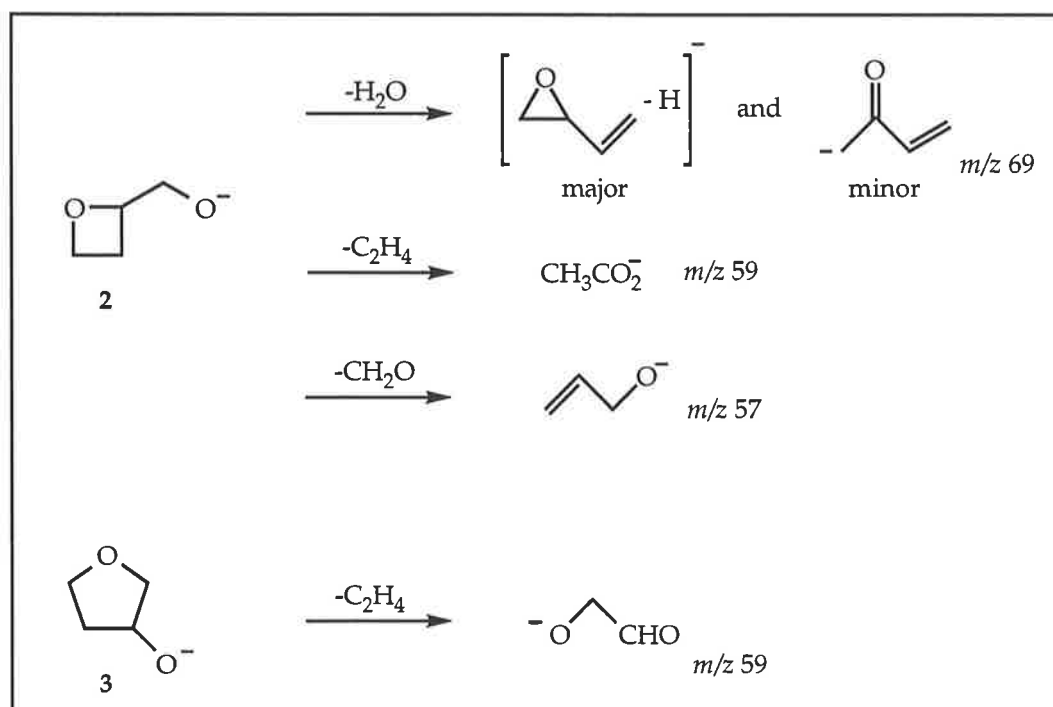
Precursor ion ( $m/z$ )	Product ion [ $m/z$ (loss)]	Mode	Spectrum [CA, $m/z$ (loss) abundance] [CR, $m/z$ (abundance)]
(4)	69 (-H <sub>2</sub> O)	CR	69(1), 68(59), 66(3), 55(10), 54(16), 53(17), 52(11), 51(16), 50(19), 42(22), 41(21), 40(12), 39(100), 38(22), 37(13), 29(22), 27(23), 26(33), 25(28).
(4)	59 (-C <sub>2</sub> H <sub>4</sub> )	CR	56(5), 45(42), 44(100), 43(34), 42(39), 41(19), 29(34), 28(28), 15(6), 14(4), 13(2), 12(1).
(5)	59 (-C <sub>2</sub> H <sub>4</sub> )	CR	59(14), 58(46), 56(42), 42(14), 41(10), 31(12), 30(32), 29(100), 28(29).
(4)	57 (-CH <sub>2</sub> O)	CA	56(H')65, 55(H <sub>2</sub> )100, 41(CH <sub>4</sub> )26, 29(C <sub>2</sub> H <sub>4</sub> )33, 27(CH <sub>2</sub> O)55.

<sup>a</sup>The abundances in both CA and CR spectra are dependent on both source conditions and collision gas pressure. As a general guide when comparing spectra, the abundance of an individual peak should be correct to  $\pm 10\%$ .

The processes observed for anions **2** and **3** are summarised in scheme 4.6. The loss of water from **2** forms a mixture of deprotonated methyl vinyl ketone and deprotonated butadiene monoxide, a similar scenario to that observed for **1**. However, the ratio of the two products is different from that observed in the spectrum of **1**. The loss of formaldehyde from **2** affords deprotonated allyl alcohol ( $m/z$  57).

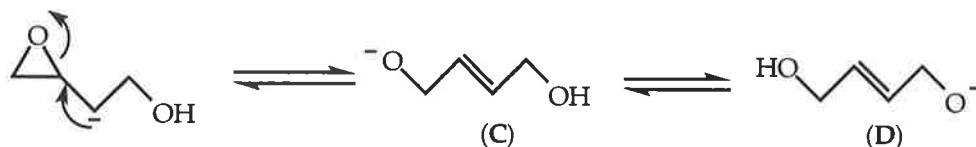
The losses of ethene from **2** and **3** give different product anions. The product ion studies identify the dish-shaped peaks from **2** and **3** to be deprotonated acetic acid and deprotonated hydroxyacetaldehyde respectively and exclusively. This should be contrasted with **1**, where  $m/z$  59 is a mixture of the two product anions.

Scheme 4.6

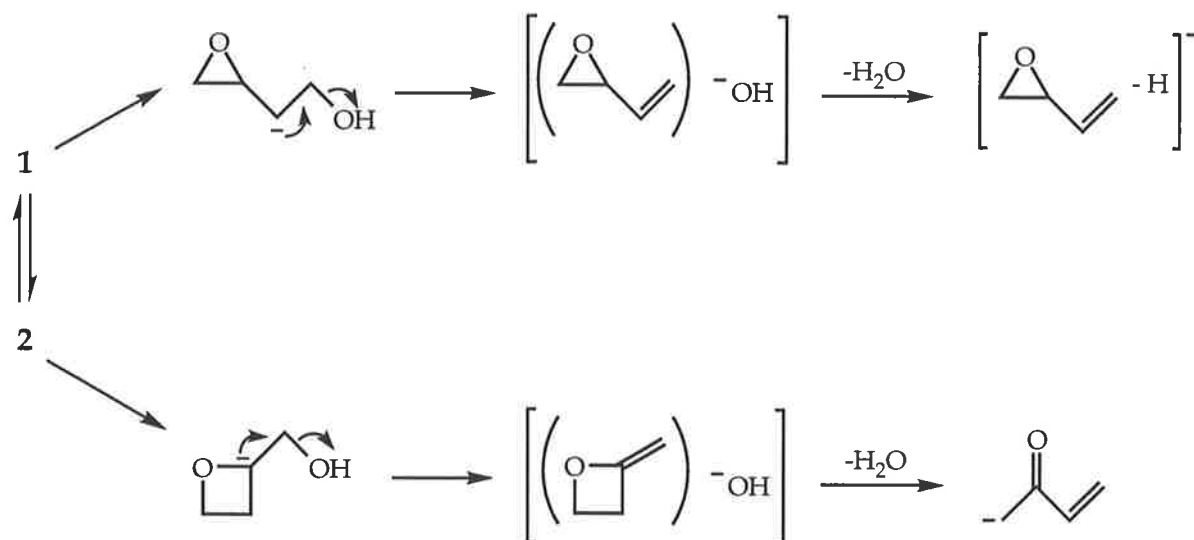


Taking the product ion studies (Tables 4.2 and 4.4) into consideration, we can conclude that under the gas-phase experimental conditions, the 3,4-epoxybutoxide anion does undergo both  $S_Ni$  processes outlined in scheme 4.4. As predicted by the *ab initio* results (Fig. 4.1) anions **1** and **2** do interconvert and the process is reversible. This equilibrium leads to the similarities in the two spectra. There are, however, subtle differences in the spectra of **1** and **2**, these being due to (i) the differences in equilibria and (ii) some interconversion of **1** to **3** (an irreversible process). We propose that the losses of  $CH_2O$  and  $H_2O$  from **1** and **2** are principally fragmentations of **1**, with a minor proportion of these losses following equilibration of the two oxygens by formation of **C** and **D** *via* a proton transfer followed by ring opening (scheme 4.7).

Scheme 4.7

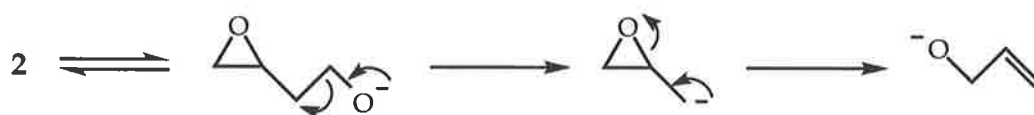


Deprotonated butadiene monoxide (the major product resulting from loss of water) is formed exclusively from **1**, and the formation of the methyl vinyl ketone enolate anion (the minor product resulting from loss of water) is formed exclusively from **2** (scheme 4.8).

Scheme 4.8<sup>a</sup>

The formation of deprotonated allyl alcohol ( $m/z$  57) occurs from the characteristic alkoxide loss of formaldehyde to afford an intermediate epoxy carbanion which ring opens to form the more stable alkoxide ion (scheme 4.9).

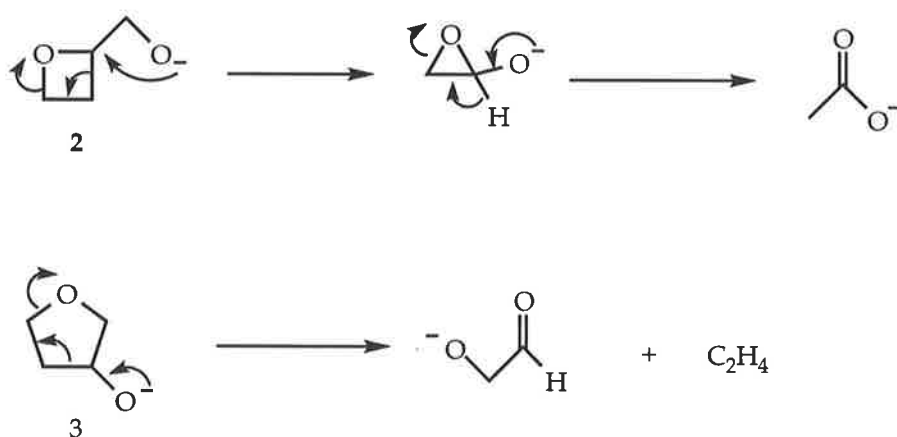
Scheme 4.9



<sup>a</sup> The key observation here is that the CR spectra of the  $m/z$  69 daughter ions of 1 and 2 are identical. If deprotonation of butadiene monoxide occurs at the allylic centre, that ion should ring open to afford deprotonated methyl vinyl ketone. However, the CA and CR spectra of the  $(M-H)^-$  ion of authentic butadiene monoxide are different from those of the  $(M-H)^-$  ion of methyl vinyl ketone (see Table 4.2, page 106). A study of deuterium labelled butadiene monoxide analogues may verify the site of deprotonation. At least two labelled derivatives of butadiene monoxide are required for this purpose, the syntheses of which are not trivial and have not been attempted. In summary, it is evident that deprotonated butadiene monoxide does not rearrange to yield deprotonated methyl vinyl ketone, and that the loss of  $H_2O$  from 1 and 2 produce a composite CR spectrum of the two product ions.

The product ion data summarised in Table 4.4 indicate that the loss of  $C_2H_4$  from **2** yields  $CH_3CO_2^-$ , whereas the analogous loss from **3** forms  $^-OCH_2CHO$ . Suggested mechanisms for the formation of these ions are shown in scheme 4.10. The formation of the acetate anion from **2** is unusual, but is analogous to the mechanism proposed to account for the formation of  $(MeCOCH_2)^-$  from the cyclopropanol alkoxide ion.<sup>83</sup> The high electron affinity of the acetate radical is probably the driving force of this reaction.

Scheme 4.10



Both losses of ethene shown in scheme 4.10 yield broad dish-shaped peaks (see Figs. 4.2, 4.4 and 4.5). The analogous peak in the spectrum (Fig. 4.2) of **1** corresponds to a mixture of  $CH_3CO_2^-$  and  $^-OCH_2CHO$  with the latter being the major contributor. It is also noteworthy that the width at half height of the composite peak for the loss of  $C_2H_4$  from **1** ( $95.8 \pm 1.0$  v) is intermediate between those for the losses  $C_2H_4$  from **2** ( $93.1 \pm 1.0$  v) and **3** ( $100.0 \pm 1.0$  v).



Thus both **2** and **3** are formed from energised **1**, but since the spectra shown in Figures 4.4 and 4.5 are different, ions **2** and **3** are not interconvertable under the reaction conditions.

#### 4.2.1.3 Condensed Phase Reactions of **1**, **2** and **3**

The results described thus far apply to reactions carried out in the absence of solvent. It would be interesting to see whether we could observe a similar trend for the analogous base catalysed reaction in solution. We have investigated the reactions of the neutrals of **1**, **2** and **3** in two solvent systems, (A) 10% aqueous sodium hydroxide at 100°C, and (B) sodium hydride-tetrahydrofuran at 66°C. These two systems mimic the conditions investigated by Payne in his original study of the Payne-rearrangement.<sup>102</sup> The products were monitored at different times using GCMS (conditions outlined in the experimental section) and the results are recorded in Table 4.5. The following observations can be made from this study:

- (i) The anion **1** converts to both **2** and **3**, with **3** being the major product,
- (ii) The four-membered ring system **2** converts slowly to the 3,4-epoxybutoxide anion **1**, which in turn forms **2** and **3**,
- (iii) The five-membered ring system **3**, is stable under the reaction conditions and no conversion to either **1** or **2** occurs,
- (iv) The conversions of **1** to **2** and **3** are more facile than the conversion of **2** to **1**, and
- (v) The S<sub>N</sub>i reaction of both **1** and **2** proceed more readily in the NaH-tetrahydrofuran system.

The reaction of **1** to **2** is more favourable than the reverse reaction **2** to **1**. This is in contrast to the scenario predicted from the *ab initio* results (Fig. 4.1). The slow conversion of **2** to **1** is not reflected in the ratio of products **2**

and 3 (from 1) with increasing time because 2 constitutes only some 10% of the product mixture 2 and 3.

Table 4.5. Base catalysed solution reactions of the neutrals of 1, 2 and 3.

Reactant	Time	Method A <sup>a</sup>	Method B <sup>a</sup>
2-(2-oxiranyl)-1-ethanol	10 min.	100:0:0 <sup>b</sup>	73:3:24 <sup>b</sup>
	1 hr.	77:3:20	21:7:62
	15 hrs.	22:11:67	11:11:78
	30 hrs.	20:10:70	10:11:79
	60 hrs.	20:10:70	9:10:81
2-oxetanyl-methanol	3 hrs.	0:100:0	0:100:0
	15 hrs.	19:100:0	50:100:1
	30 hrs.	27:100:9	24:100:20
tetrahydro-3-furanol	30 hrs.	0:0:100	0:0:100

<sup>a</sup>For experimental conditions see experimental section.

<sup>b</sup>The ratio of products refers to the 3:4:5 membered cyclic alcohols and is obtained by comparing the areas under each peak (this ratio correlates closely with the ratios obtained using ion counts/peak). The error in each number within a ratio is *ca.*  $\pm 5\%$ .

#### 4.2.1.4 Summary

Overall, for this system, *ab initio* calculations suggest that energised 1 should, in the absence of solvent, and under conditions of kinetic control, convert to the S<sub>N</sub>i products 2 and 3 in comparable yield. Also 1 and 2 should be interconvertible in the gas phase, and this may lead to the thermodynamic product 3 being the major isomer formed.

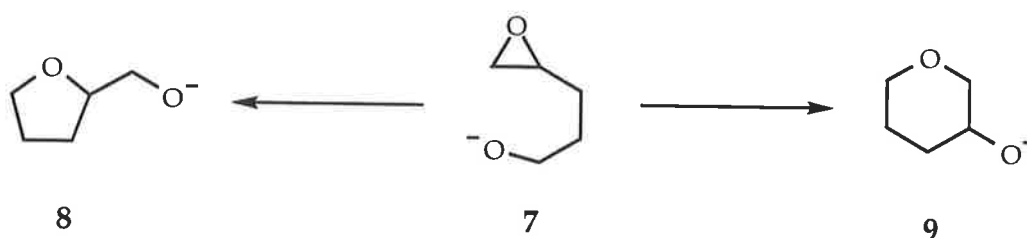
The experimental gas phase studies indicate that upon collisional activation **1** does undergo the two competitive  $S_Ni$  processes to yield **2** and **3** in comparable amounts. Compound **2** does interconvert with **1**, and thermodynamic product **3** is stable under the reaction conditions. These results are directly compatible with the theoretical predictions above.

The condensed phase studies also agree with the theoretical predictions and gas phase results above, with the exception that in the solvent systems used, the major product from **1** is **3** rather than **2**, whereas in the gas phase it appears that **2** and **3** are formed to a similar degree.

#### 4.2.2 Competitive Cyclisations of 4,5-Epoxy pentoxide Anion

Scheme 4.11 summarises the scenario we now wish to investigate. We have seen that for the energised 3,4-epoxybutoxide anion, both possible  $S_Ni$  reactions occur to similar extents. We are interested to now observe whether the energised 4,5-epoxy pentoxide anion (**7**) will follow a similar trend leading to the formation of both the five-membered anion (**8**) and the six-membered isomer (**9**) in both the gas and condensed phases.

Scheme 4.11



#### 4.2.2.1 *Ab Initio* Calculations for Competing Cyclisations of the 4,5-Epoxy-pentoxide Anion

The results of an *ab initio* computational study for the reactions shown in scheme 4.11 are summarised in Figure 4.6, and indicate that the barriers to the two transition states E and F are both 48 kJ mol<sup>-1</sup> with anion 9 being the more thermodynamically stable product. Since gas phase reactions are generally kinetically controlled the calculations shown in Figure 4.11 predict that both products 8 and 9 should be formed following the S<sub>N</sub>i reactions of the epoxy-alkoxide ion 7. This prediction is based on the assumption that the two reaction processes are controlled primarily by the transition state barriers and that the probabilities of both cyclisations are of the same order and the Arrhenius factor therefore does not contribute greatly to the reaction pathway.

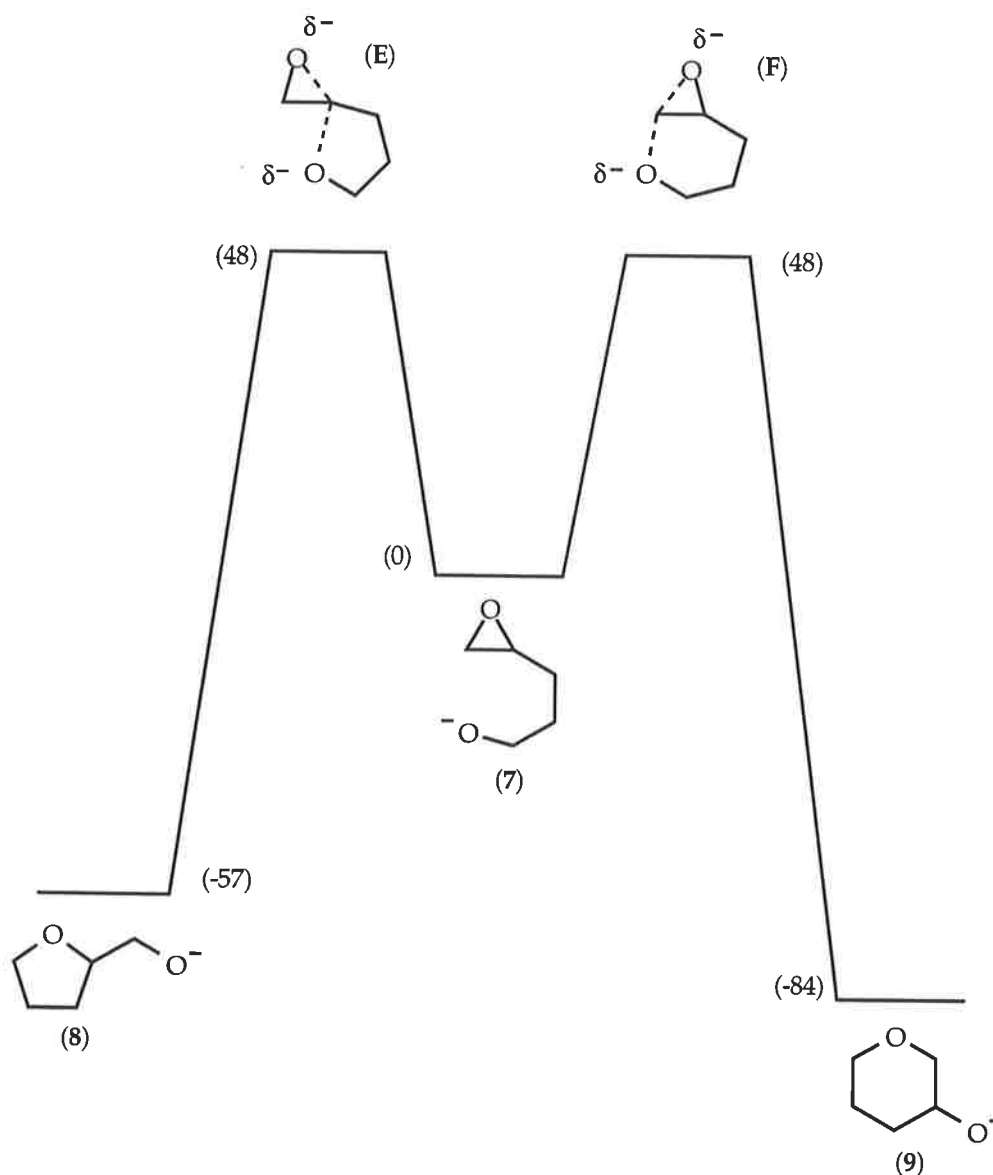


Figure 4.6 *Ab initio* calculations [Gaussian94, geometries RHF/6-31+G(d), energies MP2-fc/6-31+G(d)] for the competitive  $S_Ni$  cyclisations of the 4,5-epoxypentoxide anion. The energies are shown in  $\text{kJ mol}^{-1}$ . For full discussion of transition structures see section 4.3. Full details of geometries and energies are recorded in Appendix B.

#### 4.2.2.2 Gas Phase Reactions of 7, 8 and 9

The three alkoxide anions 7, 8 and 9 were formed following the  $S_N2$  displacement of methanol by the reaction of  $^-\text{OH}$  with the corresponding methyl ethers in the source of the ZAB (scheme 4.12). This method of anion

formation was necessary since the synthesis of the epoxy-alcohol from the usual method of epoxidation (reaction of 4-penten-1-ol with 3-chloroperbenzoic acid) affords a mixture of the cyclised isomers with the desired epoxide formed in poor yield.<sup>116,117</sup> Forming the desired anions from the corresponding ethers has an advantage over straight deprotonation with  $^-\text{OH}$ , in that deprotonation may occur both at OH and elsewhere in this system. Following the method outlined in scheme 4.12 the anion formed, at least initially, is the desired alkoxide ion.

Scheme 4.12



The collision induced mass spectra of the three isomers 7, 8 and 9 are recorded in Figures 4.7, 4.8, and 4.9 respectively.

The spectra of 7 and 8 (Figs. 4.7 and 4.8) appear to be identical and look deceptively simple. The major processes involve competitive losses of water and formaldehyde to yield  $m/z$  83 and 71 respectively. The widths at half height of the major peaks in both spectra are the same within experimental error (Table 4.6). In contrast, the spectra of 7 and 8 are quite different from that of 9 (Fig. 4.9), and the peak widths of  $m/z$  83 and 71 in this spectrum are quite different from those in the spectra of 7 and 8 (Table 4.6). This indicates that either (i) the structures of  $m/z$  83 and 71 from 9 are different from the corresponding ions formed from 7 and 8, or (ii) if they have the same structure, the mechanism and energetics of the respective processes are different.

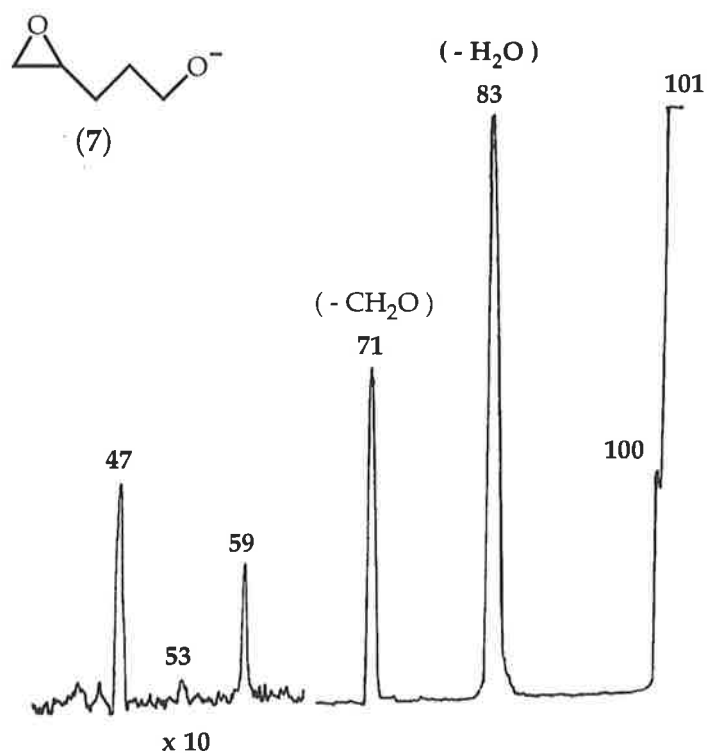


Figure 4.7 Collisional activated mass spectrum (MS/MS) of 7. Produced by the S<sub>N</sub>2 reaction between the methyl ether and <sup>-</sup>OH.

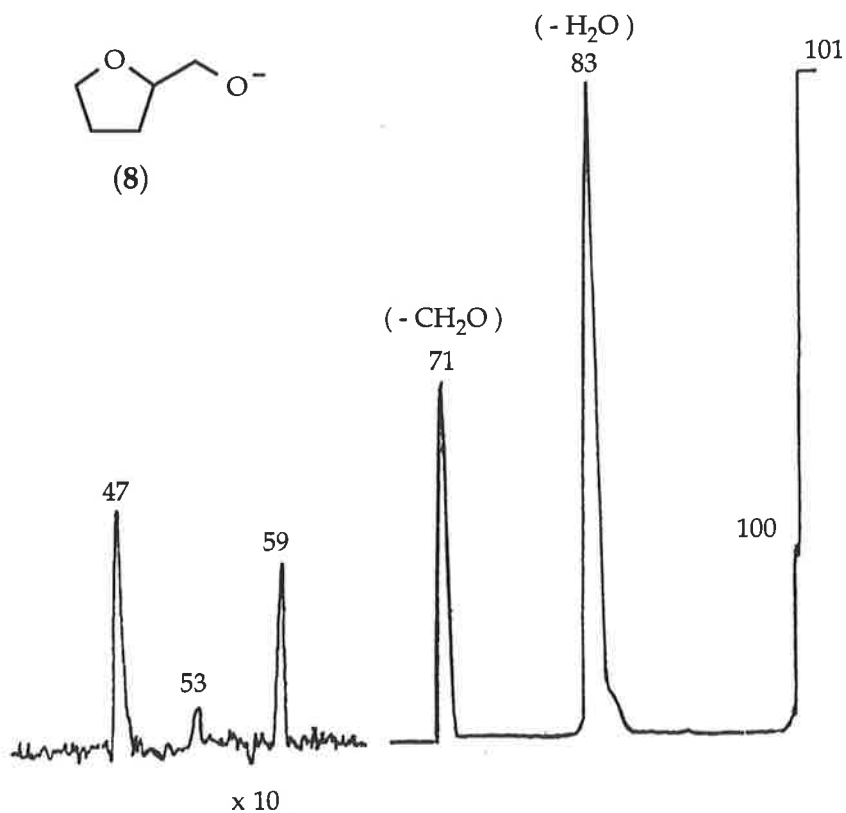


Figure 4.8 Collisional activated mass spectrum (MS/MS) of 8. Produced by the S<sub>N</sub>2 reaction between the methyl ether and <sup>-</sup>OH.

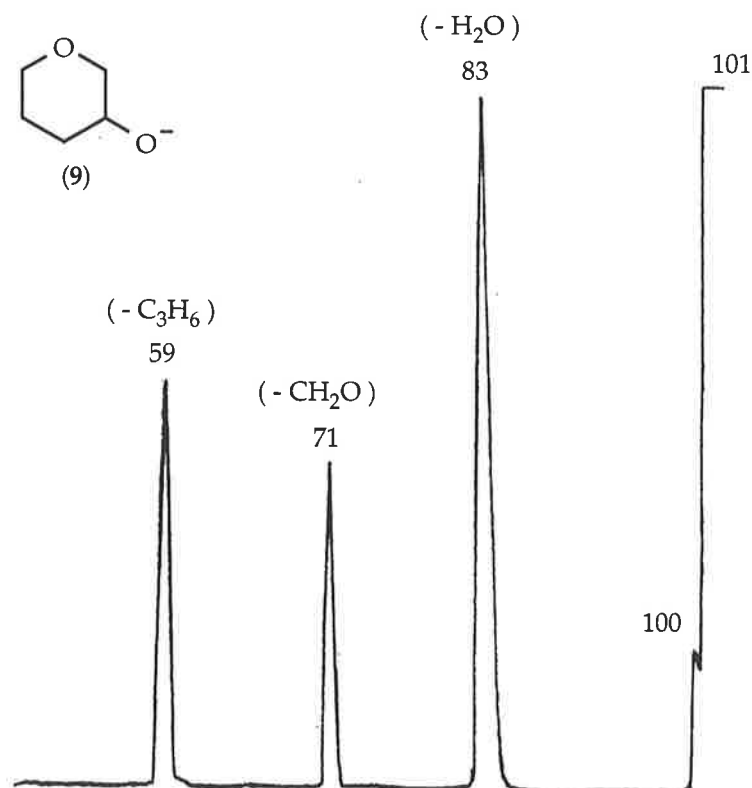


Figure 4.9 Collisional activated mass spectrum (MS/MS) of 9. Produced by the  $S_N2$  reaction between the methyl ether and  $^-OH$ .

Table 4.6 Peak width measurements of  $m/z$  71 and 83 from 7, 8 and 9.

Isomer	Peak width [ $m/z$ (width at half height)]
7	71 ( $25.2 \pm 0.2$ v), 83 ( $24.8 \pm 0.2$ v)
8	71 ( $25.3 \pm 0.2$ v), 83 ( $24.9 \pm 0.2$ v)
9	71 ( $29.5 \pm 0.2$ v), 83 ( $27.5 \pm 0.2$ v)

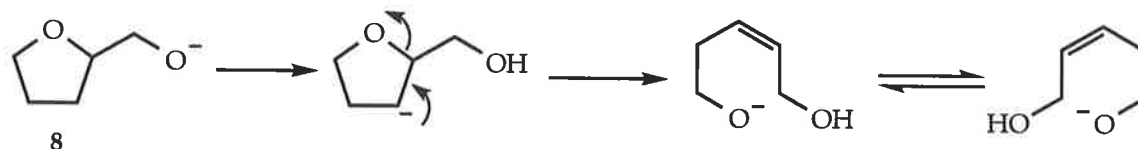
The evidence thus far suggests that the epoxy-alkoxide anion 7 is converting to the five-membered product 8, but cyclisation to the six-membered product 9 is not occurring under the reaction conditions. In order to prove this proposal it is necessary to confirm that (i) the fragment ions formed from 7



and **8** have the same structures, (ii) there are differences between these structures and those of the fragment anions from **9**, and (iii) anion **7** cyclises to anion **8** prior to fragmentation.

The five-membered species **8** has been fully investigated in a previous study.<sup>118</sup> Dua *et al.* showed, by investigating deuterium and <sup>18</sup>O-labelled derivatives of **8**, that the losses of water and formaldehyde from **8** are complex processes, with ring opening preceding fragmentation and resulting in equilibration of the two oxygens. Deprotonation occurs principally at the OH group of tetrahydrofuran methanol with minor deprotonation at the 3-position on the ring. Following collisional activation, the alkoxide and the 3-carbanion interconvert. The 3-carbanion may undergo an E<sub>2</sub> reaction to form the equilibrative ring-opened alkoxides (scheme 4.13), which then fragment by loss of H<sub>2</sub>O and CH<sub>2</sub>O.

Scheme 4.13



Product ion studies (Table 4.7) have determined that the major product ions of **7**, **8** and **9** are those shown in scheme 4.14. The structures of the product anions have been determined by comparison with the spectra of anions formed by independent syntheses. The spectra shown in Table 4.7 are all charge reversal spectra since the collisional activation spectra of the source formed product ions of **7**, **8** and **9** were either not diagnostic, or the spectra were too weak for meaningful comparisons to be made. A problem present

with charge reversal spectra is that rearrangement reactions (particularly those involving movement of H) are more prevalent in positive ion spectra than in negative ion spectra, and as a consequence caution must be taken when using charge reversal spectra alone to determine the structure of the precursor negative ion.

Table 4.7 Product Ion Studies using Charge Reversal spectra.<sup>a</sup>

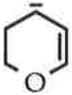
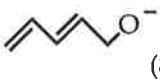

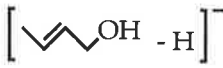

Parent Ion ( <i>m/z</i> )	Product Ion ( <i>m/z</i> )	Spectrum:- CR [ <i>m/z</i> (abundance)]
7 (101)		100(4), 81(4), 71(100), 69(14), 57(3), 55(14), 53(5), 45(6), 43(38), 42(46), 41(55), 39(53), 31(14), 29(28), 27(20).
8 (101)		100(3), 81(3), 71(100), 69(15), 57(4), 55(14), 53(4), 45(4), 43(35), 42(39), 41(52), 39(48), 31(15), 29(34), 27(19).
9 (101)		100(9), 71(52), 69(12), 55(13), 53(4), 45(10), 43(24), 42(100), 41(80), 39(71), 31(10), 29(46), 27(28).
7 (101)	- H <sub>2</sub> O (83)	83(31), 82(100), 81(52), 68(12), 55(40), 54(28), 53(43), 51(23), 50(21), 41(7), 39(55), 29(30), 27(28), 26(10).
8 (101)	- H <sub>2</sub> O (83)	83(33), 82(100), 81(60), 68(14), 55(50), 54(33), 53(55), 51(28), 50(28), 41(10), 39(66), 29(30), 27(32), 26(14).
9 (101)	- H <sub>2</sub> O (83)	83(15), 82(100), 81(63), 68(6), 55(30), 54(40), 53(60), 51(35), 50(30), 49(12), 39(72), 29(33), 27(53), 26(16).
 (83) <sup>b</sup>		83(26), 82(100), 81(66), 68(5), 55(48), 54(32), 53(60), 51(30), 50(30), 41(12), 39(58), 29(32), 27(37), 26(15).
 (83) <sup>c</sup>		83(27), 82(100), 81(65), 68(5), 55(49), 54(32), 53(60), 51(32), 50(32), 41(13), 39(59), 29(32), 27(37), 26(16).

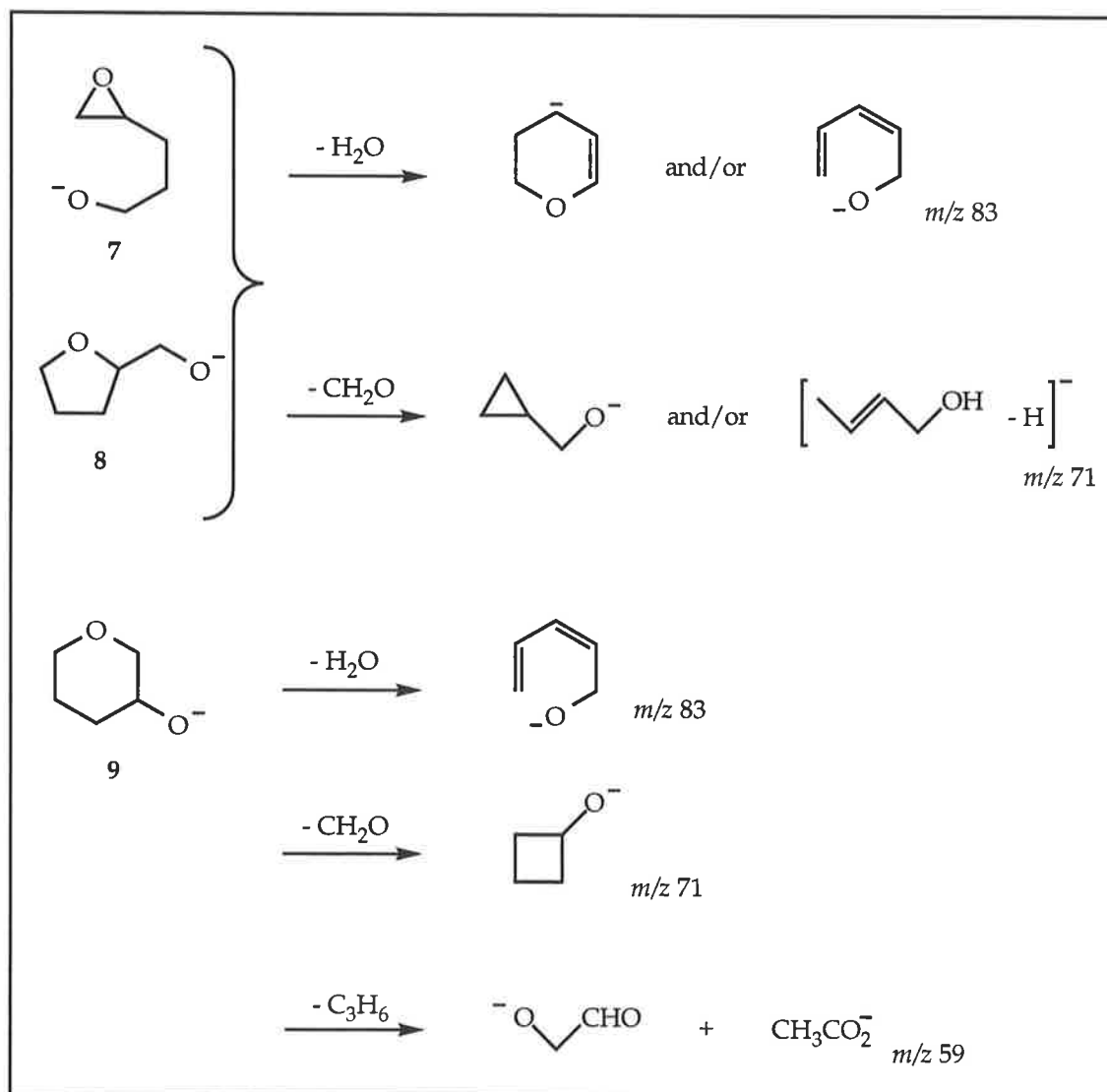
Table 4.7 continued

Parent Ion ( <i>m/z</i> )	Product Ion ( <i>m/z</i> )	Spectrum:- CR [ <i>m/z</i> (abundance)]
7 (101)	- CH <sub>2</sub> O (71)	71(4), 70(46), 69(75), 68(15), 56(21), 55(52), 54(32), 53(35), 51(14), 50(16), 44(6), 43(24), 42(65), 41(78), 39(100), 29(42), 27(36), 26(16).
8 (101)	- CH <sub>2</sub> O (71)	71(2), 70(52), 69(72), 68(15), 56(20), 55(45), 54(28), 53(30), 51(12), 50(13), 44(6), 43(19), 42(65), 41(78), 39(100), 29(42), 27(36), 26(16).
 O <sup>-</sup> (71) <sup>d</sup>		71(1), 70(26), 69(75), 68(20), 56(15), 55(45), 54(31), 53(31), 51(18), 50(20), 44(5), 43(13), 42(48), 41(65), 39(100), 29(38), 27(28), 26(22).
 - H <sup>-</sup> (71) <sup>e</sup>		71(2), 70(26), 69(85), 68(15), 56(12), 55(50), 54(32), 53(35), 51(21), 50(23), 44(4), 43(12), 42(45), 41(58), 39(100), 29(25), 27(20), 26(16).
9 (101)	- CH <sub>2</sub> O (71)	71(18), 70(93), 69(100), 68(33), 55(36), 42(14), 41(28), 39(30), 29(18), 27(19).
 O <sup>-</sup> (71) <sup>f</sup>		71(12), 70(88), 69(100), 68(36), 55(37), 42(14), 41(25), 39(28), 29(14), 27(20).
9 (101)	- C <sub>3</sub> H <sub>6</sub> (59)	59(17), 58(27), 56(38), 45(15), 44(45), 42(40), 41(38), 31(33), 39(46), 29(100), 28(38).
<sup>-</sup> OCH <sub>2</sub> CHO (59) <sup>g</sup>		59(10), 58(24), 56(38), 42(42), 41(40), 31(31), 30(44), 29(100), 28(39).
CH <sub>3</sub> CO <sub>2</sub> <sup>-</sup> (59) <sup>h</sup>		56(4), 45(28), 44(100), 43(36), 42(38), 41(18), 29(12), 28(15), 15(10), 14(5), 13(2).

<sup>a</sup>The abundances in CR spectra are dependent on both source conditions and collision gas pressure. As a general guide when comparing spectra, the abundance of an individual peak should be correct to  $\pm 10\%$ . <sup>b</sup>Produced by deprotonation of 3,4-dihydro-2H-pyran with HO<sup>-</sup> in the source. <sup>c</sup>Produced by deprotonation of 2,4-pentadiene-1-ol with HO<sup>-</sup> in the source. <sup>d</sup>Produced by deprotonation of cyclopropylmethanol by HO<sup>-</sup> in the source. <sup>e</sup>Produced by deprotonation of but-2-ene-1-ol by HO<sup>-</sup> in the source. <sup>f</sup>Produced by deprotonation of cyclobutanol by HO<sup>-</sup> in the source. <sup>g</sup>Formed by reaction of HO<sup>-</sup> with glycoaldehyde dimer. <sup>h</sup>Produced by deprotonation of CH<sub>3</sub>CO<sub>2</sub>H with HO<sup>-</sup> in the source.

The charge reversal spectra of the parent anions **7**, **8** and **9** are recorded in Table 4.7. The charge reversal spectra for **7** and **8** are identical within experimental error: in contrast, the charge reversal spectrum for **9** is significantly different from those of **7** and **9**. This suggests that **7** and **8** may interconvert, but there is no interconversion to **9**.

Scheme 4.14



Scheme 4.14 summarises the product anions formed from **7**, **8** and **9**. The loss of water from **7** and **8** produces peaks ( $m/z$  83) with identical peak width measurements at half height and identical charge reversal spectra. Thus the structure(s) and mechanism(s) of formation of these product ions are the same in both cases. The charge reversal spectra of  $m/z$  83 from **7** and **8** are identical with those of deprotonated 3,4-dihydro-2H-pyran and deprotonated 2,4-pentadien-1-ol (Table 4.7). Thus the deprotonated form of dihydropyran and deprotonated 2,4-pentadien-1-ol are in equilibrium under the reaction conditions. Possible mechanisms for the formation of both of these anions are shown in schemes 4.15 and 4.16: both processes involve prior ring opening of **8** as described by Dua.<sup>118</sup>

Scheme 4.15



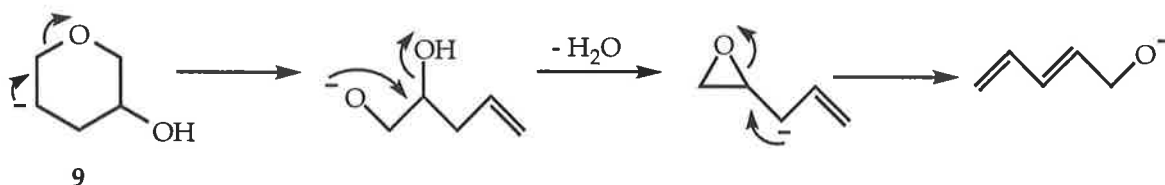
Scheme 4.16



Loss of water from **9** gives a peak at  $m/z$  83 which has a different peak profile at half height when compared with those of the corresponding peaks from **7** and **8** (Table 4.6), but the  $m/z$  83 ions in all three spectra show identical charge reversal spectra. A proposed mechanism for the loss of water from **9** is outlined in scheme 4.17 and may involve the  $S_N2$

displacement of  $^-OH$  to form an epoxide which may ring open to afford the more stable alkoxide ion.

Scheme 4.17



The losses of formaldehyde from 7, 8 and 9 are more informative. Losses of  $CH_2O$  from 7 and 8 give peaks at  $m/z$  71 with both identical peak widths and charge reversal spectra. The charge reversal spectra of the  $m/z$  71 ions from 7 and 8 and those of authentic cyclopropylmethanol and but-2-en-1-ol are identical (Table 4.7). The formation of deprotonated cyclopropylmethanol could, in principle, occur directly from 7 (scheme 4.18), or loss of  $CH_2O$  from the opened form of 8 to yield deprotonated but-2-en-1-ol (scheme 4.19). The latter process is the more likely possibility since all evidence thus far indicate that cyclisation of 7 to 8 is facile and occurs prior to fragmentation.

Scheme 4.18

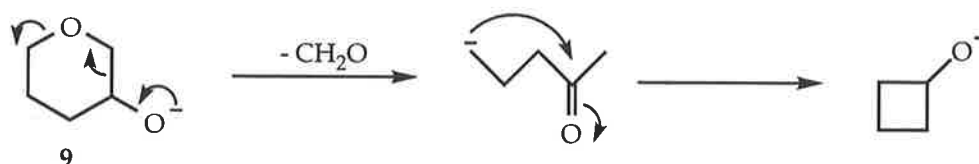


Scheme 4.19



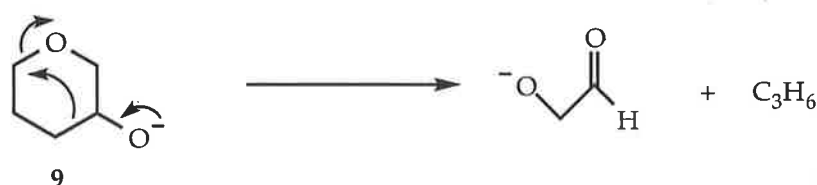
In contrast, loss of formaldehyde from **9** gives a product anion ( $m/z$  71) which has a charge reversal spectrum identical to that of deprotonated cyclobutanol (Table 4.7). A proposed mechanism for this process is outlined in scheme 4.20.

Scheme 4.20

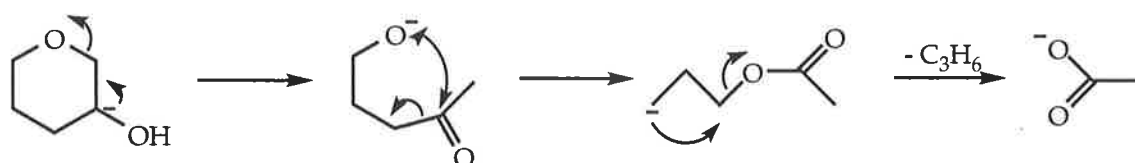


The final peak which is predominant in these spectra is the pronounced peak  $m/z$  59 observed in the spectrum of **9** (Fig. 4.9). This peak arises by loss of  $C_3H_6$ , and comparison of the charge reversal spectrum of this anion with those of the hydroxyacetaldehyde anion and the acetate anion indicate that both product anions are formed, but the former is the more abundant. The formation of hydroxyacetaldehyde anion is straightforward (scheme 4.21), but the acetate anion is an unexpected product. The proposed mechanism for the formation of the acetate anion relies on some deprotonation occurring at the 3-position of the ring. Cyclic ethers such as tetrahydrofuran and tetrahydropyran are known to deprotonate in this position in the gas phase to afford the ring opened alkoxide anion.<sup>118-120</sup> This type of deprotonation may lead to the formation of the acetate anion (scheme 4.22).

Scheme 4.21



Scheme 4.22

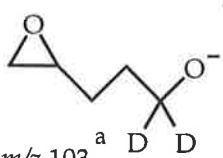
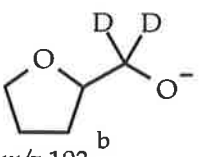
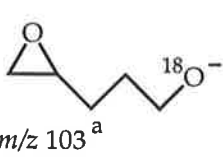
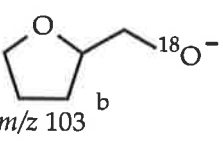


The experimental gas phase data considered to date clearly indicates that **7** and **8** have identical fragmentations, but they do not reveal whether or not **7** cyclises to **8** before fragmentation occurs.

In order to further investigate this problem we must consider the spectra of deuterium and <sup>18</sup>O-labelled derivatives of **7**: these are compared with those deuterium and <sup>18</sup>O-labelled derivatives of **8** previously studied by Dua *et al.*<sup>118</sup> These spectra are listed in Table 4.8, with the spectra of the <sup>18</sup>O-labelled derivatives reproduced in Figure 4.10. Only general comparisons between the labelled derivatives of **7** and **8** should be made, since the labelled derivatives of **8** were published around six years ago and the source conditions and collision gas pressures are not likely to be identical (both of these factors can affect ion abundances). Even so, the spectra of the two labelled derivatives demonstrate that there is significant equilibration of the two oxygens before fragmentation of **7** occurs.



Table 4.8 CA MS/MS of Labelled Derivatives.

Precursor ion	<i>m/z</i> (loss) abundance
 $m/z$ 103 <sup>a</sup>	102(H <sup>+</sup> )10, 101(D <sup>+</sup> )7, 85(H <sub>2</sub> O)100, 73(CH <sub>2</sub> O)34, 71(CD <sub>2</sub> O)68, 59(C <sub>3</sub> H <sub>4</sub> D <sub>2</sub> )4, 49(C <sub>4</sub> H <sub>6</sub> )8, 47(C <sub>4</sub> H <sub>4</sub> D <sub>2</sub> )4.
 $m/z$ 103 <sup>b</sup>	102(H <sup>+</sup> )4, 101(D <sup>+</sup> )2, 85(H <sub>2</sub> O)100, 73(CH <sub>2</sub> O)43, 71(CD <sub>2</sub> O)12, 61(C <sub>3</sub> H <sub>6</sub> )4, 49(C <sub>4</sub> H <sub>6</sub> )5, 47(C <sub>4</sub> H <sub>4</sub> D <sub>2</sub> )3.
 $m/z$ 103 <sup>a</sup>	102(H <sup>+</sup> )15, 85(H <sub>2</sub> O)70, 83(H <sub>2</sub> <sup>18</sup> O)97, 73(CH <sub>2</sub> O)61, 71(CH <sub>2</sub> <sup>18</sup> O)100, 61(C <sub>3</sub> H <sub>6</sub> )4, 49(C <sub>4</sub> H <sub>6</sub> )15.
 $m/z$ 103 <sup>b</sup>	102(H <sup>+</sup> )15, 85(H <sub>2</sub> O)52, 83(H <sub>2</sub> <sup>18</sup> O)35, 73(CH <sub>2</sub> O)100, 71(CH <sub>2</sub> <sup>18</sup> O)37, 61(C <sub>3</sub> H <sub>6</sub> )6, 49(C <sub>4</sub> H <sub>6</sub> )12.

<sup>a</sup>Anions produced by the S<sub>N</sub>2 reaction between the corresponding methyl ether and <sup>-</sup>OH.  
 Spectra reported by Dua *et al.*<sup>118</sup>

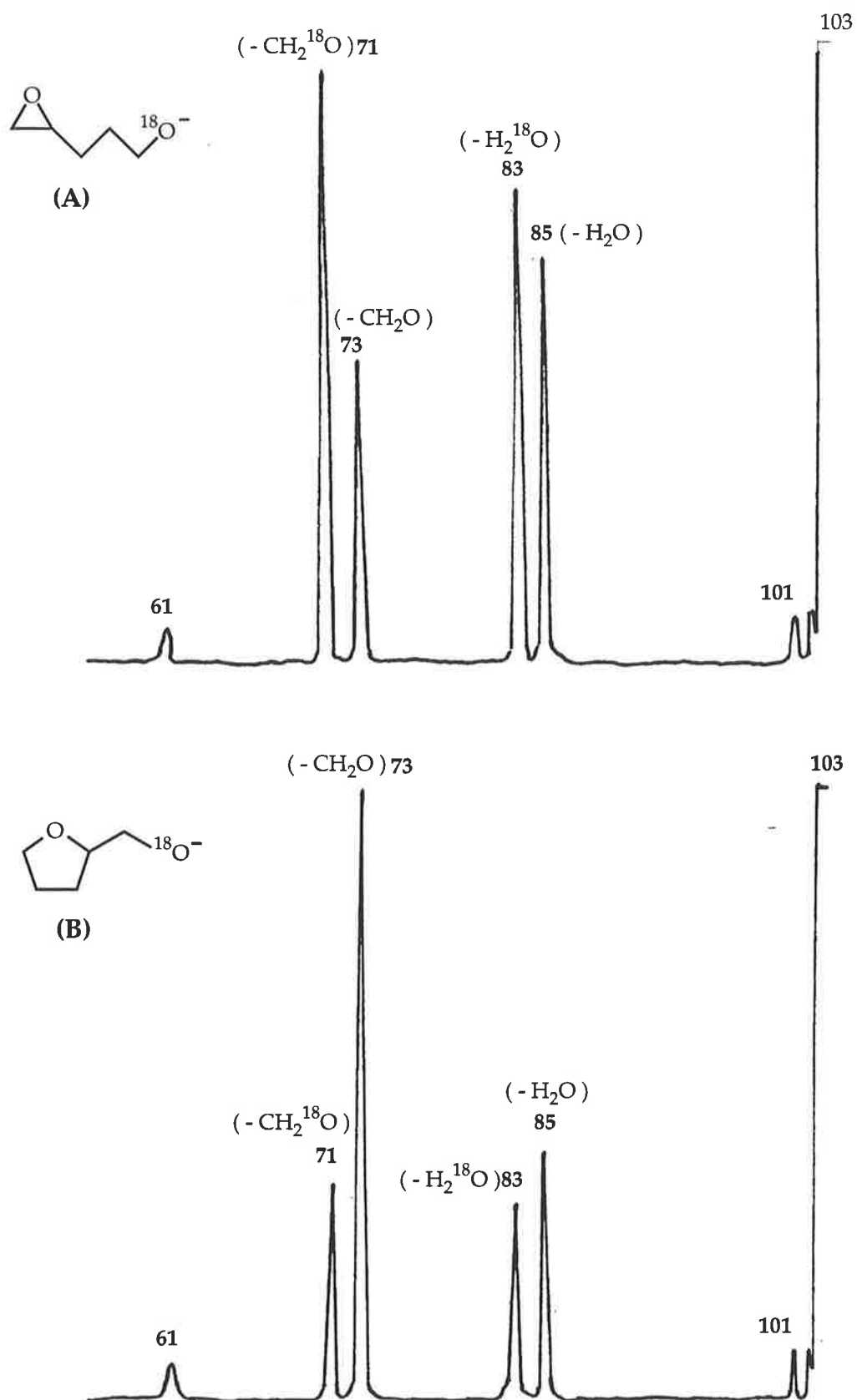


Figure 4.10. CA MIKE Spectra for the  $^{18}\text{O}$ -labelled analogues of 7 and 8.<sup>118</sup>

An interesting observation is that with the two  $^{18}\text{O}$ -labelled derivatives the ratios of the losses of  $\text{H}_2\text{O}$  and  $\text{H}_2^{18}\text{O}$  are reversed. This is also the case for the losses of  $\text{CH}_2\text{O}$  and  $\text{CH}_2^{18}\text{O}$  from these anions (Fig. 4.10 and Table 4.8). This trend is expected if **7** cyclises to **8** prior to fragmentation, since the labelled derivative of **7** (Fig. 4.10a) would incorporate the  $^{18}\text{O}$ -label in the ring following cyclisation (scheme 4.23), while the labelled derivative of **8** (Fig. 4.10b) has the  $^{18}\text{O}$ -label in the side chain.

Scheme 4.23



This trend would also be expected for the deuterium labelled anions, since for the  $d_2$ -labelled derivative of **7** cyclisation would afford the label on the ring, whereas the  $d_2$ -labelled derivative of **8** has the label on the alkyl chain. The evidence recorded in Table 4.8 shows that the ratio of losses of  $\text{CH}_2\text{O}$  and  $\text{CD}_2\text{O}$  from anion **7** is the reverse of that observed for anion **8**.

We conclude that (i) **7** does cyclise to **8** before fragmentation, (ii) the fragmentations of both **7** and **8** occur following ring opening of **8**, and (iii) **7** does not cyclise to **9** in the gas phase.

#### 4.2.2.3 Condensed Phase Reactions of 7, 8 and 9

The base catalysed reactions of the acetate of 7 have been investigated previously under a number of conditions.<sup>117,121</sup> Both the five-membered and six-membered neutrals of 8 and 9 are formed, with the former being formed in the higher yield. We have repeated these base catalysed cyclisation reactions of the acetate of 7, and the neutrals of 8 and 9 in 10% aqueous sodium hydroxide at both 20°C and at reflux and analysed the ratios of the two products by gas chromatography/mass spectrometry. The results of this study are shown in Table 4.9: the five-membered ring system is the predominant product. The cyclisation of 7 to 8 and 9 occurs very rapidly. Both anions 8 and 9 are stable under these conditions and do not revert back to 7, even when the reaction mixture is heated under reflux for 60 hrs.

Table 4.9 Base Catalysed Solution Reactions of 3-(2-oxiranyl)propyl acetate, tetrahydrofurfuryl alcohol and tetrahydro-2H-3-pyranol.<sup>a</sup>

Reactant	Time	20°C/10% NaOH	100°C/10% NaOH
3-(2-oxiranyl) propyl acetate	5 min.	95:9 <sup>b</sup>	91:9 <sup>b</sup>
	1 hr.	95:5	91:9
	60 hrs.	95:5	91:9
Tetrahydro- furfuryl alcohol	1 hr.	100:0	100:0
	60 hrs.	100:0	100:0
tetrahydro-2H-3- pyranol	1 hr.	0:100	0:100
	60 hrs.	0:100	0:100

<sup>a</sup>For experimental conditions see experimental section. <sup>b</sup>The ratio represents the neutrals of 8:9. The title compound 7 is not detected under the experimental conditions. Hydrolysis of the acetate gives the anion of 7, which immediately cyclises (in quantitative yield) to yield the listed products.

#### 4.2.2.4 Summary

The experimental results and *ab initio* calculations appear to be at a variance. The *ab initio* results indicate that the barriers to the formation of 8 and 9 from 7 are small and comparable. If the barrier heights alone are controlling the rates of the kinetically controlled reactions, then both 8 and 9 should be formed in equivalent proportions. This is the first occasion in our studies of  $S_Ni$  reactions where the *ab initio* calculations seem to predict a different outcome to that obtained experimentally.

The condensed phase results indicate that both possible  $S_Ni$  reactions of the epoxy-alkoxide ion occur to afford the neutrals derived from 8 and 9, with the smaller ring (tetrahydrofurfuryl alcohol) being formed in significantly higher yield.

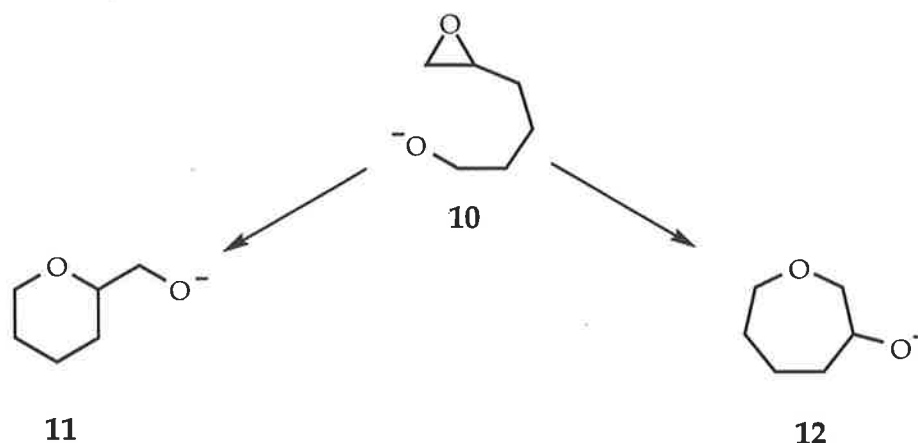
In contrast, the experimental gas phase results indicate that 7 cyclises exclusively to 8, and that all fragmentations seen in Figures 4.7 and 4.8 arise from the ring opened form of 8. There is no evidence to suggest that 7 cyclises to 9.

These results will be discussed in detail in section 4.3.

#### 4.2.3 Competitive Cyclisations of 5,6-Epoxyhexoxide Anion

We have studied and reported, in this thesis, the competitive gas and condensed phase  $S_Ni$  reactions of 3,4-epoxybutoxide and 4,5-epoxypentoxide anions both theoretically and experimentally. We now investigate the behaviour in both the condensed phase and gas phase of the next homologue, i.e. the possible  $S_Ni$  reactions of 5,6-epoxyhexoxide anion (10) (scheme 4.24).

Scheme 4.24



#### 4.2.3.1 *Ab Initio* Calculations for Competing Cyclisations of 5,6-Epoxyhexoxide Anion

The results of an *ab initio* computational study of the possible  $S_Ni$  processes of 5,6-epoxyhexoxide anion (**10**) are shown in Figure 4.11. The data presented show the barriers to the two transition states **G** and **H** are a modest 35.0 and 39.7 kJ mol<sup>-1</sup> respectively at MP2-Fc level of theory. The six-membered alkoxide anion (**11**) is some 11 kJ mol<sup>-1</sup> more thermodynamically stable than the competing seven-membered isomer (**12**). The results from these *ab initio* calculations suggest that, if these modest barriers are controlling the relative rates of the two processes, both **11** and **12** should be formed following collisional activation of **10** in the gas phase, with the formation of **11** being marginally more favourable.

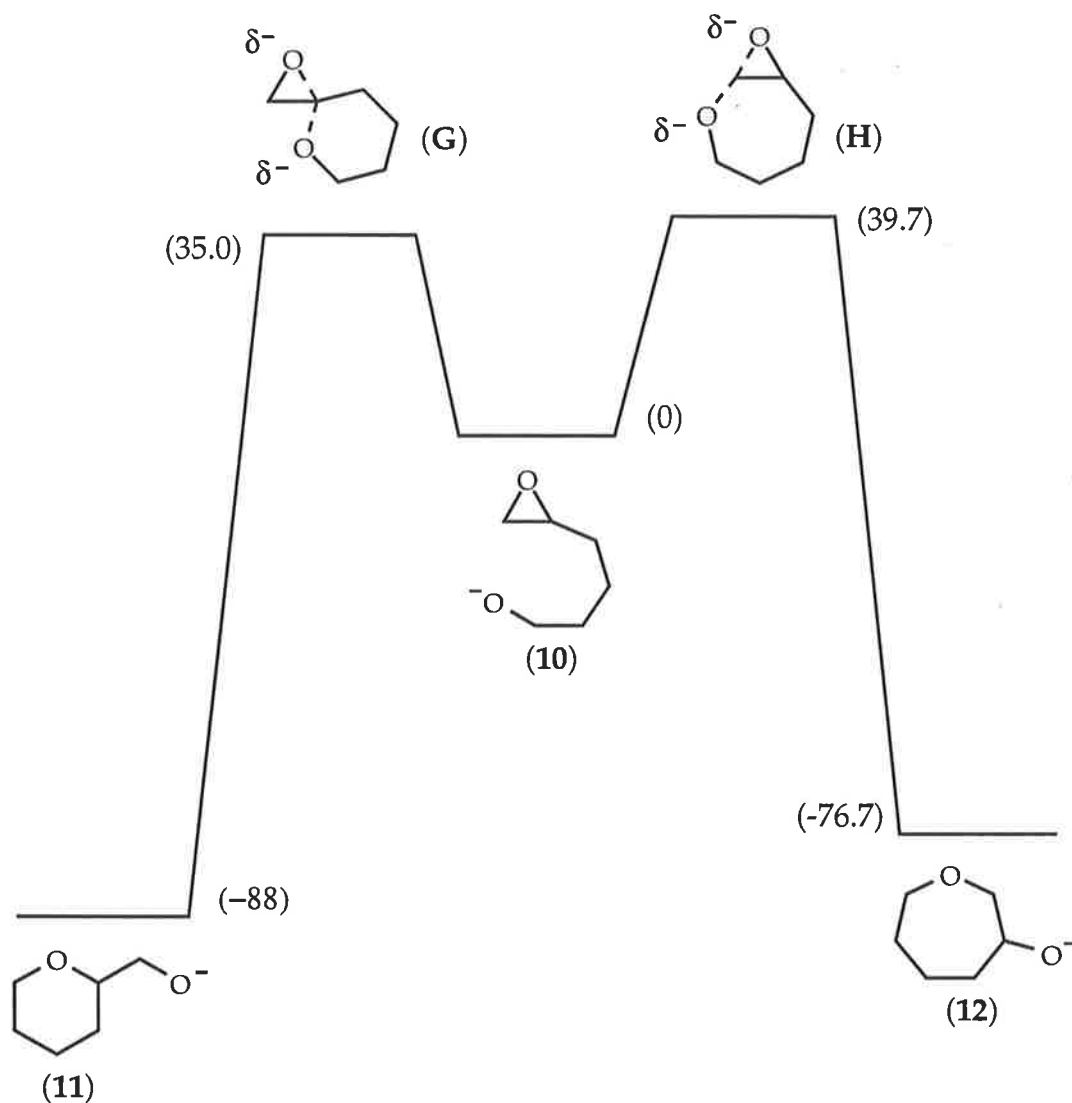


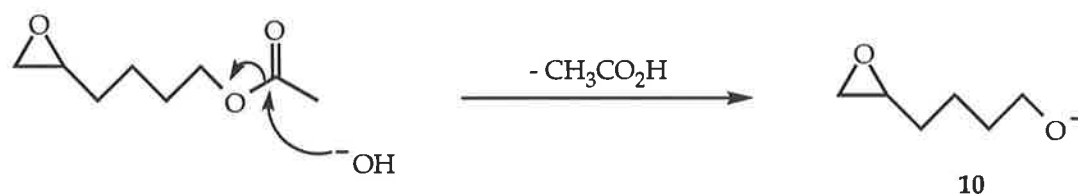
Figure 4.11 *Ab initio* calculations [Gaussian94, geometries RHF/6-31+G(d), energies MP2-fc/6-31+G(d)] for the competitive  $S_Ni$  cyclisations of the 5,6-epoxyhexoxide anion. The energies are shown in  $\text{kJ mol}^{-1}$ . For a full discussion of transition structures see section 4.3. Full details of geometries and energies are in Appendix C.

#### 4.2.3.2 Gas Phase Reactions of 10, 11 and 12

The alkoxide ions **10**, **11** and **12** were formed in the gas phase independently by deprotonation of the appropriate alcohols and also by nucleophilic addition/elimination of the appropriate acetate in the source of the ZAB 2HF. Although the spectra formed *via* both methods were identical, forming the alkoxide ions indirectly from the acetates (scheme 4.25) is

necessary, since gas phase deprotonation of the alcohols with  $^-\text{OH}$  may occur both at OH and elsewhere on the molecules.

Scheme 4.25



The collision induced mass spectra of the three alkoxide anions **10**, **11** and **12** are recorded in Figures 4.12, 4.13 and 4.14 respectively, and the peak widths at half height of the major peaks in these spectra are shown, for comparison in Table 4.10.

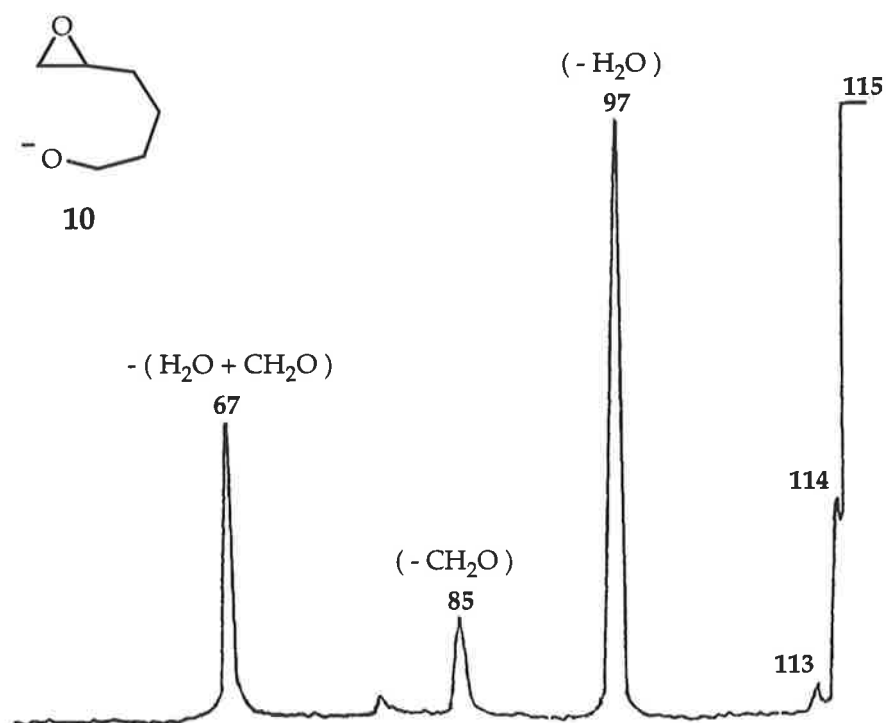


Figure 4.12 Collisionally activated MS/MS data for **10**.



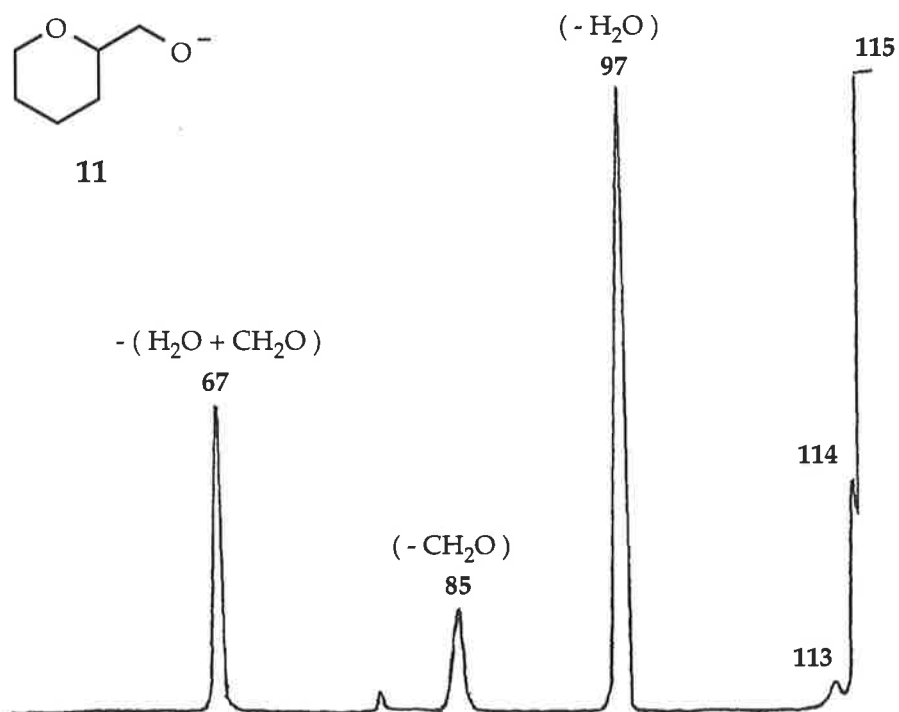


Figure 4.13 Collisionally activated MS/MS data for 11.

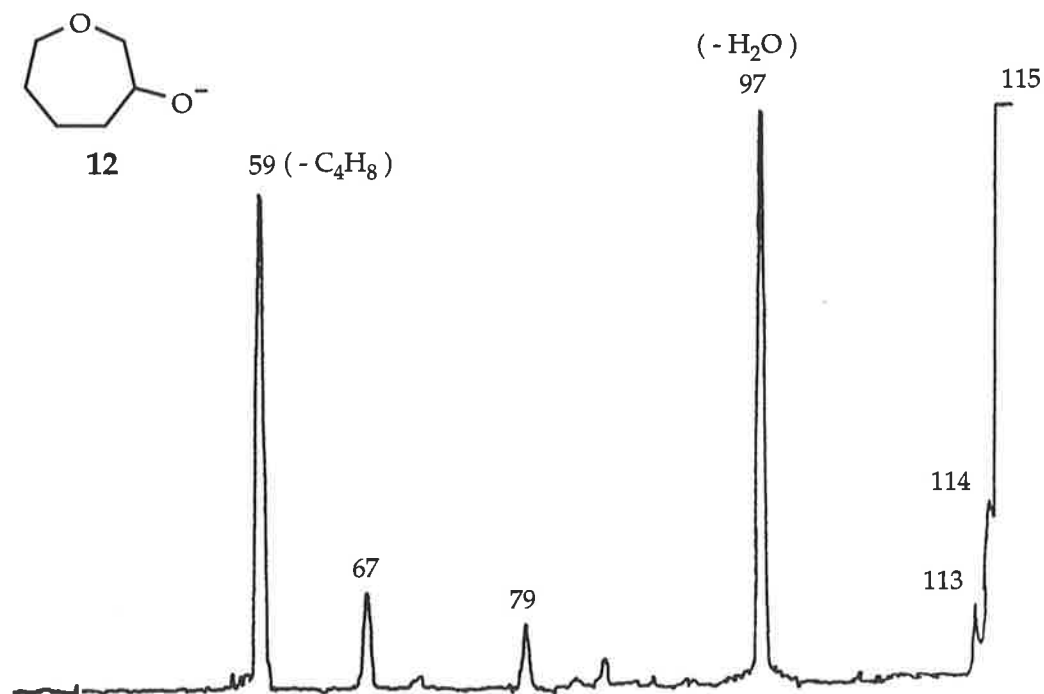


Figure 4.14 Collisionally activated MS/MS data for 12.

Table 4.10 Peak width measurements of  $m/z$  97, and/or 85 and 67 from **10**, **11** and **12**.

Isomer	Peak width:- [ $m/z$ (width at half height)]
<b>10</b>	97 ( $27.4 \pm 0.2$ v), 85 ( $33.1 \pm 0.2$ v), 67 ( $30.7 \pm 0.2$ v)
<b>11</b>	97 ( $27.7 \pm 0.2$ v), 85 ( $33.1 \pm 0.2$ v), 67 ( $30.7 \pm 0.2$ v)
<b>12</b>	97 ( $33.4 \pm 0.2$ v)

Initial inspection of the three spectra immediately indicate similarities between the spectra of **10** and **11**. A closer inspection reveals that the intensities and the peak widths at half height of the major peaks  $m/z$  97, 85 and 67 are the same within experimental error in those spectra. These spectra are, however, quite different from that of **12** (Fig. 4.14). These observations suggest that **10** and **11** are fragmenting through a common intermediate (perhaps following cyclisation of **10** to **11**), but that cyclisation of **10** to **12** does not occur under the reaction conditions. In order to confirm these proposals we now need to confirm that:

- (i) the product anions in the spectra of **10** and **11** have the same structures,
- (ii) these structures are different to those of the fragment anions derived from **12**, and
- (iii) the fragmentations of anion **10** occur following conversion of **10** to **11**.

The identities of the product anions have been investigated by comparison of the spectra of product anions with those of particular anions synthesised by unequivocal routes: these data are recorded in Table 4.11. Whenever possible, both collisional activation and charge reversal mass spectra of anions are compared.

Table 4.11 Product ion studies using CA and CR spectra.<sup>a</sup>




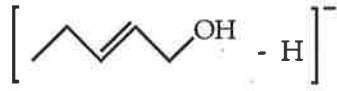

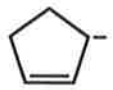
Parent ( <i>m/z</i> )	Product ion [loss ( <i>m/z</i> )]	Mode	Spectrum [CA, <i>m/z</i> (loss) abundance] [CR, <i>m/z</i> (abundance)]
10 (115)	- H <sub>2</sub> O (97)	CA	96(H <sup>+</sup> )100, 95(H <sub>2</sub> )26, 82( <sup>•</sup> CH <sub>3</sub> )11, 79(H <sub>2</sub> O)59, 67(CH <sub>2</sub> O)68.
		CR	97(70), 96(100), 96(78), 81(56), 79(54), 77(34), 69(22), 67(78), 66(44), 65(50), 63(16), 57(4), 55(14), 53(33), 52(34), 51(38), 59(33), 43(8), 41(45), 39(53), 31(6), 29(14), 27(21), 26(16).
11 (115)	- H <sub>2</sub> O (97)	CA	96(H <sup>+</sup> )100, 95(H <sub>2</sub> )22, 82( <sup>•</sup> CH <sub>3</sub> )13, 79(H <sub>2</sub> O)66, 67(CH <sub>2</sub> O)70.
		CR	97(67), 96(100), 95(75), 81(49), 79(52), 77(38), 69(24), 67(84), 66(47), 65(54), 63(19), 57(4), 55(12), 53(29), 52(30), 51(29), 50(30), 43(6), 41(35), 39(46), 31(3), 29(12), 27(20), 26(15).
12 (115)	- H <sub>2</sub> O (97)	CA	95(H <sub>2</sub> )24, 79(H <sub>2</sub> O)100, 67(CH <sub>2</sub> O)1, 41(C <sub>3</sub> H <sub>5</sub> <sup>-</sup> )2.
		CR	97(21), 96(76), 95(100), 94(8), 81(52), 79(77), 77(45), 69(18), 67(45), 66(32), 65(28), 63(12), 57(4), 55(8), 53(12), 51(14), 41(21), 39(34), 31(4), 29(8), 27(15), 26(4).
 (97) <sup>b</sup>		CA	96(H <sup>+</sup> )100, 95(H <sub>2</sub> )28, 82( <sup>•</sup> CH <sub>3</sub> )5, 79(H <sub>2</sub> O)65, 67(CH <sub>2</sub> O)52.
		CR	97(68), 96(100), 95(72), 81(52), 79(58), 77(39), 69(21), 67(83), 66(50), 65(55), 63(21), 57(4), 55(12), 53(31), 52(39), 51(32), 50(30), 43(6), 41(37), 39(46), 31(6), 29(12), 27(19), 26(12).
 (97) <sup>b</sup>		CA	95(H <sub>2</sub> )24, 79(H <sub>2</sub> O)100, 67(CH <sub>2</sub> O)1, 41(C <sub>3</sub> H <sub>5</sub> <sup>-</sup> )1.
		CR	97(19), 96(70), 95(100), 94(8), 81(53), 79(66), 77(46), 69(18), 67(39), 66(29), 65(25), 63(11), 57(4), 55(8), 53(13), 51(15), 41(22), 39(37), 31(4), 29(6), 27(11), 26(4).
10 (115)	- CH <sub>2</sub> O (85)	CA	83(H <sub>2</sub> )<20 <sup>c</sup> , 67(H <sub>2</sub> O)60, 55(CH <sub>2</sub> O)100.
		CR	85(4), 84(22), 83(12), 82(5), 81(2), 68(9), 67(60), 66(35), 65(36), 56(28), 55(85), 53(32), 51(26), 50(21), 43(6), 41(42), 39(100), 29(62), 28(16), 27(45), 26(20).
11 (115)	- CH <sub>2</sub> O (85)	CA	83(H <sub>2</sub> ), 20 <sup>c</sup> , 67(H <sub>2</sub> O)68, 55(CH <sub>2</sub> O)100.
		CR	85(6), 84(21), 83(13), 82(8), 81(4), 68(14), 67(62), 66(34), 65(38), 56(32), 55(87), 53(33), 51(28), 50(18), 43(8), 41(45), 39(100), 29(65), 28(18), 27(51), 26(20).
 (85) <sup>d</sup>		CA	83(H <sub>2</sub> )6, 67(H <sub>2</sub> O)38, 55(CH <sub>2</sub> O)100.
		CR	85(3), 84(9), 83(12), 82(6), 81(4), 70(5), 69(5), 67(7), 66(6), 65(5), 56(36), 55(100), 54(48), 53(46), 51(22), 50(22), 43(3), 41(24), 39(77), 29(52), 28(28), 27(42), 26(16).

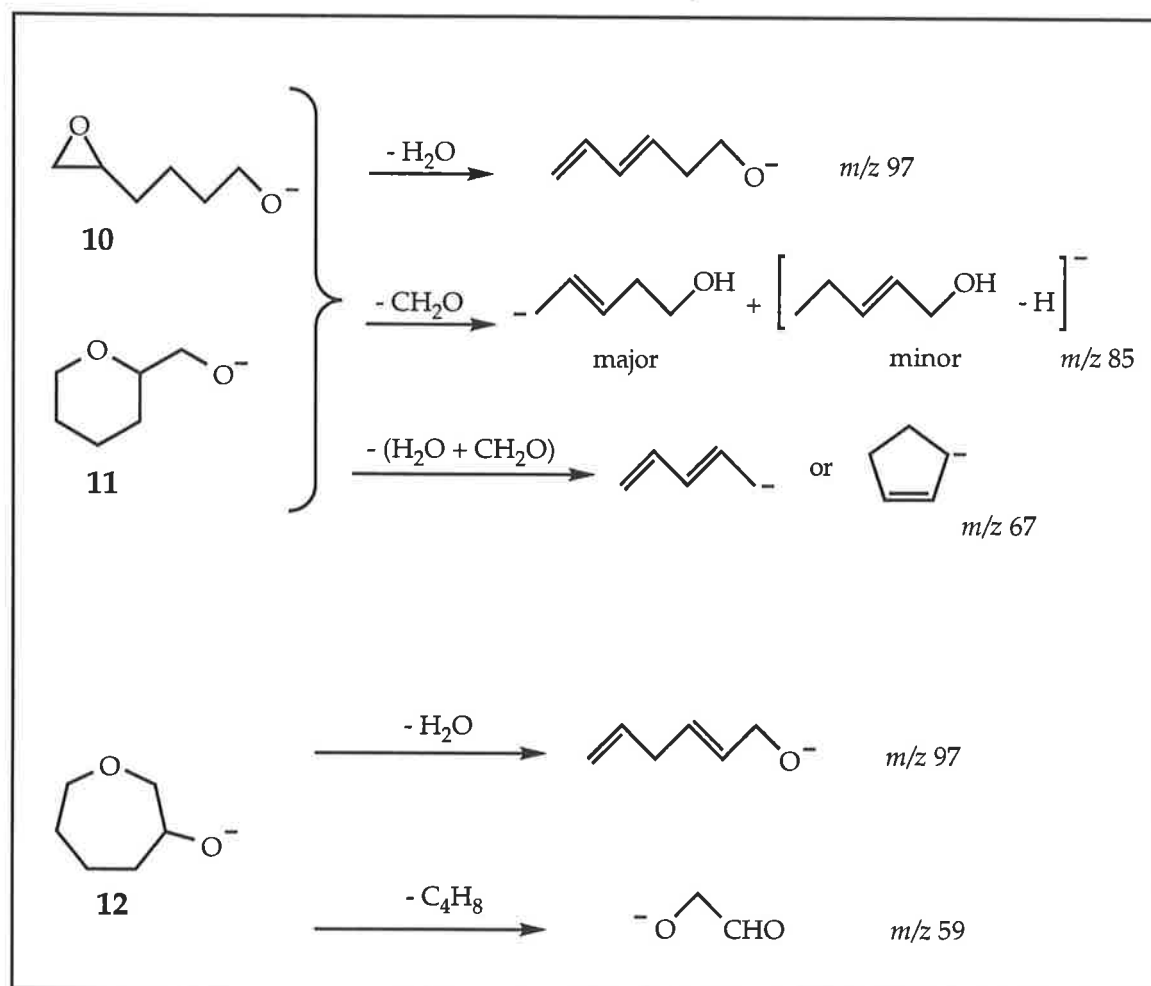
Table 4.11 Cont.

 (85) <sup>e</sup>		CA	67(H <sub>2</sub> O)100, 55(CH <sub>2</sub> O)1.
		CR	85(3), 84(83), 83(97), 82(5), 81(2), 70(1), 69(2), 68(15), 67(17), 66(10), 65(10), 57(2), 56(8), 55(29), 53(12), 51(9), 50(10), 43(6), 41(43), 39(100), 29(76), 28(26), 27(64), 26(18).
10 (115)	- (H <sub>2</sub> O + CH <sub>2</sub> O) (67)	CR	67(100), 66(48), 65(34), 64(3), 63(6), 62(3), 61(2), 53(1), 52(4), 51(6), 50(5), 49(2), 41(7), 40(3), 39(10), 38(2), 37(1), 27(2), 26(1).
11 (115)	- (H <sub>2</sub> O + CH <sub>2</sub> O) (67)	CR	67(100), 66(50), 65(35), 64(2), 63(7), 62(3), 61(2), 53(1), 52(4), 51(6), 50(5), 49(2), 41(7), 40(2), 39(8), 38(2), 37(1), 27(2), 26(1).
 (67) <sup>f</sup>		CR	67(100), 66(54), 65(36), 64(2), 63(7), 62(3), 61(2), 53(1), 52(4), 51(4), 50(3), 49(1), 41(6), 40(2), 39(7), 38(2), 37(1), 27(2), 26(1).
 (67) <sup>g</sup>		CR	67(100), 66(51), 65(39), 64(2), 63(7), 62(2), 61(1), 53(1), 52(5), 51(8), 50(7), 49(2), 41(22), 40(10), 39(39), 38(7), 37(4), 27(8), 26(3).
12 (115)	- C <sub>4</sub> H <sub>8</sub> (59)	CR	59(8), 58(29), 57(6), 56(8), 45(2), 44(4), 42(13), 41(15), 31(34), 30(48), 29(100), 28(32).
<sup>-</sup> OCH <sub>2</sub> CHO (59) <sup>h</sup>		CR	59(10), 58(28), 57(4), 56(12), 45(2), 44(6), 42(18), 41(19), 31(29), 30(43), 29(100), 28(34).

<sup>a</sup>The abundances in both CA and CR spectra are dependent on both source conditions and collision gas pressure. As a general guide when comparing spectra, the abundance of an individual peak should be correct to  $\pm 10\%$ . <sup>b</sup>Formed by deprotonation of the appropriate alcohol with <sup>-</sup>OH. <sup>c</sup>Weak spectrum: difficult to measure the abundance of the peak formed by loss of H<sub>2</sub> because of baseline noise. <sup>d</sup>Formed by decarboxylation of HOCH<sub>2</sub>CH<sub>2</sub>CH=CHCH<sub>2</sub>CO<sub>2</sub><sup>-</sup>. <sup>e</sup>Formed by deprotonation of MeCH<sub>2</sub>CH=CHCH<sub>2</sub>OH with <sup>-</sup>OH. <sup>f</sup>Formed by deprotonation of 1,3-pentadiene with <sup>-</sup>OH. <sup>g</sup>Formed by deprotonation of cyclopentene with <sup>-</sup>OH. <sup>h</sup>Formed by reaction of HO<sup>-</sup> with glycoaldehyde dimer.

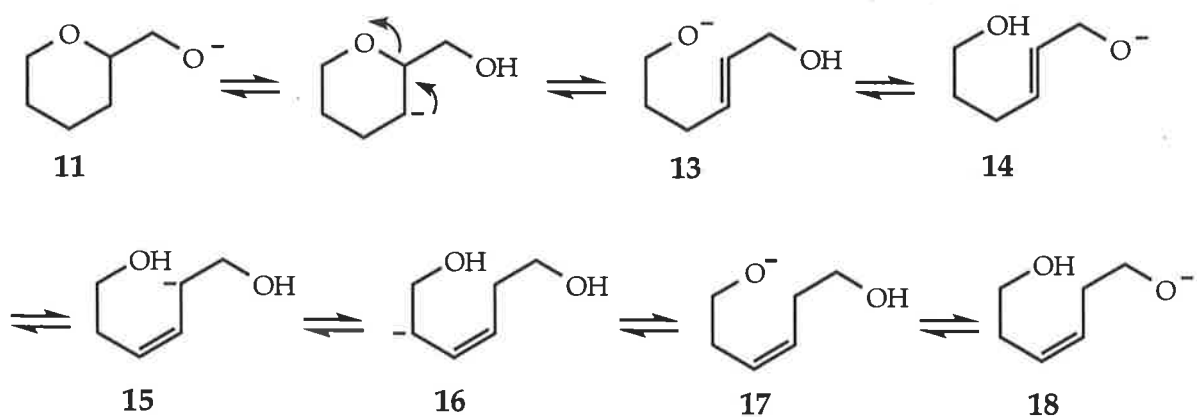
The data shown in Table 4.11 show that the product anions in the spectra of **10** and **11** are the same, but that the product ions of **12** are different. The results of these comparisons are summarised in scheme 4.26.

Scheme 4.26



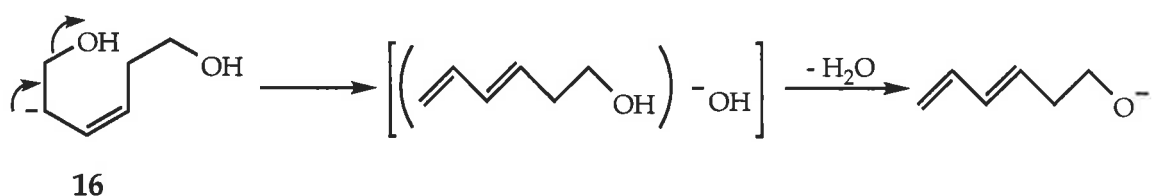
The fragmentations of **11** have been considered in a previous study.<sup>118</sup> Dua *et al.* have proposed that fragmentations of **11** arise following ring opening of the tetrahydropyran ring (*cf.* scheme 4.13, page 119). The evidence put forward to support this hypothesis is the occurrence of equilibration of the two oxygen atoms. Scheme 4.27 illustrates the possible processes which may occur following the proposed proton transfer/ring opening equilibria.

Scheme 4.27



The losses of water from **10** and **11** afford peak  $m/z$  97, identified as deprotonated 3,5-hexadien-1-ol (Table 4.11). The proposed mechanism for formation of this anion occurs from the ring opened isomers **15** and **16** (e.g. see scheme 4.28 for **16**).

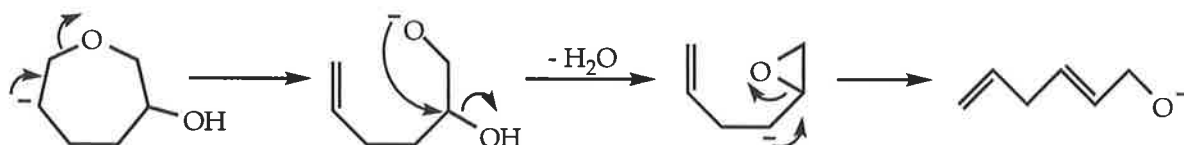
Scheme 4.28



The loss of water from **12** affords a different product ion to that formed from **10** and **11**. The peak width at half height is also different from those from **10** and **11** (which are identical). The product ion studies indicate that  $m/z$  97 from **12** is deprotonated 2,5-hexadien-1-ol which gives both a CA and CR spectrum characteristically different to **10**, **11** and deprotonated 3,5-hexadien-

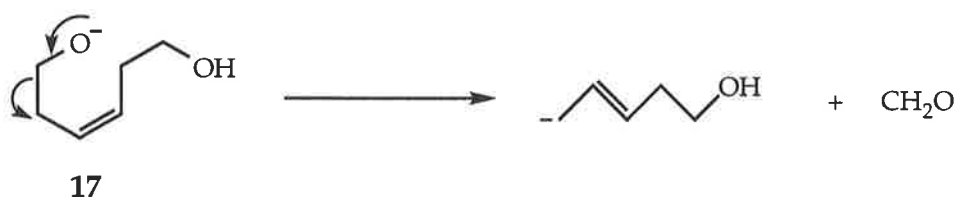
1-ol (Table 4.11). The mechanism for this process is directly analogous to the loss of water from deprotonated tetrahydro-2*H*-3-pyranol (*cf.* scheme 4.17, page 124) and is illustrated in scheme 4.29.

Scheme 4.29



The loss of formaldehyde to yield  $m/z$  85 is absent in the spectrum of **12**, but is present in the spectra for both **10** and **11** giving peaks with the same half height. Product ion studies indicate that this process affords a mixture of both  $^-\text{CH}_2\text{CH}=\text{CHCH}_2\text{CH}_2\text{OH}$  and deprotonated 2-penten-1-ol (Table 4.11). We propose that formation of the former occurs from ring opened isomers **17** and **18** (e.g. **17** scheme 4.30), and that deprotonated 2-penten-1-ol is formed from the ring opened isomer **13** in a similar fashion.

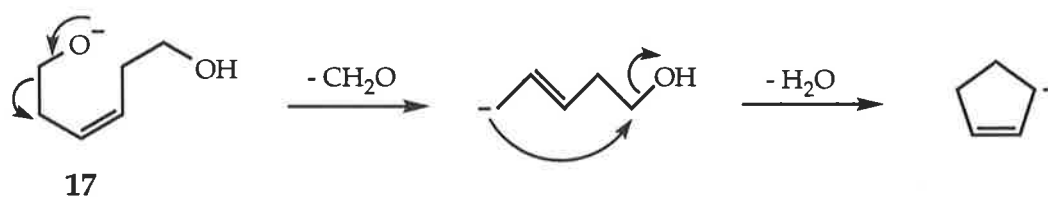
Scheme 4.30



The final fragmentation process of **10** and **11** which requires discussion is the formation of major peak  $m/z$  67. This results from the losses of water

and formaldehyde from the parent anion(s). Product ion studies indicate that the reaction may lead to formation of either deprotonated 1,3-pentadiene or deprotonated cyclopentene: both give similar CA and CR spectra and therefore cannot be differentiated. Mechanisms of formation of both of these anions are proposed. Deprotonated cyclopentene may result from the loss of formaldehyde followed by water loss from the ring opened isomers **13**, **17** and **18** (e.g. **17** scheme 4.31), while the losses of water and formaldehyde from **15** and **16** will yield deprotonated 1,3-pentadiene (e.g. **16** scheme 4.32).

Scheme 4.31



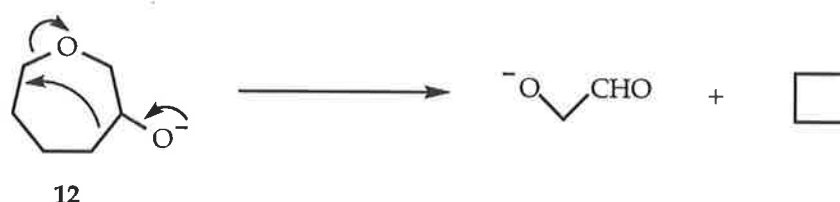
Scheme 4.32



There is one more process which deserves some comment. The major peak at  $m/z$  59 from **12** corresponds to the hydroxyacetaldehyde anion (Table 4.11). A possible mechanism for this process involves the loss of cyclobutane (scheme 4.33).


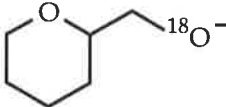


Scheme 4.33



The data considered to date show that **10** and **11** have identical fragmentations but do not indicate whether or not **10** cyclises to **11** before fragmentation occurs. This problem is resolved by consideration of the spectra of  $^{18}\text{O}$ -labelled derivatives of **10** and **11**<sup>118</sup> (Table 4.12). These spectra are consistent with the mechanisms proposed to date and demonstrate the equilibration of the two oxygens of **10** and **11** prior to fragmentation. As mentioned for the labelled derivatives in Section 4.2.2.2 (page 126), only a general comparison may be made as the labelled derivatives of **10** and **11** were analysed some six years apart, this however does not effect the critical ratios of the losses of  $\text{H}_2\text{O}:\text{H}_2^{18}\text{O}$  and  $\text{CH}_2\text{O}:\text{CH}_2^{18}\text{O}$  at  $m/z$  99:97 and 87:85 respectively, which are reversed for the two spectra shown in Table 4.12. This is the expected scenario, indicating that the cyclisation of **10** to **11** precedes fragmentation, and that the fragmentations of **10** and **11** are occurring from the same intermediate.

Table 4.12 CA MS/MS data for  $^{18}\text{O}$ -labelled derivatives of **10** and **11**.

Precursor ion	$m/z$ (loss) abundance
 $m/z$ 117 <sup>b</sup>	116/115 <sup>a</sup> (H <sup>+</sup> , H <sub>2</sub> )20, 99(H <sub>2</sub> O)100, 97(H <sub>2</sub> <sup>18</sup> O)85, 87(CH <sub>2</sub> O)8, 85(CH <sub>2</sub> <sup>18</sup> O)10, 79(H <sub>2</sub> O + H <sub>2</sub> <sup>18</sup> O)5, 67(C <sub>5</sub> H <sub>7</sub> <sup>-</sup> )47.
 $m/z$ 117 <sup>b</sup>	116(H <sup>+</sup> )24, 115(H <sub>2</sub> )5, 99(H <sub>2</sub> O)64, 97(H <sub>2</sub> <sup>18</sup> O)70, 87(CH <sub>2</sub> O)17, 85(CH <sub>2</sub> <sup>18</sup> O)18, 79(H <sub>2</sub> O + H <sub>2</sub> <sup>18</sup> O)8, 67(C <sub>5</sub> H <sub>7</sub> <sup>-</sup> )100.

<sup>a</sup>Unresolved peaks. <sup>b</sup>Cyclisation of the epoxy-anion will afford the tetrahydropyran-2-methanol anion with the  $^{18}\text{O}$ -label in the ring. Thus the relative ratios of  $m/z$  99:97 and 87:85 will be reversed in the two spectra, as observed.  
*different*

#### 4.2.3.3 Condensed Phase Reactions of **10**, **11** and **12**

The base catalysed reactions of the neutral alcohols of **10**, **11** and **12** have been studied in 10% aqueous sodium hydroxide at both 20°C and at reflux (Table 4.13). Tetrahydropyran-2-methanol is the major product formed from the epoxide. At 20°C the reaction reaches completion within 1 hour, with the product ratio of tetrahydropyran-2-methanol to 3-oxepanol being 72:28. Completion of reaction at 100°C occurs within 10 minutes with a product ratio of 61:39. There is no significant change in these product ratios (at constant temperature) with increasing time implying that the two competing S<sub>N</sub>i reactions of 5,6-epoxyhexoxide anion are kinetically controlled under these reaction conditions. Both tetrahydropyran-2-methanol and 3-oxepanol are stable under these conditions, and even after

60 hours at reflux neither reactant reverts back to 4-(2-oxiranyl)-1-butanol (Table 4.13).

Table 4.13 Condensed Phase Reactions of 4-(2-oxiranyl)-1-butanol, tetrahydropyran-2-methanol, and 3-oxepanol.<sup>a</sup>

Reactant	Time	20°C/10% NaOH	100°C/10%NaOH
4-(2-oxiranyl)- 1-butanol	5 min.	70:24:6	0:61:39
	1 hr.	0:72:28	0:60:40
	60 hrs.	0:70:30	0:63:37
Tetrahydro- pyran-2- methanol	1 hr.	0:100:0	0:100:0
	60 hrs.	0:100:0	0:100:0
3-oxepanol	1 hr.	0:0:100	0:0:100
	60 hrs.	0:0:100	0:0:100

<sup>a</sup>For experimental conditions see experimental section. <sup>b</sup>The ratio represents the isomeric neutral alcohol of 10:11:12.

#### 4.2.3.4 Summary

The *ab initio* results for this system indicate that **10** should cyclise to both **11** and **12**, provided that the barriers to the transition states control the reactions.

It is evident that experimentally in the gas phase **10** cyclises to give exclusively **11**: product anion **12** is not detected.

In the condensed phase, in aqueous solvent, **10** cyclises to afford both **11** and **12** in apparently kinetically controlled reactions, with **11** being the predominant product.

The situation for this system appears to be analogous to the scenario observed for the  $S_Ni$  processes of 4,5-epoxypentoxide anion. The theoretical results appear to predict a different outcome to that observed experimentally in the gas phase.

These results are considered further in Section 4.3.

### 4.3 Competing $S_Ni$ Reactions - the Arrhenius Factor

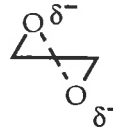
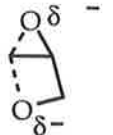
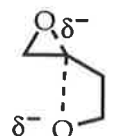
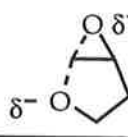
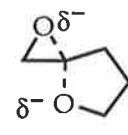
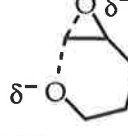
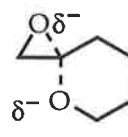
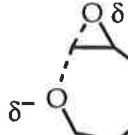
The results of the three homologous systems for which competing  $S_Ni$  processes have been discussed are now considered together along with the results for the Payne system studied by Dua *et al.*<sup>112</sup> Table 4.14 lists the computed transition state barriers as well as the parameters which appear to most influence these barriers, i.e.:

- (i) the angle of approach of each nucleophilic alkoxide ion to the receptor carbon, i.e. the more the transition state represents a classical  $S_N2$  mechanism (angle of approach close to  $180^\circ$ ) the more favourable the reaction, and
- (ii) the maximum ring strain energies involved in forming the transition states.

The ring strain energy for ethylene oxide is  $112.5 \text{ kJ mol}^{-1}$ ,<sup>114</sup> therefore there will be release of ring strain in going from the reactant epoxy-alkoxide anions to all of the larger ring systems. However the competing  $S_Ni$  products may have substantially differing ring strain energies. Take for example System 4.2 (Table 4.14). The two  $S_Ni$  products have ring strain

energies which are significantly different (ring strains of oxetane and tetrahydrofuran are 107.5 and 25 kJ mol<sup>-1</sup> respectively).<sup>114</sup> This difference in ring strain would be reflected, at least partially, in the barriers to the two respective transition states with the formation of the least strained transition state being the more favoured. The more strained transition state **C**, however, is in a better configuration for an S<sub>N</sub>2 attack with the nucleophilic alkoxide attacking the electrophilic carbon at an angle of 163.4° compared with 140.4° for transition state **D**. These considerations may explain why the two different transition states have similar energy barriers. This trend is also observed for the energy barriers of competing transition states **E** and **F**, and **G** and **H** (Table 4.14). The transition state barriers for the two competing S<sub>N</sub>i processes from 2,3-epoxypropoxide anion (System 4.1, Table 4.14) are, however, significantly in favour of the Payne product. The maximum ring strain for both competing products are comparable (ring strain values for ethylene oxide and oxetane are 112.5 and 107.5 kJ mol<sup>-1</sup> respectively).<sup>114</sup> The angle of nucleophilic attack for the Payne product is 160° compared with 116.5° for formation of the alternative four-membered counterpart. The difference in nucleophilic approach is reflected in the relative energy barriers to the two corresponding transition states (Table 4.14).

Table 4.14 Parameters Influencing the Kinetics of the  $S_Ni$  Processes. Major Products

TransitionState	Barrier (kJ mol <sup>-1</sup> ) <sup>a</sup>	Angle O-C-O	Ring Strain (kJ mol <sup>-1</sup> ) <sup>b</sup>	Product(s)	
				Gas Phase	Condensed Phase <sup>c</sup>
System 4.1					
 <b>A</b>	45 <sup>d</sup>	160.1	112.5	Major	e
 <b>B</b>	122 <sup>d</sup>	116.5	107.5	Minor	
System 4.2					
 <b>C</b>	70	163.4	107.5	Major <sup>f</sup>	Minor
 <b>D</b>	69	140.4	25	Major <sup>f</sup>	Major
System 4.3					
 <b>E</b>	48	156.1	25	Sole product	Major
 <b>F</b>	48	152.8	6.3	-	Minor
System 4.4					
 <b>G</b>	35	154.4	6.3	Sole product	Major
 <b>H</b>	40	156.4	26.7	-	Minor

<sup>a</sup>Calculations at MP2-Fc/6-31+G(d) level. <sup>b</sup>Maximum ring strain values from reference.<sup>114</sup>

<sup>c</sup>Carried out in 10% aqueous sodium hydroxide (for full details see experimental section).

<sup>d</sup>Calculations at G2 level in these two cases.<sup>112</sup> <sup>e</sup>Not performed. However alkyl substituted 2,3-epoxypropoxide anions exclusively undergo the Payne rearrangement.<sup>102</sup> <sup>f</sup>Gas phase experiments only indicate that both are formed in approximately comparable yield.

The major and minor products obtained both in the gas and condensed phases from each system are also listed in Table 4.14. If the size of the transition state barriers control the reaction rates of these  $S_Ni$  processes, then our *ab initio* calculations predict, with the exception of System 4.1, that all competing processes should occur in the gas phase in comparable yields. This is indeed the situation for System 4.2, i.e. 3,4-epoxybutoxide anion cyclises in the gas phase to give comparable amounts of both  $S_Ni$  products. The remaining systems, however, do not follow this prediction. The smaller ring product, as predicted from "Baldwin's rules", which occurs by attack of the alkoxide ion on the more substituted epoxide carbon atom, is the major product for system 4.1 and the sole product for Systems ~~4.1~~, 4.3 and 4.4.

It is important to remember that from the Arrhenius equation (equation 4.1), the rate constant  $k$  is the product of a pre-exponential factor  $A$  and an exponential energy term.

$$k = A \exp\left(\frac{-E_a}{RT}\right) \quad \text{Equation 4.1}$$

where  $R$  is the gas constant,  $T$  is the temperature and  $E_a$  is the activation energy (transition state barrier). The reaction rate is therefore not only dependent on the activation energy, but the  $A$  factor needs also to be considered. The pre-exponential factors for the competitive  $S_Ni$  processes may be influenced by factors such as:

- (i) the initial nucleophilic attack to form the transition state (i.e. the ability of the nucleophile to access the appropriate channel), and/or
- (ii) the nature of the transition state, i.e. whichever is "looser" (more disordered) should result in a higher reaction rate.

The minimum energy pathway for these  $S_Ni$  processes are a complex function of coordinates representing stretches and bends of various bonds, and so the reaction coordinates should not be directly associated with any one degree of freedom. To fully visualise and understand the relative abilities of the nucleophile to access the two possible  $S_Ni$  channels would require an intimate knowledge of the potential surface maps for those processes, which we have not calculated. We may, however, determine the entropic natures of the two competing transition states by calculating the relative pre-exponential values. By considering transition state theory<sup>122</sup> we have assessed the relative pre-exponential values for the two competing cyclisation channels from each system. The expression for the unimolecular rate constant ( $k$ ) for a canonical ensemble of molecules at temperature,  $T$ , is given by equation 4.2.

$$k(T) = \frac{k_B T}{h} \frac{Q^\ddagger}{Q_R} \exp\left(\frac{-E_0}{k_B T}\right) \quad \text{Equation 4.2}$$

where  $k_B$  is Boltzman's constant,  $h$  is Planck's constant,  $E_0$  is the energy difference between reactant and transition state at 0°K and  $Q^\ddagger$  and  $Q_R$  are the molecular partition function densities of the transition state and reactants respectively. This equation consists of an exponential factor which is primarily dependent on the transition state barrier (activation energy) and a pre-exponential factor which describes the entropy of the transition state, i.e. the shape of the potential energy surface orthogonal to the reaction coordinate in the region of the transition state.



Comparing equation 4.2 with the Arrhenius rate expression (equation 4.1), shows that the Arrhenius  $A$  factor is equivalent to the pre-exponential term of equation 4.2, viz

$$A \approx \left( \frac{k_B T}{h} \right) \left( \frac{Q^\ddagger}{Q_R} \right)$$

The partition function density of a molecule,  $Q$ , is a number that gives an approximate measure of the number of internal and translational energy states accessible to that molecule at a given temperature. It can be factorised into partition function densities for translation, rotation, vibration and electronic state as shown in equation 4.3.

$$Q = Q_{Trans} Q_{Rot} Q_{Vib} Q_{Elec}.$$

Equation 4.3

Since we are dealing with anions, there will in general be only one electronic state accessible, hence  $Q_{Elec} = 1$ . As we are treating a unimolecular rearrangement, the translational partition functions ( $Q_{Trans}$ ) of the transition state and the reactant will be identical. To a reasonable approximation, so will the rotational partition functions ( $Q_{Rot}$ ). Thus approximation of the  $A$  factor for each process simplifies to evaluating the vibrational partition functions for the reactant, and the competing transition states. Since the reactant is the same for each competing  $S_Ni$  process, we need only to consider  $Q_{Vib}$  of the two competing transition states. It must be noted at this stage that the anions in our mass spectrometer before and especially after collisional activation do not follow a

Boltzman (thermalised) distribution of internal energies (hence do not form a canonical ensemble). The use of partition functions in assessing the relative frequency factors must only be considered in a semi-quantitative sense. To evaluate these functions, we have calculated the harmonic vibrational frequencies of each structure at the HF/6-31+G(d) level of theory using the Gaussian 94 suite of programs.<sup>51</sup> The vibrational partition function at temperature  $T$  is then given within the normal mode - harmonic approximation by equation 4.4.

$$Q_{vib.} = \prod_{n=1}^{3n-(6+1)} \frac{1}{\left(1 - \exp\left(\frac{-h\lambda\nu_n}{k_B T}\right)\right)} \quad \text{Equation 4.4}$$

where  $\nu_n$  is the harmonic vibrational frequency belonging to vibrational mode  $n$  (there being  $3n-(6+1)$  normal modes of vibration in a non-linear molecule excluding the vibrational mode corresponding to the reaction coordinate).  $\lambda$  is a scaling factor introduced in order to minimise the absolute error in HF/6-31+G(d) calculated harmonic vibrational frequencies at the low end of the range ( $\lambda = 0.9131$ ).<sup>123</sup>

A difficulty often encountered in evaluating vibrational partition function densities from calculated harmonic vibrational frequencies arises due to the problem of hindered rotors.<sup>124,125</sup> Stated simply, the potential energy surface along low frequency modes corresponding to bond torsions is of a sinusoidal rather than a parabolic shape. The harmonic vibrational partition functions for these modes underestimate the actual hindered rotor partition functions (which are best included in the rotational partition function). As the reactant anion contains an alkyl chain, it is expected that

the hindered rotor problem may lead to errors in the vibrational partition function density. Since (i) we are only interested in the ratio of the frequency factors for the two competing cyclisation channels, and (ii) they both begin from the same reactant, it is sufficient to simply compare the harmonic vibrational partition function densities of the two transition states. The calculated vibrational frequencies of each of the transition states consist of one negative frequency. This purely imaginary frequency corresponds to the reaction coordinate. The degree of freedom corresponding to the reaction coordinate is not included in calculating  $Q^\ddagger$ . The other frequencies, however, are used to find the transition state vibrational partition function. The  $Q_{Vib}$  values for the transition states are listed in Table 4.15.

Table 4.15 Harmonic Vibrational Partition Functions of  $S_{Ni}$  Transition States at 298°K.<sup>a,b</sup>

Transition state	$Q_{Vib}$ (298K)
Transition state <b>A</b>	3.4
Transition state <b>B</b>	2.5
Transition state <b>C</b>	9.8
Transition state <b>D</b>	4.7
Transition state <b>E</b>	20.4
Transition state <b>F</b>	10.2
Transition state <b>G</b>	63.1
Transition state <b>H</b>	26.3

<sup>a</sup>Representations of **A** - **H** are given in Table 4.14 (page 148).

<sup>b</sup>Harmonic vibrational frequencies for the transition states are shown in Appendices D - G.

The values listed in Table 4.15 represent the partition function density. A large partition function density represents a large density of states which results from a broad transition state potential, i.e. the transition state is "loose" and readily accessible. In contrast, if a transition state has a narrow partition function density then the transition state will be "tight" and less accessible, since the narrow potential will hinder a reaction occurring *via* this pathway. Consider, for example, System 4.4 (page 148). The vibrational partition functions for transition state **G** is 63.1 compared with 26.3 for the

\* See appendix p 227 d

competing transition state **H** (Table 4.15). The significantly larger partition function for **G** suggests that this transition state is "looser" than **H** and that the probability of reaction *via* transition state **G** would be higher than the reaction through **H**. This situation is summarised (in exaggerated form) in Figure 4.15. Comparable amounts of energy are required for the reactant anion to reach the two competing transition states, however, transition state **G** has a higher density of states and is therefore 'looser' and more accessible. The probability of formation of the six-membered ring is higher than formation of the competing seven-membered product.

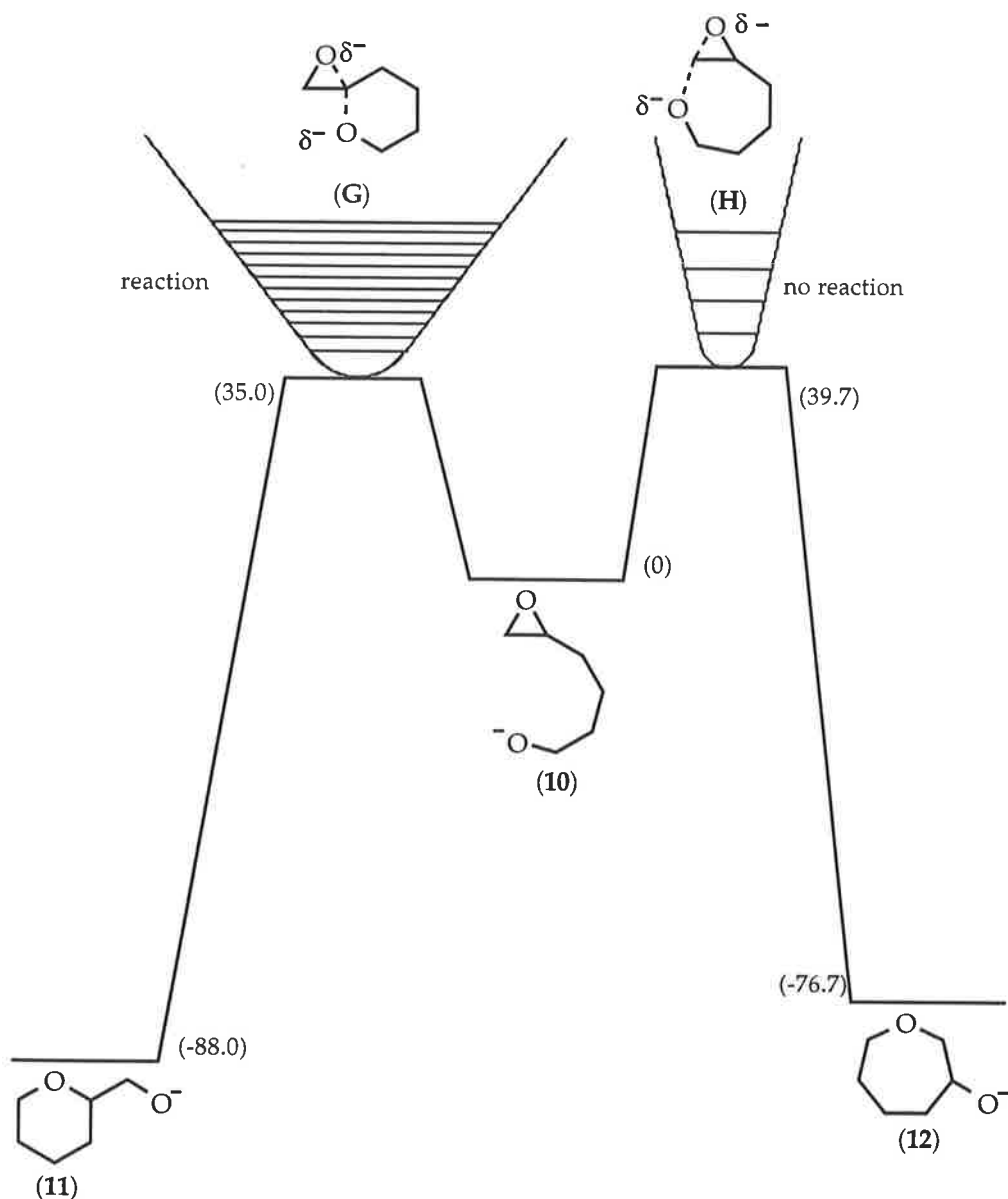


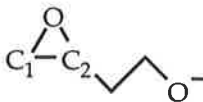
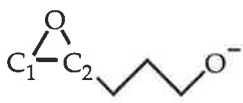

Figure 4.15 The transition state **G** has a greater density of states and is therefore the "looser" transition state. The probability of reaction passing through transition state **G** is greater than reaction proceeding through **H**.

The vibrational partition functions for System 4.3 suggest that formation of the five-membered ring is more likely to occur in preference of the six-membered cyclic isomer. Although the  $Q_{Vib}$  values for System 4.2 are significantly smaller than the calculated values for the other two systems,

they predict that transition state **C** is 'looser' than **D** and should be more accessible.

The atomic Mulliken charge distribution<sup>126</sup> for the reactant epoxy-alkoxide anions have also been calculated<sup>51</sup> and the Mulliken charge ratio (the relative electrophilicities) of C<sub>1</sub> and C<sub>2</sub> (the carbons on the ethylene oxide ring) of the reactants are shown in Table 4.16.

Table 4.16 Mulliken Charge Ratios for the Oxirane Carbons for the Reactant Anions.

Reactant anion	Mulliken charge ratio <sup>a</sup> C <sub>1</sub> : C <sub>2</sub>
 (1)	0.158 : 0.336
 (7)	0.181 : 0.329
 (10)	0.168 : 0.419

<sup>a</sup>The Mulliken charge distribution is that of C<sub>1</sub> and C<sub>2</sub> in the reactant.<sup>51</sup>

The more substituted oxirane carbon (C<sub>2</sub>) in each system is more electron deficient than the unsubstituted (C<sub>1</sub>) position. The nucleophilic alkoxide anion would have a greater tendency to attack the more electrophilic site, thus favouring formation of the smaller ring system *via* S<sub>N</sub>i cyclisation of the epoxy-alkoxide anions.<sup>a</sup>

The experimental gas phase results for System 4.3 and 4.4 (Table 4.14) are perhaps at first a little surprising but they are consistent and qualitatively similar to the predictions of the *ab initio* studies. The computed barriers for each of the competing reactions are comparable in each system (48 kJ mol<sup>-1</sup> for **E** and **F**; 35 and 40 kJ mol<sup>-1</sup> for **G** and **H**), yet in both cases there is only one product formed in the gas phase, viz the products predicted from "Baldwin's rules": i.e. those formed through **E** and **G** respectively. The frequency factor must control the gas phase reactions for System 4.3, since the transition state energy barriers predict formation of both S<sub>N</sub>i products. The same scenario probably also pertains for System 4.4. Although the barriers in System 4.4 are different (35 and 40 kJ mol<sup>-1</sup>), they are very modest, and if they are a major influence in determining the product ratio, then products should be observed from both processes. The Mulliken data (Table 4.16) also supports the observed formation of the smaller ring system, since nucleophilic attack is initiated at the more electrophilic carbon centre.

We propose that for both Systems 4.3 and 4.4, the gas phase S<sub>N</sub>i reactions are controlled by frequency factors. The condensed phase reactions (in 10% aqueous sodium hydroxide at 20°C and reflux) reflect the expected trend. The smaller ring system, as predicted from "Baldwin's rules", is formed predominantly in each case.

---

<sup>a</sup> The transition state geometries (see Appendices A - C) indicate that the forming C-O bond length is consistently longer than the breaking C-O epoxide bond suggesting, that in the gas phase, these S<sub>N</sub>i reactions have S<sub>N</sub>2 character.



System 4.1 illustrates the Payne rearrangement which may compete with formation of an alternative oxetane alkoxide ion. In the gas phase the Payne rearrangement is the major process: a feature in accord with the *ab initio* data. The Payne rearrangement (which proceeds through transition state **A**) is favoured by the lower barrier of 45 kJ mol<sup>-1</sup> (*cf.* 122 kJ mol<sup>-1</sup> for **B**, Table 4.14). The major contributor to the large barrier to transition state **B** is the unfavourable geometry of the transition state, i.e. angle O-C-O is computed to be 116.5° (*cf.* 160.1° for **A**: the closer the O-C-O angle is to the ideal S<sub>N</sub>2 angle of 180°, the more favoured will be the reaction if other parameters are equal). Although the larger Arrhenius factor (Table 4.15) also favours the formation of transition state **A**, the large barrier difference is a major factor influencing the competing S<sub>N</sub>i reactions for this system.

The situation with regard to competing S<sub>N</sub>i reactions of 2,3 epoxybutoxide anion (System 4.2, Table 4.14) is not as clear as the three other systems. System 4.2 shows similarities to that of System 4.3, i.e. the barriers to the two processes are comparable (Table 4.14), as are the Mulliken and  $Q_{Vib}$  ratios (Table 4.15 and Table 4.16)). However, there is one feature which distinguishes this system from the other three, viz the two product alkoxides have very different thermodynamic stabilities. The five-membered product ion is 82 kJ mol<sup>-1</sup> more negative in energy than the four-membered counterpart (see Figure 4.1, page 97). This large difference of 82 kJ mol<sup>-1</sup> is due principally to the significant difference in ring strain between the oxetane and tetrahydrofuran systems (Table 4.14).

Condensed phase reactions of System 4.2 (Table 4.5, page 112) have been studied in two different solvent systems (10% aqueous sodium hydroxide and sodium hydride/tetrahydrofuran) at reflux and the experimental results show that tetrahydrofuran methanol is the major product in both solvent systems. We anticipated that this might be explained in terms of the

reactions being thermodynamically controlled in solution. This, however, appears not to be the case. The product ratios at reaction times between 10 minutes and 60 hours are the same within experimental error leading to the conclusion that the five-membered ring is the kinetic product.

From an experimental viewpoint, System 4.2 (Table 4.14) is the most complex  $S_Ni$  process to have been studied. Consideration of the spectra of the  $(M-H)^-$  ion of 2-(2-oxiranyl)-1-ethanol (**1**), the two possible  $S_Ni$  product anions (**2**) and (**3**), and the deuterium and  $^{18}O$ -labelled analogues of **1** show that in the gas phase:

- (i) both cyclisation products are formed in comparable yield,
- (ii) the three and four membered anions are interconvertible under conditions of collisional activation, and
- (iii) the tetrahydrofuranyl methoxide product **3** does not interconvert to the reactant anion **1**. These observations are in agreement with the *ab initio* results, and from the studies of this system we conclude that although the Mulliken charge data and the slightly larger  $Q_{Vib}$  favours formation of transition state **C**, the similar barriers to the transition states are the major factor influencing the competing  $S_Ni$  reactions. This result is not in accord with "Baldwin's rules" which predict that cyclisation to the smaller ring would be preferred over the  $S_Ni$  process to form the competing five-membered isomer.

"Baldwin's rules" are, however, based on the stereochemical requirements of the transition states. The alkyl chain of the epoxy-alkoxide anions discussed, restricts the relative motions of the terminal nucleophile and the electrophilic oxirane carbon. Thus the nature and length of alkyl chain, and the ring size, will determine whether the nucleophilic alkoxide anions and the electrophilic oxirane carbons can attain the required transition state geometry in order to effect ring closure. The favoured transition state for

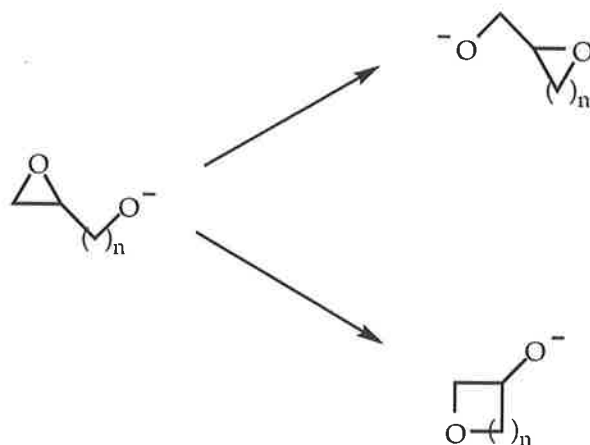
opening three-membered rings to form cyclic structures requires the incoming nucleophile to attack the electrophile at an angle close to  $180^\circ$  (i.e. the classical Walden  $S_N2$  reaction).<sup>113</sup> The angle of attack calculated for the transition states leading to formation of the four-membered and five-membered isomers is  $163.4^\circ$  and  $140.4^\circ$  respectively (Table 4.14). Although this nucleophilic attack favours the transition state leading to the smaller ring system, the large difference in ring strain, which favours formation of the larger ring system, needs also to be considered. The theoretical results predict that, provided these kinetically controlled reactions are influenced by the transition state barriers, formation of both  $S_Ni$  products would occur in the gas phase in comparable amounts, and our experimental gas phase studies indicate that this is the scenario for the  $S_Ni$  reactions of the 2,3-epoxybutoxide anion.

#### 4.4 Conclusions

In conclusion, for the scenario outlined in scheme 4.33:-

- (i) the gas phase  $S_Ni$  reactions for the systems ( $n = 1,^{112} 3$  and  $4$ ) give the smaller ring system either exclusively or in the larger yield, in accord with "Baldwin's rules".<sup>113</sup> When  $n = 2$ , both products are formed in comparable yields, as predicted from the *ab initio* results.
- (ii) the corresponding condensed phase reactions preferentially give the smaller ring system in higher yield when  $n = 1,^{102} 3$  and  $4$ . When  $n=2$ , the larger ring system is formed in the higher yield.

Scheme 4.33



These  $S_Ni$  reactions are controlled by both the barriers to the transition states and the Arrhenius factor (frequency factor). The barriers to the transition states of competing  $S_Ni$  reactions are dependent on a number of factors including, (i) the angle of approach of each nucleophile to the receptor atom (the closer to  $180^\circ$ , the more favourable the reaction), (ii) the relative ring strain energies involved in forming the competing transition states, and (iii) the electrophilicities of the recipient carbon centre. The Arrhenius factor for the competitive  $S_Ni$  processes may be influenced by (i) the initial nucleophilic attack to form the transition state, i.e. the ability of the nucleophile to access the appropriate channel, and the depth of that channel, and/or (ii) the entropic nature of the transition state, i.e. whichever is "looser" (more disordered) should result in a higher reaction rate. We propose that when  $n = 2$  and  $3$  (scheme 4.33) the barriers to the competing transition states are a major factor influencing the reaction rates. For the higher homologues, i.e. when  $n = 3$  and  $4$  (scheme 4.33), the frequency factors are controlling the  $S_Ni$  reactions.

# Chapter 5

## Experimental

### 5.1 General Experimental

Melting points were determined on a Kofler hot-stage apparatus equipped with a Reichert microscope, and are uncorrected.  $^1\text{H}$  and  $^{13}\text{C}$  spectra were measured using Varian Gemini-2000 spectrometers operating VNMR 5.3B software with operating frequencies of 200 MHz and 300 MHz.  $\text{CDCl}_3$  was used as solvent unless otherwise indicated.  $^1\text{H}$  resonances are quoted in parts per million downfield from the  $^1\text{H}$  resonance of tetramethylsilane (TMS),  $^{13}\text{C}$  resonances are referenced using the  $\text{CDCl}_3$  resonance (which falls  $\delta$  77.0 ppm downfield from the TMS resonance). The multiplicities of signals are reported as being: s, singlet; d, doublet; t, triplet; q, quartet; m, an unassignable multiplicity or overlapping signal; br, broadened signal.

Infra-red spectra were recorded on a Hitachi 270-30 spectrometer using nujol mulls or neat liquid films on sodium chloride plates. The conventional electron impact (EI) mass spectra were recorded on a VG ZAB 2HF mass spectrometer operating with an ionisation energy of 70 eV.

Flash column chromatography was performed using Merck silica gel 60 (particle size: 0.04 - 0.063 mm (230 - 240 mesh ASTM)).

Anhydrous diethyl ether and tetrahydrofuran (THF) were obtained by distillation from sodium using benzophenone ketyl as indicator immediately prior to use. All solvents used for chromatography were

distilled before use. Other reagents were purified according to literature procedures.<sup>127</sup>

Mineral oil was removed from sodium hydride 60% suspension by washing with hexane several times under a nitrogen atmosphere.

All organic extracts were dried over anhydrous magnesium sulphate unless otherwise specified.

Collisional activation (CA) mass spectra (MS-MS) were determined with a VG ZAB 2HF mass spectrometer operating in the negative ion chemical ionisation (NICI) mode. The ionising energy was 70 eV (tungsten filament), the ion source temperature was 100°C, and the accelerating voltage was 7 kV. The liquid samples were introduced through the septum inlet whilst solids were inserted *via* a direct probe with no heating [measured pressure of sample  $1 \times 10^{-6}$  Torr (1 Torr = 133.322 Pa)]. Deprotonation was effected using  $\text{HO}^-$  (from  $\text{H}_2\text{O}$ : measured pressure  $1 \times 10^{-5}$  Torr). The estimated source pressure was  $10^{-1}$  Torr. Argon was used in the second collision cell (measured pressure, outside the cell,  $2 \times 10^{-7}$  Torr), giving a 10% reduction in the main beam, equivalent to single collision conditions. Collisionally activated dissociations [(CA) MS-MS] measurements involved using the magnet to choose the ion under study [normally the  $(\text{M-H})^-$  species], collision activating it (see above), and scanning the electric sector to analyse the resultant product anions. Charge reversal (CR) (positive ion) MS-MS data for negative ions were obtained as for CA MS-MS data, except that the electric sector potential was reversed to allow the transmission of positively charged product ion. Oxygen was used in the second collision cell for CR spectra recorded in this thesis. The recorded peak widths at half height are an average of ten individual measurements. Gas chromatography-mass spectrometry (GC-MS) spectra were recorded on a Finnigan MAT GCQ mass spectrometer. Conditions: column phase RTX-SMS (length 30 m, internal

diameter 0.25 mm, GC fused silica capillary), He gas. Initial column temperature was held at 50°C for 2 minutes, then the temperature was increased at 15°C per minute to a maximum temperature of 210°C if necessary. Product ratios were determined by comparing the areas under the corresponding peaks (this ratio correlates closely with the ratios obtained using ion counts/peak).

*Ab initio* molecular orbital calculations were carried out using the Gaussian 94<sup>51</sup> suite of programs. Computational platforms used were a Silicon Graphics Indigo<sup>2</sup> xZ workstation and two SGI Power Challenge supercomputers.

The geometries of the local minima and the transition states were optimised at the RHF/6-31+G(d) level of theory. Harmonic frequency analysis as performed on each stationary point in order to characterise it as either a local minimum or a transition state. A local minimum is characterised by possessing all real vibrational frequencies and its hessian matrix possessing all negative eigenvalues. A transition state is characterised by possessing one (and only one) imaginary frequency and its hessian matrix possessing one (and only one) negative eigenvalue. Intrinsic Reaction Coordinate (IRC) calculations were performed (beginning from transition structures) to verify that each transition structure connected particular local minima.

All compounds examined in this thesis which are not described in the experimental section are commercial samples purchased from Aldrich Chemical Co.

## 5.2 Compounds Described in Chapter 2

### Preparation of N-(methoxyphenyl)benzamides - General Procedure

Benzoyl chloride (1.16 g) was added dropwise to a suspension of the appropriate anisidine (1 g) in aqueous sodium hydroxide (10%, 10 ml) at 0°C with stirring.<sup>128</sup> The precipitate was collected by filtration, washed with water (2 x 2 ml) and recrystallised from methanol.

The physical and spectral data for the N-(methoxyphenyl)-benzamide series is given below.

*Para*<sup>129</sup>- (1.4g, 76%) as greyish white plates. m.p. 154°C. (lit. m.p. 155 - 156°C).<sup>129</sup>

<sup>1</sup>H n.m.r. (200 MHz/CDCl<sub>3</sub>): δ 3.82 (3H, s), 6.89 - 7.89 (9H, m).

*Meta*<sup>130</sup>- as white crystals. m.p. 112 - 113°C. (lit. m.p. 111 - 112°C).<sup>131</sup>

<sup>1</sup>H n.m.r. (200 MHz/CDCl<sub>3</sub>): δ 3.83 (3H, s), 6.69 - 7.98 (9H, m).

*Ortho*<sup>132</sup>- as light brown needles (0.9g, 50%). m.p. 65 - 67°C. (lit. 66 - 67°C).<sup>133</sup>

<sup>1</sup>H n.m.r. (200 MHz/CDCl<sub>3</sub>): δ 3.89 (3H, s), 6.87 - 8.56 (9H, m).

### N-(2-Methoxyphenyl)-d<sub>5</sub>-benzamide

Benzoyl-d<sub>5</sub> chloride (0.45 g) was added dropwise to a suspension of *o*-anisidine (0.45 g) in aqueous sodium hydroxide (10%, 5 ml). The precipitate was collected by vacuum filtration and recrystallised from methanol to afford N-(2-methoxy phenyl)-d<sub>5</sub>-benzamide as light brown crystals (0.5 g, 72%). m.p. 62 - 63°C.



$^1\text{H}$  n.m.r. (200 MHz/ $\text{CDCl}_3$ ):  $\delta$  3.19 (3H, s), 6.89 - 7.1 (3H, m), 8.5 - 8.56 (1H, m).

### Preparation of N-(ethoxyphenyl)benzamides - General Procedure

To a suspension of the appropriate phenetidine (1 g) in aqueous sodium hydroxide (10%, 10 ml) at  $0^\circ\text{C}$  was added dropwise benzoyl chloride (1 g). The precipitate was collected *via* vacuum filtration and recrystallised from methanol.

The physical and spectral data for the N-(ethoxyphenyl)-benzamides series are given below.

*Para*<sup>134</sup>- (1.3 g, 74%) as fine white needles. m.p.  $172 - 173^\circ\text{C}$  (lit. m.p.  $169 - 170^\circ\text{C}$ ).<sup>134</sup>

$^1\text{H}$  n.m.r. (200 MHz/ $\text{CDCl}_3$ ):  $\delta$  1.41 (3H, t), 4.03 (2H, q), 6.88 - 7.88 (9H, m).

*Meta*- (1.3 g, 74%) as white needles. m.p.  $108 - 109^\circ\text{C}$ . Found: C 74.72, H 6.19, N 5.78%;  $\text{C}_{15}\text{H}_{15}\text{NO}_2$  requires C 74.66, H 6.27, N 5.81%.

$\nu_{\text{max}}$  (nujol); 3270 (NH), 1652 (C=O), 1600, 1540  $\text{cm}^{-1}$ ;  $m/z$ (rel. abund.): 241( $\text{M}^+$ , 33), 105(100), 77(53), 51(13);  $^1\text{H}$  n.m.r. (300 MHz/ $\text{CDCl}_3$ ):  $\delta$  1.42 (3H, t), 4.07 (2H, q), 6.68 - 7.89 (9H, m);  $^{13}\text{C}$  n.m.r. (75 MHz/ $\text{CDCl}_3$ ):  $\delta$  10.25 ( $\text{CH}_3$ ), 59.05 ( $\text{CH}_2$ ), (101.85, 106.65, 107.53, 122.42, 124.28, 125.19, 127.31, 130.8, 134.2, 154.87 (aromatics)), 161.3 (C=O).

*Ortho*:- The reaction mixture was extracted with dichloromethane (3 x 5 ml), the combined extracts dried ( $\text{MgSO}_4$ ), concentrated *in vacuo* and the residue distilled to afford N-(2-ethoxyphenyl)-benzamide (1 g, 57%) as a colourless liquid, (b.p.  $142 - 146^\circ\text{C}/0.07$  mm Hg) which solidified upon

cooling. m.p. 42 - 43°C. Found: C 74.63, H 6.12, N 5.71%;  $C_{15}H_{15}NO_2$  requires C 74.66, H 6.27, N 5.81%.

$\nu_{\max}$  (nujol); 3310 (NH), 1675 (C=O), 1603, 1581, 1522;  $m/z$ (rel. abund.): 241( $M^+$ , 35), 196(4), 136(6), 105(100), 77(56), 51(20);  $^1H$  n.m.r. (300 MHz/ $CDCl_3$ ):  $\delta$  1.48 (3H, t), 4.14 (2H, q), 6.88 - 8.64 (9H, m);  $^{13}C$  n.m.r. (75 MHz/ $CDCl_3$ ):  $\delta$  14.92 ( $CH_3$ ), 64.33 ( $CH_2$ ), (111.01, 119.84, 121.18, 123.79, 126.98, 128.03, 128.79, 131.64, 135.46, 147.49 (aromatics)), 165.05 (C=O).

### Preparation of Methyl(N-benzoyl)amino benzoates

#### (i) Amino methylbenzoates - General Procedure

Prepared by a procedure adapted from that of Dougherty *et al.*<sup>135</sup>

The appropriate aminobenzoic acid (2 g) in anhydrous methanol (10 ml) containing concentrated sulfuric acid (0.1 ml) was refluxed for 90 mins., cooled to 20°C, the methanol removed *in vacuo*, and the residue dissolved in water (10 ml). The reaction mixture was neutralised with aqueous sodium hydrogen carbonate (10%, 10 ml), extracted with dichloromethane (3 x 5 ml), the combined extracts washed with water (10 ml), aqueous sodium chloride (10 ml) and dried ( $MgSO_4$ ). Removal of the solvent *in vacuo* afforded the amino methyl benzoate which was recrystallised from methanol. The physical and spectral data for the amino methylbenzoates are given below.

*Para*-<sup>136</sup> (2 g, 90.7%) as white plates. m.p. 110°C (lit. m.p. 112°C).<sup>137</sup>

$^1H$  nmr (200 MHz/ $CDCl_3$ ):  $\delta$  3.86 (3H, s), 4.05 (2H, br s), 6.63 (2H, d), 7.85 (2H, d).

*Meta*<sup>138</sup> (1 g, 90%) as white plates. m.p. 53 - 54°C (lit. m.p. 54°C).<sup>137,139</sup>

<sup>1</sup>H n.m.r. (200 MHz/CDCl<sub>3</sub>): δ 3.88 (3H, s), 6.83 - 7.44 (4H, m).

*Ortho*<sup>140</sup> (1 g, 90%) as a colourless liquid, b.p. 115 - 116°C/6 mm Hg (lit. b.p. 133.5°C/15 mm Hg).<sup>139</sup>

<sup>1</sup>H n.m.r. (200 MHz/CDCl<sub>3</sub>): δ 3.86 (3H, s), 5.75 (2H, br s), 6.6 - 7.87 (4H, m).

### (ii) Methyl (N-benzoyl)amino benzoate - General Procedure

Benzoyl chloride (1.16 g) was added dropwise to a suspension of the appropriate amino methylbenzoate (1 g) in aqueous sodium hydroxide (10%, 10 ml) at 0°C with stirring.<sup>128</sup> The precipitate was collected by filtration, washed with water (2 x 2 ml) and recrystallised from methanol.

The physical and spectral data for the N-(methoxyphenyl)-benzamide series are given below.

*Para*<sup>141</sup>- (1.3 g, 77%) as white needles. m.p. 172 - 173°C. (lit. m.p. 170 - 171°C)<sup>141</sup>

<sup>1</sup>H n.m.r. (200 MHz/CDCl<sub>3</sub>): δ 3.91 (3H, s), 7.51 - 8.09 (9H, m).

*Meta*<sup>141</sup>- (1.2 g, 71%) as pink pale needles. m.p. 133 - 134°C. (lit. m.p. 130 - 131°C)<sup>141</sup>

<sup>1</sup>H n.m.r. (200 MHz/CDCl<sub>3</sub>): δ 3.93 (3H, s), 7.47 - 8.15 (9H, m).

*Ortho*<sup>142</sup>- (1.4 g, 83%) as white needles. m.p. 99 - 100°C. (lit. m.p. 99 - 101°C)<sup>142</sup>

<sup>1</sup>H n.m.r. (200 MHz/CDCl<sub>3</sub>): δ 3.97 (3H, s), 7.13 - 8.96 (9H, m).

### 5.3 Compounds Described in Chapter 3

#### 5-Hydroxy-2-pentanone<sup>143</sup>

Method modified from that of Stacey *et al.*<sup>144</sup>

A solution of mercury(II)oxide (0.15 g) in water (5.7 ml) and concentrated sulfuric acid (0.24 ml) was stirred at 60°C. To the reaction mixture was added, dropwise, 4-pentyn-1-ol (1 g). The solution was stirred for 15 mins., cooled to 20°C and extracted with dichloromethane (3 x 5 ml). The combined organic extracts were dried (MgSO<sub>4</sub>) and concentrated to afford a dark oil. Distillation of the crude oil afforded 5-hydroxy-2-pentanone (0.6 g, 52%) as a colourless oil. b.p. 140 - 142°C/100 mm Hg (lit. b.p. 144 - 145°C/100 mm Hg)<sup>137, 145</sup>

<sup>1</sup>H n.m.r. (200 MHz/CDCl<sub>3</sub>): δ 1.82 (2H, m), 2.18 (3H, s), 2.59 (2H, t), 3.64 (2H, t).

#### 5-Deutero-5-hydroxy-2-pentanone

The labelled hydroxy compound was produced by exchange of the unlabelled compound with D<sub>2</sub>O in the source of the mass spectrometer. (positive ion mass spectrometry indicated *d*<sub>1</sub> > 95%)

#### 5,5-*d*<sub>2</sub>-5-Hydroxy-2-pentanone<sup>146</sup>

(i) A solution of levulinic acid (5 g) and 1,2-ethanediol (3.2 g) in benzene (10 ml) with a catalytic amount of *p*-toluenesulphonic acid monohydrate was heated under reflux for 14 hrs. such that water (0.75 ml) was collected in a

Dean-Stark trap.<sup>147</sup> The reaction mixture was washed successively with aqueous sodium hydroxide (10%, 10 ml) and water (2 x 5 ml). The organic layer was dried (anhydrous NaHCO<sub>3</sub>) and concentrated *in vacuo* to afford 3-(2-methyl-1,3-dioxolan-2-yl) propanoic acid (4.8 g, 70%) as an oil. This was used in the next step without further purification.

(ii) Reduction<sup>148</sup> of the acid was carried out by dissolving 3-(2-methyl-1,3-dioxolan-2-yl) propanoic acid (4.8 g) in anhydrous diethyl ether (20 ml) and adding this dropwise to a suspension of lithium aluminium deuteride (1.3 g) in anhydrous diethyl ether (20 ml) which was stirred at reflux for 1 hr. Aqueous ammonium chloride (saturated, 10 ml) was added, the organic layer separated, the aqueous phase extracted with diethyl ether (2 x 20 ml), the combined organic extracts dried (NaHCO<sub>3</sub>) and concentrated under reduced pressure to afford the 1,1-*d*<sub>2</sub>-3-(2-methyl-1,3-dioxolan-2-yl)-1-propanol (3.1 g, 70%) as a light brown residue. This was used in the next step without purification.

(iii) Deprotection of the carbonyl was achieved by stirring the residue at 20°C for 20 hrs. in a solution of tetrahydrofuran (10 ml) and aqueous hydrogen chloride (2 M, 4 ml).<sup>149</sup> The organic layer was separated, dried (NaHCO<sub>3</sub>), and the solvent removed *via* rotary evaporation, and the brown residue distilled to yield 5,5-*d*<sub>2</sub>-5-hydroxy-2-pentanone (1.8 g, 81%, *d*<sub>2</sub> > 99%) as a colourless liquid, b.p. 144 - 145°C/100 mm Hg.

<sup>1</sup>H n.m.r. (200 MHz/CDCl<sub>3</sub>): δ 1.83 (2H, t), 2.18 (3H, s), 2.59 (2H, t).

#### 5-Hydroxy-5-methyl-2-hexanone<sup>150</sup>

A solution of acetonylacetone (2 g) in anhydrous diethyl ether (5 ml) was stirred at 0°C under nitrogen. Methyl lithium (1.5 M, 15 ml) was added dropwise to the reaction mixture which was refluxed for 2 hrs. The reaction

mixture was cooled to 0°C and quenched by slow addition of aqueous ammonium chloride (saturated, 2 ml). The organic phase was separated, the aqueous layer extracted with diethyl ether (3 x 5 ml), the combined organic extracts dried (MgSO<sub>4</sub>) and concentrated *in vacuo*. The residue was distilled using a Kugelrohr apparatus (oven temperature 110 - 120°C/10 mm Hg) to yield 5-hydroxy-5-methyl-2-hexanone (1.9 g, 83%) as a colourless oil. (lit. Kugelrohr dist. 110 - 130°C/10 mm Hg).<sup>150</sup>

<sup>1</sup>H n.m.r. (200 MHz/CDCl<sub>3</sub>): δ 1.22 (6H, s), 1.76 (2H, t), 2.18 (3H, s), 2.59 (2H, t).

*It has been reported<sup>150,151</sup> that 5-hydroxy-5-methyl-hexanone exists partially as the cyclic hemiketal, tetrahydro-2,5,5-trimethyl-2-furanol. From the <sup>1</sup>H n.m.r. obtained for our sample we see no evidence to support the occurrence of this tautomerism.*

#### 5-Deutero-5-hydroxy-5-methyl-2-hexanone

Prepared in the ZAB 2HF as described above for 5-deutero-hydroxy-2-pentanone; (positive ion mass spectrometry indicated *d*<sub>1</sub> > 95%).

#### 1,1,1,3,3-*d*<sub>5</sub>-5-Hydroxy-5-methyl-2-hexanone

5-Hydroxy-pentanone (1 g) was stirred in methanol-*d* (3 ml) at 20°C with the addition of a small piece of sodium metal. After 1 hr. of stirring, D<sub>2</sub>O (2 ml) was added and the solution stirred a further 30 mins. The reaction mixture was extracted with anhydrous diethyl ether (3 x 4 ml) and the combined ethereal extracts dried (MgSO<sub>4</sub>), concentrated *in vacuo* and distilled using a Kugelrohr apparatus (oven temperature 110 - 130°C/10 mm Hg) to afford 1,1,1,3,3-*d*<sub>5</sub>-5-hydroxy-5-methyl-2-hexanone (0.98 g, 93%, *d*<sub>5</sub> > 90%) as a colourless liquid.

$^1\text{H}$  n.m.r. (200 MHz/ $\text{CDCl}_3$ ):  $\delta$  1.2 (6H, s), 1.72 (2H, s).

#### 6-Hydroxy-2-hexanone<sup>152</sup>

5-Hexyn-1-ol (1 g) was added dropwise to a solution of mercury(II)oxide (0.15 g), water (5.5 ml) and concentrated sulfuric acid (0.22 ml) at reflux. After 30 mins. the reaction mixture was cooled to 20°C and extracted with dichloromethane (3 x 5 ml). The combined organic extract was dried ( $\text{MgSO}_4$ ), and concentrated under reduced pressure. Distillation of the crude oil produced 6-hydroxy-2-hexanone (0.53 g, 45%) as a colourless liquid. b.p. 112°C/15 mm Hg (lit. b.p. 65°C/0.7 mm Hg)<sup>152</sup>

$^1\text{H}$  n.m.r. (200 MHz/ $\text{CDCl}_3$ ):  $\delta$  1.45 - 1.8 (4H, m), 2.16 (3H, s), 2.49 (2H, t), 3.63 (2H, t), 4.75 (1H, br s).

#### 6-Deutero-6-hydroxy-2-hexanone

Prepared in the ZAB 2HF as described above for 5-deutero-hydroxy-2-pentanone (positive ion mass spectrometry indicated  $d_1 > 95\%$ ).

#### 6,6- $d_2$ -6-Hydroxy-2-hexanone

Method modified from that of Eisenbraun.<sup>153</sup>

(i) A solution of chromium trioxide (2.7 g), distilled water (5 ml) and concentrated sulfuric acid (2.3 ml)<sup>153</sup> was added to a stirred solution of 5-hexyn-1-ol (1 g) in acetone (20 ml) at 0°C. The solution was stirred a further 15 mins at 20°C, water (20 ml) was added, the aqueous mixture extracted

with dichloromethane (3 x 10 ml), the combined extracts washed with water (20 ml), dried (MgSO<sub>4</sub>), and concentrated *in vacuo*. The residue was distilled to afford 5-hexynoic acid (1 g, 86%) as a colourless liquid. b.p. 110 - 112°C/8 mm Hg (lit. b.p. 122 - 124°C/760 mm Hg)<sup>154</sup>

(ii) A solution of 5-hexynoic acid (1 g) in anhydrous diethyl ether (3 ml) was added dropwise to a suspension of lithium aluminium deuteride (0.37 g) in anhydrous diethyl ether (6 ml). The reaction mixture was stirred at reflux for 30 mins., cooled to 20°C and quenched by the cautious addition of water (5 ml) followed by aqueous hydrogen chloride (20%, 0.5 ml). The organic layer was separated and the aqueous layer extracted with diethyl ether (3 x 10 ml). The combined organic extracts were dried (MgSO<sub>4</sub>), concentrated *in vacuo* and distilled to afford 1,1-*d*<sub>2</sub>-5-hexyn-1-ol (0.8 g, 89%) as a colourless liquid. b.p. 180 - 182°C/20 mm Hg.

(iii) 1,1-*d*<sub>2</sub>-5-Hexyn-1-ol (0.8 g) was added dropwise to a refluxing solution of mercury(II)oxide (0.1 g) in water (4 ml) and concentrated sulfuric acid (0.15 ml). After 30 mins. reflux the solution was cooled to 20°C and extracted with dichloromethane (3 x 5 ml). The combined extracts were dried (MgSO<sub>4</sub>), concentrated under reduced pressure, and the residue distilled to afford 6,6-*d*<sub>2</sub>-6-hydroxy-2-hexanone (0.45 g, 47%, *d*<sub>2</sub> > 99%) as a colourless oil. b.p. 68°C/0.7 mm Hg.

<sup>1</sup>H n.m.r. (200 MHz/CDCl<sub>3</sub>): δ 1.45-1.8 (4H, m), 2.16 (3H, s), 2.49 (2H, t).

#### 1,1,1,3,3-*d*<sub>5</sub>-6-Hydroxy-2-hexanone

6-Hydroxy-2-hexanone (0.5 g) was stirred in methanol-*d* (1.5 ml) containing a small piece of sodium metal at 20°C. After stirring for 1 hr., D<sub>2</sub>O (1 ml) was added and the solution stirred a further 30 mins. The aqueous solution was extracted with diethyl ether (3 x 2 ml), the combined extracts dried



(MgSO<sub>4</sub>), concentrated *in vacuo* and the residue distilled using a Kugelrohr apparatus (oven temperature 90 - 100°C/0.7 mm Hg) to afford 1,1,1,3,3-*d*<sub>5</sub>-6-hydroxy-2-hexanone (0.48, 92%, *d*<sub>5</sub> > 90%) as a colourless liquid.

<sup>1</sup>H n.m.r. (200 MHz/CDCl<sub>3</sub>): δ 1.45 - 1.8 (4H, m), 3.64 (2H, t).

#### 6-Hydroxy-6-methyl-2-heptanone<sup>155</sup>

A solution of 4-acetylbutyric acid (2 g) in anhydrous tetrahydrofuran (2 ml), was stirred at 0°C under an atmosphere of nitrogen. Methyl lithium (1.5 M, 33 ml) was added dropwise and the solution refluxed for 2 hrs. The reaction mixture was cooled to 20°C, the milky white suspension quenched by slow addition of aqueous ammonium chloride (saturated, 5 ml), and the reaction mixture extracted with diethyl ether (3 x 5 ml). The combined organic extracts were dried (MgSO<sub>4</sub>), concentrated *in vacuo* and distilled to afford 6-hydroxy-6-methyl-2-heptanone (1.9 g, 86%) as a colourless liquid, b.p. 132 - 135°C/10 mm Hg (lit. b.p. 135°C/10 mm Hg)<sup>155</sup>

<sup>1</sup>H n.m.r. (200 MHz/CDCl<sub>3</sub>): δ 1.23 (6H, br s), 1.4 - 1.55 (4H, m), 2.15 (3H, s), 2.47 (2H, t).

#### 6-Deutero-6-hydroxy-6-methyl-2-heptanone

Produced in the ZAB 2HF as described above for 5-deutero-5-hydroxy-2-pentanone (positive ion mass spectrometry indicated *d*<sub>1</sub> > 95%)

### 1,1,1,3,3,-d<sub>5</sub>-6-Hydroxy-6-methyl-2-heptanone

6-Hydroxy-6-methyl-2-heptanone (0.5g) was stirred in methanol-*d* (1.5 ml) containing a small piece of sodium metal. After 1 hr. stirring, D<sub>2</sub>O (1 ml) was added and the solution stirred a further 30 mins. The aqueous solution was extracted with dichloromethane (3 x 5 ml), the combined organic extracts dried (MgSO<sub>4</sub>), concentrated under reduced pressure, and the residue distilled using a Kugelrohr apparatus (oven temperature 130 - 145°C/8 mm Hg) to afford 1,1,1,3,3,-d<sub>5</sub>-6-hydroxy-6-methyl-2-heptanone (0.46g, 86%, *d*<sub>5</sub> > 90%) as a colourless liquid.

<sup>1</sup>H n.m.r. (200 MHz/CDCl<sub>3</sub>): δ 1.23 (6H, br s), 1.4 - 1.55 (4H, m).

### 7-Hydroxy-2-heptanone<sup>156</sup>

(i) A mixture of 1,5-pentanediol (5 g), benzene (100 ml) and aqueous hydrogen bromide (48%, 6.5 ml) was refluxed for 16 hrs: water (0.9 ml) was collected in a Dean-Stark trap. The reaction mixture was washed successively with aqueous sodium hydroxide (10%, 50 ml), aqueous hydrogen chloride (2 M, 50 ml) and water (2 x 50 ml). The organic phase was dried (MgSO<sub>4</sub>), concentrated under reduced pressure and the residue distilled to afford 5-bromo-1-pentanol (5.3 g, 66%) as a colourless liquid, b.p. 105 - 107°C/20 mm Hg (lit. b.p. 66-69°C/3 mm Hg).<sup>157</sup>

(ii) A slurry of lithium acetylide-ethylenediamine complex (7 g) in anhydrous dimethylsulphoxide (35 ml) was stirred at 5°C. 5-Bromo-1-pentanol (5.3 g) was added over a 1 hr. period, stirred at 20°C for 1 hr., quenched by slow addition of water (30 ml), and stirred for a further 1 hr.<sup>158</sup> The solution was saturated with water (100 ml), extracted with diethyl ether (3 x 50 ml), the combined organic extract washed with water (3 x 100 ml),

dried ( $\text{MgSO}_4$ ), concentrated *in vacuo* and distilled to afford 6-heptyn-1-ol (2.65 g, 74%) as a clear yellow oil, b.p. 99 - 101°C/20 mm Hg (lit. b.p. 98 - 99°C/20 mm Hg)<sup>159</sup>

(iii) A solution of mercury(II)oxide (0.4 g) in water (15 ml) and concentrated sulfuric acid (0.6 ml) was stirred at 60°C. 6-Heptyn-1-ol (2.65 g) was added dropwise to the reaction mixture and stirred at 60°C for a further 15 mins. The reaction mixture was cooled to 20°C and extracted with dichloromethane (3 x 10 ml). The combined organic extract was dried ( $\text{MgSO}_4$ ) and concentrated to afford a brown residue which was distilled to give 7-hydroxy-2-heptanone (1.3 g, 44%) as a colourless liquid, b.p. 135 - 137°C/20 mm Hg (lit. b.p. 172°C/13 mm Hg).<sup>156</sup>

$^1\text{H}$  n.m.r. (200 MHz/ $\text{CDCl}_3$ ):  $\delta$  1.3 - 1.7 (6H, m), 2.14 (3H, s), 2.45 (2H, t), 3.65 (2H, t).

#### 7-Deutero-7-hydroxy-2-heptanone

Prepared in the ZAB 2HF as described above for 5-deutero-5-hydroxy-2-pentanone (positive ion mass spectrometry indicated  $d_1 > 95\%$ ).

#### 5-Oxohexanal<sup>152</sup>

Method modified from that of Garnick *et al.*<sup>152</sup>

6-Hydroxy-2-hexanone (1 g) was added to a stirred suspension of pyridinium chlorochromate (2.8 g) in anhydrous dichloromethane (17 ml) under an atmosphere of nitrogen. After stirring for 2 hrs., anhydrous diethyl ether (10 ml) was added and the supernatant liquid decanted from insoluble material. The residue was washed thoroughly with diethylether (3 x 10 ml), the

combined organic extract passed through a thin pad of celite, dried ( $\text{MgSO}_4$ ) and concentrated under reduced pressure. The residue was distilled to give 5-oxohexanal (0.89 g, 91%) as a colourless liquid, b.p. 65 - 67°C/0.1 mm Hg (lit. b.p. 65°C/0.1 mm Hg).<sup>152</sup>

$^1\text{H}$  n.m.r. (200 MHz/ $\text{CDCl}_3$ ):  $\delta$  1.85 (2H, p), 2.15 (3H, s), 2.34 (2H, t), 2.52 (2H, dt), 9.77 (1H, s).

#### 4-Oxopentanal<sup>160</sup>

5-Hydroxy-2-pentanone (0.2 g) was oxidised as described above for 5-oxohexanal, to afford 4-oxopentanal (0.18 g, 90%) as a colourless liquid, b.p. 83 - 84°C/20 mm Hg (lit. b.p. 66°C/8.5 mm Hg).<sup>137,161</sup>

$^1\text{H}$  n.m.r. (200 MHz/ $\text{CDCl}_3$ ):  $\delta$  2.13 (3H, s), 2.41 - 2.58 (4H, m), 9.61 (1H, s).

#### 6-Oxoheptanal<sup>162</sup>

7-Hydroxy-2-heptanone (0.1 g) was oxidised as described above for 5-oxohexanal, and distilled to afford 6-oxoheptanal (0.09 g, 86%) as a colourless liquid. b.p. 115 - 116°C/20 mm Hg. (lit. b.p. 91 - 96°C/4 mm Hg).<sup>163</sup>

$^1\text{H}$  n.m.r. (200 MHz/ $\text{CDCl}_3$ ):  $\delta$  1.48 - 1.71 (4H, m), 2.15 (3H, s), 2.34 (2H, t), 2.53 (2H, dt), 9.68 (1H, s).

#### 4-Penten-2-one<sup>164</sup>

4-Penten-2-ol (1 g) was oxidised as described above for 5-oxohexanal, to afford 4-penten-2-one (0.86 g, 88%) as a colourless liquid. b.p. 108 - 109°C/760 mm Hg. (lit. b.p. 107 - 108°C/760 mm Hg).<sup>137</sup>

<sup>1</sup>H n.m.r. (200 MHz/CDCl<sub>3</sub>): δ 2.11 (3H, s), 3.08 (2H, d), 4.95 - 5.05 (2H, m), 5.71 - 5.87 (1H, m).

#### 6-Hepten-2-one<sup>165</sup>

Method modified from that of Kongkathip *et al.*<sup>165</sup>

(i) A mixture of ethyl acetoacetate (0.96 g), 4-bromo-1-butene (1 g) and ethanol (10 ml) containing sodium ethoxide (8 g) was heated at reflux for 16 hrs. The reaction mixture was cooled to 20°C, concentrated *in vacuo*, water (10 ml) was added to the residue and the aqueous solution extracted with dichloromethane (3 x 10 ml). The combined organic extract was dried (MgSO<sub>4</sub>), and concentrated to afford ethyl-2-acetyl-5-hexenoate (1.25 g, 92%) as a clear oil. This was used in the next step without further purification.

(ii) The unpurified ester (1.25 g) was hydrolysed and decarboxylated by stirring in aqueous potassium hydroxide (20%, 10 ml) for 15 min., after which sulfuric acid (5%, 10 ml) was added, the reaction mixture allowed to reflux for 1 hr., cooled to 20°C, and extracted with dichloromethane (3 x 10 ml). The combined organic extract was dried (MgSO<sub>4</sub>), the solvent removed under reduced pressure and the residue distilled to afford 6-hepten-2-one (0.53 g, 70%) as a colourless liquid, b.p. 50°C/20 mm Hg (lit. b.p. 72 - 73°C/50 mm Hg).<sup>137,166</sup>

<sup>1</sup>H n.m.r. (200 MHz/CDCl<sub>3</sub>): δ 1.38 - 1.49 (2H, m), 2.15 (3H, s), 2.21 - 2.41 (4H, m), 4.86 - 5.00 (2H, m), 5.83 - 5.98 (1H, m).

### 5-Methyl-4-hexen-2-one<sup>167</sup>

Method adapted from that of Kosugi *et al.*<sup>167</sup>

A solution of tributyltin methoxide (4.8 g), isoprenyl acetate (1.5 g), 1-bromo-2-methylpropene (1.35 g) and PdCl<sub>2</sub>-[(*o*-tolyl)<sub>3</sub>P]<sub>2</sub> (0.01 g) in toluene (5 ml) was heated at 100°C under an atmosphere of nitrogen for 12 hrs. The solution was concentrated *in vacuo* and water (5 ml) added to the residue. The solution was extracted with dichloromethane (3 x 5 ml), the combined organic extract dried (MgSO<sub>4</sub>), concentrated under reduced pressure and the residue distilled to afford 5-methyl-4-hexen-2-one (0.52 g, 46%) as a colourless liquid, b.p. 58 - 59°C/20 mm Hg (lit. b.p. 43 - 45°C/17 mm Hg).<sup>167</sup> <sup>1</sup>H n.m.r. (200 MHz/CDCl<sub>3</sub>): δ 1.68 (3H, s), 1.72 (3H, s), 2.06 (3H, s), 2.99 (2H, d), 5.25 - 5.32 (1H, m).

## **5.4 Compounds Described in Chapter 4**

### 5.4.1 Compounds Described in Section 4.2.1

#### 2-(2-Oxiranyl)-1-ethanol<sup>168</sup>

Method modified from that of Brown and Lynch.<sup>168</sup>

3-Chloroperbenzoic acid (70%, 3.4 g) was added portionwise at 0°C to a solution of 3-buten-1-ol (1 g) in dichloromethane (30 ml) and the mixture was stirred at 20°C for 20 hrs. Aqueous sodium hydroxide (10%, 15 ml) was added to the suspension, the organic layer separated and the aqueous phase extracted with dichloromethane (5 x 20 ml). The combined organic extract was dried (MgSO<sub>4</sub>), concentrated under reduced pressure and the residue distilled to afford 2-(2-oxiranyl)-1-ethanol (0.7 g, 58%) as a colourless liquid, b.p. 79 - 81°C/16 mm Hg (lit. b.p. 89 - 90°C/19 mm Hg).<sup>168</sup>

$^1\text{H}$  n.m.r. (200 MHz/ $\text{CDCl}_3$ ):  $\delta$  1.56 - 1.92 (2H, m), 2.51 (1H, m), 2.74 (1H, t), 3.02 (1H, m), 3.73 (2H, t), 4.67 (1H, br s).

### 2-Oxetanylmethanol<sup>169</sup>

Method modified from that of Fitton *et al.*<sup>169</sup>

(i) A solution of propylene oxide (4 g) in ethyl vinyl ether (20 ml) and *p*-toluenesulfonic acid (0.1 g) was stirred at 20°C for 12 hrs. Aqueous sodium hydrogen carbonate (saturated, 10 ml) was added to the reaction mixture, the organic layer separated, dried ( $\text{MgSO}_4$ ) and evaporated under reduced pressure. Distillation of the residue produced 2-[(1-ethoxyethoxy)methyl]oxirane (7 g, 89%) as a colourless liquid, b.p. 85°C/70 mm Hg (lit. b.p. 152 - 154°C/760 mm Hg).<sup>169</sup>

(ii) A mixture of potassium-*tert*-butoxide (4.6 g) and trimethyloxosulphonium iodide (9 g) in dry *tert*-butanol (50 ml) was stirred at 50°C for 1 hr. 2-[(1-ethoxyethoxy)methyl]oxirane (3 g) in *tert*-butanol (8 ml) was added dropwise and the reaction mixture stirred at 50°C for 3 days. The solvent was removed *under vacuo* and water (30 ml) was added to the residue. The mixture was extracted with dichloromethane (3 x 20 ml), the combined organic extracts dried ( $\text{MgSO}_4$ ), concentrated under reduced pressure and the residue distilled to afford 2-[(1-ethoxyethoxy)methyl]oxetane (2.2 g, 68%) as a colourless liquid, b.p. 48 - 50°C/0.34 mm Hg (lit. b.p. 55 - 58°C/0.4 mm Hg).<sup>169</sup>

(iii) A solution of 2-[(1-ethoxyethoxy)methyl]oxetane (1 g) and acetic acid (10%, 5 ml) was stirred at 20°C for 12 hrs. The reaction mixture was neutralised with solid sodium hydrogen carbonate (0.65 g) and extracted with dichloromethane (3 x 5 ml). The combined organic extract was washed with aqueous sodium hydroxide (10%, 2 x 5 ml), dried ( $\text{MgSO}_4$ ),

concentrated *in vacuo*, and the residue distilled to produce 2-oxetanylmethanol (0.38 g, 69%) as a colourless liquid, b.p. 90 - 92°C/15 mm Hg (lit. b.p. 94 - 98°C/15 mm Hg).<sup>169</sup>

<sup>1</sup>H n.m.r. (200 MHz/CDCl<sub>3</sub>): δ 2.65 (2H, m), 3.75 (2H, m), 4.5 - 4.95 (3H, m).

1,1-*d*<sub>2</sub>-2-(2-Oxiranyl)-1-ethan-[<sup>18</sup>O]-ol

(i) A mixture of vinylacetic acid (1 g), oxalyl chloride (1.22 g) and *N,N*-dimethyl-formamide (1 drop) in anhydrous diethyl ether (30 ml) was stirred at 20°C for 2 hrs. under nitrogen and the reaction mixture distilled to yield 3-butenoyl chloride (0.8 g, 64%). b.p. 99°C/760 mm Hg. (lit. b.p. 95 - 95°C/760 mm Hg).<sup>170</sup>

(ii) 3-Butenoyl chloride (0.8 g) was added to a mixture of anhydrous tetrahydrofuran (10 ml) and H<sub>2</sub><sup>18</sup>O (160 mg, 96% <sup>18</sup>O). The mixture was stirred at 20°C for 12 hrs., the solvent removed *in vacuo*, the residue dissolved in anhydrous diethyl ether (20 ml), and added at 0°C to a slurry of lithium aluminium deuteride (0.5 g) in anhydrous diethyl ether (10 ml). The mixture was heated at reflux for 3 hrs., cooled to 0°C, water (5 ml) was cautiously added followed by aqueous hydrogen chloride (20%, 2 ml). The organic layer was separated, the aqueous layer extracted with diethyl ether (2 x 30 ml) and the combined organic extract dried (MgSO<sub>4</sub>), concentrated *in vacuo* and distilled to give 1,1-*d*<sub>2</sub>-but-3-en-1-[<sup>18</sup>O]-ol (0.38 g, 66%) as a colourless liquid, b.p. 109 - 111°C/760 mm Hg.

(iii) Epoxidation with 3-chloroperbenzoic acid as described for 2-(2-oxiranyl)-1-ethanol afforded 1,1-*d*<sub>2</sub>-2-(2-oxiranyl)-1-ethan-[<sup>18</sup>O]-ol (0.26 g, 57%, <sup>18</sup>O = 48%, *d*<sub>2</sub> = 99%) as a colourless liquid, b.p. 82 - 84°C/16 mm Hg.

<sup>1</sup>H n.m.r. (200 MHz/CDCl<sub>3</sub>): δ 1.62 - 1.9 (2H, m), 2.53 (1H, m), 2.76 (1H, t), 3.04 (1H, m).



### 2-(2-Oxiranyl)-1-ethan-[<sup>18</sup>O]-ol

Preparation of the title compound was achieved by the same method as that described above for 1,1-*d*<sub>2</sub>-2-(2-oxiranyl)-1-ethan-[<sup>18</sup>O]-ol, except that lithium aluminium hydride was used to reduce <sup>18</sup>O-labelled vinylacetic acid. Distillation afforded 2-(2-oxiranyl)-1-ethan-[O<sup>18</sup>]ol (0.5 g, 46%, <sup>18</sup>O = 48%) as a colourless liquid, b.p. 78 - 82°C/16 mm Hg.

<sup>1</sup>H n.m.r. (200 MHz/CDCl<sub>3</sub>): δ 1.54 - 1.93 (2H, m), 2.5 (1H, m), 2.72 (1H, t), 3.03 (1H, m), 3.73 (2H, t).

### 1,1-*d*<sub>2</sub>-2-(2-Oxiranyl)-1-ethanol

Vinylacetic acid (1 g) was reduced with lithium aluminium deuteride (0.49 g) and epoxidised using 3-chloroperbenzoic acid (70%, 2.9 g) as described above for 1,1-*d*<sub>2</sub>-2-(2-oxiranyl)-1-ethan-[<sup>18</sup>O]-ol, to afford 1,1-*d*<sub>2</sub>-2-(2-oxiranyl)-1-ethanol (0.6 g, 57%, *d*<sub>2</sub> > 99%) as a colourless liquid, b.p. 80 - 81°C/16 mm Hg.

<sup>1</sup>H n.m.r. (200 MHz/CDCl<sub>3</sub>): δ 1.62 - 1.91 (2H, m), 2.53 (1H, m), 2.75 (1H, t), 3.03 (1H, m).

## Condensed Phase Reactions

### Method A

A mixture of 2-(2-oxiranyl)-1-ethanol (0.5 g) in aqueous sodium hydroxide (10%, 5 ml) was stirred under reflux for 60 hrs., cooled to 20°C, and aqueous hydrogen chloride (10%) was added dropwise until the solution was slightly acidic (pH 6). The mixture was extracted with dichloromethane (4 x 5 ml)

and the combined organic extracts were dried ( $\text{MgSO}_4$ ) and concentrated to give an oil (0.25 g). The reaction mixture was sampled at particular times, and the product composition analysed by GC-MS (see Table 4.5).

#### Method B

2-(2-Oxiranyl)-1-ethanol (0.5 g) was added dropwise to a slurry of sodium hydride (1 mol equiv.) in anhydrous tetrahydrofuran (10 ml) maintained at  $0^\circ\text{C}$ . The mixture was then heated at reflux for 60 hrs., cooled to  $0^\circ\text{C}$ , water (5 ml) was added, the mixture extracted with dichloromethane (4 x 5 ml), the combined organic extracts dried ( $\text{MgSO}_4$ ), and concentrated under reduced pressure to afford an oil (0.4 g). The reaction mixture was sampled at particular times, and the product composition analysed by GC-MS (see Table 4.5).

Identical procedures were used for both 2-oxetanylmethanol and tetrahydro-3-furanol and the reaction mixtures were again analysed at particular times to determine the product composition by GC-MS (see Table 4.5).

Table 4.5. Base catalysed solution reactions of 2-(2-oxiranyl)-1-ethanol, 2-oxetanylmethanol and tetrahydro-3-furanol.<sup>a</sup>

Reactant <sup>b</sup>	Time	Method A	Method B
2-(2-oxiranyl)-1-ethanol	10 min.	100:0:0 <sup>a</sup>	73:3:24 <sup>a</sup>
	1 hr.	77:3:20	21:7:62
	15 hrs.	22:11:67	11:11:78
	30 hrs.	20:10:70	10:11:79
	60 hrs.	20:10:70	9:10:81
2-oxetanyl-methanol	3 hrs.	0:100:0	0:100:0
	15 hrs.	19:100:0	50:100:1
	30 hrs.	27:100:9	24:100:20
tetrahydro-3-furanol	30 hrs.	0:0:100	0:0:100

<sup>a</sup>The ratio of products refers to the 3:4:5 membered cyclic ethers and is obtained by comparing the areas under each peak (this ratio correlates closely with the ratios obtained using ion counts/peak). The error in each number within a ratio is *ca.*  $\pm 5\%$ .

<sup>b</sup>The retention times for the reactants are: 2-(2-oxiranyl)-1-ethanol (4.05 min.), 2-oxetanylmethanol (3.25 min.) and tetrahydro-3-furanol (3.48 min.).

#### 5.4.2 Compounds Described in Section 4.2.2

##### 2-(3-Methoxypropyl)oxirane<sup>171</sup>

To a suspension of potassium hydroxide (1.3 g) in dimethylsulphoxide (10 ml) was added 4-penten-1-ol (0.5 g) and iodomethane (1.65 g), and the reaction mixture allowed to stir at 20°C for 30 min. The solution was poured onto water (60 ml), extracted with dichloromethane (3 x 20 ml) and the combined organic extract dried (MgSO<sub>4</sub>), and stirred at 0°C with the

addition of 3-chloroperbenzoic acid (70%, 1.43 g). After 20 hrs. stirring at 20°C, aqueous sodium hydroxide (10%, 15 ml) was added, the organic layer separated and the aqueous phase extracted with dichloromethane (3 x 15 ml). The combined organic extract was dried (MgSO<sub>4</sub>), concentrated under reduced pressure and distilled using a Kugelrohr apparatus (oven temp. of 50 - 60°C/20 mm Hg) to afford 2-(3-methoxypropyl)oxirane (0.56 g, 83%) as a colourless liquid. (lit. b.p. 156°C/760 mm Hg)<sup>172</sup>

<sup>1</sup>H n.m.r. (200 MHz/CDCl<sub>3</sub>): δ 1.50 - 1.75 (4H, m), 2.51 (1H, m), 2.75 (1H, t), 3.02 (1H, m), 3.35 (3H, s), 3.44 (2H, m).

### 3-(2-Oxiranyl)propyl acetate<sup>117</sup>

Pyridine (1.2 g) and acetic anhydride (1.4 g) were added to a solution of 4-penten-1-ol (1 g) in anhydrous dichloromethane (10 ml) and the mixture was allowed to stir at 20°C for 12 hrs. Water (10 ml) was added followed by aqueous hydrogen chloride (10%, 5 ml). The organic layer was separated, the aqueous phase extracted with dichloromethane (3 x 10 ml) and the combined organic extract dried (MgSO<sub>4</sub>). 3-Chloroperbenzoic acid (70%, 2.86 g) was added to the organic solution and the mixture allowed to stir for 15 hrs. Aqueous sodium hydroxide (10%, 10 ml) was added to the suspension, the organic layer separated and the aqueous phase extracted with dichloromethane (3 x 10 ml). The combined organic extract was dried (MgSO<sub>4</sub>), concentrated under reduced pressure and the residue distilled to afford 3-(2-oxiranyl)propyl acetate (1.5 g, 92%) as a colourless liquid, b.p. 110 - 112°C/40 mm Hg. (lit. b.p. not recorded).

<sup>1</sup>H n.m.r. (200 MHz/CDCl<sub>3</sub>): δ 1.50 - 1.82 (4H, m), 2.05 (3H, s), 2.50 (1H, m), 2.77 (1H, t), 2.95 (1H, m), 4.12 (2H, m).

### Tetrahydro-2H-3-pyranol<sup>173</sup>

Method modified from that of Brown *et al.*<sup>173</sup>

3,4-Dihydro-2H-pyran (0.84 g) was added dropwise to a solution of 9-borobicyclo[3.3.1]nonane in tetrahydrofuran (0.5 M, 20 ml) under an atmosphere of nitrogen and allowed to stir at 0°C for 3 hrs. Aqueous sodium hydroxide (10%, 10 ml) and hydrogen peroxide (30%, 4.25 ml) were added, and the mixture then maintained at 55°C for 1 hr. The reaction mixture was cooled to 20°C, anhydrous potassium carbonate (15 g) was added, and the solution stirred a further 15 min. The organic layer was separated, the aqueous phase extracted with dichloromethane (3 x 20 ml), the combined organic extract dried (MgSO<sub>4</sub>) and concentrated under reduced pressure. The residue was distilled to afford tetrahydro-2H-3-pyranol (0.82 g, 81%) as a colourless liquid, b.p. 85 - 89°C/20 mm Hg (lit. b.p. 90°C/20 mm Hg).<sup>173</sup>

<sup>1</sup>H n.m.r. (200 MHz/CDCl<sub>3</sub>): δ 1.45 - 1.98 (4H, m), 3.4 - 3.8 (5H, m).

### 3-Methoxytetrahydro-2H-pyran<sup>171</sup>

Tetrahydro-2H-3-pyranol (0.5 g) was converted to the methyl ether with sodium hydride and iodomethane as described for 2-(methoxymethyl) tetrahydrofuran. 3-Methoxytetrahydro-2H-pyran (0.35 g, 62%) was isolated as a colourless liquid, b.p. 139 - 142°C/760 mm Hg (lit. b.p. 141 - 142°C/760 mm Hg).<sup>174</sup>

<sup>1</sup>H n.m.r. (200 MHz/CDCl<sub>3</sub>): δ 1.40 - 1.91 (4H, m), 3.25 (3H, s), 3.46 - 3.84 (5H, m).

### 2,4-Pentadien-1-ol<sup>175</sup>

*trans*-2,4-Pentadienoic acid (1 g) was added dropwise at 0°C, to a suspension of lithium aluminium hydride (0.4 g) in tetrahydrofuran (20 ml). The reaction mixture was allowed to reflux for 2 hrs., cooled to 0°C and aqueous hydrogen chloride (20%, 5 ml) was cautiously added. The organic layer was separated and the aqueous phase extracted with dichloromethane (3 x 10 ml). The combined organic extract was dried (MgSO<sub>4</sub>), concentrated *in vacuo* and distilled to afford 2,4-pentadien-1-ol (0.6g, 71%) as a colourless liquid, b.p. 91 - 93°C/60 mm Hg (lit. b.p. 86 - 88°C/66 mm Hg).<sup>175</sup>

<sup>1</sup>H n.m.r. (200 MHz/CDCl<sub>3</sub>): δ 3.72 (1H, br s), 4.04 (2H, d), 5.05 - 6.32 (5H, m).

### 1,1-*d*<sub>2</sub>-3-(2-Oxiranyl) propylmethyl ether

(i) To a suspension of lithium aluminium deuteride (0.24 g) in anhydrous diethyl ether (10 ml) at 0°C was added dropwise 4-pentenoic acid (0.5 g), and the mixture heated under reflux for 2 hrs. Aqueous hydrogen chloride (20%, 3 ml) was added, the organic layer separated, the aqueous phase extracted with dichloromethane (3 x 5 ml) and the combined organic extract dried (MgSO<sub>4</sub>) and concentrated under reduced pressure. Distillation of the residue afforded 1,1-*d*<sub>2</sub>-4-penten-1-ol (0.4 g, 91%), b.p. 131 - 132°C/760 mm Hg.

(ii) 1,1-*d*<sub>2</sub>-4-Penten-1-ol (0.4 g) was converted to the methyl ether and then epoxidised to 3,3-*d*<sub>2</sub>-3-methoxypropyl oxirane following the same method described for 2-(3-methoxypropyl) oxirane. Kugelrohr distillation (oven temperature of 55 - 65°C/20 mm Hg) afforded 1,1-*d*<sub>2</sub>-3-(2-oxiranyl) propylmethyl ether (0.4 g, 76%) as a colourless liquid.

$^1\text{H}$  n.m.r. (200 MHz/ $\text{CDCl}_3$ ):  $\delta$  1.51 - 1.75 (4H, m), 2.52 (1H, m), 2.75 (1H, t), 3.03 (1H, m), 3.35 (3H, s).

#### 2-(3- $^{18}\text{O}$ -Methoxypropyl) oxirane

A mixture of 4-pentenoic acid (1 g), oxalyl chloride (1.14 ml), *N,N*-dimethylformamide (1 drop) and anhydrous diethyl ether (30 ml) was allowed to stir at 20°C for 3 hrs. Distillation afforded 4-pentenoyl chloride (0.83 g) which was added to a mixture of anhydrous tetrahydrofuran (10 ml) and  $\text{H}_2^{18}\text{O}$  (0.15 g, 96%  $^{18}\text{O}$ ), stirred at 20°C for 24 hrs., the solvent removed *in vacuo* and the residue treated with lithium aluminium hydride [as for 4-pentenoic acid (above)] to afford 4-penten-1- $^{18}\text{O}$ -ol (0.7 g) which was converted to the methyl ether and then epoxidised to 2-(3- $^{18}\text{O}$ -methoxypropyl) oxirane as described above for 2-(3-methoxypropyl) oxirane. Kugelrohr distillation (oven temperature 50 - 60°C/20 mm Hg) afforded 2-(3- $^{18}\text{O}$ -methoxypropyl) oxirane (0.55 g, overall yield 47%) as a colourless liquid.  $^1\text{H}$  n.m.r. (200 MHz/ $\text{CDCl}_3$ ):  $\delta$  1.50 - 1.75 (4H, m), 2.51 (1H, m), 2.75 (1H, t), 3.02 (1H, m), 3.35 (3H, s), 3.44 (2H, m).

#### Condensed Phase Reactions

A mixture of 3-(2-oxiranyl)propyl acetate (0.5 g) and aqueous sodium hydroxide (10%, 5 ml) was allowed to stir for 60 hrs. at (i) 20°C, and (ii) at 100°C (see Table 4.9). The reaction mixtures were sampled at various times. Each sample was acidified with aqueous hydrogen chloride (10%) until the pH was 6, extracted with dichloromethane (5 ml), the organic extract dried

(MgSO<sub>4</sub>) and concentrated. The product composition was analysed by GC/MS and the results are outlined in Table 4.9.

Tetrahydrofurfuryl alcohol and tetrahydro-2H-3-pyranol were each treated with aqueous sodium hydroxide (10%) as detailed above. No reaction was observed in either case (see Table 4.9).

Table 4.9 Base Catalysed Solution Reactions of 3-(2-oxiranyl)propyl acetate, tetrahydrofurfuryl alcohol and tetrahydro-2H-3-pyranol.<sup>a</sup>

Reactant <sup>b</sup>	Time	20°C/10% NaOH	100°C/10% NaOH
3-(2-Oxiranyl)-propyl acetate	5 min.	95:9 <sup>b</sup>	91:9 <sup>b</sup>
	1 hr.	95:5	91:9
	60 hrs.	95:5	91:9
Tetrahydro-furfuryl-alcohol	1 hr.	100:0	100:0
	60 hrs.	100:0	100:0
Tetrahydro-2H-3-pyranol	1 hr.	0:100	0:100
	60 hrs.	0:100	0:100

<sup>a</sup>The ratio of products refers to the 5:6 membered cyclic ethers and is obtained by comparing the areas under each peak (this ratio correlates closely with the ratios obtained using ion counts/peak). The error in each number within a ratio is *ca.* ± 5%. Hydrolysis of the acetate immediately cyclises (in quantitative yield) to yield the listed products. <sup>b</sup>The retention times for the reactants/products are: tetrahydrofurfuryl alcohol (5.39min.) and tetrahydro-2H-3-pyranol (3.58min.).



### 5.4.3 Compounds Discussed in Section 4.2.3

#### 4-(2-Oxiranyl)-1-butanol<sup>165</sup>

To 5-hexen-1-ol (0.5 g) in dichloromethane (20 ml) was added 3-chloroperbenzoic acid (70%, 1.23 g), the solution stirred at 20°C for 16 hrs., aqueous sodium hydroxide (10%, 10 ml) was added and the organic layer separated. The aqueous phase was extracted with dichloromethane (2 x 10 ml) and the combined organic extract dried (MgSO<sub>4</sub>), concentrated *in vacuo* and distilled using a Kugelrohr apparatus (oven temperature 70 - 80°C/20 mm Hg) to afford 4-(2-oxiranyl)-1-butanol (0.48 g, 83%) as a colourless liquid. (lit. b.p. not recorded).

<sup>1</sup>H n.m.r. (200 MHz/CDCl<sub>3</sub>): δ 1.50 - 1.67 (6H, m), 2.49 (1H, m), 2.76 (1H, t), 2.93 (1H, m), 3.67 (2H, m).

#### 4-(2-Oxiranyl)butyl acetate<sup>121</sup>

Pyridine (0.7 g) and acetic anhydride (0.85 g) was added to a solution of 5-hexen-1-ol (1 g) in dichloromethane (10 ml), the reaction mixture allowed to stir at 20°C for 8 hrs., water (10 ml) was added, and the organic phase separated, the aqueous layer was extracted with dichloromethane (2 x 10 ml), the combined organic extract washed with aqueous ammonium chloride (10%, 20 ml), dried (MgSO<sub>4</sub>), 3-chloroperbenzoic acid (70%, 2.47 g) was added and the organic solution was stirred at 20°C for 14 hrs. Workup as described above for 4-(2-oxiranyl)-1-butanol afforded a residue which was distilled using a Kugelrohr apparatus (oven temperature 80 - 90°C/20 mm Hg) to afford 4-(2-oxiranyl)butyl acetate (1.2 g, 76%) as a colourless liquid. (lit. b.p. not recorded).

$^1\text{H}$  n.m.r. (200 MHz/ $\text{CDCl}_3$ ):  $\delta$  1.50 - 1.72 (6H, m), 2.06 (3H, s), 2.44 (1H, m), 2.76 (1H, t), 2.91 (1H, m), 4.08 (2H, m).

#### Tetrahydro-2H-2-pyranylmethyl acetate<sup>176</sup>

Tetrahydropyran-2-methanol (1 g) was acetylated as described for 4-(2-oxiranyl)butyl acetate above. Distillation of the crude residue produced tetrahydro-2H-2-pyranylmethyl acetate (1.17 g, 86%) as a colourless liquid, b.p. 78 - 80°C/20 mm Hg (lit. b.p. 80 - 85°C/20 mm Hg).<sup>137,177</sup>

$^1\text{H}$  n.m.r. (200 MHz/ $\text{CDCl}_3$ ):  $\delta$  1.21 - 1.69 (6H, m), 2.04 (3H, s), 3.45 - 3.93 (5H, m).

#### 3-Oxepanol<sup>121</sup>

A mixture of oxirane butanol acetate (0.5 g) and aqueous sodium hydroxide (10%, 10 ml) was heated at reflux for 2 hrs. The solution was extracted with dichloromethane (3 x 5 ml), the combined organic extract dried ( $\text{MgSO}_4$ ) and concentrated under reduced pressure to afford a clear oil consisting of a mixture of tetrahydropyran-2-methanol and 3-oxepanol (see Table 4.13). 3-Oxepanol was separated *via* column chromatography over silica gel using acetone/dichloromethane (1:3) as the eluent. 3-Oxepanol (0.15 g, 30%) was isolated as a colourless liquid, which was shown to be pure from GC/MS and  $^1\text{H}$  n.m.r, and was used in the next reaction without further purification.

$^1\text{H}$  n.m.r. (200 MHz/ $\text{CDCl}_3$ ):  $\delta$  1.15 - 2.13 (6H, m), 3.00 - 3.24 (3H, m), 3.72 (2H, t).

### 3-Oxepanol acetate

3-Oxepanol (0.1 g) was acetylated as described for 4-(2-oxiranyl)butyl acetate above. Distillation of the crude residue using a Kugelrohr apparatus (oven temperature 110 - 120°C/26 mm Hg) afforded 3-oxepanol acetate (0.11 g, 81%) as a colourless liquid. Found: C 60.6, H 9.2%;  $C_8H_{14}O_3$  requires: C 60.7, H 8.9%.

$m/z$ (rel. abund.): 159(MH<sup>+</sup>, 18), 17(8), 99(7), 83(32), 67(12), 57(43), 55(34), 43(100), 41(70), 39(82), 31(13), 29(24), 27(27). <sup>1</sup>H n.m.r. (200 MHz/ $CDCl_3$ ):  $\delta$  1.35 - 1.52 (4H, m), 1.7 - 1.82 (2H, q), 2.01 (3H, s), 3.4 (2H, d), 3.69 (2H, t), 4.1 (1H, p). <sup>13</sup>C n.m.r (75 MHz/ $CDCl_3$ ):  $\delta$  21.1 (CH<sub>3</sub>), 21.3 (CH<sub>2</sub>), 27.5 (CH<sub>2</sub>), 31.82 (CH<sub>2</sub>), 64.1 (CH), 70.4 (CH<sub>2</sub>), 70.71 (CH<sub>2</sub>), 170.5 (C=O).

### 3,5-Hexadien-1-ol<sup>178</sup>

(i) A mixture of sorbic acid (2 g), methanol (10 ml) and concentrated sulfuric acid (0.1 ml) was heated under reflux for 15 hrs. The solution was cooled to 20°C, aqueous sodium hydrogen carbonate (saturated, 3 ml) was added, and the solution extracted with dichloromethane (3 x 10 ml). The combined organic extract was dried (MgSO<sub>4</sub>) and concentrated under reduced pressure to afford methyl sorbate (2 g, 90%) as a colourless liquid which was used in the next step without further purification.

(ii) Method from that of Stevens *et al.*<sup>179</sup> Hexamethylphosphoramide (4.35 ml) was added dropwise to a solution of lithium diisopropylamide in tetrahydrofuran (2 M, 10 ml) maintained at -78°C, the solution stirred for 30 mins., methyl sorbate (2 g) was added dropwise and the mixture stirred at -78°C for 1 hr. The mixture was poured onto a stirred solution of aqueous acetic acid (10%, 60 ml) at 0°C, the resultant solution extracted with diethyl

ether (3 x 40 ml), the combined organic extract washed with aqueous sodium hydrogen carbonate (10%, 30 ml), dried (MgSO<sub>4</sub>), concentrated under reduced pressure and the residue distilled to yield methyl 3,5-hexadienoate (1.62 g, 81%). b.p. 75 - 77°C/20 mm Hg (lit. b.p. 73 - 75°C/20 mm Hg)<sup>179</sup>

(iii) Methyl 3,5-hexadienoate (1.62 g) was added dropwise to a suspension of lithium aluminium hydride (0.48 g) in dry diethyl ether (40 ml) at 0°C. After stirring for 1 hr. at 20°C, water (20 ml) was added followed by aqueous hydrogen chloride (30%, 2 ml), the organic layer separated, the aqueous portion extracted with diethyl ether (2 x 10 ml) and the combined organic extract dried (MgSO<sub>4</sub>), concentrated *in vacuo* and the residue distilled to afford 3,5-hexadien-1-ol (0.93 g, 74%) as a colourless liquid, b.p. 81 - 82°C/20 mm Hg (lit. b.p. 79 - 80°C/20 mm Hg)<sup>178</sup>

<sup>1</sup>H n.m.r. (200 MHz/CDCl<sub>3</sub>): δ 2.31 (2H, q), 3.62 (2H, t), 5.2 - 6.4 (5H, m).

### 2,5-Hexadiene-1-ol<sup>180</sup>

(i) A mixture of propargyl alcohol (5 g), 3,4-dihydro-2H-pyran (7.5 g), *p*-toluenesulphonic acid (1 crystal) and dichloromethane (30 ml) was allowed to stir at 20°C for 2 hrs. Aqueous sodium hydrogen carbonate (saturated, 30 ml) was added to the reaction mixture and the organic layer separated. The aqueous layer was extracted with dichloromethane (2 x 10 ml), the combined organic extract dried (MgSO<sub>4</sub>), and concentrated under reduced pressure to afford tetrahydropyranyl-protected propargyl alcohol (12.3 g, 98%) as a colourless liquid. This was used in the next step without purification.

(ii) Method modified from that of Durand *et al.*<sup>181</sup> A mixture of potassium carbonate (2.27 g), sodium iodide (2.48 g), copper(I) iodide (1.57 g), the protected propargyl alcohol (2.31 g), allyl bromide (2 g) and *N,N*-dimethylformamide (35 ml), was stirred under nitrogen at 20°C for 10 hrs.

Aqueous ammonium chloride (saturated, 15 ml) was added and the mixture extracted with diethyl ether (3 x 10 ml). The combined organic extract was dried ( $\text{MgSO}_4$ ), concentrated *in vacuo*, and the residue distilled using a Kugelrohr apparatus (oven temperature 75 - 85°C/0.07 mm Hg) to afford tetrahydropyranyl-protected 5-hexen-2-yn-1-ol (2.16 g, 73%) as a colourless liquid.

(iii) Deprotection<sup>182</sup> of the alcohol function was achieved by stirring the protected 5-hexen-2-yn-1-ol for 2 hrs. in methanol (15 ml) containing *p*-toluene sulfonic acid (0.05 g). The aqueous solution was extracted with dichloromethane (3 x 10 ml) and the combined organic extract dried ( $\text{MgSO}_4$ ), and concentrated *in vacuo* to afford a residue which was distilled to afford 5-hexen-2-yn-1-ol (1.04 g, 90%) as a colourless liquid, b.p. 70 - 71°C/15 mm Hg. (lit. b.p. 68 - 70°C/14 mm Hg).<sup>183</sup>

(iv) Method modified from that of Rao *et al.*<sup>180</sup> A mixture of 5-hexen-2-yn-1-ol (0.5g) in anhydrous tetrahydrofuran (5 ml) was added dropwise to a suspension of lithium aluminium hydride (0.19g) in anhydrous tetrahydrofuran (10 ml), and the reaction mixture was heated at reflux for 3 hrs., cooled to 0°C, and aqueous hydrogen chloride (10%, 15 ml) was added dropwise. The mixture was extracted with diethyl ether (3 x 10 ml), the combined extract dried ( $\text{MgSO}_4$ ), concentrated *in vacuo*, and distilled to afford 2,5-hexadien-1-ol (0.41 g, 80%) as a colourless liquid, b.p. 70 - 72°C/18 mm Hg. (lit. b.p. 73 - 75°C/20 mm Hg)<sup>180</sup>

<sup>1</sup>H nmr (300 MHz,  $\text{CDCl}_3$ ):  $\delta$  2.82 (2H, t), 4.14 (2H, d), 4.99 - 5.1 (2H, m), 5.68 - 5.9 (3H, m).

### 3-Penten-1-ol<sup>184</sup>

3-Pentenoic acid methyl ester (1 g) was added dropwise to a suspension of lithium aluminium hydride (0.33 g) in tetrahydrofuran (10 ml) at 0°C. The reaction mixture was stirred at 20°C for 3 hrs., then cooled to 0°C, aqueous hydrogen chloride (20%, 5 ml) was added, the organic layer separated and the aqueous phase extracted with dichloromethane (3 x 10 ml). The combined organic extract was dried (MgSO<sub>4</sub>), the solvent removed *in vacuo* and the residue distilled to yield 3-penten-1-ol (0.71 g, 93%) as a colourless liquid, b.p. 134 - 135°C/760 mm Hg (lit. b.p. 45 - 46°C/35 mm Hg).<sup>184</sup>

<sup>1</sup>H n.m.r. (200 MHz/CDCl<sub>3</sub>): δ 1.66 (2H, d), 2.24 (2H, q), 3.62 (2H, t), 5.38 - 5.62 (2H, m).

### 6-Hydroxy-3-hexenoic acid<sup>185</sup>

(i) A mixture of *trans*-β-hydromuconic acid (2 g), methanol (20ml) and concentrated sulfuric acid (0.2 ml) was heated under reflux for 12 hrs. The reaction mixture was allowed to cool to 20°C, aqueous sodium hydrogen carbonate (10%, 20 ml) was added and the solution extracted with dichloromethane (3 x 10 ml). The combined organic extract was dried (MgSO<sub>4</sub>), the solvent removed under reduced pressure and the residue distilled to afford dimethyl-*trans*-3-hexene-1,6-dioate (1.93 g, 80%). b.p. 68 - 69°C/0.2 mm Hg (lit. b.p. 71 - 74°C/0.15 mm Hg).<sup>186</sup>

(ii) Method adapted from that of Eaton *et al.*<sup>187</sup> Methanolic sodium hydroxide (2.5 M, 6.5 ml) was added dropwise to a solution of dimethyl-*trans*-3-hexene-1,6-dioate (1.93 g) in tetrahydrofuran (40 ml) and this mixture was allowed to stir at 20°C for 16 hrs. The solvent was removed under reduced pressure, water (50 ml) was added and the mixture extracted

with dichloromethane (3 x 20 ml). The aqueous layer was acidified to pH 3 with concentrated hydrogen chloride and extracted with dichloromethane (2 x 20 ml). The combined organic extract was dried (MgSO<sub>4</sub>), the solvent removed *in vacuo* to afford mono-methyl-*trans*-3-hexenedioate (1.56 g, 88%). This was used in the next step without further purification.

(iii) Mono-methyl-*trans*-3-hexenedioate (1.56 g) was added dropwise to a suspension of lithium aluminium hydride (0.38 g) in tetrahydrofuran (10 ml) at 0°C. The reaction mixture was stirred at 20°C for 2 hrs., aqueous hydrogen chloride (20%, 3 ml) was added dropwise, the organic layer separated, the aqueous layer extracted with dichloromethane (3 x 10 ml), the combined organic extract dried (MgSO<sub>4</sub>) and concentrated under reduced pressure. The crude residue was purified by flash column chromatography over silica gel using hexane/acetone (1:1) as the eluent to give 6-hydroxy-3-hexenoic acid (0.66 g, 52%) as a colourless liquid. (lit. b.p. not recorded).

<sup>1</sup>H n.m.r. (200 MHz/CDCl<sub>3</sub>): δ 2.38 (2H, p), 3.02 (2H, d), 3.62 (2H, t), 5.51 (1H, m), 5.63 (1H, m).

#### 4-(2-Oxiranyl)-1-butan-[<sup>18</sup>O]-ol

(i) A solution of chromium trioxide (2.7 g), distilled water (5 ml) and concentrated sulfuric acid (2.3 ml) was added dropwise to a solution of 5-hexen-1-ol (2 g) in anhydrous acetone (30 ml) and the mixture allowed to stir at 20°C for 15 mins.<sup>153</sup> The solvent was removed under reduced pressure, water (50 ml) was added to the residue, the solution was extracted with dichloromethane (3 x 20 ml), the combined organic extract dried (MgSO<sub>4</sub>), concentrated *in vacuo*, and the residue distilled to afford 5-hexenoic acid (1.9 g, 85%). b.p. 90 - 92°C/20 mm Hg (lit. b.p. 203°C/760 mm Hg).<sup>137,188</sup>

(ii) A mixture of 5-hexenoic acid (1.9 g), oxalyl chloride (1.5 ml), *N,N*-dimethylformamide (1 drop) and diethyl ether (30 ml) was stirred at 20°C for 3 hrs. Removal of the solvent *in vacuo* followed by distillation of the residue afforded 5-hexenoyl chloride (1.4 g, 63%) which was added to a mixture of H<sub>2</sub><sup>18</sup>O (0.26 g, 96% <sup>18</sup>O) and tetrahydrofuran (10 ml) and stirred at 20°C for 24 hrs. The resultant mixture was dried (MgSO<sub>4</sub>), concentrated under reduced pressure to afford a colourless liquid which was added dropwise to a suspension of lithium aluminium hydride (0.5 g) in diethyl ether (20 ml), the mixture heated under reflux for 2 hrs., cooled to 0°C, aqueous hydrogen chloride (30%, 2 ml) was added, and the organic layer separated. The aqueous layer was extracted with diethyl ether (2 x 5 ml), the combined organic extract dried (MgSO<sub>4</sub>), concentrated *in vacuo*, and the residue distilled to afford 5-hexen-1-<sup>18</sup>O-ol (0.75 g, 64%) as a colourless liquid, b.p. 68 - 70°C/20 mm Hg.

(iii) 5-hexen-1-<sup>18</sup>O-ol (0.75 g) was epoxidised with 3-chloroperbenzoic acid (as described for 4-(2-oxiranyl)-1-butanol) and the residue distilled using a Kugelrohr apparatus (oven temp. 60°C/20 mm Hg) to afford 4-(2-oxiranyl)-1-butan-[<sup>18</sup>O]-ol (0.5 g, 66%, <sup>18</sup>O = 48%).

<sup>1</sup>H n.m.r. (200 MHz/CDCl<sub>3</sub>): δ 1.51 - 1.68 (6H, m), 2.50 (1H, m), 2.77 (1H, t), 2.93 (1H, m), 3.68 (2H, m).

### Condensed Phase Reactions

A mixture of 4-(2-oxiranyl)-1-butanol (0.5 g) and aqueous sodium hydroxide (10%, 5 ml) was allowed to stir for 60 hrs. at: (i) 20°C, and (ii) at 100°C (see Table 4.13 page 199). The reaction mixtures were sampled at various times. Each sample was acidified with aqueous hydrogen chloride (10%) until the pH was 6, extracted with dichloromethane (5 ml), the organic extract dried



(MgSO<sub>4</sub>) and concentrated. The product composition was analysed by GC/MS and is outlined in Table 4.13.

Tetrahydropyran-2-methanol and 3-oxepanol were each treated with aqueous sodium hydroxide as detailed above. No reaction was observed in either case (see Table 4.13).

Table 4.13 Condensed Phase Reactions of 4-(2-oxiranyl)-1-butanol, tetrahydropyran-2-methanol and 3-oxepanol.<sup>a</sup>

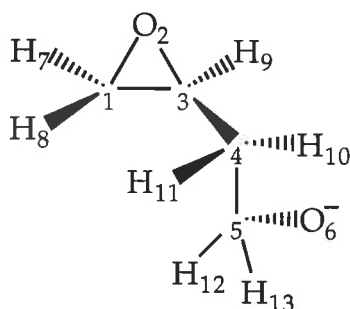
Reactant <sup>b</sup>	Time	20°C/10% NaOH <sup>a</sup>	100°C/10% NaOH <sup>a</sup>
4-(2-oxiranyl)-1-butanol	5 min.	70:24:6	0:61:39
	1 hr.	0:72:28	0:60:40
	60 hrs.	0:70:30	0:63:37
Tetrahydropyran-2-methanol	1 hr.	0:100:0	0:100:0
	60 hrs.	0:100:0	0:100:0
3-oxepanol	1 hr.	0:0:100	0:0:100
	60 hrs.	0:0:100	0:0:100

<sup>a</sup>The ratio of products refers to the 3:6:7 membered cyclic ethers and is obtained by comparing the areas under each peak (this ratio correlates closely with the ratios obtained using ion counts/peak). The error in each number within a ratio is *ca.* ± 5%.

<sup>b</sup>The retention times for the reactants are: oxirane butanol (7.00 min.), tetrahydropyran-2-methanol (6.02 min.) and 3-oxepanol (6.32 min.).

## Appendix A

Geometries and MP2(fc)/6-31+G(d) energies of species shown in Figure 4.1.

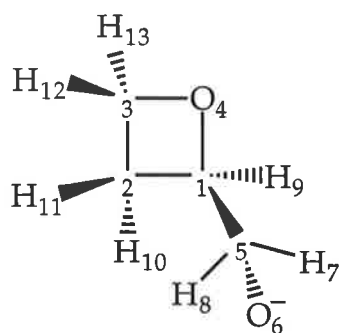


(1)

$E = -305.9967521$  hartrees  
(0 kJ mol<sup>-1</sup>).

O <sub>2</sub> C <sub>1</sub>	1.4513 Å	C <sub>3</sub> C <sub>1</sub> H <sub>8</sub>	118.9969
C <sub>3</sub> O <sub>2</sub>	1.4772	H <sub>7</sub> C <sub>1</sub> H <sub>8</sub>	115.2846
C <sub>4</sub> C <sub>3</sub>	1.4957	C <sub>1</sub> C <sub>3</sub> H <sub>9</sub>	117.4727
C <sub>5</sub> C <sub>4</sub>	1.557	O <sub>2</sub> C <sub>3</sub> H <sub>9</sub>	113.1833
O <sub>6</sub> C <sub>5</sub>	1.3555	C <sub>4</sub> C <sub>3</sub> H <sub>9</sub> <sup>-</sup>	114.9339
H <sub>7</sub> C <sub>1</sub>	1.0897	C <sub>3</sub> C <sub>4</sub> H <sub>10</sub>	109.1066
H <sub>8</sub> C <sub>1</sub>	1.0897	C <sub>5</sub> C <sub>4</sub> H <sub>10</sub>	108.2217
H <sub>9</sub> C <sub>3</sub>	1.0865	C <sub>3</sub> C <sub>4</sub> H <sub>11</sub>	109.363
H <sub>10</sub> C <sub>4</sub>	1.0986	C <sub>5</sub> C <sub>4</sub> H <sub>11</sub>	111.96
H <sub>11</sub> C <sub>4</sub>	1.1036	H <sub>10</sub> C <sub>4</sub> H <sub>11</sub>	108.6711
H <sub>12</sub> C <sub>5</sub>	1.1309	C <sub>4</sub> C <sub>5</sub> H <sub>12</sub>	104.8911
H <sub>13</sub> C <sub>5</sub>	1.1286	O <sub>6</sub> C <sub>5</sub> H <sub>12</sub>	114.2662
O <sub>2</sub> C <sub>1</sub> C <sub>3</sub>	60.891°	C <sub>4</sub> C <sub>5</sub> H <sub>13</sub>	104.8619
C <sub>1</sub> O <sub>2</sub> C <sub>3</sub>	59.9748	O <sub>6</sub> C <sub>5</sub> H <sub>13</sub>	114.8931
C <sub>1</sub> C <sub>3</sub> O <sub>2</sub>	59.1342	H <sub>12</sub> C <sub>5</sub> H <sub>13</sub>	103.9432
C <sub>1</sub> C <sub>3</sub> C <sub>4</sub>	121.8632	C <sub>3</sub> O <sub>2</sub> C <sub>1</sub> H <sub>7</sub>	-112.4447
O <sub>2</sub> C <sub>3</sub> C <sub>4</sub>	118.2606	C <sub>3</sub> O <sub>2</sub> C <sub>1</sub> H <sub>8</sub>	110.8151
C <sub>3</sub> C <sub>4</sub> C <sub>5</sub>	109.4685	O <sub>2</sub> C <sub>3</sub> C <sub>1</sub> H <sub>7</sub>	103.2173
C <sub>4</sub> C <sub>5</sub> O <sub>6</sub>	112.9006	O <sub>2</sub> C <sub>3</sub> C <sub>1</sub> H <sub>8</sub>	-103.9506
O <sub>2</sub> C <sub>1</sub> H <sub>7</sub>	114.7515	C <sub>4</sub> C <sub>3</sub> C <sub>1</sub> O <sub>2</sub>	106.14
C <sub>3</sub> C <sub>1</sub> H <sub>7</sub>	120.4379	C <sub>4</sub> C <sub>3</sub> C <sub>1</sub> H <sub>7</sub>	-150.6426
O <sub>2</sub> C <sub>1</sub> H <sub>8</sub>	114.593	C <sub>4</sub> C <sub>3</sub> C <sub>1</sub> H <sub>8</sub>	2.4894

H <sub>9</sub> C <sub>3</sub> C <sub>1</sub> O <sub>2</sub>	-101.897	H <sub>11</sub> C <sub>4</sub> C <sub>3</sub> O <sub>2</sub>	41.5404
H <sub>9</sub> C <sub>3</sub> C <sub>1</sub> H <sub>7</sub>	1.3204	H <sub>11</sub> C <sub>4</sub> C <sub>3</sub> H <sub>9</sub>	179.511
H <sub>9</sub> C <sub>3</sub> C <sub>1</sub> H <sub>8</sub>	154.4524	O <sub>6</sub> C <sub>5</sub> C <sub>4</sub> C <sub>3</sub>	55.0393
C <sub>4</sub> C <sub>3</sub> O <sub>2</sub> C <sub>1</sub>	-112.1439	O <sub>6</sub> C <sub>5</sub> C <sub>4</sub> H <sub>10</sub>	-63.7689
H <sub>9</sub> C <sub>3</sub> O <sub>2</sub> C <sub>1</sub>	109.1896	O <sub>6</sub> C <sub>5</sub> C <sub>4</sub> H <sub>11</sub>	176.4861
C <sub>5</sub> C <sub>4</sub> C <sub>3</sub> C <sub>1</sub>	95.1309	H <sub>12</sub> C <sub>5</sub> C <sub>4</sub> C <sub>3</sub>	-69.9885
C <sub>5</sub> C <sub>4</sub> C <sub>3</sub> O <sub>2</sub>	164.541	H <sub>12</sub> C <sub>5</sub> C <sub>4</sub> H <sub>10</sub>	171.2033
C <sub>5</sub> C <sub>4</sub> C <sub>3</sub> H <sub>9</sub>	-57.4884	H <sub>12</sub> C <sub>5</sub> C <sub>4</sub> H <sub>11</sub>	51.4583
H <sub>10</sub> C <sub>4</sub> C <sub>3</sub> C <sub>1</sub>	-146.6107	H <sub>13</sub> C <sub>5</sub> C <sub>4</sub> C <sub>3</sub>	-179.1697
H <sub>10</sub> C <sub>4</sub> C <sub>3</sub> O <sub>2</sub>	-77.2005	H <sub>13</sub> C <sub>5</sub> C <sub>4</sub> H <sub>10</sub>	62.0239
H <sub>10</sub> C <sub>4</sub> C <sub>3</sub> H <sub>9</sub>	60.77	H <sub>13</sub> C <sub>5</sub> C <sub>4</sub> H <sub>11</sub>	-57.7211
H <sub>11</sub> C <sub>4</sub> C <sub>3</sub> C <sub>1</sub>	-27.8697		

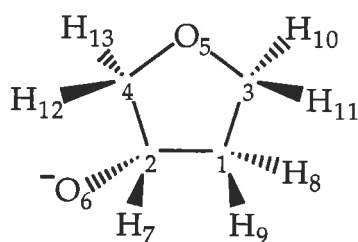


(2)

E = -305.997086 hartrees  
(-1 kJ mol<sup>-1</sup>)

C <sub>2</sub> C <sub>1</sub>	1.5332Å	C <sub>2</sub> C <sub>1</sub> O <sub>4</sub>	90.6938
C <sub>3</sub> C <sub>2</sub>	1.5337	C <sub>2</sub> C <sub>3</sub> O <sub>4</sub>	92.5555
O <sub>4</sub> C <sub>1</sub>	1.4989	C <sub>1</sub> O <sub>4</sub> C <sub>3</sub>	89.967
O <sub>4</sub> C <sub>3</sub>	1.45	C <sub>2</sub> C <sub>1</sub> C <sub>5</sub>	113.9266
C <sub>5</sub> C <sub>1</sub>	1.5284	O <sub>4</sub> C <sub>1</sub> C <sub>5</sub>	115.4172
O <sub>6</sub> C <sub>5</sub>	1.3625	C <sub>1</sub> C <sub>5</sub> O <sub>6</sub>	109.9332
H <sub>7</sub> C <sub>5</sub>	1.1243	C <sub>1</sub> C <sub>5</sub> H <sub>7</sub>	106.133
H <sub>8</sub> C <sub>5</sub>	1.1288	O <sub>6</sub> C <sub>5</sub> H <sub>7</sub>	115.2835
H <sub>9</sub> C <sub>1</sub>	1.0965	C <sub>1</sub> C <sub>5</sub> H <sub>8</sub>	105.2367
H <sub>10</sub> C <sub>2</sub>	1.0949	O <sub>6</sub> C <sub>5</sub> H <sub>8</sub>	114.9327
H <sub>11</sub> C <sub>2</sub>	1.093	H <sub>7</sub> C <sub>5</sub> H <sub>8</sub>	104.4809
H <sub>12</sub> C <sub>3</sub>	1.0992	C <sub>2</sub> C <sub>1</sub> H <sub>9</sub>	116.288
H <sub>13</sub> C <sub>3</sub>	1.0996	O <sub>4</sub> C <sub>1</sub> H <sub>9</sub>	109.7673
C <sub>1</sub> C <sub>2</sub> C <sub>3</sub>	85.6526°	C <sub>5</sub> C <sub>1</sub> H <sub>9</sub>	109.7153

C <sub>1</sub> C <sub>2</sub> H <sub>10</sub>	115.1454	H <sub>12</sub> C <sub>3</sub> C <sub>2</sub> C <sub>1</sub>	-106.8918
C <sub>3</sub> C <sub>2</sub> H <sub>10</sub>	114.0354	H <sub>12</sub> C <sub>3</sub> C <sub>2</sub> H <sub>10</sub>	137.4694
C <sub>1</sub> C <sub>2</sub> H <sub>11</sub>	112.9782	H <sub>12</sub> C <sub>3</sub> C <sub>2</sub> H <sub>11</sub>	6.8436
C <sub>3</sub> C <sub>2</sub> H <sub>11</sub>	117.8018	H <sub>13</sub> C <sub>3</sub> C <sub>2</sub> C <sub>1</sub>	123.574
H <sub>10</sub> C <sub>2</sub> H <sub>11</sub>	109.6361	H <sub>13</sub> C <sub>3</sub> C <sub>2</sub> H <sub>10</sub>	7.9352
C <sub>2</sub> C <sub>3</sub> H <sub>12</sub>	114.911	H <sub>13</sub> C <sub>3</sub> C <sub>2</sub> H <sub>11</sub>	-122.6906
O <sub>4</sub> C <sub>3</sub> H <sub>12</sub>	111.2854	C <sub>3</sub> O <sub>4</sub> C <sub>1</sub> C <sub>2</sub>	8.1863
C <sub>2</sub> C <sub>3</sub> H <sub>13</sub>	116.9336	C <sub>3</sub> O <sub>4</sub> C <sub>1</sub> C <sub>5</sub>	-108.8668
O <sub>4</sub> C <sub>3</sub> H <sub>13</sub>	111.3373	C <sub>3</sub> O <sub>4</sub> C <sub>1</sub> H <sub>9</sub>	126.5457
H <sub>12</sub> C <sub>3</sub> H <sub>13</sub>	108.8993	C <sub>1</sub> O <sub>4</sub> C <sub>3</sub> C <sub>2</sub>	-8.1914
C <sub>3</sub> C <sub>2</sub> C <sub>1</sub> O <sub>4</sub>	-7.7591	C <sub>1</sub> O <sub>4</sub> C <sub>3</sub> H <sub>12</sub>	109.8355
C <sub>3</sub> C <sub>2</sub> C <sub>1</sub> C <sub>5</sub>	110.598	C <sub>1</sub> O <sub>4</sub> C <sub>3</sub> H <sub>13</sub>	-128.4702
C <sub>3</sub> C <sub>2</sub> C <sub>1</sub> H <sub>9</sub>	-120.2925	O <sub>6</sub> C <sub>5</sub> C <sub>1</sub> C <sub>2</sub>	69.4895
H <sub>10</sub> C <sub>2</sub> C <sub>1</sub> O <sub>4</sub>	106.7951	O <sub>6</sub> C <sub>5</sub> C <sub>1</sub> O <sub>4</sub>	172.5225
H <sub>10</sub> C <sub>2</sub> C <sub>1</sub> C <sub>5</sub>	-134.8478	O <sub>6</sub> C <sub>5</sub> C <sub>1</sub> H <sub>9</sub>	-62.863
H <sub>10</sub> C <sub>2</sub> C <sub>1</sub> H <sub>9</sub>	-5.7383	H <sub>7</sub> C <sub>5</sub> C <sub>1</sub> C <sub>2</sub>	-165.2117
H <sub>11</sub> C <sub>2</sub> C <sub>1</sub> O <sub>4</sub>	-126.1731	H <sub>7</sub> C <sub>5</sub> C <sub>1</sub> O <sub>4</sub>	-62.1787
H <sub>11</sub> C <sub>2</sub> C <sub>1</sub> C <sub>5</sub>	-7.816	H <sub>7</sub> C <sub>5</sub> C <sub>1</sub> H <sub>9</sub>	62.4358
H <sub>11</sub> C <sub>2</sub> C <sub>1</sub> H <sub>9</sub>	121.2935	H <sub>8</sub> C <sub>5</sub> C <sub>1</sub> C <sub>2</sub>	-54.8111
O <sub>4</sub> C <sub>3</sub> C <sub>2</sub> C <sub>1</sub>	8.0297	H <sub>8</sub> C <sub>5</sub> C <sub>1</sub> O <sub>4</sub>	48.2219
O <sub>4</sub> C <sub>3</sub> C <sub>2</sub> H <sub>10</sub>	-107.6091	H <sub>8</sub> C <sub>5</sub> C <sub>1</sub> H <sub>9</sub>	172.8364
O <sub>4</sub> C <sub>3</sub> C <sub>2</sub> H <sub>11</sub>	121.7651		

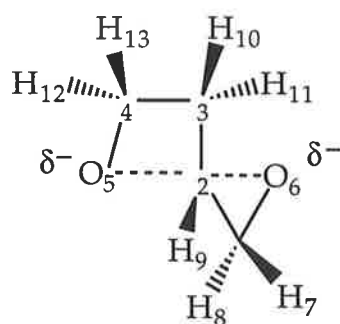


(3)

E = -306.0284004 hartrees  
(-83 kJ mol<sup>-1</sup>)

C <sub>2</sub> C <sub>1</sub>	1.5608Å	H <sub>7</sub> C <sub>2</sub>	1.1297
C <sub>3</sub> C <sub>1</sub>	1.5184	H <sub>8</sub> C <sub>1</sub>	1.0981
C <sub>4</sub> C <sub>2</sub>	1.546	H <sub>9</sub> C <sub>1</sub>	1.0967
O <sub>5</sub> C <sub>3</sub>	1.4522	H <sub>10</sub> C <sub>3</sub>	1.099
O <sub>5</sub> C <sub>4</sub>	1.4556	H <sub>11</sub> C <sub>3</sub>	1.1012
O <sub>6</sub> C <sub>2</sub>	1.3498	H <sub>12</sub> C <sub>4</sub>	1.0961

H <sub>13</sub> C <sub>4</sub>	1.0999	O <sub>6</sub> C <sub>2</sub> C <sub>1</sub> H <sub>8</sub>	44.1887
C <sub>2</sub> C <sub>1</sub> C <sub>3</sub>	103.6675°	O <sub>6</sub> C <sub>2</sub> C <sub>1</sub> H <sub>9</sub>	-74.6527
C <sub>1</sub> C <sub>2</sub> C <sub>4</sub>	97.8684	H <sub>7</sub> C <sub>2</sub> C <sub>1</sub> C <sub>3</sub>	-70.0284
C <sub>1</sub> C <sub>3</sub> O <sub>5</sub>	106.4253	H <sub>7</sub> C <sub>2</sub> C <sub>1</sub> H <sub>8</sub>	171.4436
C <sub>2</sub> C <sub>4</sub> O <sub>5</sub>	108.1649	H <sub>7</sub> C <sub>2</sub> C <sub>1</sub> H <sub>9</sub>	52.6022
C <sub>3</sub> O <sub>5</sub> C <sub>4</sub>	107.9203	O <sub>5</sub> C <sub>3</sub> C <sub>1</sub> C <sub>2</sub>	-31.3461
C <sub>1</sub> C <sub>2</sub> O <sub>6</sub>	117.3423	O <sub>5</sub> C <sub>3</sub> C <sub>1</sub> H <sub>8</sub>	83.5101
C <sub>4</sub> C <sub>2</sub> O <sub>6</sub>	115.5725	O <sub>5</sub> C <sub>3</sub> C <sub>1</sub> H <sub>9</sub>	-152.8711
C <sub>1</sub> C <sub>2</sub> H <sub>7</sub>	104.9715	H <sub>10</sub> C <sub>3</sub> C <sub>1</sub> C <sub>2</sub>	-150.1252
C <sub>4</sub> C <sub>2</sub> H <sub>7</sub>	105.6086	H <sub>10</sub> C <sub>3</sub> C <sub>1</sub> H <sub>8</sub>	-35.269
O <sub>6</sub> C <sub>2</sub> H <sub>7</sub>	113.6295	H <sub>10</sub> C <sub>3</sub> C <sub>1</sub> H <sub>9</sub>	88.3499
C <sub>2</sub> C <sub>1</sub> H <sub>8</sub>	106.8428	H <sub>11</sub> C <sub>3</sub> C <sub>1</sub> C <sub>2</sub>	86.6247
C <sub>3</sub> C <sub>1</sub> H <sub>8</sub>	112.0671	H <sub>11</sub> C <sub>3</sub> C <sub>1</sub> H <sub>8</sub>	-158.5191
C <sub>2</sub> C <sub>1</sub> H <sub>9</sub>	111.8267	H <sub>11</sub> C <sub>3</sub> C <sub>1</sub> H <sub>9</sub>	-34.9002
C <sub>3</sub> C <sub>1</sub> H <sub>9</sub>	113.4869	O <sub>5</sub> C <sub>4</sub> C <sub>2</sub> C <sub>1</sub>	-34.1049
H <sub>8</sub> C <sub>1</sub> H <sub>9</sub>	108.7154	O <sub>5</sub> C <sub>4</sub> C <sub>2</sub> O <sub>6</sub>	-159.5665
C <sub>1</sub> C <sub>3</sub> H <sub>10</sub>	114.7952	O <sub>5</sub> C <sub>4</sub> C <sub>2</sub> H <sub>7</sub>	73.9174
O <sub>5</sub> C <sub>3</sub> H <sub>10</sub>	107.4954	H <sub>12</sub> C <sub>4</sub> C <sub>2</sub> C <sub>1</sub>	-153.2947
C <sub>1</sub> C <sub>3</sub> H <sub>11</sub>	111.5518	H <sub>12</sub> C <sub>4</sub> C <sub>2</sub> O <sub>6</sub>	81.2437
O <sub>5</sub> C <sub>3</sub> H <sub>11</sub>	108.334	H <sub>12</sub> C <sub>4</sub> C <sub>2</sub> H <sub>7</sub>	-45.2724
H <sub>10</sub> C <sub>3</sub> H <sub>11</sub>	107.9927	H <sub>13</sub> C <sub>4</sub> C <sub>2</sub> C <sub>1</sub>	84.9876
C <sub>2</sub> C <sub>4</sub> H <sub>12</sub>	113.3491	H <sub>13</sub> C <sub>4</sub> C <sub>2</sub> O <sub>6</sub>	-40.474
O <sub>5</sub> C <sub>4</sub> H <sub>12</sub>	107.5713	H <sub>13</sub> C <sub>4</sub> C <sub>2</sub> H <sub>7</sub>	-166.9901
C <sub>2</sub> C <sub>4</sub> H <sub>13</sub>	108.1777	C <sub>4</sub> O <sub>5</sub> C <sub>3</sub> C <sub>1</sub>	9.5026
O <sub>5</sub> C <sub>4</sub> H <sub>13</sub>	109.9791	C <sub>4</sub> O <sub>5</sub> C <sub>3</sub> H <sub>10</sub>	132.9622
H <sub>12</sub> C <sub>4</sub> H <sub>13</sub>	109.5695	C <sub>4</sub> O <sub>5</sub> C <sub>3</sub> H <sub>11</sub>	-110.5728
C <sub>4</sub> C <sub>2</sub> C <sub>1</sub> C <sub>3</sub>	38.5209	C <sub>3</sub> O <sub>5</sub> C <sub>4</sub> C <sub>2</sub>	16.566
C <sub>4</sub> C <sub>2</sub> C <sub>1</sub> H <sub>8</sub>	-80.007	C <sub>3</sub> O <sub>5</sub> C <sub>4</sub> H <sub>12</sub>	139.3474
C <sub>4</sub> C <sub>2</sub> C <sub>1</sub> H <sub>9</sub>	161.1516	C <sub>3</sub> O <sub>5</sub> C <sub>4</sub> H <sub>13</sub>	-101.3799
O <sub>6</sub> C <sub>2</sub> C <sub>1</sub> C <sub>3</sub>	162.7166		

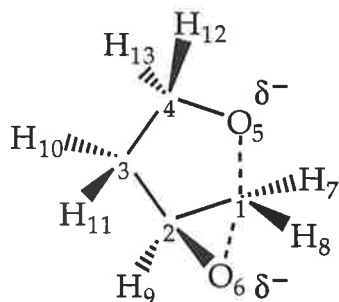


(C)

E = -305.9701383 hartrees  
(+70 kJ mol<sup>-1</sup>)

C <sub>2</sub> C <sub>1</sub>	1.4523Å	C <sub>2</sub> C <sub>3</sub> H <sub>11</sub>	108.7817
C <sub>3</sub> C <sub>2</sub>	1.5092	C <sub>4</sub> C <sub>3</sub> H <sub>11</sub>	111.7735
C <sub>4</sub> C <sub>3</sub>	1.5249	H <sub>10</sub> C <sub>3</sub> H <sub>11</sub>	108.591
O <sub>5</sub> C <sub>4</sub>	1.4044	C <sub>3</sub> C <sub>4</sub> H <sub>12</sub>	114.3563
O <sub>6</sub> C <sub>1</sub>	1.4101	O <sub>5</sub> C <sub>4</sub> H <sub>12</sub>	114.0568
O <sub>6</sub> C <sub>2</sub>	1.85	C <sub>3</sub> C <sub>4</sub> H <sub>13</sub>	109.8998
O <sub>5</sub> C <sub>2</sub>	2.0	O <sub>5</sub> C <sub>4</sub> H <sub>13</sub>	112.9481
H <sub>7</sub> C <sub>1</sub>	1.1021	H <sub>12</sub> C <sub>4</sub> H <sub>13</sub>	106.185
H <sub>8</sub> C <sub>1</sub>	1.102	O <sub>5</sub> C <sub>2</sub> O <sub>6</sub>	163.4
H <sub>9</sub> C <sub>2</sub>	1.0839	C <sub>3</sub> C <sub>2</sub> C <sub>1</sub> O <sub>6</sub>	80.8322
H <sub>10</sub> C <sub>3</sub>	1.0998	C <sub>3</sub> C <sub>2</sub> C <sub>1</sub> H <sub>7</sub>	-164.7473
H <sub>11</sub> C <sub>3</sub>	1.0968	C <sub>3</sub> C <sub>2</sub> C <sub>1</sub> H <sub>8</sub>	-33.3667
H <sub>12</sub> C <sub>4</sub>	1.1108	H <sub>9</sub> C <sub>2</sub> C <sub>1</sub> O <sub>6</sub>	-78.8448
H <sub>13</sub> C <sub>4</sub>	1.116	H <sub>9</sub> C <sub>2</sub> C <sub>1</sub> H <sub>7</sub>	35.5756
C <sub>1</sub> C <sub>2</sub> C <sub>3</sub>	122.4492°	H <sub>9</sub> C <sub>2</sub> C <sub>1</sub> H <sub>8</sub>	166.9563
C <sub>2</sub> C <sub>3</sub> C <sub>4</sub>	95.0889	C <sub>4</sub> C <sub>3</sub> C <sub>2</sub> C <sub>1</sub>	131.2633
C <sub>3</sub> C <sub>4</sub> O <sub>5</sub>	99.4898	C <sub>4</sub> C <sub>3</sub> C <sub>2</sub> H <sub>9</sub>	-69.457
C <sub>2</sub> C <sub>1</sub> O <sub>6</sub>	80.7688	H <sub>10</sub> C <sub>3</sub> C <sub>2</sub> C <sub>1</sub>	-105.0601
C <sub>2</sub> C <sub>1</sub> H <sub>7</sub>	116.5862	H <sub>10</sub> C <sub>3</sub> C <sub>2</sub> H <sub>9</sub>	54.2196
O <sub>6</sub> C <sub>1</sub> H <sub>7</sub>	115.8948	H <sub>11</sub> C <sub>3</sub> C <sub>2</sub> C <sub>1</sub>	16.199
C <sub>2</sub> C <sub>1</sub> H <sub>8</sub>	115.1379	H <sub>11</sub> C <sub>3</sub> C <sub>2</sub> H <sub>9</sub>	175.4787
O <sub>6</sub> C <sub>1</sub> H <sub>8</sub>	115.7485	O <sub>5</sub> C <sub>4</sub> C <sub>3</sub> C <sub>2</sub>	-26.1005
H <sub>7</sub> C <sub>1</sub> H <sub>8</sub>	110.1851	O <sub>5</sub> C <sub>4</sub> C <sub>3</sub> H <sub>10</sub>	-146.6083
C <sub>1</sub> C <sub>2</sub> H <sub>9</sub>	116.1869	O <sub>5</sub> C <sub>4</sub> C <sub>3</sub> H <sub>11</sub>	86.4588
C <sub>3</sub> C <sub>2</sub> H <sub>9</sub>	118.2508	H <sub>12</sub> C <sub>4</sub> C <sub>3</sub> C <sub>2</sub>	-148.062
C <sub>2</sub> C <sub>3</sub> H <sub>10</sub>	113.8887	H <sub>12</sub> C <sub>4</sub> C <sub>3</sub> H <sub>10</sub>	91.4303
C <sub>4</sub> C <sub>3</sub> H <sub>10</sub>	117.9748	H <sub>12</sub> C <sub>4</sub> C <sub>3</sub> H <sub>11</sub>	-35.5027

H <sub>13</sub> C <sub>4</sub> C <sub>3</sub> C <sub>2</sub>	92.6451	H <sub>13</sub> C <sub>4</sub> C <sub>3</sub> H <sub>11</sub>	-154.7956
H <sub>13</sub> C <sub>4</sub> C <sub>3</sub> H <sub>10</sub>	-27.8627	O <sub>5</sub> C <sub>2</sub> C <sub>1</sub> O <sub>6</sub>	172.52



(D)

E = -305.9645415 hartrees  
(+69 kJ mol<sup>-1</sup>)

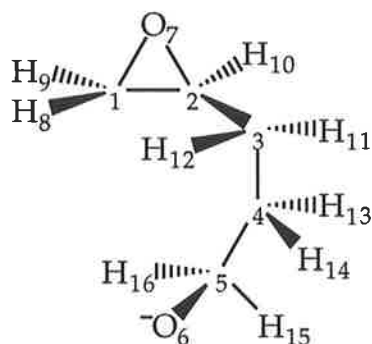
C <sub>2</sub> C <sub>1</sub>	1.4367Å	C <sub>4</sub> C <sub>3</sub> H <sub>10</sub>	112.0912
C <sub>3</sub> C <sub>2</sub>	1.5092	C <sub>2</sub> C <sub>3</sub> H <sub>11</sub>	108.4488
C <sub>4</sub> C <sub>3</sub>	1.5623	C <sub>4</sub> C <sub>3</sub> H <sub>11</sub>	110.6941
O <sub>5</sub> C <sub>4</sub>	1.3902	H <sub>10</sub> C <sub>3</sub> H <sub>11</sub>	108.7182
O <sub>6</sub> C <sub>2</sub>	1.4261	C <sub>3</sub> C <sub>4</sub> H <sub>12</sub>	108.2555
H <sub>7</sub> C <sub>1</sub>	1.084	O <sub>5</sub> C <sub>4</sub> H <sub>12</sub>	112.2997
H <sub>8</sub> C <sub>1</sub>	1.0773	C <sub>3</sub> C <sub>4</sub> H <sub>12</sub>	106.5561
H <sub>9</sub> C <sub>2</sub>	1.1028	O <sub>5</sub> C <sub>4</sub> H <sub>13</sub>	112.3076
H <sub>10</sub> C <sub>3</sub>	1.101	H <sub>12</sub> C <sub>4</sub> H <sub>13</sub>	105.5592
H <sub>11</sub> C <sub>3</sub>	1.0987	O <sub>5</sub> C <sub>1</sub> O <sub>6</sub>	140.3
H <sub>12</sub> C <sub>4</sub>	1.1128	C <sub>3</sub> C <sub>2</sub> C <sub>1</sub> H <sub>7</sub>	-147.5812
H <sub>13</sub> C <sub>4</sub>	1.1183	C <sub>3</sub> C <sub>2</sub> C <sub>1</sub> H <sub>8</sub>	47.8126
O <sub>5</sub> C <sub>1</sub>	2.09	O <sub>6</sub> C <sub>2</sub> C <sub>1</sub> H <sub>7</sub>	88.7611
O <sub>6</sub> C <sub>1</sub>	1.84	O <sub>6</sub> C <sub>2</sub> C <sub>1</sub> H <sub>8</sub>	-75.8451
C <sub>1</sub> C <sub>2</sub> C <sub>3</sub>	108.532°	H <sub>9</sub> C <sub>2</sub> C <sub>1</sub> H <sub>7</sub>	-21.9648
C <sub>2</sub> C <sub>3</sub> C <sub>4</sub>	102.3988	H <sub>9</sub> C <sub>2</sub> C <sub>1</sub> H <sub>8</sub>	173.429
C <sub>3</sub> C <sub>4</sub> O <sub>5</sub>	111.4957	C <sub>4</sub> C <sub>3</sub> C <sub>2</sub> C <sub>1</sub>	55.1723
C <sub>1</sub> C <sub>2</sub> O <sub>6</sub>	79.8035	C <sub>4</sub> C <sub>3</sub> C <sub>2</sub> O <sub>6</sub>	145.5587
C <sub>3</sub> C <sub>2</sub> O <sub>6</sub>	124.9916	C <sub>4</sub> C <sub>3</sub> C <sub>2</sub> H <sub>9</sub>	-72.875
C <sub>2</sub> C <sub>1</sub> H <sub>7</sub>	121.0524	H <sub>10</sub> C <sub>3</sub> C <sub>2</sub> C <sub>1</sub>	176.6431
C <sub>2</sub> C <sub>1</sub> H <sub>8</sub>	118.7889	H <sub>10</sub> C <sub>3</sub> C <sub>2</sub> O <sub>6</sub>	-92.9705
H <sub>7</sub> C <sub>1</sub> H <sub>8</sub>	118.3894	H <sub>10</sub> C <sub>3</sub> C <sub>2</sub> H <sub>9</sub>	48.5958
C <sub>1</sub> C <sub>2</sub> H <sub>9</sub>	115.4448	H <sub>11</sub> C <sub>3</sub> C <sub>2</sub> C <sub>1</sub>	-61.8772
C <sub>3</sub> C <sub>2</sub> H <sub>9</sub>	111.2258	H <sub>11</sub> C <sub>3</sub> C <sub>2</sub> O <sub>6</sub>	28.5092
O <sub>6</sub> C <sub>2</sub> H <sub>9</sub>	112.9906	H <sub>11</sub> C <sub>3</sub> C <sub>2</sub> H <sub>9</sub>	170.0756
C <sub>2</sub> C <sub>3</sub> H <sub>10</sub>	114.3385	O <sub>5</sub> C <sub>4</sub> C <sub>3</sub> C <sub>2</sub>	-42.8959

$\text{O}_5\text{C}_4\text{C}_3\text{H}_{10}$	-165.8953	$\text{H}_{13}\text{C}_4\text{C}_3\text{C}_2$	79.97
$\text{O}_5\text{C}_4\text{C}_3\text{H}_{11}$	72.5341	$\text{H}_{13}\text{C}_4\text{C}_3\text{H}_{10}$	-43.0295
$\text{H}_{12}\text{C}_4\text{C}_3\text{C}_2$	-166.9058	$\text{H}_{13}\text{C}_4\text{C}_3\text{H}_{11}$	-164.6
$\text{H}_{12}\text{C}_4\text{C}_3\text{H}_{10}$	70.0947	$\text{O}_5\text{C}_1\text{C}_2\text{O}_6$	-163.13
$\text{H}_{12}\text{C}_4\text{C}_3\text{H}_{11}$	-51.4759		



## Appendix B

Geometries and MP2(fc)/6-31+G(d) energies of species shown in Figure 4.6.

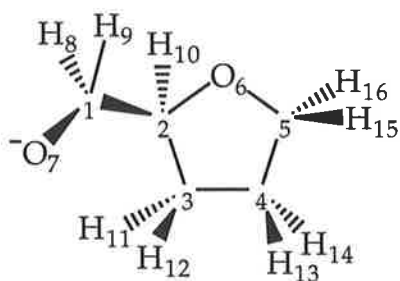


(7)

E = -345.167127 hartrees  
(0 kJ mol<sup>-1</sup>)

C1C2	1.4604Å	C2C1H8	116.398
O7C2	1.464	O7C1H8	116.3269
O7C1	1.4645	C1C2H10	117.6638
C3C2	1.5017	O7C2H10	112.1995
H8C1	1.0892	C3C2H10	116.6997
H10C2	1.0937	C2C1H9	119.7241
H9C1	1.0898	O7C1H9	113.6938
C4C3	1.5312	H8C1H9	117.6178
H11C3	1.1013	C2C3C4	112.0927
H12C3	1.0949	C2C3H11	109.3027
C5C4	1.5564	C4C3H11	111.5445
H13C4	1.1064	C2C3H12	107.7769
H14C4	1.0997	C4C3H12	107.2884
O6C5	1.3575	H11C3H12	108.6918
H15C5	1.1268	C3C4C5	111.2228
H16C5	1.1301	C3C4H13	110.9791
C1C2O7	60.1028°	C5C4H13	110.4121
C2C1O7	60.072	C3C4H14	108.1068
C2O7C1	59.8252	C5C4H14	108.4185
C1C2C3	120.3024	H13C4H14	107.5667
O7C2C3	116.9503	C4C5O6	113.3298

C <sub>4</sub> C <sub>5</sub> H <sub>15</sub>	105.0059	H <sub>11</sub> C <sub>3</sub> C <sub>2</sub> H <sub>10</sub>	56.6588
O <sub>6</sub> C <sub>5</sub> H <sub>15</sub>	114.5215	H <sub>12</sub> C <sub>3</sub> C <sub>2</sub> C <sub>1</sub>	-31.7599
C <sub>4</sub> C <sub>5</sub> H <sub>16</sub>	105.4858	H <sub>12</sub> C <sub>3</sub> C <sub>2</sub> O <sub>7</sub>	37.7207
O <sub>6</sub> C <sub>5</sub> H <sub>16</sub>	113.833	H <sub>12</sub> C <sub>3</sub> C <sub>2</sub> H <sub>10</sub>	174.6211
H <sub>15</sub> C <sub>5</sub> H <sub>16</sub>	103.6374	C <sub>5</sub> C <sub>4</sub> C <sub>3</sub> C <sub>2</sub>	-62.1188
O <sub>7</sub> C <sub>1</sub> C <sub>2</sub> C <sub>3</sub>	105.635	C <sub>5</sub> C <sub>4</sub> C <sub>3</sub> H <sub>11</sub>	174.938
O <sub>7</sub> C <sub>2</sub> C <sub>1</sub> H <sub>10</sub>	-100.9929	C <sub>5</sub> C <sub>4</sub> C <sub>3</sub> H <sub>12</sub>	56.0084
H <sub>8</sub> C <sub>1</sub> C <sub>2</sub> O <sub>7</sub>	-106.5921	H <sub>13</sub> C <sub>4</sub> C <sub>3</sub> C <sub>2</sub>	61.2215
H <sub>8</sub> C <sub>1</sub> C <sub>2</sub> C <sub>3</sub>	-0.9571	H <sub>13</sub> C <sub>4</sub> C <sub>3</sub> H <sub>11</sub>	-61.7216
H <sub>8</sub> C <sub>1</sub> C <sub>2</sub> H <sub>10</sub>	152.415	H <sub>13</sub> C <sub>4</sub> C <sub>3</sub> H <sub>12</sub>	-180.6513
H <sub>9</sub> C <sub>1</sub> C <sub>2</sub> O <sub>7</sub>	101.8442	H <sub>14</sub> C <sub>4</sub> C <sub>3</sub> C <sub>2</sub>	178.9618
H <sub>9</sub> C <sub>1</sub> C <sub>2</sub> C <sub>3</sub>	-152.5208	H <sub>14</sub> C <sub>4</sub> C <sub>3</sub> H <sub>11</sub>	56.0186
H <sub>9</sub> C <sub>1</sub> C <sub>2</sub> H <sub>10</sub>	0.8513	H <sub>14</sub> C <sub>4</sub> C <sub>3</sub> H <sub>12</sub>	-62.911
C <sub>1</sub> O <sub>7</sub> C <sub>2</sub> C <sub>3</sub>	-111.1368	O <sub>6</sub> C <sub>5</sub> C <sub>4</sub> C <sub>3</sub>	-48.6745
C <sub>1</sub> O <sub>7</sub> C <sub>2</sub> H <sub>10</sub>	110.1085	O <sub>6</sub> C <sub>5</sub> C <sub>4</sub> H <sub>13</sub>	-172.3384
C <sub>2</sub> O <sub>7</sub> C <sub>1</sub> H <sub>8</sub>	106.7101	O <sub>6</sub> C <sub>5</sub> C <sub>4</sub> H <sub>14</sub>	70.058
C <sub>2</sub> O <sub>7</sub> C <sub>1</sub> H <sub>9</sub>	-111.8424	H <sub>15</sub> C <sub>5</sub> C <sub>4</sub> C <sub>3</sub>	-174.3756
C <sub>4</sub> C <sub>3</sub> C <sub>2</sub> C <sub>1</sub>	86.0768	H <sub>15</sub> C <sub>5</sub> C <sub>4</sub> H <sub>13</sub>	61.9605
C <sub>4</sub> C <sub>3</sub> C <sub>2</sub> O <sub>7</sub>	155.5574	H <sub>15</sub> C <sub>5</sub> C <sub>4</sub> H <sub>14</sub>	-55.6431
C <sub>4</sub> C <sub>3</sub> C <sub>2</sub> H <sub>10</sub>	-67.5422	H <sub>16</sub> C <sub>5</sub> C <sub>4</sub> C <sub>3</sub>	76.5035
H <sub>11</sub> C <sub>3</sub> C <sub>2</sub> C <sub>1</sub>	-149.7222	H <sub>16</sub> C <sub>5</sub> C <sub>4</sub> H <sub>13</sub>	-47.1605
H <sub>11</sub> C <sub>3</sub> C <sub>2</sub> O <sub>7</sub>	-80.2416	H <sub>16</sub> C <sub>5</sub> C <sub>4</sub> H <sub>14</sub>	-164.764



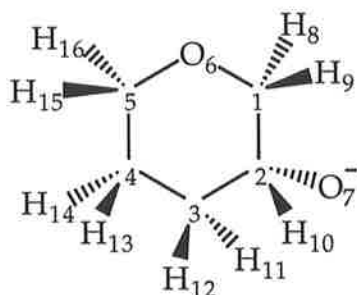
(8)

E = -345.1713646 hartrees  
(-57.1 kJ mol<sup>-1</sup>)

C <sub>2</sub> O <sub>6</sub>	1.4774Å	H <sub>14</sub> C <sub>4</sub>	1.0979
C <sub>3</sub> C <sub>2</sub>	1.535	H <sub>12</sub> C <sub>3</sub>	1.0968
C <sub>4</sub> C <sub>3</sub>	1.5315	H <sub>11</sub> C <sub>3</sub>	1.0935
C <sub>5</sub> O <sub>6</sub>	1.4246	C <sub>1</sub> C <sub>2</sub>	1.5371
C <sub>5</sub> C <sub>4</sub>	1.5233	H <sub>10</sub> C <sub>2</sub>	1.0978

H <sub>16</sub> C <sub>5</sub>	1.0974	C <sub>1</sub> C <sub>2</sub> O <sub>6</sub> C <sub>5</sub>	109.8163
H <sub>15</sub> C <sub>5</sub>	1.1033	H <sub>10</sub> C <sub>2</sub> O <sub>6</sub> C <sub>5</sub>	-131.1929
H <sub>13</sub> C <sub>4</sub>	1.0981	C <sub>4</sub> C <sub>3</sub> C <sub>2</sub> O <sub>6</sub>	-13.6589
H <sub>8</sub> C <sub>1</sub>	1.1231	C <sub>4</sub> C <sub>3</sub> C <sub>2</sub> C <sub>1</sub>	-136.8422
O <sub>7</sub> C <sub>1</sub>	1.3613	C <sub>4</sub> C <sub>3</sub> C <sub>2</sub> H <sub>10</sub>	100.8285
H <sub>9</sub> C <sub>1</sub>	1.1317	H <sub>12</sub> C <sub>3</sub> C <sub>2</sub> O <sub>6</sub>	105.1444
O <sub>6</sub> C <sub>2</sub> C <sub>3</sub>	105.5317°	H <sub>12</sub> C <sub>3</sub> C <sub>2</sub> C <sub>1</sub>	-18.0389
C <sub>2</sub> C <sub>3</sub> C <sub>4</sub>	104.2065	H <sub>12</sub> C <sub>3</sub> C <sub>2</sub> H <sub>10</sub>	-140.3682
C <sub>2</sub> O <sub>6</sub> C <sub>5</sub>	108.1137	H <sub>11</sub> C <sub>3</sub> C <sub>2</sub> O <sub>6</sub>	-136.9769
C <sub>3</sub> C <sub>4</sub> C <sub>5</sub>	100.8711	H <sub>11</sub> C <sub>3</sub> C <sub>2</sub> C <sub>1</sub>	99.8398
O <sub>6</sub> C <sub>5</sub> C <sub>4</sub>	104.5849	H <sub>11</sub> C <sub>3</sub> C <sub>2</sub> H <sub>10</sub>	-22.4895
C <sub>3</sub> C <sub>4</sub> H <sub>14</sub>	111.1285	C <sub>5</sub> C <sub>4</sub> C <sub>3</sub> C <sub>2</sub>	32.5827
C <sub>5</sub> C <sub>4</sub> H <sub>14</sub>	109.3427	C <sub>5</sub> C <sub>4</sub> C <sub>3</sub> H <sub>12</sub>	-84.25
C <sub>2</sub> C <sub>3</sub> H <sub>12</sub>	108.5352	C <sub>5</sub> C <sub>4</sub> C <sub>3</sub> H <sub>11</sub>	154.8029
C <sub>4</sub> C <sub>3</sub> H <sub>12</sub>	111.3969	H <sub>14</sub> C <sub>4</sub> C <sub>3</sub> C <sub>2</sub>	-83.2529
C <sub>2</sub> C <sub>3</sub> H <sub>11</sub>	112.0083	H <sub>14</sub> C <sub>4</sub> C <sub>3</sub> H <sub>12</sub>	159.9144
C <sub>4</sub> C <sub>3</sub> H <sub>11</sub>	113.6855	H <sub>14</sub> C <sub>4</sub> C <sub>3</sub> H <sub>11</sub>	38.9673
H <sub>12</sub> C <sub>3</sub> H <sub>11</sub>	106.9725	H <sub>13</sub> C <sub>4</sub> C <sub>3</sub> C <sub>2</sub>	154.1108
O <sub>6</sub> C <sub>2</sub> C <sub>1</sub>	113.0199	H <sub>13</sub> C <sub>4</sub> C <sub>3</sub> H <sub>12</sub>	37.278
C <sub>3</sub> C <sub>2</sub> C <sub>1</sub>	111.6875	H <sub>13</sub> C <sub>4</sub> C <sub>3</sub> H <sub>11</sub>	-83.669
O <sub>6</sub> C <sub>2</sub> H <sub>10</sub>	105.715	C <sub>4</sub> C <sub>5</sub> O <sub>6</sub> C <sub>2</sub>	34.0259
C <sub>3</sub> C <sub>2</sub> H <sub>10</sub>	111.8728	H <sub>16</sub> C <sub>5</sub> O <sub>6</sub> C <sub>2</sub>	156.2968
C <sub>1</sub> C <sub>2</sub> H <sub>10</sub>	108.8738	H <sub>15</sub> C <sub>5</sub> O <sub>6</sub> C <sub>2</sub>	-85.0229
O <sub>6</sub> C <sub>5</sub> H <sub>16</sub>	107.6792	O <sub>6</sub> C <sub>5</sub> C <sub>4</sub> C <sub>3</sub>	-41.1607
C <sub>4</sub> C <sub>5</sub> H <sub>16</sub>	114.5723	O <sub>6</sub> C <sub>5</sub> C <sub>4</sub> H <sub>14</sub>	75.9955
O <sub>6</sub> C <sub>5</sub> H <sub>15</sub>	110.8683	O <sub>6</sub> C <sub>5</sub> C <sub>4</sub> H <sub>13</sub>	-163.0265
C <sub>4</sub> C <sub>5</sub> H <sub>15</sub>	110.4495	H <sub>16</sub> C <sub>5</sub> C <sub>4</sub> C <sub>3</sub>	-158.8078
H <sub>16</sub> C <sub>5</sub> H <sub>15</sub>	108.6073	H <sub>16</sub> C <sub>5</sub> C <sub>4</sub> H <sub>14</sub>	-41.6516
C <sub>3</sub> C <sub>4</sub> H <sub>13</sub>	113.707	H <sub>16</sub> C <sub>5</sub> C <sub>4</sub> H <sub>13</sub>	79.3264
C <sub>5</sub> C <sub>4</sub> H <sub>13</sub>	113.2265	H <sub>15</sub> C <sub>5</sub> C <sub>4</sub> C <sub>3</sub>	78.1707
H <sub>14</sub> C <sub>4</sub> H <sub>13</sub>	108.4015	H <sub>15</sub> C <sub>5</sub> C <sub>4</sub> H <sub>14</sub>	-164.673
C <sub>2</sub> C <sub>1</sub> H <sub>8</sub>	106.182	H <sub>15</sub> C <sub>5</sub> C <sub>4</sub> H <sub>13</sub>	-43.6951
C <sub>2</sub> C <sub>1</sub> O <sub>7</sub>	110.9607	H <sub>8</sub> C <sub>1</sub> C <sub>2</sub> O <sub>6</sub>	56.1877
H <sub>8</sub> C <sub>1</sub> O <sub>7</sub>	115.0545	H <sub>8</sub> C <sub>1</sub> C <sub>2</sub> C <sub>3</sub>	175.0088
C <sub>2</sub> C <sub>1</sub> H <sub>9</sub>	104.4273	H <sub>8</sub> C <sub>1</sub> C <sub>2</sub> H <sub>10</sub>	-60.9584
H <sub>8</sub> C <sub>1</sub> H <sub>9</sub>	104.4276	O <sub>7</sub> C <sub>1</sub> C <sub>2</sub> O <sub>6</sub>	-178.1251
O <sub>7</sub> C <sub>1</sub> H <sub>9</sub>	114.8515	O <sub>7</sub> C <sub>1</sub> C <sub>2</sub> C <sub>3</sub>	-59.304
C <sub>3</sub> C <sub>2</sub> O <sub>6</sub> C <sub>5</sub>	-12.5153	O <sub>7</sub> C <sub>1</sub> C <sub>2</sub> H <sub>10</sub>	64.7288

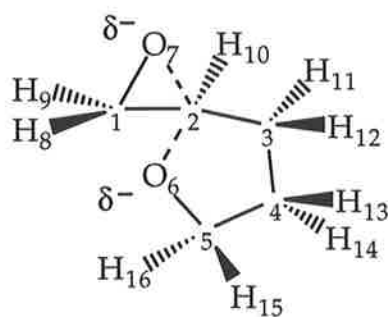
H <sub>9</sub> C <sub>1</sub> C <sub>2</sub> O <sub>6</sub>	-53.8438	H <sub>9</sub> C <sub>1</sub> C <sub>2</sub> H <sub>10</sub>	-170.9899
H <sub>9</sub> C <sub>1</sub> C <sub>2</sub> C <sub>3</sub>	64.9773		



E = -345.1815112 hartrees  
(-83.7 kJ mol<sup>-1</sup>)

C <sub>5</sub> C <sub>4</sub>	1.5232Å	C <sub>1</sub> C <sub>2</sub> H <sub>10</sub>	105.2
C <sub>3</sub> C <sub>4</sub>	1.5312	O <sub>7</sub> C <sub>2</sub> H <sub>10</sub>	113.9058
C <sub>2</sub> C <sub>3</sub>	1.5483	C <sub>4</sub> C <sub>3</sub> H <sub>12</sub>	111.8285
C <sub>1</sub> C <sub>2</sub>	1.5411	C <sub>2</sub> C <sub>3</sub> H <sub>12</sub>	108.5085
O <sub>6</sub> C <sub>5</sub>	1.4232	C <sub>4</sub> C <sub>3</sub> H <sub>11</sub>	110.4077
O <sub>6</sub> C <sub>1</sub>	1.4577	C <sub>2</sub> C <sub>3</sub> H <sub>11</sub>	106.5888
O <sub>7</sub> C <sub>2</sub>	1.3583	H <sub>12</sub> C <sub>3</sub> H <sub>11</sub>	106.9548
H <sub>10</sub> C <sub>2</sub>	1.1282	C <sub>5</sub> C <sub>4</sub> H <sub>13</sub>	108.1977
H <sub>12</sub> C <sub>3</sub>	1.0984	C <sub>3</sub> C <sub>4</sub> H <sub>13</sub>	110.0775
H <sub>11</sub> C <sub>3</sub>	1.1015	C <sub>5</sub> C <sub>4</sub> H <sub>14</sub>	109.145
H <sub>13</sub> C <sub>4</sub>	1.0992	C <sub>3</sub> C <sub>4</sub> H <sub>14</sub>	111.9954
H <sub>14</sub> C <sub>4</sub>	1.1029	H <sub>13</sub> C <sub>4</sub> H <sub>14</sub>	107.2617
H <sub>16</sub> C <sub>5</sub>	1.1069	C <sub>4</sub> C <sub>5</sub> H <sub>16</sub>	109.4979
H <sub>15</sub> C <sub>5</sub>	1.0976	O <sub>6</sub> C <sub>5</sub> H <sub>16</sub>	109.4982
H <sub>8</sub> C <sub>1</sub>	1.1041	C <sub>4</sub> C <sub>5</sub> H <sub>15</sub>	111.8302
H <sub>9</sub> C <sub>1</sub>	1.0934	O <sub>6</sub> C <sub>5</sub> H <sub>15</sub>	105.7616
C <sub>5</sub> C <sub>4</sub> C <sub>3</sub>	110.0519°	H <sub>16</sub> C <sub>5</sub> H <sub>15</sub>	108.1779
C <sub>4</sub> C <sub>3</sub> C <sub>2</sub>	112.2756	C <sub>2</sub> C <sub>1</sub> H <sub>8</sub>	108.0651
C <sub>3</sub> C <sub>2</sub> C <sub>1</sub>	106.7792	O <sub>6</sub> C <sub>1</sub> H <sub>8</sub>	109.0874
C <sub>4</sub> C <sub>5</sub> O <sub>6</sub>	111.9446	C <sub>2</sub> C <sub>1</sub> H <sub>9</sub>	109.9436
C <sub>2</sub> C <sub>1</sub> O <sub>6</sub>	115.0505	O <sub>6</sub> C <sub>1</sub> H <sub>9</sub>	105.6278
C <sub>5</sub> O <sub>6</sub> C <sub>1</sub>	110.4498	H <sub>8</sub> C <sub>1</sub> H <sub>9</sub>	108.9328
C <sub>3</sub> C <sub>2</sub> O <sub>7</sub>	113.965	O <sub>6</sub> C <sub>5</sub> C <sub>4</sub> C <sub>3</sub>	-57.4147
C <sub>1</sub> C <sub>2</sub> O <sub>7</sub>	110.8569	O <sub>6</sub> C <sub>5</sub> C <sub>4</sub> H <sub>13</sub>	62.8949
C <sub>3</sub> C <sub>2</sub> H <sub>10</sub>	105.4786	O <sub>6</sub> C <sub>5</sub> C <sub>4</sub> H <sub>14</sub>	-180.6964

H <sub>16</sub> C <sub>5</sub> C <sub>4</sub> C <sub>3</sub>	64.2131	O <sub>7</sub> C <sub>2</sub> C <sub>3</sub> H <sub>11</sub>	-52.3382
H <sub>16</sub> C <sub>5</sub> C <sub>4</sub> H <sub>13</sub>	-175.4773	H <sub>10</sub> C <sub>2</sub> C <sub>3</sub> C <sub>4</sub>	60.9709
H <sub>16</sub> C <sub>5</sub> C <sub>4</sub> H <sub>14</sub>	-59.0685	H <sub>10</sub> C <sub>2</sub> C <sub>3</sub> H <sub>12</sub>	-63.1446
H <sub>15</sub> C <sub>5</sub> C <sub>4</sub> C <sub>3</sub>	-175.8961	H <sub>10</sub> C <sub>2</sub> C <sub>3</sub> H <sub>11</sub>	-178.0173
H <sub>15</sub> C <sub>5</sub> C <sub>4</sub> H <sub>13</sub>	-55.5865	O <sub>6</sub> C <sub>1</sub> C <sub>2</sub> C <sub>3</sub>	53.9229
H <sub>15</sub> C <sub>5</sub> C <sub>4</sub> H <sub>14</sub>	60.8223	O <sub>6</sub> C <sub>1</sub> C <sub>2</sub> O <sub>7</sub>	178.5944
C <sub>2</sub> C <sub>3</sub> C <sub>4</sub> C <sub>5</sub>	53.6727	O <sub>6</sub> C <sub>1</sub> C <sub>2</sub> H <sub>10</sub>	-57.8404
C <sub>2</sub> C <sub>3</sub> C <sub>4</sub> H <sub>13</sub>	-65.4949	H <sub>8</sub> C <sub>1</sub> C <sub>2</sub> C <sub>3</sub>	-68.2266
C <sub>2</sub> C <sub>3</sub> C <sub>4</sub> H <sub>14</sub>	175.2712	H <sub>8</sub> C <sub>1</sub> C <sub>2</sub> O <sub>7</sub>	56.4449
H <sub>12</sub> C <sub>3</sub> C <sub>4</sub> C <sub>5</sub>	175.9231	H <sub>8</sub> C <sub>1</sub> C <sub>2</sub> H <sub>10</sub>	180.0101
H <sub>12</sub> C <sub>3</sub> C <sub>4</sub> H <sub>13</sub>	56.7555	H <sub>9</sub> C <sub>1</sub> C <sub>2</sub> C <sub>3</sub>	172.9958
H <sub>12</sub> C <sub>3</sub> C <sub>4</sub> H <sub>14</sub>	-62.4784	H <sub>9</sub> C <sub>1</sub> C <sub>2</sub> O <sub>7</sub>	-62.3327
H <sub>11</sub> C <sub>3</sub> C <sub>4</sub> C <sub>5</sub>	-65.1167	H <sub>9</sub> C <sub>1</sub> C <sub>2</sub> H <sub>10</sub>	61.2325
H <sub>11</sub> C <sub>3</sub> C <sub>4</sub> H <sub>13</sub>	175.7157	C <sub>1</sub> O <sub>6</sub> C <sub>5</sub> C <sub>4</sub>	59.3675
H <sub>11</sub> C <sub>3</sub> C <sub>4</sub> H <sub>14</sub>	56.4818	C <sub>1</sub> O <sub>6</sub> C <sub>5</sub> H <sub>16</sub>	-62.2602
C <sub>1</sub> C <sub>2</sub> C <sub>3</sub> C <sub>4</sub>	-50.6	C <sub>1</sub> O <sub>6</sub> C <sub>5</sub> H <sub>15</sub>	-178.6078
C <sub>1</sub> C <sub>2</sub> C <sub>3</sub> H <sub>12</sub>	-174.7155	C <sub>5</sub> O <sub>6</sub> C <sub>1</sub> C <sub>2</sub>	-59.6092
C <sub>1</sub> C <sub>2</sub> C <sub>3</sub> H <sub>11</sub>	70.4117	C <sub>5</sub> O <sub>6</sub> C <sub>1</sub> H <sub>8</sub>	61.9878
O <sub>7</sub> C <sub>2</sub> C <sub>3</sub> C <sub>4</sub>	-173.35	C <sub>5</sub> O <sub>6</sub> C <sub>1</sub> H <sub>9</sub>	178.9441
O <sub>7</sub> C <sub>2</sub> C <sub>3</sub> H <sub>12</sub>	62.5345		

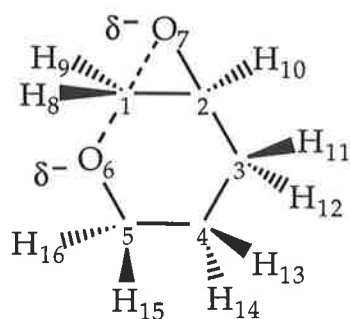


(E)

E = -345.1313611 hartrees  
(+48 kJ mol<sup>-1</sup>)

O <sub>7</sub> C <sub>2</sub>	1.7989 Å	C <sub>5</sub> C <sub>4</sub>	1.5323
O <sub>6</sub> C <sub>2</sub>	2.1019	O <sub>6</sub> C <sub>5</sub>	1.3789
O <sub>7</sub> C <sub>1</sub>	1.4207	H <sub>8</sub> C <sub>1</sub>	1.1006
C <sub>2</sub> C <sub>1</sub>	1.4461	H <sub>10</sub> C <sub>2</sub>	1.0814
C <sub>2</sub> O <sub>7</sub>	1.7989	H <sub>9</sub> C <sub>1</sub>	1.0984
C <sub>3</sub> C <sub>2</sub>	1.5061	H <sub>15</sub> C <sub>3</sub>	1.0971
C <sub>4</sub> C <sub>3</sub>	1.529	H <sub>16</sub> C <sub>3</sub>	1.0993

H <sub>13</sub> C <sub>4</sub>	1.0995	C <sub>2</sub> O <sub>7</sub> C <sub>1</sub> H <sub>9</sub>	-114.5317
H <sub>14</sub> C <sub>4</sub>	1.1039	O <sub>7</sub> C <sub>2</sub> C <sub>1</sub> H <sub>8</sub>	-112.6824
H <sub>11</sub> C <sub>5</sub>	1.1209	O <sub>7</sub> C <sub>2</sub> C <sub>1</sub> H <sub>9</sub>	113.1519
H <sub>12</sub> C <sub>5</sub>	1.1154	C <sub>3</sub> C <sub>2</sub> C <sub>1</sub> O <sub>7</sub>	81.1691
O <sub>7</sub> C <sub>2</sub> O <sub>6</sub>	156.078°	C <sub>3</sub> C <sub>2</sub> C <sub>1</sub> H <sub>8</sub>	-31.5133
O <sub>7</sub> C <sub>1</sub> C <sub>2</sub>	77.7252	C <sub>3</sub> C <sub>2</sub> C <sub>1</sub> H <sub>9</sub>	-165.679
C <sub>1</sub> O <sub>7</sub> C <sub>2</sub>	51.767	H <sub>10</sub> C <sub>2</sub> C <sub>1</sub> O <sub>7</sub>	-81.9907
C <sub>1</sub> C <sub>2</sub> O <sub>7</sub>	50.5078	H <sub>10</sub> C <sub>2</sub> C <sub>1</sub> H <sub>8</sub>	165.3269
C <sub>1</sub> C <sub>2</sub> C <sub>3</sub>	121.3847	H <sub>10</sub> C <sub>2</sub> C <sub>1</sub> H <sub>9</sub>	31.1612
O <sub>7</sub> C <sub>2</sub> C <sub>3</sub>	103.3009	C <sub>3</sub> C <sub>2</sub> O <sub>7</sub> C <sub>1</sub>	-119.9086
C <sub>2</sub> C <sub>3</sub> C <sub>4</sub>	111.176	H <sub>10</sub> C <sub>2</sub> O <sub>7</sub> C <sub>1</sub>	115.9088
C <sub>3</sub> C <sub>4</sub> C <sub>5</sub>	106.1834	C <sub>4</sub> C <sub>3</sub> C <sub>2</sub> C <sub>1</sub>	133.716
C <sub>4</sub> C <sub>5</sub> O <sub>6</sub>	107.7423	C <sub>4</sub> C <sub>3</sub> C <sub>2</sub> O <sub>7</sub>	-174.6941
O <sub>7</sub> C <sub>1</sub> H <sub>8</sub>	115.587	C <sub>4</sub> C <sub>3</sub> C <sub>2</sub> H <sub>10</sub>	-63.5418
C <sub>2</sub> C <sub>1</sub> H <sub>8</sub>	116.0242	H <sub>15</sub> C <sub>3</sub> C <sub>2</sub> C <sub>1</sub>	-103.178
C <sub>1</sub> C <sub>2</sub> H <sub>10</sub>	116.9532	H <sub>15</sub> C <sub>3</sub> C <sub>2</sub> O <sub>7</sub>	-51.5882
O <sub>7</sub> C <sub>2</sub> H <sub>10</sub>	101.0939	H <sub>15</sub> C <sub>3</sub> C <sub>2</sub> H <sub>10</sub>	59.5642
C <sub>3</sub> C <sub>2</sub> H <sub>10</sub>	119.4903	H <sub>16</sub> C <sub>3</sub> C <sub>2</sub> C <sub>1</sub>	12.8588
O <sub>7</sub> C <sub>1</sub> H <sub>9</sub>	116.0329	H <sub>16</sub> C <sub>3</sub> C <sub>2</sub> O <sub>7</sub>	64.4486
C <sub>2</sub> C <sub>1</sub> H <sub>9</sub>	117.2485	H <sub>16</sub> C <sub>3</sub> C <sub>2</sub> H <sub>10</sub>	175.601
H <sub>8</sub> C <sub>1</sub> H <sub>9</sub>	110.8383	C <sub>5</sub> C <sub>4</sub> C <sub>3</sub> C <sub>2</sub>	-45.6864
C <sub>2</sub> C <sub>3</sub> H <sub>15</sub>	109.3039	C <sub>5</sub> C <sub>4</sub> C <sub>3</sub> H <sub>15</sub>	-167.7106
C <sub>4</sub> C <sub>3</sub> H <sub>15</sub>	111.1774	C <sub>5</sub> C <sub>4</sub> C <sub>3</sub> H <sub>16</sub>	74.1
C <sub>2</sub> C <sub>3</sub> H <sub>16</sub>	108.1727	H <sub>13</sub> C <sub>4</sub> C <sub>3</sub> C <sub>2</sub>	71.2531
C <sub>4</sub> C <sub>3</sub> H <sub>16</sub>	109.9835	H <sub>13</sub> C <sub>4</sub> C <sub>3</sub> H <sub>15</sub>	-50.7711
H <sub>15</sub> C <sub>3</sub> H <sub>16</sub>	106.8882	H <sub>13</sub> C <sub>4</sub> C <sub>3</sub> H <sub>16</sub>	-168.9605
C <sub>3</sub> C <sub>4</sub> H <sub>13</sub>	109.5934	H <sub>14</sub> C <sub>4</sub> C <sub>3</sub> C <sub>2</sub>	-169.5801
C <sub>5</sub> C <sub>4</sub> H <sub>13</sub>	108.4477	H <sub>14</sub> C <sub>4</sub> C <sub>3</sub> H <sub>15</sub>	68.3956
C <sub>3</sub> C <sub>4</sub> H <sub>14</sub>	111.0922	H <sub>14</sub> C <sub>4</sub> C <sub>3</sub> H <sub>16</sub>	-49.7937
C <sub>5</sub> C <sub>4</sub> H <sub>14</sub>	113.5391	O <sub>6</sub> C <sub>5</sub> C <sub>4</sub> C <sub>3</sub>	47.463
H <sub>13</sub> C <sub>4</sub> H <sub>14</sub>	107.9203	O <sub>6</sub> C <sub>5</sub> C <sub>4</sub> H <sub>13</sub>	-70.241
C <sub>4</sub> C <sub>5</sub> H <sub>11</sub>	107.6176	O <sub>6</sub> C <sub>5</sub> C <sub>4</sub> H <sub>14</sub>	169.8173
O <sub>6</sub> C <sub>5</sub> H <sub>11</sub>	113.2684	H <sub>11</sub> C <sub>5</sub> C <sub>4</sub> C <sub>3</sub>	-75.0018
C <sub>4</sub> C <sub>5</sub> H <sub>12</sub>	109.2839	H <sub>11</sub> C <sub>5</sub> C <sub>4</sub> H <sub>13</sub>	167.2942
O <sub>6</sub> C <sub>5</sub> H <sub>16</sub>	113.1448	H <sub>11</sub> C <sub>5</sub> C <sub>4</sub> H <sub>14</sub>	47.3525
H <sub>15</sub> C <sub>6</sub> H <sub>12</sub>	105.6161	H <sub>12</sub> C <sub>5</sub> C <sub>4</sub> C <sub>3</sub>	170.7725
O <sub>7</sub> C <sub>1</sub> C <sub>2</sub> O <sub>6</sub>	-176.131	H <sub>12</sub> C <sub>5</sub> C <sub>4</sub> H <sub>13</sub>	53.0685
C <sub>2</sub> O <sub>7</sub> C <sub>1</sub> H <sub>8</sub>	113.1821	H <sub>12</sub> C <sub>5</sub> C <sub>4</sub> H <sub>14</sub>	-66.8732



(F)

E = -345.1314998 hartrees  
(+47.7 kJ mol<sup>-1</sup>)

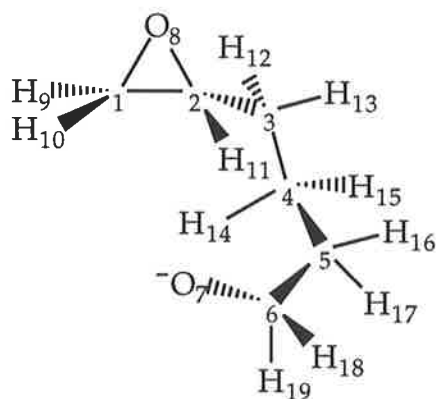
C5O6	1.3786Å	C1C2H10	115.5788
C4C5	1.5486	O7C2H10	113.8039
C3C4	1.5348	C4C3H12	111.8532
C2C3	1.5128	C2C3H12	110.5602
C1C2	1.4374	C4C3H11	109.9397
O7C2	1.4261	C2C3H11	107.5837
O7C1	1.7644	H12C3H11	107.1064
O6C1	2.1044	C5C4H14	107.5766
H10C2	1.1003	C3C4H14	109.8593
H12C3	1.1022	C5C4H13	109.345
H11C3	1.0994	C3C4H13	109.5654
H14C4	1.1003	H11C3H12	107.4225
H13C4	1.1044	O6C5H15	112.6773
H15C5	1.1251	C4C5H15	105.6943
H16C5	1.1158	O6C5H16	111.6769
H8C1	1.0807	C4C5H16	106.4737
H9C1	1.0801	H15C5H16	104.8966
O6C1O7	152.817°	C2C1H8	119.1986
O6C5C4	114.6975	O7C1H8	102.1161
C5C4C3	112.9088	C2C1H9	120.6656
C4C3C2	109.6769	O7C1H9	106.273
C3C2C1	115.6918	H8C1H9	119.2523
C3C2O7	119.6248	O7C2C1O6	175.313
C1C2O7	76.0731	C3C4C5O6	-65.5283
C2C1O7	51.674	C3C4C5H15	59.2229
C2O7C1	52.2529	C3C4C5H16	170.4148
C3C2H10	111.8615	H14C4C5O6	55.8528

H <sub>14</sub> C <sub>4</sub> C <sub>5</sub> H <sub>15</sub>	-179.396	O <sub>7</sub> C <sub>2</sub> C <sub>3</sub> H <sub>12</sub>	82.3589
H <sub>14</sub> C <sub>4</sub> C <sub>5</sub> H <sub>16</sub>	-68.2005	O <sub>7</sub> C <sub>2</sub> C <sub>3</sub> H <sub>11</sub>	-34.2836
H <sub>13</sub> C <sub>4</sub> C <sub>5</sub> O <sub>6</sub>	172.2174	H <sub>10</sub> C <sub>2</sub> C <sub>3</sub> C <sub>4</sub>	69.4067
H <sub>13</sub> C <sub>4</sub> C <sub>5</sub> H <sub>15</sub>	-63.0314	H <sub>10</sub> C <sub>2</sub> C <sub>3</sub> H <sub>12</sub>	-54.396
H <sub>13</sub> C <sub>4</sub> C <sub>5</sub> H <sub>16</sub>	48.1641	H <sub>10</sub> C <sub>2</sub> C <sub>3</sub> H <sub>11</sub>	-171.0385
C <sub>2</sub> C <sub>3</sub> C <sub>4</sub> C <sub>5</sub>	57.8851	O <sub>7</sub> C <sub>1</sub> C <sub>2</sub> C <sub>3</sub>	-116.4787
C <sub>2</sub> C <sub>3</sub> C <sub>4</sub> H <sub>14</sub>	-62.1949	O <sub>7</sub> C <sub>1</sub> C <sub>2</sub> H <sub>10</sub>	110.0182
C <sub>2</sub> C <sub>3</sub> C <sub>4</sub> H <sub>13</sub>	-179.9843	H <sub>8</sub> C <sub>1</sub> C <sub>2</sub> C <sub>3</sub>	-34.2527
H <sub>12</sub> C <sub>3</sub> C <sub>4</sub> C <sub>5</sub>	-179.0724	H <sub>8</sub> C <sub>1</sub> C <sub>2</sub> O <sub>7</sub>	82.226
H <sub>12</sub> C <sub>3</sub> C <sub>4</sub> H <sub>14</sub>	60.8476	H <sub>8</sub> C <sub>1</sub> C <sub>2</sub> H <sub>10</sub>	-167.7559
H <sub>12</sub> C <sub>3</sub> C <sub>4</sub> H <sub>13</sub>	-56.9418	H <sub>9</sub> C <sub>1</sub> C <sub>2</sub> C <sub>3</sub>	156.5856
H <sub>11</sub> C <sub>3</sub> C <sub>4</sub> C <sub>5</sub>	-60.2156	H <sub>9</sub> C <sub>1</sub> C <sub>2</sub> O <sub>7</sub>	-86.9358
H <sub>11</sub> C <sub>3</sub> C <sub>4</sub> H <sub>14</sub>	179.7045	H <sub>9</sub> C <sub>1</sub> C <sub>2</sub> H <sub>10</sub>	23.0824
H <sub>11</sub> C <sub>3</sub> C <sub>4</sub> H <sub>13</sub>	61.915	C <sub>1</sub> O <sub>7</sub> C <sub>2</sub> C <sub>3</sub>	111.8894
C <sub>1</sub> C <sub>2</sub> C <sub>3</sub> C <sub>4</sub>	-65.7684	C <sub>1</sub> O <sub>7</sub> C <sub>2</sub> H <sub>10</sub>	-112.1355
C <sub>1</sub> C <sub>2</sub> C <sub>3</sub> H <sub>12</sub>	170.4289	C <sub>2</sub> O <sub>7</sub> C <sub>1</sub> H <sub>8</sub>	-117.7957
C <sub>1</sub> C <sub>2</sub> C <sub>3</sub> H <sub>11</sub>	53.7864	C <sub>2</sub> O <sub>7</sub> C <sub>1</sub> H <sub>9</sub>	116.5204
O <sub>7</sub> C <sub>2</sub> C <sub>3</sub> C <sub>4</sub>	-153.8384		



## Appendix C

Geometries and MP2(fc)/6-31+G(d) energies of species shown in Figure 4.10.



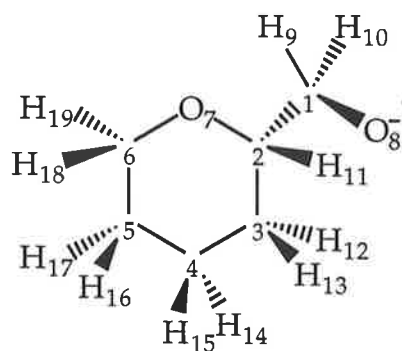
(10)

E = -384.4306105 hartrees

(0 kJ mol<sup>-1</sup>)

O8C2	1.475Å	O8C2C1	59.1452°
C1C2	1.4646	C2O8C1	60.0724
C1O8	1.4508	C2C1O8	60.7824
C3C2	1.5023	O8C2C3	114.993
C4C3	1.5383	C1C2C3	119.9933
C5C4	1.5367	C2C3C4	113.974
C6C5	1.5502	C3C4C5	117.0066
O7C6	1.3584	C4C5C6	116.3855
H11C2	1.0943	C5C6O7	115.3881
H11O7	1.9744	O8C2H11	116.9216
H9C1	1.0914	C1C2H11	118.9084
H10C1	1.0889	C3C2H11	115.0355
H13C3	1.0995	C6O7H11	117.7062
H12C3	1.1009	C2H11O7	141.1154
H14C4	1.1018	C2C1H9	119.7077
H15C4	1.1012	O8C1H9	114.3076
H17C5	1.106	C2C1H10	119.6994
H16C5	1.1011	O8C1H10	114.8596
H19C6	1.1309	H9C1H10	115.4237
H18C6	1.1277	C2C3H13	108.7875

C <sub>4</sub> C <sub>3</sub> H <sub>13</sub>	109.2473	H <sub>12</sub> C <sub>3</sub> C <sub>2</sub> O <sub>8</sub>	-39.9208
C <sub>2</sub> C <sub>3</sub> H <sub>12</sub>	107.8068	H <sub>12</sub> C <sub>3</sub> C <sub>2</sub> C <sub>1</sub>	27.4801
C <sub>4</sub> C <sub>3</sub> H <sub>12</sub>	109.7897	H <sub>12</sub> C <sub>3</sub> C <sub>2</sub> H <sub>11</sub>	-180.1918
H <sub>13</sub> C <sub>3</sub> H <sub>12</sub>	106.9968	C <sub>5</sub> C <sub>4</sub> C <sub>3</sub> C <sub>2</sub>	-77.6297
C <sub>3</sub> C <sub>4</sub> H <sub>14</sub>	109.0434	C <sub>5</sub> C <sub>4</sub> C <sub>3</sub> H <sub>13</sub>	44.2814
C <sub>5</sub> C <sub>4</sub> H <sub>14</sub>	108.8074	C <sub>5</sub> C <sub>4</sub> C <sub>3</sub> H <sub>12</sub>	161.3266
C <sub>3</sub> C <sub>4</sub> H <sub>15</sub>	106.6971	H <sub>14</sub> C <sub>4</sub> C <sub>3</sub> C <sub>2</sub>	46.3376
C <sub>5</sub> C <sub>4</sub> H <sub>15</sub>	108.5109	H <sub>14</sub> C <sub>4</sub> C <sub>3</sub> H <sub>13</sub>	168.2487
H <sub>14</sub> C <sub>4</sub> H <sub>15</sub>	106.252	H <sub>14</sub> C <sub>4</sub> C <sub>3</sub> H <sub>12</sub>	-74.7061
C <sub>4</sub> C <sub>5</sub> H <sub>17</sub>	107.8652	H <sub>15</sub> C <sub>4</sub> C <sub>3</sub> C <sub>2</sub>	160.7082
C <sub>6</sub> C <sub>5</sub> H <sub>17</sub>	107.6528	H <sub>15</sub> C <sub>4</sub> C <sub>3</sub> H <sub>13</sub>	-77.3807
C <sub>4</sub> C <sub>5</sub> H <sub>16</sub>	109.3692	H <sub>15</sub> C <sub>4</sub> C <sub>3</sub> H <sub>12</sub>	39.6645
C <sub>6</sub> C <sub>5</sub> H <sub>16</sub>	107.9101	C <sub>6</sub> C <sub>5</sub> C <sub>4</sub> C <sub>3</sub>	83.6164
H <sub>17</sub> C <sub>5</sub> H <sub>16</sub>	107.3059	C <sub>6</sub> C <sub>5</sub> C <sub>4</sub> H <sub>14</sub>	-40.4707
C <sub>5</sub> C <sub>6</sub> H <sub>19</sub>	104.5966	C <sub>6</sub> C <sub>5</sub> C <sub>4</sub> H <sub>15</sub>	-155.6723
O <sub>7</sub> C <sub>6</sub> H <sub>19</sub>	113.785	H <sub>17</sub> C <sub>5</sub> C <sub>4</sub> C <sub>3</sub>	-155.3486
C <sub>5</sub> C <sub>6</sub> H <sub>18</sub>	104.1972	H <sub>17</sub> C <sub>5</sub> C <sub>4</sub> H <sub>14</sub>	80.5642
O <sub>7</sub> C <sub>6</sub> H <sub>18</sub>	113.6767	H <sub>17</sub> C <sub>5</sub> C <sub>4</sub> H <sub>15</sub>	-34.6374
H <sub>19</sub> C <sub>6</sub> H <sub>18</sub>	103.9676	H <sub>16</sub> C <sub>5</sub> C <sub>4</sub> C <sub>3</sub>	-38.9504
C <sub>1</sub> O <sub>8</sub> C <sub>2</sub> C <sub>3</sub>	111.3451 <sup>o</sup>	H <sub>16</sub> C <sub>5</sub> C <sub>4</sub> H <sub>14</sub>	-163.0375
C <sub>1</sub> O <sub>8</sub> C <sub>2</sub> H <sub>11</sub>	-109.1583	H <sub>16</sub> C <sub>5</sub> C <sub>4</sub> H <sub>15</sub>	81.7609
O <sub>8</sub> C <sub>1</sub> C <sub>2</sub> C <sub>3</sub>	-102.911	O <sub>7</sub> C <sub>6</sub> C <sub>5</sub> C <sub>4</sub>	-65.7163
O <sub>8</sub> C <sub>1</sub> C <sub>2</sub> H <sub>11</sub>	105.8181	O <sup>7</sup> C <sub>6</sub> C <sub>5</sub> H <sub>17</sub>	173.1359
H <sub>9</sub> C <sub>1</sub> C <sub>2</sub> O <sub>8</sub>	102.9384	O <sub>7</sub> C <sub>6</sub> C <sub>5</sub> H <sub>16</sub>	57.61
H <sub>9</sub> C <sub>1</sub> C <sub>2</sub> C <sub>3</sub>	0.0274	H <sub>19</sub> C <sub>6</sub> C <sub>5</sub> C <sub>4</sub>	60.0795
H <sub>9</sub> C <sub>1</sub> C <sub>2</sub> H <sub>11</sub>	-151.2435	H <sub>19</sub> C <sub>6</sub> C <sub>5</sub> H <sub>17</sub>	-61.0683
H <sub>10</sub> C <sub>1</sub> C <sub>2</sub> O <sub>8</sub>	-103.6223	H <sub>19</sub> C <sub>6</sub> C <sub>5</sub> H <sub>16</sub>	-176.5943
H <sub>10</sub> C <sub>1</sub> C <sub>2</sub> C <sub>3</sub>	153.4668	H <sub>18</sub> C <sub>6</sub> C <sub>5</sub> C <sub>4</sub>	168.9338
H <sub>10</sub> C <sub>1</sub> C <sub>2</sub> H <sub>11</sub>	2.1959	H <sub>18</sub> C <sub>6</sub> C <sub>5</sub> H <sub>17</sub>	47.786
H <sub>9</sub> C <sub>1</sub> O <sub>8</sub> C <sub>2</sub>	-111.7425	H <sub>18</sub> C <sub>6</sub> C <sub>5</sub> H <sub>16</sub>	-67.74
H <sub>10</sub> C <sub>1</sub> O <sub>8</sub> C <sub>2</sub>	111.5008	H <sub>11</sub> O <sub>7</sub> C <sub>6</sub> C <sub>5</sub>	35.9652
C <sub>4</sub> C <sub>3</sub> C <sub>2</sub> O <sub>8</sub>	-162.0621	H <sub>11</sub> O <sub>7</sub> C <sub>6</sub> H <sub>19</sub>	-84.9661
C <sub>4</sub> C <sub>3</sub> C <sub>2</sub> C <sub>1</sub>	-94.6612	H <sub>11</sub> O <sub>7</sub> C <sub>6</sub> H <sub>18</sub>	156.265
C <sub>4</sub> C <sub>3</sub> C <sub>2</sub> H <sub>11</sub>	57.6669	O <sub>7</sub> H <sub>11</sub> C <sub>2</sub> O <sub>8</sub>	-178.6556
H <sub>13</sub> C <sub>3</sub> C <sub>2</sub> O <sub>8</sub>	75.7736	O <sub>7</sub> H <sub>11</sub> C <sub>2</sub> C <sub>3</sub>	113.4712
H <sub>13</sub> C <sub>3</sub> C <sub>2</sub> C <sub>1</sub>	143.1745	O <sub>7</sub> H <sub>11</sub> C <sub>2</sub> C <sub>3</sub>	-39.176
H <sub>13</sub> C <sub>3</sub> C <sub>2</sub> H <sub>11</sub>	-64.4974	C <sub>2</sub> H <sub>11</sub> O <sub>7</sub> C <sub>6</sub>	3.8377



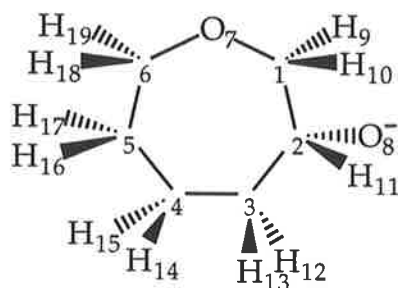
(11)

E = -384.4678042 hartrees

(-88.0 kJ mol<sup>-1</sup>)

C2O7	1.4574Å	C3C4H14	111.3461
C3C2	1.5172	C5C4H14	110.4995
C4C3	1.5288	C3C4H15	109.2776
C5C4	1.5297	C5C4H15	109.0725
C6O7	1.4186	H14C4H15	106.7029
C6C5	1.5257	C2C3H12	107.5327
H17C5	1.0988	C4C3H12	109.9917
H14C4	1.1	C2C3H13	107.1412
H15C4	1.1011	C4C3H13	112.9339
H12C3	1.1011	H12C3H13	107.3865
H13C3	1.095	O7C2H11	107.7136
H11C2	1.106	C3C2H11	109.7161
H18C6	1.1068	O7C6H18	109.8088
H19C6	1.0976	C5C6H18	109.5276
H16C5	1.1013	O7C6H19	106.2456
C1C2	1.5408	C5C6H19	111.241
O8C1	1.363	H18C6H19	108.0591
H9C1	1.1238	C4C5H16	111.6151
H10C1	1.1268	C6C5H16	109.7835
O7C2C3	109.7095°	H17C5H16	107.57
C2C3C4	111.6085	O7C2C1	110.1121
C3C4C5	109.8626	C3C2C1	111.8709
C2O7C6	111.4525	H11C2C1	107.609
C4C5C6	109.8787	C2C1O8	111.5223
O7C6C5	111.8468	C2C1H9	105.0681
C4C5H17	109.6491	O8C1H9	114.9918
C6C5H17	108.2587	C2C1H10	104.8812

O8C1H10	114.6406	H17C5C4H14	-55.6841
H9C1H10	104.7552	H17C5C4H15	-172.6799
C3C2O7C6	60.9329	H16C5C4C3	-173.3419
H11C2O7C6	-58.4479	H16C5C4H14	63.4107
C1C2O7C6	-175.523	H16C5C4H15	-53.5851
C4C3C2O7	-56.3558	C5C6O7C2	-61.9779
C4C3C2H11	61.789	H18C6O7C2	59.8374
C4C3C2C1	-178.8616	H19C6O7C2	176.4628
H12C3C2O7	64.3601	O7C6C5C4	56.844
H12C3C2H11	-177.4951	O7C6C5H17	-62.8793
H12C3C2C1	-58.1457	O7C6C5H16	179.9601
H13C3C2O7	-180.4652	H18C6C5C4	-65.1328
H13C3C2H11	-62.3204	H18C6C5H17	175.1439
H13C3C2C1	57.029	H18C6C5H16	57.9833
C5C4C3C2	52.5268	H19C6C5C4	175.4776
C5C4C3H12	-66.7417	H19C6C5H17	55.7543
C5C4C3H13	173.3112	H19C6C5H16	-61.4063
H14C4C3C2	175.2757	O8C1C2O7	178.8906
H14C4C3H12	56.0072	O8C1C2C3	-58.8336
H14C4C3H13	-63.9398	O8C1C2H11	61.7503
H15C4C3C2	-67.1049	H9C1C2O7	53.686
H15C4C3H12	173.6266	H9C1C2C3	175.9619
H15C4C3H13	53.6796	H9C1C2H11	-63.4542
C6C5C4C3	-51.3091	H10C1C2O7	-56.4623
C6C5C4H14	-174.5565	H10C1C2C3	65.8135
C6C5C4H15	68.4477	H10C1C2H11	-173.6026
H17C5C4C3	67.5632		



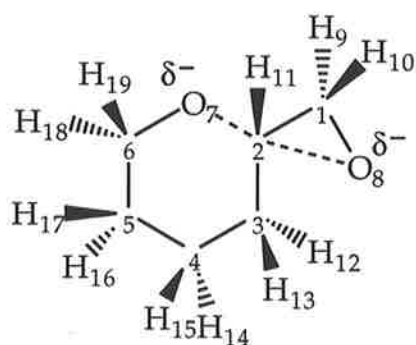
(12)

E = -384.4636616 hartrees  
(-76.7 kJ mol<sup>-1</sup>)

C6C5	1.5259Å	C4C5	1.5325
------	---------	------	--------

C <sub>3</sub> C <sub>4</sub>	1.5312	H <sub>18</sub> C <sub>6</sub> H <sub>19</sub>	107.7634
C <sub>2</sub> C <sub>3</sub>	1.5532	C <sub>6</sub> C <sub>5</sub> H <sub>17</sub>	107.0493
C <sub>1</sub> C <sub>2</sub>	1.5479	C <sub>4</sub> C <sub>5</sub> H <sub>17</sub>	110.4426
O <sub>7</sub> C <sub>6</sub>	1.4203	C <sub>6</sub> C <sub>5</sub> H <sub>16</sub>	108.436
O <sub>7</sub> C <sub>1</sub>	1.4592	C <sub>4</sub> C <sub>5</sub> H <sub>16</sub>	108.5504
O <sub>8</sub> C <sub>2</sub>	1.3634	H <sub>17</sub> C <sub>5</sub> H <sub>16</sub>	106.8208
H <sub>11</sub> C <sub>2</sub>	1.1262	C <sub>5</sub> C <sub>4</sub> H <sub>15</sub>	107.555
H <sub>10</sub> C <sub>1</sub>	1.096	C <sub>3</sub> C <sub>4</sub> H <sub>15</sub>	110.2529
H <sub>9</sub> C <sub>1</sub>	1.0991	C <sub>5</sub> C <sub>4</sub> H <sub>14</sub>	111.2043
H <sub>18</sub> C <sub>6</sub>	1.0991	C <sub>3</sub> C <sub>4</sub> H <sub>14</sub>	108.6581
H <sub>19</sub> C <sub>6</sub>	1.1044	H <sub>15</sub> C <sub>4</sub> H <sub>14</sub>	106.3688
H <sub>17</sub> C <sub>5</sub>	1.1034	C <sub>4</sub> C <sub>3</sub> H <sub>13</sub>	108.8645
H <sub>16</sub> C <sub>5</sub>	1.0998	C <sub>2</sub> C <sup>3</sup> H <sub>13</sub>	110.5948
H <sub>15</sub> C <sub>4</sub>	1.1008	C <sub>4</sub> C <sub>3</sub> H <sub>12</sub>	110.2867
H <sub>14</sub> C <sub>4</sub>	1.0992	C <sub>2</sub> C <sub>3</sub> H <sub>12</sub>	104.4376
H <sub>13</sub> C <sub>3</sub>	1.1039	H <sub>13</sub> C <sub>3</sub> H <sub>12</sub>	107.7418
H <sub>12</sub> C <sub>3</sub>	1.0974	O <sub>7</sub> C <sub>6</sub> C <sub>5</sub> C <sub>4</sub>	-54.0283
C <sub>6</sub> C <sub>5</sub> C <sub>4</sub>	115.2107°	O <sub>7</sub> C <sub>6</sub> C <sub>5</sub> H <sub>17</sub>	-177.2694
C <sub>5</sub> C <sub>4</sub> C <sub>3</sub>	112.6173	O <sub>7</sub> C <sub>6</sub> C <sub>5</sub> H <sub>16</sub>	67.8147
C <sub>4</sub> C <sub>3</sub> C <sub>2</sub>	114.6576	H <sub>18</sub> C <sub>6</sub> C <sub>5</sub> C <sub>4</sub>	-172.883
C <sub>3</sub> C <sub>2</sub> C <sub>1</sub>	110.7298	H <sub>18</sub> C <sub>6</sub> C <sub>5</sub> H <sub>17</sub>	63.8759
C <sub>5</sub> C <sub>6</sub> O <sub>7</sub>	114.7546	H <sub>18</sub> C <sub>6</sub> C <sub>5</sub> H <sub>16</sub>	-51.0399
C <sub>2</sub> C <sub>1</sub> O <sub>7</sub>	117.9504	H <sub>19</sub> C <sub>6</sub> C <sub>5</sub> C <sub>4</sub>	69.1714
C <sub>6</sub> O <sub>7</sub> C <sub>1</sub>	112.2106	H <sub>19</sub> C <sub>6</sub> C <sub>5</sub> H <sub>17</sub>	-54.0697
C <sub>3</sub> C <sub>2</sub> O <sub>8</sub>	113.8202	H <sub>19</sub> C <sub>6</sub> C <sub>5</sub> H <sub>16</sub>	-168.9855
C <sub>1</sub> C <sub>2</sub> O <sub>8</sub>	108.1521	C <sub>3</sub> C <sub>4</sub> C <sub>5</sub> C <sub>6</sub>	67.1262
C <sub>3</sub> C <sub>2</sub> H <sub>11</sub>	104.4754	C <sub>3</sub> C <sub>4</sub> C <sub>5</sub> H <sub>17</sub>	-171.4525
C <sub>1</sub> C <sub>2</sub> H <sub>11</sub>	106.3102	C <sub>3</sub> C <sub>4</sub> C <sub>5</sub> H <sub>16</sub>	-54.6552
O <sub>8</sub> C <sub>2</sub> H <sub>11</sub>	113.1024	H <sub>15</sub> C <sub>4</sub> C <sub>5</sub> C <sub>6</sub>	-171.1974
C <sub>2</sub> C <sub>1</sub> H <sub>10</sub>	109.2836	H <sub>15</sub> C <sub>4</sub> C <sub>5</sub> H <sub>17</sub>	-49.7761
O <sub>8</sub> C <sub>1</sub> H <sub>10</sub>	105.624	H <sub>15</sub> C <sub>4</sub> C <sub>5</sub> H <sub>16</sub>	67.0212
C <sub>2</sub> C <sub>1</sub> H <sub>9</sub>	106.4604	H <sub>14</sub> C <sub>4</sub> C <sub>5</sub> C <sub>6</sub>	-55.1073
O <sub>7</sub> C <sub>1</sub> H <sub>9</sub>	108.9287	H <sub>14</sub> C <sub>4</sub> C <sub>5</sub> H <sub>17</sub>	66.3139
H <sub>10</sub> C <sub>1</sub> H <sub>9</sub>	108.3032	H <sub>14</sub> C <sub>4</sub> C <sub>5</sub> H <sub>16</sub>	-176.8887
C <sub>5</sub> C <sub>6</sub> H <sub>18</sub>	109.5414	C <sub>2</sub> C <sub>3</sub> C <sub>4</sub> C <sub>5</sub>	-88.6739
O <sub>7</sub> C <sub>6</sub> H <sub>18</sub>	105.8393	C <sub>2</sub> C <sub>3</sub> C <sub>4</sub> H <sub>15</sub>	151.1933
C <sub>5</sub> C <sub>6</sub> H <sub>19</sub>	109.4462	C <sub>2</sub> C <sub>3</sub> C <sub>4</sub> H <sub>14</sub>	34.9844
O <sub>7</sub> C <sub>6</sub> H <sub>19</sub>	109.2368	H <sub>13</sub> C <sub>3</sub> C <sub>4</sub> H <sub>15</sub>	35.7889

H <sub>13</sub> C <sub>3</sub> C <sub>4</sub> H <sub>15</sub>	-84.3439	O <sub>7</sub> C <sub>1</sub> C <sub>2</sub> O <sub>8</sub>	159.2496
H <sub>13</sub> C <sub>3</sub> C <sub>4</sub> H <sub>14</sub>	159.4472	O <sub>7</sub> C <sub>1</sub> C <sub>2</sub> H <sub>11</sub>	-79.003
H <sub>12</sub> C <sub>3</sub> C <sub>4</sub> H <sub>14</sub>	153.7988	H <sub>10</sub> C <sub>1</sub> C <sub>2</sub> C <sub>3</sub>	154.477
H <sub>12</sub> C <sub>3</sub> C <sub>4</sub> H <sub>15</sub>	33.6661	H <sub>10</sub> C <sub>1</sub> C <sub>2</sub> O <sub>8</sub>	-80.1763
H <sub>12</sub> C <sub>3</sub> C <sub>4</sub> H <sub>14</sub>	-82.5428	H <sub>10</sub> C <sub>1</sub> C <sub>2</sub> H <sub>11</sub>	41.5711
C <sub>1</sub> C <sub>2</sub> C <sub>3</sub> C <sub>4</sub>	46.3976	H <sub>9</sub> C <sub>1</sub> C <sub>2</sub> C <sub>3</sub>	-88.7598
C <sub>1</sub> C <sub>2</sub> C <sub>3</sub> H <sub>13</sub>	-77.1452	H <sub>9</sub> C <sub>1</sub> C <sub>2</sub> O <sub>8</sub>	36.5869
C <sub>1</sub> C <sub>2</sub> C <sub>3</sub> H <sub>12</sub>	167.2034	H <sub>9</sub> C <sub>1</sub> C <sub>2</sub> H <sub>11</sub>	158.3343
O <sub>8</sub> C <sub>2</sub> C <sub>3</sub> C <sub>4</sub>	-75.6893	C <sub>1</sub> O <sub>7</sub> C <sub>6</sub> C <sub>5</sub>	77.6471
O <sub>8</sub> C <sub>2</sub> C <sub>3</sub> H <sub>13</sub>	160.7679	C <sub>1</sub> O <sub>7</sub> C <sub>6</sub> H <sub>18</sub>	-161.4428
O <sub>8</sub> C <sub>2</sub> C <sub>3</sub> H <sub>12</sub>	45.1165	C <sub>1</sub> O <sub>7</sub> C <sub>6</sub> H <sub>19</sub>	-45.6648
H <sub>11</sub> C <sub>2</sub> C <sub>3</sub> C <sub>4</sub>	160.466	C <sub>6</sub> O <sub>7</sub> C <sub>1</sub> C <sub>2</sub>	-92.6862
H <sub>11</sub> C <sub>2</sub> C <sub>3</sub> H <sub>13</sub>	36.9231	C <sub>6</sub> O <sub>7</sub> C <sub>1</sub> H <sub>10</sub>	144.8625
H <sub>11</sub> C <sub>2</sub> C <sub>3</sub> H <sub>12</sub>	-78.7282	C <sub>6</sub> O <sub>7</sub> C <sub>1</sub> H <sub>9</sub>	28.7177
O <sub>7</sub> C <sub>1</sub> C <sub>2</sub> C <sub>3</sub>	33.9029		



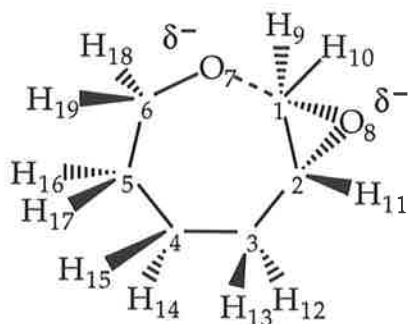
(G)

E = -384.4172435 hartrees  
(+35.0 kJ mol<sup>-1</sup>)

C <sub>2</sub> O <sub>7</sub>	2.0844Å	H <sub>14</sub> C <sub>4</sub>	1.1012
C <sub>2</sub> O <sub>8</sub>	1.7837	H <sub>15</sub> C <sub>4</sub>	1.1015
O <sub>7</sub> C <sub>6</sub>	1.3767	H <sub>12</sub> C <sub>3</sub>	1.0981
C <sub>3</sub> C <sub>2</sub>	1.5068	H <sub>13</sub> C <sub>3</sub>	1.0979
C <sub>4</sub> C <sub>3</sub>	1.5333	H <sub>11</sub> C <sub>2</sub>	1.0837
C <sub>5</sub> C <sub>6</sub>	1.5356	H <sub>19</sub> C <sub>6</sub>	1.1254
C <sub>5</sub> C <sub>4</sub>	1.5282	H <sub>18</sub> C <sub>6</sub>	1.1156
C <sub>1</sub> C <sub>2</sub>	1.445	H <sub>17</sub> C <sub>5</sub>	1.1049
O <sub>8</sub> C <sub>2</sub>	1.7837	H <sub>10</sub> C <sub>1</sub>	1.0977
O <sub>8</sub> C <sub>1</sub>	1.4236	H <sub>9</sub> C <sub>1</sub>	1.0998
H <sub>16</sub> C <sub>5</sub>	1.1	O <sub>7</sub> C <sub>2</sub> O <sub>8</sub>	154.417°

C <sub>2</sub> C <sub>3</sub> C <sub>4</sub>	113.6771	C <sub>4</sub> C <sub>3</sub> C <sub>2</sub> C <sub>1</sub>	-171.1246
O <sub>7</sub> C <sub>6</sub> C <sub>5</sub>	111.6274	C <sub>4</sub> C <sub>3</sub> C <sub>2</sub> O <sub>8</sub>	135.4068
C <sub>3</sub> C <sub>4</sub> C <sub>5</sub>	114.0991	C <sub>4</sub> C <sub>3</sub> C <sub>2</sub> H <sub>11</sub>	24.1046
C <sub>6</sub> C <sub>5</sub> C <sub>4</sub>	111.3707	H <sub>12</sub> C <sub>3</sub> C <sub>2</sub> C <sub>1</sub>	-49.6009
C <sub>3</sub> C <sub>2</sub> C <sub>1</sub>	121.5806	H <sub>12</sub> C <sub>3</sub> C <sub>2</sub> O <sub>8</sub>	-103.0695
C <sub>3</sub> C <sub>2</sub> O <sub>8</sub>	105.5773	H <sub>12</sub> C <sub>3</sub> C <sub>2</sub> H <sub>11</sub>	145.6283
C <sub>1</sub> C <sub>2</sub> O <sub>8</sub>	51.0152	H <sub>13</sub> C <sub>3</sub> C <sub>2</sub> C <sub>1</sub>	67.1967
C <sub>2</sub> C <sub>1</sub> O <sub>8</sub>	76.8937	H <sub>13</sub> C <sub>3</sub> C <sub>2</sub> O <sub>8</sub>	13.7281
C <sub>2</sub> O <sub>8</sub> C <sub>1</sub>	52.0911	H <sub>13</sub> C <sub>3</sub> C <sub>2</sub> H <sub>11</sub>	-97.574
C <sub>6</sub> C <sub>5</sub> H <sub>16</sub>	107.6511	C <sub>5</sub> C <sub>4</sub> C <sub>3</sub> C <sub>2</sub>	68.2822
C <sub>4</sub> C <sub>5</sub> H <sub>16</sub>	109.3091	C <sub>5</sub> C <sub>4</sub> C <sub>3</sub> H <sub>12</sub>	-52.6709
C <sub>3</sub> C <sub>4</sub> H <sub>14</sub>	108.5329	C <sub>5</sub> C <sub>4</sub> C <sub>3</sub> H <sub>13</sub>	-170.4649
C <sub>5</sub> C <sub>4</sub> H <sub>14</sub>	109.7431	H <sub>14</sub> C <sub>4</sub> C <sub>3</sub> C <sub>2</sub>	-169.0172
C <sub>3</sub> C <sub>4</sub> H <sub>15</sub>	108.6831	H <sub>14</sub> C <sub>4</sub> C <sub>3</sub> H <sub>12</sub>	70.0297
C <sub>5</sub> C <sub>4</sub> H <sub>15</sub>	109.2837	H <sub>14</sub> C <sub>4</sub> C <sub>3</sub> H <sub>13</sub>	-47.7644
H <sub>14</sub> C <sub>4</sub> H <sub>15</sub>	106.1951	H <sub>15</sub> C <sub>4</sub> C <sub>3</sub> C <sub>2</sub>	-53.937
C <sub>2</sub> C <sub>3</sub> H <sub>12</sub>	108.2093	H <sub>15</sub> C <sub>4</sub> C <sub>3</sub> H <sub>12</sub>	-174.8901
C <sub>4</sub> C <sub>3</sub> H <sub>12</sub>	109.2305	H <sub>15</sub> C <sub>4</sub> C <sub>3</sub> H <sub>13</sub>	67.3159
C <sub>2</sub> C <sub>3</sub> H <sub>13</sub>	108.4515	C <sub>4</sub> C <sub>5</sub> C <sub>6</sub> O <sub>7</sub>	59.2537
C <sub>4</sub> C <sub>3</sub> H <sub>13</sub>	109.2155	C <sub>4</sub> C <sub>5</sub> C <sub>6</sub> H <sub>19</sub>	-64.2726
H <sub>12</sub> C <sub>3</sub> H <sub>13</sub>	107.8992	C <sub>4</sub> C <sub>5</sub> C <sub>6</sub> H <sub>18</sub>	183.3903
C <sub>3</sub> C <sub>2</sub> H <sub>11</sub>	119.8153	H <sub>16</sub> C <sub>5</sub> C <sub>6</sub> O <sub>7</sub>	-60.5569
C <sub>1</sub> C <sub>2</sub> H <sub>11</sub>	116.9233	H <sub>16</sub> C <sub>5</sub> C <sub>6</sub> H <sub>19</sub>	175.9167
O <sub>8</sub> C <sub>2</sub> H <sub>11</sub>	99.7938	H <sub>16</sub> C <sub>5</sub> C <sub>6</sub> H <sub>18</sub>	63.5797
O <sub>7</sub> C <sub>6</sub> H <sub>19</sub>	112.734	H <sub>17</sub> C <sub>5</sub> C <sub>6</sub> O <sub>7</sub>	181.8515
C <sub>5</sub> C <sub>6</sub> H <sub>19</sub>	106.6331	H <sub>17</sub> C <sub>5</sub> C <sub>6</sub> H <sub>19</sub>	58.3251
O <sub>7</sub> C <sub>6</sub> H <sub>18</sub>	112.3639	H <sub>17</sub> C <sub>5</sub> C <sub>6</sub> H <sub>18</sub>	-54.0119
C <sub>5</sub> C <sub>6</sub> H <sub>18</sub>	108.1655	C <sub>6</sub> C <sub>5</sub> C <sub>4</sub> C <sub>3</sub>	-52.82
H <sub>19</sub> C <sub>6</sub> H <sub>18</sub>	104.8661	C <sub>6</sub> C <sub>5</sub> C <sub>4</sub> H <sub>14</sub>	-174.858
C <sub>6</sub> C <sub>5</sub> H <sub>17</sub>	110.9187	C <sub>6</sub> C <sub>5</sub> C <sub>4</sub> H <sub>15</sub>	69.0692
C <sub>4</sub> C <sub>5</sub> H <sub>17</sub>	109.7868	H <sub>16</sub> C <sub>5</sub> C <sub>4</sub> C <sub>3</sub>	66.0038
H <sub>16</sub> C <sub>5</sub> H <sub>17</sub>	107.6984	H <sub>16</sub> C <sub>5</sub> C <sub>4</sub> H <sub>14</sub>	-56.0341
C <sub>2</sub> C <sub>1</sub> H <sub>10</sub>	117.1838	H <sub>16</sub> C <sub>5</sub> C <sub>4</sub> H <sub>15</sub>	-172.1069
O <sub>8</sub> C <sub>1</sub> H <sub>10</sub>	116.1951	H <sub>17</sub> C <sub>5</sub> C <sub>4</sub> C <sub>3</sub>	183.9337
C <sub>2</sub> C <sub>1</sub> H <sub>9</sub>	116.4212	H <sub>17</sub> C <sub>5</sub> C <sub>4</sub> H <sub>14</sub>	61.8957
O <sub>8</sub> C <sub>1</sub> H <sub>9</sub>	115.3504	H <sub>17</sub> C <sub>5</sub> C <sub>4</sub> H <sub>15</sub>	-54.1771
H <sub>10</sub> C <sub>1</sub> H <sub>9</sub>	111.1091	O <sub>8</sub> C <sub>1</sub> C <sub>2</sub> C <sub>3</sub>	-84.7209
O <sub>8</sub> C <sub>1</sub> C <sub>2</sub> O <sub>7</sub>	172.933	O <sub>8</sub> C <sub>1</sub> C <sub>2</sub> H <sub>11</sub>	80.469

H <sub>10</sub> C <sub>1</sub> C <sub>2</sub> C <sub>3</sub>	162.3282	H <sub>9</sub> C <sub>1</sub> C <sub>2</sub> H <sub>11</sub>	-167.4946
H <sub>10</sub> C <sub>1</sub> C <sub>2</sub> O <sub>8</sub>	-112.9509	C <sub>1</sub> O <sub>8</sub> C <sub>2</sub> C <sub>3</sub>	118.2807
H <sub>10</sub> C <sub>1</sub> C <sub>2</sub> H <sub>11</sub>	-32.4819	C <sub>1</sub> O <sub>8</sub> C <sub>2</sub> H <sub>11</sub>	-116.835
H <sub>9</sub> C <sub>1</sub> C <sub>2</sub> C <sub>3</sub>	27.3155	C <sub>2</sub> O <sub>8</sub> C <sub>1</sub> H <sub>10</sub>	114.0928
H <sub>9</sub> C <sub>1</sub> C <sub>2</sub> O <sub>8</sub>	112.0364	C <sub>2</sub> O <sub>8</sub> C <sub>1</sub> H <sub>9</sub>	-113.2811



(H)

E = -384.2565604 hartrees  
(+39.7 kJ mol<sup>-1</sup>)

C <sub>1</sub> O <sub>7</sub>	2.07514Å	C <sub>5</sub> C <sub>4</sub> C <sub>3</sub>	115.3355
C <sub>1</sub> O <sub>8</sub>	1.7467	C <sub>4</sub> C <sub>3</sub> C <sub>2</sub>	116.5452
C <sub>4</sub> C <sub>5</sub>	1.538	C <sub>3</sub> C <sub>2</sub> O <sub>8</sub>	118.18
C <sub>3</sub> C <sub>4</sub>	1.5326	C <sub>4</sub> C <sub>5</sub> C <sub>6</sub>	117.2212
C <sub>2</sub> C <sub>3</sub>	1.5199	C <sub>5</sub> C <sub>6</sub> O <sub>7</sub>	115.633
O <sub>8</sub> C <sub>2</sub>	1.4283	C <sub>3</sub> C <sub>2</sub> C <sub>1</sub>	121.0486
C <sub>6</sub> C <sub>5</sub>	1.5445	O <sub>8</sub> C <sub>2</sub> C <sub>1</sub>	74.9274
O <sub>7</sub> C <sub>6</sub>	1.3741	C <sub>2</sub> O <sub>8</sub> C <sub>1</sub>	52.9226
C <sub>1</sub> C <sub>2</sub>	1.4432	C <sub>2</sub> C <sub>1</sub> O <sub>8</sub>	52.15
H <sub>11</sub> C <sub>2</sub>	1.1005	C <sub>3</sub> C <sub>2</sub> H <sub>11</sub>	110.907
H <sub>10</sub> C <sub>1</sub>	1.0808	O <sub>8</sub> C <sub>2</sub> H <sub>11</sub>	112.63
H <sub>9</sub> C <sub>1</sub>	1.079	C <sub>1</sub> C <sub>2</sub> H <sub>11</sub>	114.8511
H <sub>19</sub> C <sub>6</sub>	1.1161	C <sub>2</sub> C <sub>1</sub> H <sub>10</sub>	119.5018
H <sub>18</sub> C <sub>6</sub>	1.1268	O <sub>8</sub> C <sub>1</sub> H <sub>10</sub>	106.4122
H <sub>16</sub> C <sub>5</sub>	1.1054	C <sub>2</sub> C <sub>1</sub> H <sub>9</sub>	120.292
H <sub>17</sub> C <sub>5</sub>	1.1009	O <sub>8</sub> C <sub>1</sub> H <sub>9</sub>	99.7434
H <sub>15</sub> C <sub>4</sub>	1.1017	H <sub>10</sub> C <sub>1</sub> H <sub>9</sub>	118.8374
H <sub>14</sub> C <sub>4</sub>	1.0993	C <sub>5</sub> C <sub>6</sub> H <sub>19</sub>	105.9562
H <sub>13</sub> C <sub>3</sub>	1.1003	O <sub>7</sub> C <sub>6</sub> H <sub>19</sub>	111.7304
H <sub>12</sub> C <sub>3</sub>	1.1012	C <sub>5</sub> C <sub>6</sub> H <sub>18</sub>	105.5372
O <sub>7</sub> C <sub>1</sub> O <sub>8</sub>	156.379°	O <sub>7</sub> C <sub>6</sub> H <sub>18</sub>	112.6873



H <sub>19</sub> C <sub>6</sub> H <sub>18</sub>	104.412	C <sub>1</sub> C <sub>2</sub> C <sub>3</sub> C <sub>4</sub>	10.9406
C <sub>4</sub> C <sub>5</sub> H <sub>16</sub>	108.0433	C <sub>1</sub> C <sub>2</sub> C <sub>3</sub> H <sub>13</sub>	-110.9915
C <sub>6</sub> C <sub>5</sub> H <sub>16</sub>	107.4124	C <sub>1</sub> C <sub>2</sub> C <sub>3</sub> H <sub>12</sub>	134.1678
C <sub>4</sub> C <sub>5</sub> H <sub>17</sub>	108.8311	H <sub>11</sub> C <sub>2</sub> C <sub>3</sub> C <sub>4</sub>	149.9736
C <sub>6</sub> C <sub>5</sub> H <sub>17</sub>	107.7783	H <sub>11</sub> C <sub>2</sub> C <sub>3</sub> H <sub>13</sub>	28.0415
H <sub>16</sub> C <sub>5</sub> H <sub>17</sub>	107.1342	H <sub>11</sub> C <sub>2</sub> C <sub>3</sub> H <sub>12</sub>	-86.7992
C <sub>5</sub> C <sub>4</sub> H <sub>15</sub>	107.8648	C <sub>1</sub> O <sub>8</sub> C <sub>2</sub> C <sub>3</sub>	117.4961
C <sub>3</sub> C <sub>4</sub> H <sub>15</sub>	107.4673	C <sub>1</sub> O <sub>8</sub> C <sub>2</sub> H <sub>11</sub>	-111.0555
C <sub>5</sub> C <sub>4</sub> H <sub>14</sub>	110.1613	O <sub>7</sub> C <sub>6</sub> C <sub>5</sub> C <sub>4</sub>	-65.203
C <sub>3</sub> C <sub>4</sub> H <sub>14</sub>	109.7277	O <sub>7</sub> C <sub>6</sub> C <sub>5</sub> H <sub>16</sub>	173.0369
H <sub>15</sub> C <sub>4</sub> H <sub>14</sub>	105.8011	O <sub>7</sub> C <sub>6</sub> C <sub>5</sub> H <sub>17</sub>	57.8986
C <sub>4</sub> C <sub>3</sub> H <sub>13</sub>	108.0288	H <sub>19</sub> C <sub>6</sub> C <sub>5</sub> C <sub>4</sub>	170.4432
C <sub>2</sub> C <sub>3</sub> H <sub>13</sub>	108.2408	H <sub>19</sub> C <sub>6</sub> C <sub>5</sub> H <sub>16</sub>	48.6831
C <sub>4</sub> C <sub>3</sub> H <sub>12</sub>	110.0046	H <sub>19</sub> C <sub>6</sub> C <sub>5</sub> H <sub>17</sub>	-66.4552
C <sub>2</sub> C <sup>3</sup> H <sub>12</sub>	106.5995	H <sub>18</sub> C <sub>6</sub> C <sub>5</sub> C <sub>4</sub>	60.0673
H <sub>13</sub> C <sub>3</sub> H <sub>12</sub>	107.0339	H <sub>18</sub> C <sub>6</sub> C <sub>5</sub> H <sub>16</sub>	-61.6928
O <sub>7</sub> C <sub>1</sub> C <sub>2</sub> O <sub>8</sub>	172.251	H <sub>18</sub> C <sub>6</sub> C <sub>5</sub> H <sub>17</sub>	-176.8311
C <sub>3</sub> C <sub>4</sub> C <sub>5</sub> C <sub>6</sub>	75.8743	O <sub>8</sub> C <sub>1</sub> C <sub>2</sub> C <sub>3</sub>	-114.1249
C <sub>3</sub> C <sub>4</sub> C <sub>5</sub> H <sub>16</sub>	-162.6935	O <sub>8</sub> C <sub>1</sub> C <sub>2</sub> H <sub>11</sub>	108.326
C <sub>3</sub> C <sub>4</sub> C <sub>5</sub> H <sub>17</sub>	-46.6876	H <sub>10</sub> C <sub>1</sub> C <sub>2</sub> C <sub>3</sub>	157.5111
H <sub>15</sub> C <sub>4</sub> C <sub>5</sub> C <sub>6</sub>	-164.0245	H <sub>10</sub> C <sub>1</sub> C <sub>2</sub> O <sub>8</sub>	-88.364
H <sub>15</sub> C <sub>4</sub> C <sub>5</sub> H <sub>16</sub>	-42.5923	H <sub>10</sub> C <sub>1</sub> C <sub>2</sub> H <sub>11</sub>	19.962
H <sub>15</sub> C <sub>4</sub> C <sub>5</sub> H <sub>17</sub>	73.4137	H <sub>9</sub> C <sub>1</sub> C <sub>2</sub> C <sub>3</sub>	-35.997
H <sub>14</sub> C <sub>4</sub> C <sub>5</sub> C <sub>6</sub>	-48.9935	H <sub>9</sub> C <sub>1</sub> C <sub>2</sub> O <sub>8</sub>	78.1279
H <sub>14</sub> C <sub>4</sub> C <sub>5</sub> H <sub>16</sub>	72.4388	H <sub>9</sub> C <sub>1</sub> C <sub>2</sub> H <sub>11</sub>	-173.5461
H <sub>14</sub> C <sub>4</sub> C <sub>5</sub> H <sub>17</sub>	-171.5553	H <sub>10</sub> C <sub>1</sub> O <sub>8</sub> C <sub>2</sub>	114.9142
C <sub>2</sub> C <sub>3</sub> C <sub>4</sub> C <sub>5</sub>	-77.484	H <sub>9</sub> C <sub>1</sub> O <sub>8</sub> C <sub>2</sub>	-120.9782
C <sub>2</sub> C <sub>3</sub> C <sub>4</sub> H <sub>15</sub>	162.1974		
C <sub>2</sub> C <sub>3</sub> C <sub>4</sub> H <sub>14</sub>	47.6087		
H <sub>13</sub> C <sub>3</sub> C <sub>4</sub> C <sub>5</sub>	44.5593		
H <sub>13</sub> C <sub>3</sub> C <sub>4</sub> H <sub>15</sub>	-75.7594		
H <sub>13</sub> C <sub>3</sub> C <sub>4</sub> H <sub>14</sub>	169.6519		
H <sub>12</sub> C <sub>3</sub> C <sub>4</sub> C <sub>5</sub>	161.0682		
H <sub>12</sub> C <sub>3</sub> C <sub>4</sub> H <sub>15</sub>	40.7496		
H <sub>12</sub> C <sub>3</sub> C <sub>4</sub> H <sub>14</sub>	-73.8391		
O <sub>8</sub> C <sub>2</sub> C <sub>3</sub> C <sub>4</sub>	-77.8092		
O <sub>8</sub> C <sub>2</sub> C <sub>3</sub> H <sub>13</sub>	160.2586		
O <sub>8</sub> C <sub>2</sub> C <sub>3</sub> H <sub>12</sub>	45.4179		

## Appendix D

Harmonic vibrational frequencies [ $hf/6-31+G(d)$ ] of the competing transition states from System 4.1 (Table 4.14, page 148).

TS forming 3 membered ring $\nu$ (cm <sup>-1</sup> )	TS forming 4 membered ring $\nu$ (cm <sup>-1</sup> )
238.1683	247.6448
291.5725	356.3894
338.4092	496.2033
442.3735	624.089
956.4544	786.0414
984.0787	968.0274
1094.8481	994.9663
1186.7729	1137.3038
1210.3706	1173.0644
1253.9235	1211.3019
1256.7998	1254.8283
1339.0495	1286.8973
1352.166	1345.7891
1427.4524	1417.8896
1458.5443	1450.075
1565.599	1505.5309
1683.1828	1634.6148
1687.1988	1654.8612
3083.7249	2998.0877
3086.9203	3029.2264
3100.2848	3077.5531
3114.5341	3351.8231
3470.5805	3520.4099

## Appendix E

Harmonic vibrational frequencies [hf/6-31+G(d)] of the competing transition states from System 4.2 (Table 4.14, page 148).

TS forming 4 membered ring $\nu$ (cm <sup>-1</sup> )	TS forming 5 membered ring $\nu$ (cm <sup>-1</sup> )
122.2899	205.8544
235.2298	273.9004
266.6923	334.1038
317.4729	489.4422
435.7578	500.408
647.7909	603.7499
883.6261	884.1782
989.664	930.3798
1012.3455	966.5513
1038.4286	1018.6981
1126.5694	1050.7643
1182.1946	1145.0813
1221.8755	1175.3681
1247.6603	1224.1225
1277.3496	1260.3284
1319.9074	1306.445
1326.8818	1330.0707
1354.1884	1348.7898
1407.2254	1416.5173
1441.704	1443.4315
1498.4453	1500.3753
1566.2495	1546.5688
1634.0958	1626.0985
1670.1974	1651.7434
1687.4549	1657.3263
2951.4459	2920.2208
3006.0097	2979.1006
3117.4382	3118.3729
3134.2758	3155.4068
3201.0636	3189.6122
3239.7512	3415.3166
3468.8057	3551.9066

## Appendix F

Harmonic vibrational frequencies [ $hf/6-31+G(d)$ ] of the competing transition states from System 4.3 (Table 4.14, page 148).

TS forming 5 membered ring $\nu$ ( $\text{cm}^{-1}$ )	TS forming 6 membered ring $\nu$ ( $\text{cm}^{-1}$ )
157.437	96.8503
248.9617	218.6748
328.6974	259.2397
349.0703	293.1267
368.2671	318.8512
456.6176	437.773
474.7492	466.3916
576.9262	595.4249
851.9635	904.8141
907.2457	939.6597
957.8098	968.7445
1020.9847	993.959
1027.1873	1050.7703
1088.694	1095.7603
1098.9146	1139.4047
1142.056	1184.6318
1215.2838	1241.5412
1251.3729	1241.7007
1261.6875	1280.2103
1306.8693	1316.6557
1334.2357	1339.504
1351.2783	1345.4006
1388.4798	1377.3043
1420.5572	1416.608
1474.7671	1462.241
1485.8614	1483.9876
1528.1011	1516.9297
1552.6904	1580.119
1611.453	1616.8304
1631.6319	1633.5746
1643.413	1655.9089
1658.3677	1694.1428
2869.8021	2898.9173
2959.1501	2959.6052
3117.2053	3138.95
3138.4509	3142.7375
3154.7416	3167.9556
3163.7017	3175.4567
3194.9892	3206.0572
3432.0823	3246.3859
3552.7109	3487.5424

## Appendix G

Harmonic vibrational frequencies [hf/6-31+G(d)] of the competing transition states from System 4.4 (Table 4.14, page 148).

TS forming 6 membered ring $\nu$ (cm <sup>-1</sup> )	TS forming 7 membered ring $\nu$ (cm <sup>-1</sup> )
66.1078	141.4382
182.7473	214.5084
211.4131	237.55
291.684	258.6153
296.339	347.9687
335.8924	353.3443
354.5923	405.2012
407.5301	454.4485
494.0256	528.29
565.6386	610.1535
851.2685	792.1728
904.633	856.9756
922.6417	923.4059
985.5192	943.8285
1019.7469	1033.3008
1051.5519	1062.3587
1093.7621	1094.6923
1128.7435	1116.7297
1159.5618	1155.4843
1192.8497	1177.2478
1239.6402	1230.9708
1263.1688	1252.6821
1277.6613	1285.6387
1312.8955	1309.2626
1333.3107	1329.7282
1348.3901	1352.9018
1386.5768	1377.2706
1393.9629	1405.4095
1417.8369	1426.3761
1473.6993	1473.6352
1496.8531	1507.0943
1510.0437	1513.4116
1535.4851	1551.0958
1590.8701	1556.1139
1611.9505	1614.9174
1621.4804	1630.0017
1631.9781	1636.9131
1647.3944	1648.7812
1695.7221	1659.5831
2859.1602	2881.819
2948.9933	2958.0136
3113.9301	3105.7725
3149.7551	3128.8472
3150.7705	3136.9937
3154.9978	3154.1879
3175.9895	3170.4498
3189.9274	3204.2468
3218.2163	3217.9483
3255.8966	3433.8945
3478.1966	3557.6639

comment (3) page 26: line 1. An examiner has stated: caution should be used when talking about *ab initio* calculations being used to determine reaction probabilities. The actual structure and the energy of the transition states can often not be enough (as the candidate knows from his chapter 4). Further information on the dynamics may be required. I think it would be useful for the candidate to briefly discuss transition state theory in the introduction.

Papers referred to: *J. Chem. Soc. Faraday Trans.*, 1994, 90, 1715.

*J. Am. Chem. Soc.*, 1994, 116, 9644.

The determination of reaction probabilities by *ab initio* methods using transition state theory may not be completely accurate. Transition state theory supposes that as reactants approach each other closely they are momentarily in a less stable state than either the reactants or the products. In this less stable state the atoms rearrange themselves, original bonds are weakened and new bonds are partially formed. The potential energy of the system increases at this point because the approaching reactant molecules must overcome the initial repulsive forces between the outer shell electrons of their constituent atoms, and the atoms must be separated from each other as bonds are broken. This increase in potential energy corresponds to an energy barrier over which the reactant molecules must pass if the reaction is to proceed. The arrangement of atoms at the maximum of the energy barrier is called the transition state and is a transitory intermediate state between reactant and product. The transition state is an unstable transitory combination of reactant molecules which may either go on to form products or fall apart to return to the unchanged reactants.

When determining reaction probabilities, calculating the potential energies of the transition state, the reactant and the product can often not be enough, and further information on the dynamics may be required.<sup>1</sup> Dynamics calculations and potential energy surfaces may be calculated economically using semiempirical electronic structure calculations, however, in many situations semiempirical methods alone cannot provide satisfactory accuracy for quantitative dynamics calculations. Better accuracy can be achieved by using high-level *ab initio* calculations, but this is usually too expensive to calculate enough important features of a poly-atomic potential energy surface.

Truhlar<sup>2</sup> has provided a practical method to include important dynamical effects in rate calculations with a minimal number of electronic structure calculations, thereby allowing as high as possible a level of theory to be used. Truhlar has carried out high-level *ab initio* calculations at a few points (including the reactants, saddle point and products) along the reaction path and also semiempirical molecular orbital calculations for a much greater number of points. The semiempirical values can then be corrected at the selected points high-level *ab initio* calculations have been carried out. This method allows for dynamics calculations of organic systems with semiempirical potential energy surfaces to overall be more accurate.<sup>2</sup>

## REFERENCES

1. H. Wang, G.H. Peslherbe, W.L. Hase, *J. Am. Chem. Soc.*, 1994, **116**, 9644.
2. W. Hu, Y. Liu, D.G. Truhlar, *J. Chem. Faraday Trans.*, 1994, **90**(12), 1715, and references cited therein.

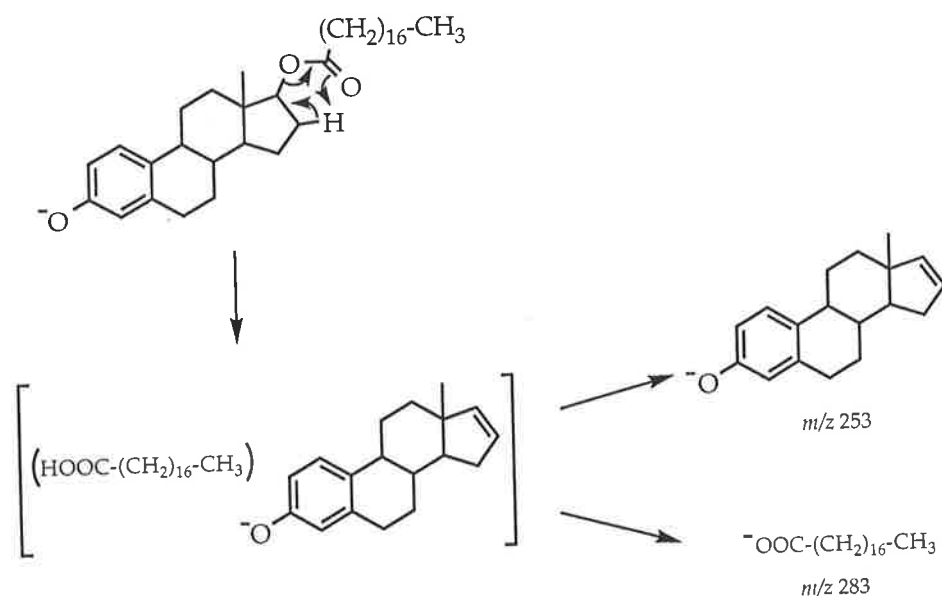
comment (7) page 56: An examiner has stated: the candidate should reference some work by Tabet, who postulated one of the first long range anion migrations within an ion neutral complex derived from CID of the  $[M-H]^-$  ions of 17  $\beta$ -estradiol-17-stearate ester.

Paper referred to: *Rapid Commun. Mass Spectrom.*, 1991, 5, 44.

To be included on page 34 after scheme 1.8 and before the closing paragraph of the introduction.

Tabet has studied the fragmentations of the  $[M-H]^-$  ions of 17- $\beta$ -estradiol-17-long chain esters.<sup>1</sup> The NICI-ND<sub>3</sub> spectra of 17- $\beta$ -estradiol-17-stearate ester afforded both  $[M-D]^-$  and  $[M-H]^-$  ions corresponding to deprotonation at the phenol and enol positions, respectively. The CID spectra of each deprotonated species was characteristic of the anion. Both parent anions, however, showed formation of daughter ions  $m/z$  253 and 283. Tabet has proposed that the formation of these daughter ions from the phenol anion occurs *via* a long-range proton transfer within the ion/neutral complex following charge remote fragmentation (scheme 1.9).

Scheme 1.9



## REFERENCES

1. F. Fournier, J.C. Tabet, L. Debrauwer, D. Rao, A. Paris, G. Bories, *Rapid Commun. Mass Spectrom.*, 1991, 5, 44.



Comment (15) page 154. An examiner has stated: I would like to see an appendix which gives a specific example (e.g. transition state A) of how  $Q_{vib}$  is calculated.

## Appendix H

Calculation of the harmonic vibrational partition function of transition state A.

$$Q_{vib} = \prod_{n=1}^{3n-(6+1)} \frac{1}{\left(1 - \exp\left(\frac{-h\lambda v_n}{k_B T}\right)\right)} \quad \text{Equation 4.4}$$

1st vibrational frequency is 238.1683 (Appendix D, page 224)

Using equation 4.4 for  $v = 238.1683$  gives:

$$Q_{vib} = \frac{1}{\left(1 - \exp\left(\frac{-(6.626 \times 10^{-34} \text{ Js})(0.9131)(238.1683 \text{ cm}^{-1})(2.9979 \times 10^{18} \text{ ms}^{-1})}{(1.38066 \times 10^{-23} \text{ JK}^{-1})(298 \text{ K})}\right)\right)} = 1.54$$

Repeating this for each vibrational frequency of transition state A (Appendix D, page 224) affords  $Q_{vib}$  values shown below (including  $Q_{vib}$  for 238.1683 calculated above).

<u>frequency</u>	<u><math>Q_{vib}</math></u>
238.1683	1.54
291.5725	1.38
338.4092	1.29
442.3735	1.17
956.4544	1.01
984.0787	1.01
1094.848	1.01
1186.773	1.01

1210.371	1.00
1253.924	1.00
1256.8	1.00
1339.05	1.00
1352.166	1.00
1427.452	1.00
1458.544	1.00
1565.599	1.00
1683.183	1.00
1687.199	1.00
3083.743	1.00
3086.92	1.00
3100.285	1.00
3114.534	1.00
3470.581	1.00

Multiplying the  $Q_{vib}$  results for transition state A affords the harmonic vibrational partition function of transition state A and equates to 3.414, as shown in table 4.15 (pg 154).

# References

- (1) J.H. Bowie, *Mass Spectrom. Rev.*, 1984, **3**, 161.
- (2) H. Budzikiewicz, *Mass Spectrom. Rev.*, 1986, **5**, 345.
- (3) C. Brunnée, *Int. J. Mass Spectrom. Ion. Proc.*, 1987, **76**, 125.
- (4) K.R. Jennings, Specialist Periodical Report, "Mass Spectrometry", Chemical Society London. 1977, **14**, 211.
- (5) A.G. Harrison in "*Chemical Ionisation Mass Spectrometry*"; CRC Press: Boca Raton, 1983, Chapt. 2.
- (6) J.E. Bartmess, *Mass Spectrom. Rev.*, 1989, **8**, 297.
- (7) D.J. Surma and J.C. Vickerman, *J. Chem. Soc. Chem. Comm.*, 1981, 342.
- (8) J.H. Zoeller, R.A. Zingaro and R.D. Macfarlane, *Int. J. Mass Spectrom. Ion. Proc.*, 1987, **77**, 21.
- (9) I. Matsumoto, *Japan. J. Toxicol. Environ. Health*, 1993, **39**, 266.
- (10) M.J. Raftery Ph.D. Thesis, University of Adelaide, 1988.
- (11) J.H. Bowie, *Mass Spectrom. Rev.*, 1990, **9**, 349.

- (12) J.H. Bowie in *"Experimental Mass Spectrometry"*; Plenum Press: New York, 1994, Chapt. 1.
- (13) H.S.W. Massey in *"Negative Ions"*; 3rd ed.; Cambridge University Press: Cambridge, 1976, Chapt. 8.
- (14) M.R. Litzow and T.R. Spalding in *"Mass Spectrometry of Inorganic and Organometallic Compounds"*; Elsevier: Amsterdam, 1973, Chapt. 1.
- (15) C.E. Melton: *"Negative Ion Mass Spectra"* in *"Mass Spectrometry of Organic Ions"*; (F.W. McLafferty ed.); Academic: New York, 1963, Chapt. 2.
- (16) J.G. Dillard, *Chem. Rev.*, 1973, **73**, 589.
- (17) L.G. Christophorou and S.R. Hunter in *"Swarms of Ions and Electrons in Gases"*; Springer-Verlag: Vienna, 1984, Chapt. 4.
- (18) C.H. DePuy, J.J. Grabowski and V.M. Bierbaum, *Science*, 1982, **218**, 955.
- (19) M.E. Rose and R.A.W. Johnstone in *"Mass Spectrometry for Chemists and Biochemists"*; Cambridge University Press: Cambridge, 1982; Chapt. 7.
- (20) I.H. Bowie, *Adv. Mass. Spectrom.*, 1986, **10A**, 553.
- (21) J.B. Westmore and M.M. Alauddin, *Mass Spectrom. Rev.*, 1986, **5**, 381.
- (22) G.B. Ellison, P.C. Engelking and W.C. Lineberger, *J. Phys. Chem.*, 1982, **86**, 4873.

- (23) P.A. Schultz, R.D. Mead, P.L. Jones and W.C. Lineberger, *J. Chem. Phys.*, 1982, **77**, 1153.
- (24) G. Caldwell and P. Kebarle, *J. Chem. Phys.*, 1984, **80**, 577.
- (25) J.J. Grabowski, J.M. Van Doren, C.H. DePuy and V.M. Bierbaum, *J. Chem. Phys.*, 1984, **80**, 575.
- (26) S.A. Sullivan, C.H. DePuy and R. Damrauer, *J. Am. Chem. Soc.*, 1981, **103**, 480.
- (27) D.J. Hajdasz and R.R. Squires, *J. Am. Chem. Soc.*, 1986, **108**, 3139.
- (28) J.C. Kleingeld and N.M.M. Nibbering, *Int. J. Mass. Spectrom. Ion Phys.*, 1983, **49**, 311.
- (29) C.H. DePuy, R. Damrauer, J.H. Bowie and J.C. Sheldon, *Acc. Chem. Res.*, 1987, **20**, 127.
- (30) C.H. DePuy, V.M. Bierbaum, R. Damrauer and J.A. Soderquist, *J. Am. Chem. Soc.*, 1985, **107**, 3385.
- (31) M.E. Rose and R.A.W. Johnstone in *"Mass spectrometry for chemists and biochemists"*; Cambridge University Press: Cambridge, 1982; Chapt. 2.
- (32) H. Hintenberger and L.A. Konig in *"Advances in Mass Spectrometry"*; Pergamon Press: New York, 1959.

- (33) T. Ast, M.H. Bozorgzadeh, J.L. Wiebers, J.H. Beynon and A.G. Brenton, *Org. Mass Spectrom.*, 1979, **14**, 313.
- (34) M.J. Lacey, C.G. Macdonald, K.F. Donchi and P.J. Derrick, *Org. Mass Spectrom.*, 1981, **16**, 351.
- (35) C.J. Porter, J.H. Beynon and T. Ast, *Org. Mass Spectrom.*, 1981, **16**, 101.
- (36) J.H. Beynon and R.G. Cooks, *Int. J. Mass. Spectrom. Ion Phys.*, 1976, **19**, 107.
- (37) J.H. Beynon, R.G. Cooks, J.W. Amy, W.E. Baitinger and T.Y. Ridley, *Anal. Chem.*, 1973, **45**, 1973.
- (38) K.R. Jennings in "*Scanning Methods for Double-Focussing Mass Spectrometers*"; D. Reidel Publishing Co.: Dordrecht, 1984, pp 7-21.
- (39) D.S. Millington and J. Smith, *Org. Mass Spectrom.*, 1977, **12**, 264.
- (40) V.H. Wysocki, H.I. Kenttämäa and R.G. Cooks, *Int. J. Mass Spectrom. Ion Proc.*, 1987, **75**, 181.
- (41) U.P. Schlünegger in "*Advanced Mass Spectrometry*"; first ed.; Pergamon Press: Oxford, 1980, Chapt. 2.
- (42) J.A. Nystrom, M.M. Bursey and J.R. Hass, *Int. J. Mass Spectrom. Ion Proc.*, 1984, **55**, 263.
- (43) J.H. Bowie and T. Blumenthal, *J. Am. Chem. Soc.*, 1975, **97**, 2959.

- (44) M.M. Bursey, D.J. Harvan, C.E. Parker, T.A. Darden and J.R. Haas, *Org. Mass Spectrom.*, 1983, **18**, 530.
- (45) R.D. Bowen and D.H. Williams in "*Gas Phase Ion Rearrangements*"; Academic Press: New York, 1980; Vol. 1, p 55.
- (46) M.S. Kim and F.W. McLafferty, *J. Am. Chem. Soc.*, 1978, **100**, 3279.
- (47) J.L. Holmes, *Org. Mass Spectrom.*, 1985, **20**, 169.
- (48) D.T. Terwilliger, J.H. Beynon and R.G. Cooks, *Proc. Roy. Soc., Ser A*, 1974, **341**, 135.
- (49) J.L. Holmes and A.D. Osborne, *Int. J. Mass Spectrom. Ion Phys.*, 1977, **23**, 189
- (50) P.W. Atkins in "*Molecular Quantum Mechanics*"; Oxford University Press: Oxford, 1983, Chapt. 2.
- (51) M.J. Frisch, G.W. Trucks, H.B. Schlegel, P.M.W. Gill, B.G. Johnson, M.A. Robb, J.R. Cheeseman, T. Keith, G.A. Petersson, J.A. Montgomery, K. Raghavachari, M.A. Al-Latham, V.G. Zakrzewski, J.V. Ortiz, J.B. Foresman, J. Cioslowski, B.B. Stefanov, A. Nanayakkara, M. Challacombe, C.Y. Peng, P.Y. Ayala, W. Chen, M.W. Wong, J.L. Andres, E.S. Replogle, R. Gomperts, R.L. Martin, D.J. Fox, J.S. Binkley, D.J. Defrees, J. Baker, J.P. Stewart, M. Head-Gordon, C. Gonzalez and J.A. Pople in "*Gaussian 94, Revision C.3*"; Gaussian, Inc., Pittsburg PA: 1995.

- (52) C. Gonzalez and H.B. Schlegel, *J. Chem. Phys.*, 1989, **90**, 2154.
- (53) J.B. Foresman and A. Frisch in *"Exploring Chemistry with Electronic Structure Methods"*; 2nd edition ed.; Gaussian, Inc.: Pittsburgh, 1996, Chapt. 1.
- (54) M.B. Stringer, J.H. Bowie, P.C.H. Eichinger and C.J. Currie, *J. Chem. Soc., Perkin Trans. 2*, 1987, 385.
- (55) R.N. Hayes and J.H. Bowie, *J. Chem. Soc. Perkin Trans. 2*, 1986, 1827.
- (56) P.C.H. Eichinger and J.H. Bowie, *Org. Mass Spectrom.*, 1987, **22**, 103.
- (57) P.C.H. Eichinger, J.H. Bowie and R.N. Hayes, *J. Org. Chem.*, 1987, **52**, 5224.
- (58) G.W. Adams, J.H. Bowie and R.N. Hayes, *J. Chem. Soc. Perkin Trans. 2*, 1989, 2159.
- (59) J. Adams, *Mass Spectrometry Reviews*, 1990, **9**, 141.
- (60) M.L. Gross, *Int. J. Mass Spectrom. Ion Processes*, 1992, **118**, 137.
- (61) S. Dua, J.H. Bowie, B.A. Cerda, C. Wesdemiotis, M.J. Raftery, J.F. Kelly, M.S. Taylor, S.J. Blanksby and M.A. Buntine, *J. Chem. Soc. Perkin Trans. 2*, 1997, 695.
- (62) V.H. Wysocki, M.E. Bier and R.G. Cooks, *Org. Mass Spectrom.*, 1988, **23**, 627.



- (63) S. Dua, J.H. Bowie, B.A. Cerda and C. Wesdemiotis, *J. Chem. Soc., Perkin Trans 2*, 1988, 1443.
- (64) M.J. Raftery and J.H. Bowie, *Int. J. Mass Spectrom. Ion Processes*, 1987, 79, 267.
- (65) S. Dua, R.B. Whait, M.J. Alexander, R.N. Hayes, A.T. Lebedev, P.C.H. Eichinger and J.H. Bowie, *J. Am. Chem. Soc.*, 1993, 115, 5709.
- (66) S.J. Blanksby, S. Dua and J.H. Bowie, *Rapid Commun. Mass Spectrom.*, 1995, 9, 177.
- (67) S. Dua, A.P. Pollnitz and J.H. Bowie, *J. Chem. Soc. Perkin Trans. 2*, 1993, 2235.
- (68) C.S.B. Chia, M.S. Taylor, S. Dua, S.J. Blanksby and J.H. Bowie, *J. Chem. Soc. Perkin Trans. 2*, 1998, 1435.
- (69) T.C. Kleingeld and N.M.M. Nibbering, *Tetrahedron*, 1983, 39, 4193.
- (70) P.C.H. Eichinger, J.H. Bowie and R.N. Hayes, *Aust. J. Chem.*, 1989, 42, 865.
- (71) S.J. Blanksby, S. Dua, J.M. Hevko, H. Christie and J.H. Bowie, *Eur. Mass Spectrom.*, 1996, 2, 33.
- (72) S.J. Blanksby, S. Dua, H. Christie and J.H. Bowie, *Rapid Commun. Mass Spectrom.*, 1996, 10, 478.

- (73) M.J. Raftery, J.H. Bowie and J.C. Sheldon, *J. Chem. Soc. Perkin Trans. 2*, 1988, 563.
- (74) G. Boand, R. Houriet and T. Gaumann, *Lecture Notes Chem*, 1982, **31**, 195.
- (75) R.N. Hayes, J.C. Sheldon, J.H. Bowie and D.E. Lewis, *J. Chem. Soc. Chem. Commun.*, 1984, 1431.
- (76) R.N. Hayes, J.C. Sheldon, J.H. Bowie and D.E. Lewis, *Aust. J. Chem.*, 1985, **38**, 1197.
- (77) W. Tumas, R.F. Foster, M.J. Pellerite and J.I. Brauman, *J. Am. Chem. Soc.*, 1983, **105**, 7464.
- (78) W. Tumas, R.F. Foster, M.J. Pellerite and J.I. Brauman, *J. Am. Chem. Soc.*, 1984, **106**, 4053.
- (79) W. Tumas, R.F. Foster, M.J. Pellerite and J.I. Brauman, *J. Am. Chem. Soc.*, 1987, **109**, 961.
- (80) W. Tumas, R.F. Foster, M.J. Pellerite and J.I. Brauman, *J. Am. Chem. Soc.*, 1988, **110**, 2714.
- (81) A.J. Noest and N.M.M. Nibbering, *Adv. Mass Spectrom.*, 1980, **8A**, 227.
- (82) J.E. Bartmess, J.A. Scott and R.T. McIver, *J. Am. Chem. Soc.*, 1989, **101**, 607.

- (83) R.J. Waugh, R.N. Hayes, P.C.H. Eichinger, K.M. Downard and J.H. Bowie, *J. Am. Chem. Soc.*, 1990, **112**, 2537.
- (84) K.M. Downard, J.C. Sheldon and J.H. Bowie, *Int. J. Mass Spectrom. Ion Processes*, 1988, **86**, 217.
- (85) R.N. Hayes, J.C. Sheldon and J.H. Bowie, *Int. J. Mass Spectrom. Ion Processes*, 1986, **71**, 233.
- (86) W.C. Brumley, D. Andrzejewski and J.A. Sphon, *Org. Mass Spectrom.*, 1988, **23**, 204.
- (87) P.C.H. Eichinger, J.H. Bowie and R.N. Hayes, *J. Am. Chem. Soc.*, 1989, **111**, 4224.
- (88) J. Adams and M.L. Gross, *J. Am. Chem. Soc.*, 1989, **111**, 435, and references cited therein.
- (89) M.M. Cordero and C. Wesdemiotis, *Anal. Chem.*, 1994, **66**, 861.
- (90) N. Kasai, T. Suzuki and Y. Furukawa, *Journal of Molecular Catalysis B-Enzymatic*, 1998, **4**(5-6), 237.
- (91) A. Archelas and R. Furstoss, *Annual Review of Microbiology*, 1997, **51**, 491.
- (92) L. Engman and V. Gupta, *J. Org. Chem.*, 1997, **62**(1), 157.

- (93) R.D. Chambers, J.F.S. Vaughan and S.J. Mullins, *Research on Chemical Intermediates*, 1996, **22**(8), 703.
- (94) D.J. Darensbourg and M.W. Holtcamp, *Coordination Chemistry Reviews*, 1996, **153**, 155.
- (95) S. Pedragosamoreau, A. Archelas and R. Furstoss, *Bulletin de la Societe Chimique de France*, 1995, **132**(8), 769.
- (96) P. Besse and H. Veschambre, *Tetrahedron*, 1994, **50**(30), 8885.
- (97) D. Seebach, B. Weidmann and L. Wilder in *"Modern Synthetic Methods"*; Otto Salle Verlag: Frankfurt, 1983, p 323.
- (98) J. Gorzynski-Smith, *Synthesis*, 1984, 629.
- (99) C.H. Behrens and K.B. Sharpless, *Aldrichimica Acta.*, 1983, **16**, 67.
- (100) S.A. Rao, S.K. Paknikar and J.G. Kirtane, *Tetrahedron*, 1983, **39**, 2323.
- (101) K.B. Sharpless, C.H. Behrens, T. Katsuki, A.W.M Lee, V.S. Martin, M. Takatani, S.M. Viti, F.J. Walker and S.S. Woodard, *Pure Appl. Chem.*, 1983, **55**, 589.
- (102) G.B. Payne, *J. Org. Chem.*, 1962, **27**, 3819.
- (103) S.J. Angyal and P.T. Gilham, *J. Chem. Soc.*, 1957, 3691.
- (104) H.B. Wood and B. Ganem, *Tetrahedron Lett.*, 1989, **30**(46), 6257.

- (105) H.J. Carlson and K. Aase, *Acta. Chemica.Scandinavica*, 1994, **48**, 273.
- (106) M.A. Tius and N.K. Reddy, *Synth. Commun.*, 1994, **24**(6), 859.
- (107) J.E. Wrobel and B. Ganem, *J. Org. Chem.*, 1983, **48**, 3761.
- (108) C.H. Behrens, S.Y. Ko, B. Sharpless and F.J. Walker, *J. Org. Chem.*, 1985, **50**, 5687.
- (109) S.Y. Ko, M. Malik and A.F. Dickinson, *J. Org. Chem.*, 1994, **59**, 2570.
- (110) P.C. Bullman Page, C.M. Rayner and I.O. Sutherland, *J. Chem. Soc. Perkin Trans. 1*, 1990, 1375.
- (111) S. Dua, P.C.H. Eichinger, G.W. Adams and J.H. Bowie, *Int. J. Mass Spectrom. Ion Processes*, 1994, **1**, 133.
- (112) S. Dua, M.S. Taylor, M.A. Buntine and J.H. Bowie, *J. Chem. Soc. Perkin Trans 2*, 1997, 1991.
- (113) J.E. Baldwin, *J. Chem. Soc. Chem. Commun.*, 1976, 734.
- (114) Data from: S.W. Benson in *"Thermochemical Kinetics"*; Wiley: New York, 1967.
- (115) S. Okada, Y. Abe, S. Tanaguchi and S. Yamabe, *J. Am. Chem. Soc.*, 1987, **109**, 295.

- (116) Y. Masaki, T. Miura, I. Mukai, A. Itoh and H. Oda, *Chem. Lett.*, 1991, 1937.
- (117) M. Lj. Mihailovic, N. Pavlovic and S. Gijkovic, *Bull. Soc. Chim. Beograd*, 1975, **40**, 309.
- (118) S. Dua, R.A.J. O'Hair, J.H. Bowie and R.N. Hayes, *J. Chem. Soc. Perkin Trans 2*, 1992, 1151.
- (119) C.H. DePuy and V.M. Bierbaum, *J. Am. Chem. Soc.*, 1981, **103**, 5034.
- (120) C.H. DePuy, E.C. Beedle and V.M. Bierbaum, *J. Am. Chem. Soc.*, 1982, **104**, 6483.
- (121) M. Lj. Mihailovic and D. Marinkovic, *Croatica Chemica Acta*, 1986, **59**(1), 109.
- (122) R.G. Gilbert and S.C. Smith in *"Theory of Unimolecular and Recombination Reactions"*; Blackwell Scientific Publications: Oxford, 1990, p 27.
- (123) A.P. Scott and L. Radom, *J. Phys. Chem.*, 1996, **100**, 16502.
- (124) J.P. A. Heuts, R.G. Gilbert and L. Radom, *Macromolecules*, 1995, **28**, 8771.
- (125) J.P.A. Heuts, R.G. Gilbert and L. Radom, *J. Phys. Chem*, 1996, **100**, 18997.
- (126) R.S. Mulliken, *J. Chem. Phys.*, 1955, **23**, 1833.

- (127) D.D. Perrin and W.L.F. Armarego in *"Purification of Laboratory Chemicals"*; Pergamon Press: Oxford, 1988.
- (128) A. Vogel in *"Vogel's Textbook of Practical Organic Chemistry"*; fourth edition ed.; Longman: London and New York, 1978, p 1129.
- (129) S. Ikenoya, M. Masui, H. Ohmori and H. Sayo, *J. Chem. Soc. Perkin Trans. II*, 1974, 571.
- (130) R.S. Mali and S.N. Yeola, *Synthesis*, 1989, **9**, 755.
- (131) R. H. Shapiro, J. Turk and J.W. Serum, *Org. Mass Spectrom.*, 1970, **3**, 171.
- (132) P. Beak and B.J. Kokko, *J. Org. Chem.*, 1982, **47**, 2822.
- (133) Amundsen and Pollard, *J. Am. Chem. Soc.*, 1935, **57**, 2005.
- (134) T. Nishiwaki, K. Azechi and F. Fujiyama, *J. Chem. Soc. Perkin Trans. I*, 1974, 1867.
- (135) C.M. Dougherty, R.L. Baumgarten, A. Sweeny and E. Concepcion, *J. Chem. Ed.*, 1977, **54**, 643.
- (136) A. Nose and T. Kudo, *Chem. Pharm. Bull.*, 1986, **34**(9), 3905.
- (137) *Dictionary of Organic Compounds*; Fifth ed.; J. Buckingham, Ed.; Chapman and Hall: New York, London, Toronto, 1982; Vol. 1, p 149.

- (138) M. Rajagopalan, K. Rao, J. Ayyer and V. Sasisekharan, *Indian J. Chem. Sect. B.*, 1987, **26B**(11), 1021.
- (139) *Dictionary of Organic Compounds*; Fifth ed.; J. Buckingham, Ed.; Chapman and Hall: New York, London, Toronto, 1982; Vol. 1, p 148.
- (140) T. Kashimura, K. Kudo, S. Mori and N. Sugita, *Chem. Letters*, 1986, **6**, 851.
- (141) A. Williams and K.T. Douglas, *J. Chem. Soc. Perkin Trans. II*, 1972, 2112.
- (142) N.P. Peet, *Synthesis*, 1984, **12**, 1065.
- (143) J.E. Whiting and J.T. Edward, *Can. J. Chem.*, 1971, **49**, 3799.
- (144) G.W. Stacey and R.A. Mikulec, *Org. Synth.*, 1963; **Col. Vol. IV**, 13.
- (145) *Dictionary of Organic Compounds*; Fifth ed.; J. Buckingham, Ed.; Chapman and Hall: New York, London, Toronto, 1982; Vol. 3, p 3202.
- (146) W. von E. Doering and W. J. Ehlhardt, *J. Am. Chem. Soc.*, 1987, **109**, 2697.
- (147) R.A. Daignault and E.L. Eliel, *Org. Synth*, **Col. Vol. V**, 303.
- (148) A. Burger, L. Turnbull and J.G. Dinwiddie, *J. Am. Chem. Soc.*, 1950, **72**, 5512.



- (149) P.A. Grieco, M. Nishizawa, T. Oguri, S.D. Burke and N. Marinovic, *J. Am. Chem. Soc.*, 1977, **99**, 5773.
- (150) H.A. Bates, *J. Am. Chem. Soc.*, 1982, **104**(9), 2490.
- (151) A. Martin, M. Jouannetaud and J. Jacquesy, *Tetrahedron Lett.*, 1996, **37**(17), 2967.
- (152) R.L. Garnick and P.W. LeQuesne, *J. Am. Chem. Soc.*, 1978, **100**, 4213.
- (153) E.J. Eisenbraun, *Org. Synth.*, **Col. Vol. V**, 310.
- (154) R.J. Ferrier and J.M. Tedder, *J. Chem. Soc.*, 1957, 1435.
- (155) S.H. Mashraqui and G.K. Trivedi, *Indian J. Chem., Sect. B*, 1978, **16b**, 849.
- (156) D. Barbry, C. Faven and A. Ajana, *Synth. Commun.*, 1993, **23**(19), 2647.
- (157) S. Kang, W. Kim and B. Moon, *Synthesis*, 1985, 1161.
- (158) W. Novis Smith and O.F. Beumel, *Synthesis*, 1974, 441.
- (159) D. Ma and X. Lu, *Tetrahedron*, 1990, **46**(18), 6319.
- (160) R.G. Salomon and M.F. Salomon, *J. Am. Chem. Soc.*, 1977, **99**, 3501.
- (161) *Dictionary of Organic Compounds*; Fifth ed.; J. Buckingham, Ed.; Chapman and Hall: New York, London, Toronto, 1982; Vol. 4, p 4454.

- (162) T. Wu, J. Mareda, Y.N. Gupta and K.N. Houk, *J. Am. Chem. Soc.*, 1983, **105**, 6996.
- (163) B.G. Kovalev, N.P. Dormidontova, E.M. Al'tmark and A.A. Shamshurin, *Probl. Poluch. Poluprod. Prom. Org. Sin.* 1967, 53.
- (164) R.M. Scarborough Jr. and A.B. Smith, *Tetrahedron Letters*, 1977, 4361.
- (165) B. Kongkathip, R. Sookkho and N. Kongkathip, *Chem. Letters*, 1985, 1849.
- (166) *Dictionary of Organic Compounds*; Fifth ed.; J. Buckingham, Ed.; Chapman and Hall: New York, London, Toronto, 1982; Vol. 3, p 2872.
- (167) M. Kosugi, I. Hagiwara and T. Migita, *Chem. Letters*, 1983, 839.
- (168) H.C. Brown and G.J. Lynch, *J Org Chem*, 1981, **46**, 930.
- (169) A.O. Fitton, J. Hill, D.E. Jane and R. Millar, *Synthesis*, 1987, **12**, 1140.
- (170) T. Ochiai, M. Yoshida and O. Simamura, *Bull. Chem. Soc. Jpn.*, 1976, **49**(9), 2641.
- (171) W. Kirmse and U. Jansen, *Chem. Ber.*, 1985, **118**, 2607.
- (172) R. Paul, *Ann. Chim. (Paris)*, 1932, **18**, 303.
- (173) H.C. Brown, J.V.N. Vara Prasad and S. Zee, *J. Org. Chem.*, 1985, **50**, 1582.

- (174) V. Prey and J. Bartsch, *Liebigs Ann Chem.*, 1968, **712**, 201.
- (175) K. Mori, *Tetrahedron*, 1974, **30**, 3807.
- (176) M.Lj. Mihailovic, D. Marinkovic, S. Konstantinovic and Z. Bugarcic, *J. Serb. Chem. Soc.*, 1985, **50**, 327.
- (177) *Dictionary of Organic Compounds*; Fifth ed.; J. Buckingham, Ed.; Chapman and Hall: New York, London, Toronto, 1982; Vol. 5, p 5226.
- (178) S.F. Martin, C. Tu and T. Chou, *J. Am. Chem. Soc.*, 1980, **102**, 5274.
- (179) R.V. Stevens, R.E. Cherpeck, B.L. Harrison, J. Lai and R. Lapalme, *J. Am. Chem. Soc.*, 1976, **98**(20), 6317.
- (180) J. Appa Rao and M.P. Cava, *J. Org. Chem.*, 1989, **54**, 2751.
- (181) S. Durand, J. Parrain and M. Santelli, *Synthesis*, 1998, 1015.
- (182) E.J. Corey, H. Niwa and J. Knolle, *J. Am. Chem. Soc.*, 1978, **100**, 1942.
- (183) M. Bourgain and J.F. Normant, *Bull. Soc. Chim. Fr.*, 1969, **7**, 2477.
- (184) W.D. Lubell, T.F. Jamison and H. Rapoport, *J. Org. Chem.*, 1990, **55**, 3511.
- (185) V. Vukov and R.J. Crawford, *Can. J. Chem.*, 1975, **53**, 1367.

- (186) P.G. Gassman, S.M. Bonser and K. Mlinaric-Majerski, *J. Am. Chem. Soc.*, 1989, **111**, 2653.
- (187) P.E. Eaton, Y. Xiong and J. Ping Zhou, *J. Org. Chem.*, 1992, **57**, 4277.
- (188) *Dictionary of Organic Compounds*; Fifth ed.; J. Buckingham, Ed.; Chapman and Hall: New York, London, Toronto, 1982; Vol. 3, p 2938.

# Publications

**1. Anionic migration in aromatic systems effected by collisional activation. Unusual fragmentations of deprotonated anilides containing methoxyl and ethoxyl substituents.**

S.J. Blanksby, S. Dua, J.M. Hevko, H. Christie and J.H. Bowie., *Eur. Mass Spectrom.*, 1996, 2, 33.

**2. Anionic migration effected by collisional activation. Hydride ion mobility in keto substituted alkoxide anions.**

J.M. Hevko, S. Dua and J.H. Bowie., *Eur. Mass Spectrom.*, 1996, 2, 287.

**3. Comparison of gas phase and condensed phase  $S_Ni$  reactions. The competitive four- and five-centre cyclisations of the 3,4-epoxybutoxide anion. A joint experimental and theoretical study.**

J.M. Hevko, S. Dua, M.S. Taylor and J.H. Bowie., *J. Chem. Soc., Perkin Trans. 2*, 1998, 1629.

**4. Gas phase and condensed phase  $S_Ni$  reactions. The competitive five and six centre cyclisations of the 4,5-epoxypentoxide anion. A joint experimental and theoretical study.**

J.M. Hevko, S. Dua, M.S. Taylor and J.H. Bowie., *Int. J. Mass Spectrom.*, 1999, in press. Dedicated to M.T. Bowers on the occasion of his 60<sup>th</sup> birthday.

**5. Gas phase and condensed phase  $S_Ni$  reactions. The competitive six and seven centre cyclisations of the 5,6-epoxyhexoxide anion. A joint experimental and *ab initio* study. A comparison with  $S_Ni$  reactions of homologous epoxyalkoxide anions.**

J.M. Hevko, S. Dua, J.H. Bowie, M.S. Taylor., *J. Chem. Soc. Perkin Trans. 2.*, 1999, in press.

Blanksby, S.J., Dua, S., Hevko, J.M., Christie, H. & Bowie, J.H. (1996) Anionic migration in aromatic systems effected by collisional activation. Unusual fragmentations of deprotonated anilides containing methoxyl and ethoxyl substituents.

*European Journal of Mass Spectrometry*, v. 2(1), pp. 33-42

NOTE:

This publication is included on pages 247-257 in the print copy  
of the thesis held in the University of Adelaide Library.

© 2006 The Authors  
Journal compilation © 2006 Blackwell Publishing Ltd

1. *Journal of Management Studies*, 1997, 34, 1, 1-14.





Hevko, J.M., Dua, S. & Bowie, J.H. (1996) Anionic migration effected by collisional activation.  
Hydride ion mobility in keto substituted alkoxide anions.  
*European Journal of Mass Spectrometry*, v. 2(4-5), pp. 287-293

NOTE:

This publication is included on pages 260-268 in the print copy  
of the thesis held in the University of Adelaide Library.





# Comparison of gas phase and condensed phase $S_Ni$ reactions. The competitive four- and five-centre cyclisations of the 3,4-epoxybutoxide anion. A joint experimental and theoretical study

2 PERKIN

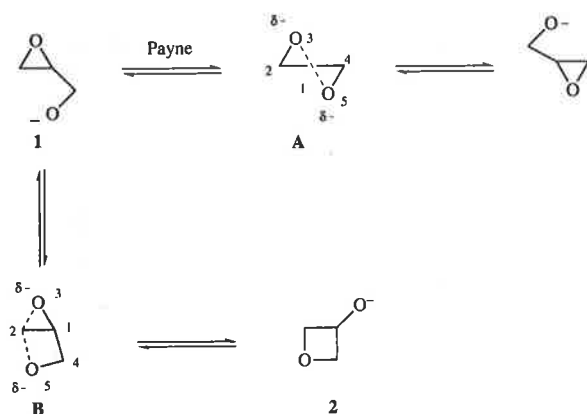
John M. Hevko, Suresh Dua, Mark S. Taylor and John H. Bowie

Department of Chemistry, The University of Adelaide, South Australia, 5005

*Ab initio* calculations [at the MP2-Fc/6-31+G(d) level] indicate that the 3,4-epoxybutoxide anion should undergo competitive  $S_Ni$  cyclisations (through four- and five-membered transition states) to yield the  $(M - H)^-$  ions of oxetan-2-ylmethanol and tetrahydrofuran-3-ol respectively. The barriers to the transition states are comparable (*ca.* 70 kJ mol<sup>-1</sup>) for each process, and the latter product is the more stable by 82 kJ mol<sup>-1</sup> at the level of theory indicated. Gas phase studies of the 3,4-epoxybutoxide anion excited by collisional activation are in accord with this scenario, and show, in addition, that deprotonated 2-oxetanylmethanol can convert to the starting material. Base treatment of 2-(oxiran-2-yl)ethan-1-ol (3,4-epoxybutan-1-ol) in two different solvent systems [10% aqueous sodium hydroxide and sodium hydride-tetrahydrofuran (both at reflux)] yields the same two products observed in the gas phase studies. However, deprotonated tetrahydrofuran-3-ol is the kinetic product in both solvent systems.

## Introduction

The energised 2,3-epoxypropoxide anion undergoes two competing  $S_Ni$  processes in the gas phase: these are summarised in Scheme 1. The more facile of the two processes is the Payne



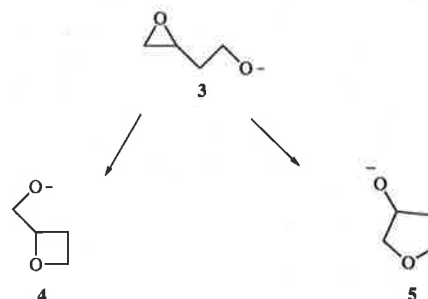
**Scheme 1** A:  $C^1O^3 = 1.89$ ,  $C^1O^5 = 1.89$  Å;  $O^3C^1O^5 = 160.15^\circ$ ,  $O^5C^1C^2O^3 = -159.7^\circ$ . B:  $C^2O^3 = 1.91$ ,  $C^2O^5 = 2.08$  Å;  $O^3C^2O^5 = 116.5^\circ$ ,  $O^5C^2C^1O^3 = -153.0^\circ$

rearrangement which has a computed barrier (*ab initio* calculations at the G2 level) of only 45 kJ mol<sup>-1</sup>. This process competes with the alternative cyclisation to yield the four-membered oxetane system 2 (barrier 122 kJ mol<sup>-1</sup>).<sup>1</sup>

The angle of approach of  $O^-$  to the receptor carbon in the transition state is the major feature influencing the relative barriers to the transition states A and B (the OCO angles in the transition states are computed to be 161.5° for the three-centred Payne process, and 116.5° for the four-centred formation of 2).<sup>1</sup> The closer the OCO angle is to 180° (*i.e.* the closer the geometry is to that of an ideal  $S_N2$  type transition state), the lower the barrier of the  $S_Ni$  process. The strain energies of the various rings have only a minor influence on the competition between the three- and four-centre cyclisations, since the strain energies of ethylene oxide and oxetane are comparable, *i.e.* 112.5 and 107.5 kJ mol<sup>-1</sup> respectively.<sup>2</sup>

In this paper we extend the above study to probe the scenario summarised in Scheme 2. We wish to investigate the  $S_Ni$

reactions of the 3,4-epoxybutoxide anion 3 both theoretically, and experimentally in the gas and condensed phases, in order to answer the following questions. Firstly, do the two  $S_Ni$  processes shown in Scheme 2 occur? Secondly, if both cyclisations do



**Scheme 2**

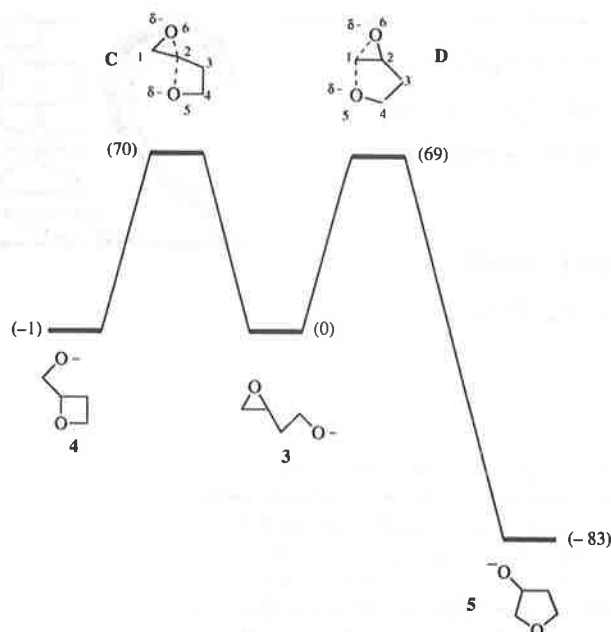
occur, then (i) is the angle of approach of  $O^-$  to each of the two possible electrophilic carbon centres a major factor controlling competition between the two processes, (ii) is the difference in strain energy (112.5, 107.5 and 25 kJ mol<sup>-1</sup> for ethylene oxide, oxetane and tetrahydrofuran respectively<sup>2</sup>) a significant factor in controlling the relative extents of the two processes, and (iii) do equilibria between 3, 4 and 5 occur during the experimental conditions, or are the processes 3 to 4 and 3 to 5 irreversible?

## Results and discussion

### 1. The results of *ab initio* calculations

The results of an *ab initio* computational study using GAUSSIAN94<sup>3</sup> for the reactions shown in Scheme 2 are summarised in Fig. 1. The geometries of the local minima and the transition states were optimised at the RHF/6-31+G(d) level of theory. Energies were then refined at the MP2-Fc/6-31+G(d) level. Geometries and energies of 3, 4 and 5 and the two transition states C and D are listed in Table 1.

The details shown in Fig. 1 and Table 1 indicate that the barriers to the two transition states are of the same order. The OCO angles in the transition state are 163.4° for the four- (C) and 140.3° for the five-centre (D) rearrangements respectively, with the dihedral angles being 172.3 and 163.4° respectively.



**Fig. 1** *Ab initio* calculations [GAUSSIAN94, geometries RHF/6-31+G(d), energies MP2-Fc/6-31+G(d)] for the competitive  $S_Ni$  cyclisations of the 3,4-epoxybutoxide anion. Partial geometries: **C**,  $C^2O^5 = 2.00$ ,  $C^2O^6 = 1.85$  Å;  $O^6C^2O^5 = 163.4^\circ$ ,  $O^5C^2C^1O^6 = +172.5^\circ$ . **D**,  $C^1O^5 = 2.09$ ,  $C^1O^6 = 1.84$  Å;  $O^6C^1O^5 = 140.3^\circ$ ,  $O^5C^1C^2O^6 = -163.1^\circ$ . For energies and further data on **C** and **D** see Table 1. For other geometries see Supplementary material.

The four-centre  $S_Ni$  reaction has the larger OCO angles in the transition state: these data taken alone favour the kinetic formation of **4**. The change in ring strain from reactant to transition state is another major factor influencing the rate of reaction. The decrease in ring strain from **3** to **C** and **3** to **D** due to the breaking C–O bond should be comparable (C–O = 1.45 Å for **3**, 1.85 Å for **C** and 1.84 Å for **D**). In contrast, the increase in ring strain as a consequence of the formation of the new C–O bond will be greater for **C** [forming C–O bond length = 2.00 Å, strain energy = 107.5 kJ mol<sup>-1</sup> for oxetane<sup>2</sup> (C–O = 1.45 Å)] than for **D** [forming C–O bond length = 2.09 Å, strain energy = 25 kJ mol<sup>-1</sup> for tetrahydrofuran<sup>2</sup> (C–O = 1.45 Å)].

There are two major features which control the rate of a gas phase reaction, *viz.* (i) the barrier to the transition state (described above) and (ii), the frequency or probability factor [of the quasi-equilibrium equation (or the *A* factor of the Arrhenius rate equation)]. The parameters controlling the frequency factor can be complex and an understanding of these depends upon an intimate knowledge of the full potential surface for the reaction (which we do not have). In the simplest scenario, the frequency factors could be a function of the relative probabilities of **3** being able to enter the two competing  $S_Ni$  channels. A Mulliken charge analysis of **3** shows that of the two recipient carbon centres, the more substituted is more electrophilic [+0.336 *vs.* +0.158 at the RHF/6-31+G(d) level]. This could mean that the probability of **3** entering the channel to form **4** is higher than that for the competing formation of **5**.

The *ab initio* calculations predict (i) that the relative proportions of products **4** and **5** (from **3**) should be comparable if the rates of the two reactions are controlled by the relative barriers to the transition states, (ii) should frequency factors control the kinetically controlled reactions, **4** will be the major product, and (iii) if the reaction of **3** to **4** is reversible under the reaction conditions, thermodynamic product **5** may be formed in the higher yield.

## 2. The reactions of **3**, **4** and **5** in the condensed phase

The computed results shown in Fig. 1 apply to reactions carried out in the absence of solvent. Does such a scenario also pertain

**Table 1** Energies of stable ions and transition states shown in Fig. 1 together with geometries of transition states at the MP2-Fc/6-31+G(d) level<sup>a</sup>

Species	Energy/ hartrees (kJ mol <sup>-1</sup> )	Geometry			
		Bond lengths/Å		Bond angles/°	
<b>3</b>	-305.996 752 1 (0)	See Supplementary data			
<b>4</b>	-305.997 086 (-1)				
<b>5</b>	-306.028 400 4 (-83)				
 <b>C</b>	-305.970 138 3 (+70)	C <sup>1</sup> C <sup>2</sup>	1.452	C <sup>1</sup> C <sup>2</sup> C <sup>3</sup>	122.45
		C <sup>2</sup> C <sup>3</sup>	1.509	C <sup>2</sup> C <sup>3</sup> C <sup>4</sup>	95.09
		C <sup>3</sup> C <sup>4</sup>	1.525	C <sup>3</sup> C <sup>4</sup> O <sup>5</sup>	99.49
		C <sup>4</sup> O <sup>5</sup>	1.404	O <sup>5</sup> C <sup>2</sup> O <sup>6</sup>	163.45
		C <sup>1</sup> O <sup>6</sup>	1.410	C <sup>2</sup> C <sup>1</sup> O <sup>6</sup>	80.77
		C <sup>2</sup> O <sup>6</sup>	1.850	O <sup>5</sup> C <sup>2</sup> C <sup>1</sup> O <sup>6</sup>	172.52
		C <sup>2</sup> O <sup>5</sup>	2.005		
		C <sup>1</sup> C <sup>2</sup>	1.437	C <sup>1</sup> C <sup>2</sup> C <sup>3</sup>	108.54
		C <sup>2</sup> C <sup>3</sup>	1.509	C <sup>2</sup> C <sup>3</sup> C <sup>4</sup>	102.40
		C <sup>3</sup> C <sup>4</sup>	1.562	C <sup>3</sup> C <sup>4</sup> O <sup>5</sup>	111.50
 <b>D</b>	-305.964 541 5 (+69)	C <sup>4</sup> O <sup>5</sup>	1.390	O <sup>5</sup> C <sup>1</sup> O <sup>6</sup>	140.35
		C <sup>1</sup> O <sup>5</sup>	2.090	C <sup>1</sup> C <sup>2</sup> O <sup>6</sup>	79.81
		C <sup>1</sup> O <sup>6</sup>	1.840	C <sup>2</sup> C <sup>2</sup> O <sup>6</sup>	125.00
		C <sup>2</sup> O <sup>6</sup>	1.426	O <sup>5</sup> C <sup>1</sup> C <sup>2</sup> O <sup>6</sup>	-163.13

<sup>a</sup> Full details of bond lengths and angles are available as supplementary material (SUPPL. NO. 57382, 5 pp.). For details of the Supplementary Publications Scheme see 'Instructions for Authors', *J. Chem. Soc., Perkin Trans. 2*, available via the RSC Web page (<http://www.rsc.org/authors>).

**Table 2** Base catalysed solution reactions of **3**, **4** and **5**<sup>a</sup>

Reactant	System <sup>b</sup>	Time/h	Ratio ( <b>3</b> : <b>4</b> : <b>5</b> ) <sup>c</sup>
<b>3</b>	A	0.17	100:0:0
	A	1	77:3:20
	A	15	22:11:67
	A	30	20:10:70
	A	60	20:10:70
	B	0.17	73:2:25
	B	1	21:7:62
	B	15	11:11:78
	B	30	10:11:79
	B	60	9:13:78
<b>4</b>	A	3	0:100:0
	A	15	19:100:0
	A	30	27:100:9
	B	3	0:100:0
	B	15	50:100:0
<b>5</b>	B	30	24:100:20
	A	30	0:0:100
	B	30	0:0:100

<sup>a</sup> For experimental conditions see Experimental section. <sup>b</sup> System A: 10% NaOH, 100 °C. System B: NaH–tetrahydrofuran, 65 °C. <sup>c</sup> The ratio is obtained by comparing the areas under each peak (this ratio correlates closely with the ratios obtained using ion counts/peak). The error in each number within a ratio is *ca.* ± 5%.

to the analogous base catalysed reaction in solution? The reactions of **3**, **4** and **5** have been examined in two solvent systems, (a) 10% aqueous sodium hydroxide at 100 °C, and (b) sodium hydride–tetrahydrofuran at 65 °C. These systems were chosen because they were used previously in investigations of the Payne rearrangement (*cf.* ref. 1). Products were monitored at different reaction times using gas chromatography–mass spectrometry. The following observations can be made from the data recorded in Table 2: (i) the anion **3** converts to both **4** and **5**, with **5** being the major product, (ii) the four-membered ring system **4** converts slowly to the 3,4-epoxybutoxide anion **3**, which in turn forms **4** and **5**, (iii) the five-membered ring system **5** is stable under the reaction conditions, (iv) conversions of **3** to **4** and **5** are more facile than conversion of **4** to **3**, and (v) the  $S_Ni$  reac-

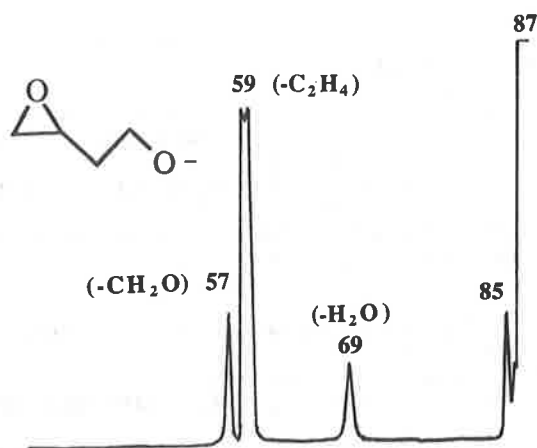


Fig. 2 Collision induced  $\text{HO}^-$  negative ion chemical ionisation (MS-MS) mass spectrum of the 3,4-epoxybutoxide anion. VG ZAB 2HF mass spectrometer. For experimental conditions see Experimental section. Peak widths at half height:  $m/z$  69 ( $75.2 \pm 1.0$  V),  $m/z$  59 ( $95.8 \pm 1.0$  V).

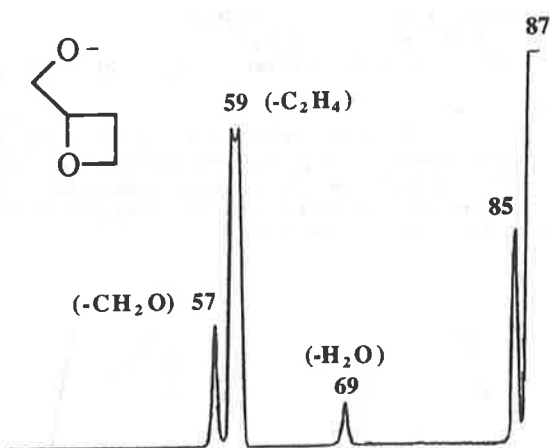


Fig. 3 Collision induced mass spectrum of the  $(M-H)^-$  ion of 2-(oxiran-2-yl)ethan-1-ol. VG ZAB 2HF mass spectrometer. Peak widths at half height:  $m/z$  69 ( $72.0 \pm 1.0$  V),  $m/z$  59 ( $93.1 \pm 1.0$  V).

tions of **3** and **4** proceed more readily in the NaH-tetrahydrofuran system.

Thus reaction **3**→**5** is more favourable in solution than **3**→**4**. This is in contrast to the scenario predicted in Fig. 1 for a gas phase reaction. The slow conversion of **4**→**3** is not reflected in the ratio of products of **4** and **5** (from **3**) with increasing time because **4** constitutes only some 10% of the product mixture **4** and **5**. The  $\text{S}_{\text{N}}\text{i}$  reactions of **3** proceed through transition states in which the charge is dispersed (relative to the reactant), so the reaction rates should not be significantly influenced by the relative permittivity of the solvent (78.5 for  $\text{H}_2\text{O}$ , 7.4 for tetrahydrofuran). Nor should the counter ion influence the relative reaction rates since it is  $\text{Na}^+$  in both systems. In contrast, the rates should be influenced by the solvating power of the solvent, *i.e.* a protic solvent like water will strongly solvate the anion centre and consequently retard an  $\text{S}_{\text{N}}\text{i}$  reaction (compared with the same reaction performed in a non-protic solvent like tetrahydrofuran), as observed for the  $\text{S}_{\text{N}}\text{i}$  reactions of **3**.

### 3. Gas phase cyclisations of the 3,4-epoxypropoxide anion

The collision induced mass spectra of the isomers **3**, **4** and **5** are shown in Figs. 2–4 (peak widths at half height of some fragment ions are recorded in the legends to Figs. 2–4). In our study of the Payne rearrangement, we used the loss of  $\text{CH}_2\text{O}$  from the  $(M-H)^-$  ion as a probe to test for the operation of the competing  $\text{S}_{\text{N}}\text{i}$  reactions shown in Scheme 1.<sup>1</sup> In the present investigation, consideration of the spectra shown in Figs. 2–4 suggests

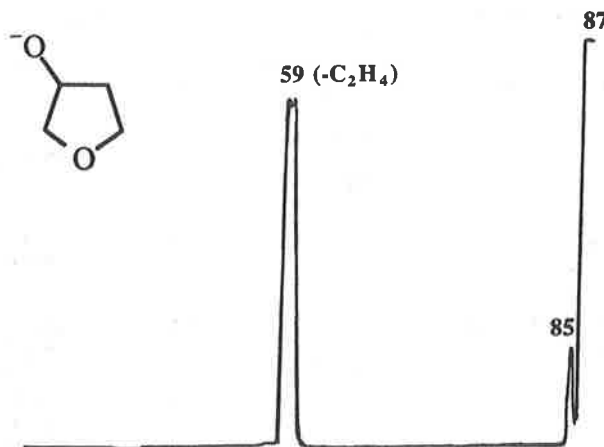
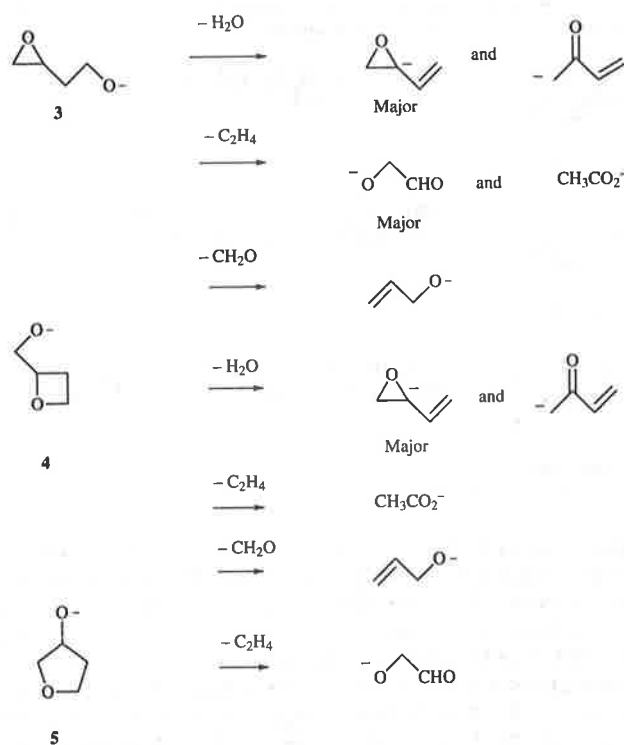


Fig. 4 Collision induced mass spectrum of the  $(M-H)^-$  ion of tetrahydrofuran-3-ol. VG ZAB 2HF mass spectrometer. Peak width at half height:  $m/z$  59 ( $100.0 \pm 1.0$  V).

that three processes might provide information concerning the operation of the two  $\text{S}_{\text{N}}\text{i}$  processes depicted in Fig. 1, *viz.*, the competitive losses of  $\text{H}_2\text{O}$ ,  $\text{C}_2\text{H}_4$  and  $\text{CH}_2\text{O}$  from  $(M-H)^-$  ions. We need to know the structures of each of these ions, together with their mechanisms of formation from **3**–**5** (as appropriate). The structures of the daughter ions formed from these processes have been determined by a comparison of the spectra [both collision induced and charge reversal (positive ion)<sup>4</sup> spectra] with those of authentic anions formed by independent syntheses. The product ion spectra are recorded in Table 3: the conclusions arising from these data are summarised in Scheme 3.



Scheme 3

The spectra of deuterium and  $^{18}\text{O}$  labelled analogues of the 3,4-epoxybutoxide anion are listed in Table 4. The peak shapes of the broad peaks in the spectra of two labelled compounds are shown in Fig. 5: the example of a Gaussian peak (loss of  $\text{CH}_2\text{O}$ ) superimposed on the dish-shaped peak (loss of  $\text{C}_2\text{H}_2\text{D}_2$ ) (see Fig. 5A) is noteworthy. These spectra show that the losses of  $\text{H}_2\text{O}$  and  $\text{CH}_2\text{O}$  from the 3,4-epoxybutoxide anion



**Table 3** Spectra of product anions from 3–5 and known anions

Precursor ion	Product ion <i>m/z</i> (loss)	Mode	Spectrum [CA: <i>m/z</i> (loss) abundance] <sup>a</sup> [CR: <i>m/z</i> (abundance)]
3	69 (–H <sub>2</sub> O)	CR	69(1), 68(73), 66(4), 55(11), 54(5), 53(8), 52(6), 51(8), 50(15), 42(43), 41(27), 40(8), 39(100), 38(20), 37(13), 29(15), 27(25), 26(41), 25(8)
4	69 (–H <sub>2</sub> O)	CR	69(1), 68(59), 66(3), 55(10), 54(16), 53(17), 52(11), 51(16), 50(19), 42(22), 41(21), 40(12), 39(100), 38(22), 37(13), 29(22), 27(23), 26(33), 25(8)
		CR	69(1), 68(100), 66(6), 54(16), 53(12), 52(8), 51(12), 50(18), 42(6), 41(27), 40(10), 39(71), 38(21), 37(9), 29(18), 27(8), 26(10), 25(12)
<sup>–</sup> [CH <sub>2</sub> COCH=CH <sub>2</sub> ] <sup>b</sup> ( <i>m/z</i> 69)		CR	68(2), 66(1), 55(33), 54(8), 53(12), 52(7), 51(9), 50(19), 42(100), 41(33), 39(38), 37(10), 29(5), 27(46), 26(28), 25(10), 14(1)
3	59 (–C <sub>2</sub> H <sub>4</sub> )	CA	58(H <sup>+</sup> )100, 57(H <sub>2</sub> )65, 44(CH <sub>3</sub> ) <sup>8</sup> , 31(CO)32, 29(CH <sub>2</sub> O)11
		CR	59(12), 58(29), 56(31), 45(11), 44(22), 43(15), 42(22), 41(20), 31(18), 30(22), 29(100), 28(29), 15(2)
4	59 (–C <sub>2</sub> H <sub>4</sub> )	CR	56(5), 45(42), 44(100), 43(34), 42(39), 41(19), 29(34), 28(28), 15(6), 14(4), 13(2), 12(1)
5	59 (–C <sub>2</sub> H <sub>4</sub> )	CR	59(14), 58(46), 56(42), 42(14), 41(10), 31(12), 30(32), 29(100), 28(29)
<sup>–</sup> OCH <sub>2</sub> CHO <sup>c</sup> ( <i>m/z</i> 59)		CA	58(H <sup>+</sup> )100, 57(H <sub>2</sub> )60, 31(CO)30, 29(CH <sub>2</sub> O)13
		CR	59(8), 58(33), 56(19), 42(24), 41(27), 31(31), 30(44), 29(100), 28(39)
CH <sub>3</sub> CO <sub>2</sub> <sup>–d</sup> ( <i>m/z</i> 59)		CR	56(4), 45(28), 44(100), 43(36), 42(38), 41(18), 29(12), 28(13), 15(10), 14(5), 13(2), 12(1)
3	57 (CH <sub>2</sub> O)	CA	56(H <sup>+</sup> )68, 55(H <sub>2</sub> )100, 41(CH <sub>4</sub> )28, 29(C <sub>2</sub> H <sub>4</sub> )36, 27(CH <sub>2</sub> O)58
		CR	56(12), 55(58), 53(14), 42(18), 41(20), 39(62), 38(18), 37(16), 29(100), 28(19), 27(68), 26(48), 25(15)
4	57 (CH <sub>2</sub> O)	CA	56(H <sup>+</sup> )65, 55(H <sub>2</sub> )100, 41(CH <sub>4</sub> )26, 29(C <sub>2</sub> H <sub>4</sub> )33, 27(CH <sub>2</sub> O)52
CH <sub>2</sub> =CHCH <sub>2</sub> O <sup>–e</sup> ( <i>m/z</i> 57)		CA	56(H <sup>+</sup> )65, 55(H <sub>2</sub> )100, 41(CH <sub>4</sub> )25, 29(C <sub>2</sub> H <sub>4</sub> )32, 27(CH <sub>2</sub> O)55
		CR	56(10), 55(64), 53(12), 42(12), 41(16), 39(54), 38(14), 37(12), 29(100), 28(26), 27(75), 26(50), 25(12)

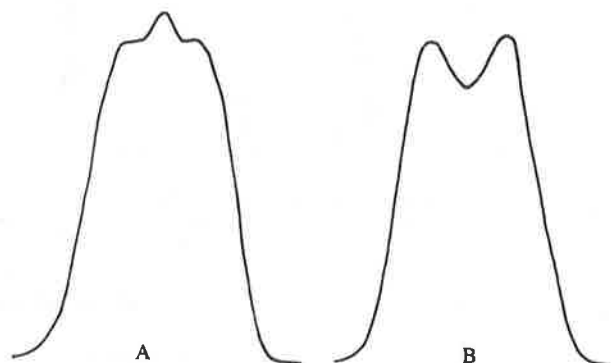
<sup>a</sup> The relative abundances of CR spectra are critically dependent upon the collision gas pressure. Discrepancies between the abundances of peaks in the charge reversal spectra of source formed product anions and in the spectra of authentic anions is to be expected. This is particularly apparent for the CR spectra of the [(M – H)<sup>–</sup> – C<sub>2</sub>H<sub>4</sub>] ions and of CH<sub>3</sub>CO<sub>2</sub><sup>–</sup> and <sup>–</sup>CH<sub>2</sub>CHO. Even so, the spectra are quite characteristic, and there can be no doubt as to the structures of the two [(M – H)<sup>–</sup> – C<sub>2</sub>H<sub>4</sub>] species. <sup>b</sup> Formed by deprotonation of methyl vinyl ketone. <sup>c</sup> Formed by reaction of HO<sup>–</sup> with 2,5-dihydroxy-1,4-dioxane. <sup>d</sup> Formed by deprotonation of acetic acid. <sup>e</sup> Formed by deprotonation of allyl alcohol.

**Table 4** Mass spectra of labelled 3,4-epoxybutoxide anions

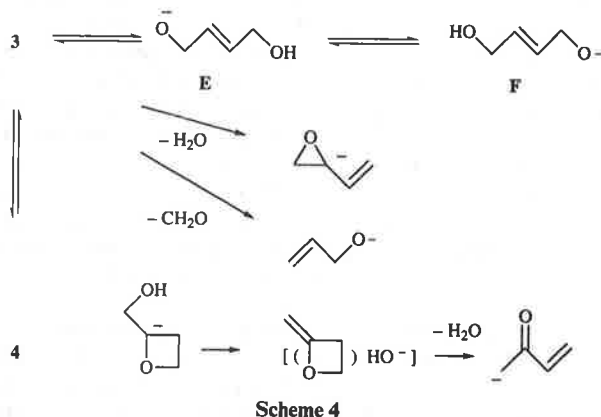
Anion	<i>m/z</i> (loss) abundance
	88(H <sup>+</sup> )55, 87(H <sub>2</sub> , D <sup>+</sup> )100, 71(H <sub>2</sub> O)20, 59(C <sub>2</sub> H <sub>2</sub> D <sub>2</sub> , CH <sub>2</sub> O)85, 57(CD <sub>2</sub> O)17 ( <i>m/z</i> 89)
	88(H <sup>+</sup> )45, 87(H <sub>2</sub> )92, 71(H <sub>2</sub> O)7, 69(H <sub>2</sub> <sup>18</sup> O)17, 61(C <sub>2</sub> H <sub>4</sub> )100, 59(CH <sub>2</sub> O)8, 57(CH <sub>2</sub> <sup>18</sup> O)16 ( <i>m/z</i> 89)
	90(H <sup>+</sup> )100, 89(H <sub>2</sub> , D <sup>+</sup> )82, 88(HD)18, 71(H <sub>2</sub> O)3, 69(H <sub>2</sub> <sup>18</sup> O)14, 61(CH <sub>2</sub> O, C <sub>2</sub> H <sub>2</sub> D <sub>2</sub> )85, 57(CD <sub>2</sub> <sup>18</sup> O)15 ( <i>m/z</i> 91)

principally involve the side chain oxygen of 3, with the epoxide oxygen being involved to a lesser extent. We propose, from a consideration of the labelling and product ion data, that (i) anions 3 and 4 can interconvert under the reaction conditions, (ii) the loss of CH<sub>2</sub>O, and the major loss of H<sub>2</sub>O from 3 (and 4) are fragmentations of 3, but a minor proportion of these losses follow equilibration of the two oxygens by formation of E and F (see Scheme 4, E is formed by proton transfer within 3 from the 2 position to O<sup>–</sup>, followed by ring opening), and (iii) the methyl vinyl ketone enolate ion (the minor product resulting from loss of water) is formed exclusively from 4 (see Scheme 4).

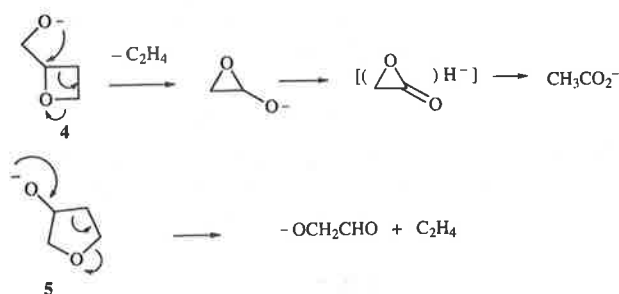
The data considered so far suggest that 3 and 4 are interconvertible, but provide no evidence concerning the relationship between 4 and 5. That information is forthcoming from a consideration of the various losses of ethene, processes which cannot occur directly from anion 3. The product ion data summarised in Scheme 3 show that loss of C<sub>2</sub>H<sub>4</sub> from 4 yields



**Fig. 5** Peak profile of the broad peaks in the spectra of the (M – H)<sup>–</sup> ions of (A), 2-(oxiran-2-yl)ethan-1-[<sup>18</sup>O]ol, and (B) [1,1-<sup>2</sup>H<sub>2</sub>]-2-(oxiran-2-yl)ethan-1-ol

**Scheme 4**

CH<sub>3</sub>CO<sub>2</sub><sup>–</sup> whereas the analogous loss from 5 forms <sup>–</sup>OCH<sub>2</sub>CHO. Suggested mechanisms for the formation of these ions are shown in Scheme 5. The formation of the acetate anion



from **4** is unusual, but is analogous to the mechanism proposed to account for the formation of  $(\text{MeCOCH}_2)^-$  from  $^-\text{CH}_2\text{CH}_2\text{-CHO}$ .<sup>5</sup> The process is slightly exothermic [ $\Delta H$  for the conversion of **4** to  $\text{CH}_3\text{CO}_2^-$  is calculated to be  $-23 \text{ kJ mol}^{-1(2)}$ ; the high electron affinity of  $\text{CH}_3\text{CO}_2^-$  ( $297 \text{ kJ mol}^{-1(2)}$ )<sup>6</sup> is primarily responsible for the exothermicity of this process]. Both losses of ethene shown in Scheme 5 yield broad dish-shaped peaks (see Figs. 2–5). The corresponding peak in the spectrum (Fig. 2) of **3** corresponds to a mixture of  $\text{CH}_3\text{CO}_2^-$  and  $^-\text{OCH}_2\text{CHO}$  with the latter ion being the major contributor (see Scheme 3 and Table 3). It is also noteworthy that the width at half height of the composite peak for the loss of  $\text{C}_2\text{H}_4$  from **3** ( $95.8 \pm 1 \text{ V}$ ) is intermediate between those for the losses of  $\text{C}_2\text{H}_4$  from **4** ( $93.1 \pm 1 \text{ V}$ ) and **5** ( $100.0 \pm 1 \text{ V}$ ). Thus both **4** and **5** are formed from energised **3**, but since the spectra shown in Figs. 3 and 4 are different, ions **4** and **5** are not interconvertible under the reaction conditions.

## Conclusions

*Ab initio* calculations suggest that energised **3** should, in the absence of solvent, and under conditions of kinetic control, convert to the two  $\text{S}_{\text{N}}1$  products, **4** and **5**, in comparable yield if barriers to transition states alone determine the rates of the reactions. The relative barrier to the transition state for each of the competitive  $\text{S}_{\text{N}}1$  processes is primarily a function of (i) the angle of approach of  $\text{O}^-$  to the recipient carbon centre, and (ii) the difference in ring strain between reactant and transition state. If frequency factors control energy into the two reaction channels, then **4** should be the predominant product. If **3** and **4** are interconvertible under the reaction conditions, thermodynamic product **5** should be the major product.

Gas phase studies indicate that upon collisional activation (i) **3** undergoes competitive  $\text{S}_{\text{N}}1$  reactions to yield both **4** and **5** in comparable amounts, (ii) **4** is able to convert to **3**, and (iii) **5** does not convert to either **3** or **4**. These results are compatible with the theoretical predictions involving similar barrier heights, with frequency factors being of lesser importance in this system.

The condensed phase studies are different from those outlined above. The evidence suggests that in the solvent systems used, the kinetic product from **3** is **5**, rather than **4** (whereas in the gas phase **4** and **5** are formed to a similar degree).

## Experimental

### Mass spectrometric methods

Collisional activation (CA) mass spectra (MS–MS) were determined with a VG ZAB 2HF mass spectrometer.<sup>7</sup> Full operating details have been reported.<sup>8</sup> Specific details were as follows: the chemical ionisation slit was used in the chemical ionisation source, the ionising energy was  $70 \text{ eV}$ , the ion source temperature was  $100^\circ\text{C}$ , and the accelerating voltage was  $7 \text{ kV}$ . The liquid samples were introduced through the septum inlet with no heating [measured pressure of sample  $1 \times 10^{-6} \text{ Torr}$  ( $1 \text{ Torr} = 133.322 \text{ Pa}$ )]. Deprotonation was effected using  $\text{HO}^-$  (from  $\text{H}_2\text{O}$ : measured pressure  $1 \times 10^{-5} \text{ Torr}$ ). The estimated

source pressure was  $10^{-1} \text{ Torr}$ . Argon was used in the second collision cell (measured pressure, outside the cell,  $2 \times 10^{-7} \text{ Torr}$ ), giving a 10% reduction in the main beam, equivalent to single collision conditions. Collision induced dissociation (CID) MS–MS measurements involved using the magnet to choose the ion under study [normally the  $(\text{M} - \text{H})^-$  species], collision activating it (see above), and scanning the electric sector to analyse the resultant product anions. Charge reversal (CR) (positive ion) MS–MS data for negative ions were obtained as for CA MS–MS data, except that the electric sector potential was reversed to allow the transmission of positively charged product ions (for full details see ref. 4). The recorded peak widths at half height are an average of five individual measurements.

### Ab initio calculations

The GAUSSIAN94<sup>3</sup> suite of programs was used for all calculations. The computational platforms used were a Silicon Graphics Indigo<sup>2</sup>xZ workstation and a Silicon Graphics Power Challenge. The geometries of the local minima and the transition states were optimised at the RHF/6-31+G(d) level of theory. Harmonic frequency analyses were performed on each stationary point in order to characterise them as either a local minimum or a transition state. A local minimum is characterised by possessing all real vibrational frequencies and its hessian matrix possessing all positive eigenvalues. A transition state is characterised by possessing one (and only one) imaginary frequency and its hessian matrix possessing one (and only one) negative eigenvalue. Intrinsic reaction coordinate (IRC) calculations were performed (beginning from both transition structures) to verify that each transition structure connected particular local minima. The energy of each structure at  $0 \text{ K}$  was calculated using MP2-Fc/6-31+G(d) level of theory. The energies include a scaled (0.8929) zero point vibrational energy correction based on the RHF/6-31+G(d) optimised geometry.

### Unlabelled compounds

Allyl alcohol, butadiene monoxide, crotonaldehyde, 2,5-dihydrofuran, 1,4-dioxane-2,3-diol and propylene oxide were commercial samples. Tetrahydrofuran-3-ol,<sup>9</sup> oxetan-2-ylmethanol<sup>10</sup> and 2-(oxiran-2-yl)ethan-1-ol<sup>11</sup> were prepared by reported procedures.

### Labelled compounds

Labelled compounds were synthesised as outlined below. The purity of all products was established by  $^1\text{H}$  NMR and positive ion mass spectrometry. The extent of incorporation (of D and/or  $^{18}\text{O}$ ) was established by either positive or negative ion mass spectrometry.

**[1,1- $^2\text{H}_2$ ]-2-(Oxiran-2-yl)ethan-1-ol- $^{18}\text{O}$ ].** A mixture of vinylacetic acid (1 g), oxalyl chloride (1.22 g) and *N,N*-dimethylformamide (1 drop) in anhydrous diethyl ether ( $30 \text{ cm}^3$ ) was stirred at  $20^\circ\text{C}$  for 2 h under nitrogen. Distillation yielded but-3-enoyl chloride (0.8 g), which was added to a mixture of anhydrous tetrahydrofuran ( $10 \text{ cm}^3$ ) and  $\text{H}_2^{18}\text{O}$  (160 mg, 96%  $^{18}\text{O}$ ). The mixture was stirred at  $20^\circ\text{C}$  for 12 h, the solvent removed *in vacuo*, the residue dissolved in diethyl ether ( $20 \text{ cm}^3$ ), and added at  $0^\circ\text{C}$  to a slurry of lithium aluminium deuteride (0.5 g) in diethyl ether ( $10 \text{ cm}^3$ ). The mixture was heated at reflux for 3 h, cooled to  $0^\circ\text{C}$ , water ( $5 \text{ cm}^3$ ) was added followed by aqueous hydrogen chloride (saturated,  $2 \text{ cm}^3$ ). The organic layer was separated, the aqueous layer extracted with diethyl ether ( $2 \times 30 \text{ cm}^3$ ) and the combined organic extract dried ( $\text{MgSO}_4$ ), concentrated *in vacuo* and distilled to give [1,1- $^2\text{H}_2$ ]-but-3-en-1-ol- $^{18}\text{O}$ ] (0.75 g, bp  $109\text{--}111^\circ\text{C}$  at atmospheric pressure). *meta*-Chloroperbenzoic acid (3 g) was added, at  $0^\circ\text{C}$ , to the labelled buten-1-ol (0.75 g) in dichloromethane ( $25 \text{ cm}^3$ ), the mixture allowed to stir at  $20^\circ\text{C}$  for 20 h, aqueous sodium hydroxide (10%,  $12 \text{ cm}^3$ ) was added, the organic layer separated and the aqueous layer extracted with dichloro-



methane ( $3 \times 20 \text{ cm}^3$ ). The combined organic extracts were dried ( $\text{MgSO}_4$ ), concentrated *in vacuo*, and the residue distilled to yield  $[1,1\text{-}^2\text{H}_2]\text{-2-(oxiran-2-yl)ethan-1-}[^{18}\text{O}]\text{ol}$  (0.45 g, overall yield 36%,  $^{18}\text{O} = 48\%$ ,  $^2\text{H}_2 = 99\%$ ).

**$[1,1\text{-}^2\text{H}_2]\text{-2-(Oxiran-2-yl)ethan-1-ol}$ .** The method is similar to that outlined above. Vinylacetic acid was reduced with lithium aluminium deuteride to yield  $[1,1\text{-}^2\text{H}_2]\text{-but-3-en-1-ol}$ , which was then epoxidised to yield  $[1,1\text{-}^2\text{H}_2]\text{-2-(oxiran-2-yl)ethan-1-ol}$  (overall yield 55%,  $^2\text{H}_2 = 99\%$ ).

**$2\text{-(Oxiran-2-yl)ethan-1-}[^{18}\text{O}]\text{ol}$ .** The method is similar to those outlined above except that  $\text{H}_2^{18}\text{O}$  and lithium aluminium hydride were used. Overall yield 46%,  $^{18}\text{O} = 48\%$ .

#### Condensed phase reactions

Products of the reactions outlined below were analysed using a Finnigan MAT GCQ mass spectrometer. Conditions: column phase RTX-SMS (length 30 cm, id 0.25 mm, GC fused silica capillary), He carrier gas. Initial column temperature, held at  $50^\circ\text{C}$  for 2 min, then the temperature increased at  $15^\circ\text{C}$  per minute. Retention times: 3 (4.05 min), 4 (3.23 min) and 5 (3.48 min).

**System A.** A mixture of  $2\text{-(oxiran-2-yl)ethan-1-ol}$  (0.5 g) in aqueous sodium hydroxide (10%,  $5 \text{ cm}^3$ ) was stirred under reflux for 15 h, cooled to  $20^\circ\text{C}$ , and aqueous hydrogen chloride (10%) was added dropwise until the pH was 6. The mixture was extracted with dichloromethane ( $4 \times 5 \text{ cm}^3$ ) and the combined organic extract was dried ( $\text{MgSO}_4$ ) and concentrated to give an oil (0.25 g). The reaction mixture was sampled at particular times, and the product composition analysed by GC-MS (see Table 2).

**System B.**  $2\text{-(Oxiran-2-yl)ethan-1-ol}$  (0.5 g) was added dropwise to a slurry of sodium hydride (1 mol equiv.) in tetrahydrofuran ( $10 \text{ cm}^3$ ) maintained at  $0^\circ\text{C}$ . The mixture was then heated at reflux for 15 h, cooled to  $0^\circ\text{C}$ , water ( $5 \text{ cm}^3$ ) was added, the mixture extracted with dichloromethane ( $4 \times 5 \text{ cm}^3$ ), the combined organic extracts dried ( $\text{MgSO}_4$ ), and concentrated to give an oil (0.4 g). The reaction mixture was sampled at particular times, and the product composition analysed by GC-MS.

Identical procedures were carried out with oxetan-2-ylmethanol and tetrahydrofuran-3-ol.

#### Acknowledgements

This project was financed by the Australian Research Council. J. M. H. and S. D. thank the ARC for a Ph.D. scholarship and a research associate position respectively.

#### References

- 1 S. Dua, M. S. Taylor, M. A. Buntine and J. H. Bowie, *J. Chem. Soc., Perkin Trans. 2*, 1997, 1991.
- 2 Data from: S. W. Benson, *Thermochemical Kinetics*, Wiley, New York, 1967.
- 3 GAUSSIAN94, Revision C3, M. J. Frish, G. W. Trucks, H. B. Schlegel, P. M. W. Gill, B. G. Johnson, M. A. Robb, J. R. Cheeseman, T. Keith, G. A. Petersson, J. A. Montgomery, K. Raghavachari, M. A. Al-Latham, V. G. Zakrzewski, J. V. Ortiz, J. B. Foresman, J. Cioslowski, B. B. Stefanov, A. Nanayakkara, M. Challacombe, C. Y. Peng, P. V. Ayala, W. Chen, M. W. Wong, J. L. Andres, E. S. Replogle, R. Gomperts, R. L. Martin, D. J. Fox, J. S. Binkley, D. J. Defrees, J. Baker, J. P. Stewart, M. Head-Gordon, C. Gonzalez and J. A. Pople, Gaussian Inc., Pittsburgh, PA, 1995.
- 4 J. H. Bowie and T. Blumenthal, *J. Am. Chem. Soc.*, 1975, **97**, 2959; I. Howe, J. H. Bowie, J. E. Szulejko and J. H. Beynon, *Int. J. Mass Spectrom. Ion Phys.*, 1980, **34**, 99.
- 5 R. J. Waugh, R. N. Hayes, P. C. H. Eichinger, K. M. Downard and J. H. Bowie, *J. Am. Chem. Soc.*, 1990, **112**, 2537.
- 6 J. B. Cumming and P. Kebarle, *Can. J. Chem.*, 1978, **56**, 1.
- 7 VG ZAB 2HF, VG Analytical, Manchester, UK.
- 8 M. B. Stringer, J. L. Holmes and J. H. Bowie, *J. Am. Chem. Soc.*, 1986, **108**, 3888.
- 9 H. Wynberg and A. Bantjes, *Org. Synth.*, 1963, Coll. Vol. **4**, 534.
- 10 A. O. Fitton, J. Hill, D. E. Jane and R. Millar, *Synthesis*, 1987, **12**, 1140.
- 11 H. C. Brown and G. J. Lynch, *J. Org. Chem.*, 1981, **46**, 930.

Paper 8/01172I

Received 10th February 1998

Accepted 21st April 1998